

University of Alberta

Synthesis of Bicyclic and Bimetallic Titanacyclobutenes

by

Jeffrey Scott Quesnel

A thesis submitted to the Faculty of Graduate Studies and Research
in partial fulfillment of the requirements for the degree of

Master of Science

Department of Chemistry

©Jeffrey Scott Quesnel

Fall 2009

Edmonton, Alberta

Permission is hereby granted to the University of Alberta Libraries to reproduce single copies of this thesis and to lend or sell such copies for private, scholarly or scientific research purposes only. Where the thesis is converted to, or otherwise made available in digital form, the University of Alberta will advise potential users of the thesis of these terms.

The author reserves all other publication and other rights in association with the copyright in the thesis and, except as herein before provided, neither the thesis nor any substantial portion thereof may be printed or otherwise reproduced in any material form whatsoever without the author's prior written permission.

Examining Committee

Jeffrey M. Stryker, Department of Chemistry

Derrick L. J. Clive, Department of Chemistry

Natalia Semagina, Department of Chemical and Materials Engineering

Abstract

In an attempt to expand the scope of titanacyclobutenes, malonate-derived α,ω -alkylpropargyl dibromides and α,ω -bis(bromopropargyl) malonates were prepared and examined for their reactivity with titanocene reagents. Unfortunately, all of the α,ω -alkylpropargyl dibromomalonates failed, presumably from chelation of the carbonyl oxygen followed by radical or nucleophilic attack. The α,ω -bis(bromopropargyl) malonate substrates allowed the successful synthesis of ester-functionalized allenyl or alkynyl-substituted bicyclic titanacyclobutene complexes. Allenyl-substitution is favoured when the being formed ring is small. When ring strain is minimal, cycloalkynes are obtained. An impressive example of a twelve-membered macrobicyclic titanacyclobutene was achieved, supported by extensive NMR spectroscopy and X-ray crystallography.

η^3 -Propargyltitanium(III) complexes were synthesized and displayed equilibrium behaviour between the monomeric propargyl and dimeric di(titanacyclobutene) forms. Both steric and electronic effects are believed to be contributing factors for dimerization. Bimetallic titanacyclobutenes are obtained from the reaction of an epoxide and titanocene monochloride in the presence of a η^3 -propargyltitanium(III) complex.

Acknowledgments

I would like to thank my supervisor, Dr. Jeff Stryker, for his enthusiasm, ideas, sense of humour and patient thesis-editing skills. I will always remember our impromptu group meetings at the faculty club.

To all my labmates throughout my stay (Kai Ylijoki, Bryan Chan, Dr. Rick Bauer, Jeremy Gauthier, Dr. Robin Hamilton, Dr. Masaki Morita, Dr. Owen Lightbody, Dominique Hebert, Shao Hui, Takahiro Saito), thank you so much for everything I have taken from you, whether it knowledge, friendship, or in the extremely generous cases, precious starting materials. I would especially like to thank Kai Ylijoki for helping me with the Spartan program.

Finally, I would like to extend out a warm thank-you to my family and (non-Stryker group) friends. Over my many years of education, I have received nothing but support from them. They also kept me in touch with the world outside of the laboratory, something essential to one's sanity.

Table of Contents

Chapter 1: Introduction-Radical Macrocyclization.....	1
1.1 Introduction	1
1.2 General mechanism.....	2
1.3 Historical perspective.....	3
1.4 Intermolecular reactions	6
1.4.1 Telomerization.....	6
1.4.2 Dimerization and trimerization.....	9
1.4.3 Other radical macrocyclization reactions.....	12
1.5 Atom-transfer reactions.....	13
1.5.1 Metal-catalyzed radical generation.....	14
1.5.2 Other atom-transfer reagents.....	16
1.6 Polymers containing macrocycles.....	18
1.7 Natural product synthesis	19
1.7.1 Macrolactams	19
1.7.2 Macrolides.....	22
1.7.3 Cembranoids.....	25
1.7.4 Cyclic peptides	27
1.8 Conclusion.....	28
Chapter 2: Background-Titanacyclobutenes <i>via</i> radical methodology	30
2.1 Introduction	30
2.2 Titanacyclobutenes from intermolecular radical addition.....	30
2.3 Mechanism and frontier orbital analysis	32

2.4 Bicyclic titanacyclobutenes from intramolecular radical addition	34
2.5 Di(titanacyclobutenes) via propargyl-propargyl radical coupling.....	36
2.6 Conclusion	37
Chapter 3: Bicyclic titanacyclobutenes from α,ω -alkylpropargyl	
dibromide malonates	39
3.1 Introduction	39
3.2 Project goals	40
3.3 Results: α,ω -alkylpropargyl dibromide substrate synthesis	41
3.3.1 Introduction.....	41
3.3.2 Synthesis of organic substrates bearing a primary halide.....	42
3.3.3 Synthesis of organic substrates bearing a secondary or tertiary halide.....	45
3.4 Results: Intramolecular addition of radicals to η^3 -propargyltitanium(III) complexes.....	51
3.4.1 Intramolecular addition with primary radicals.....	51
3.4.2 Intramolecular addition with secondary radicals.....	52
3.5 Future research and conclusion.....	56
Chapter 4: Bicyclic titanacyclobutenes from α,ω -bis(bromopropargyl) malonates...58	
4.1 Introduction	58
4.2 Results: α,ω -bis(bromopropargyl) malonate synthesis.....	58
4.3 Results: Intramolecular addition of radicals to η^3 -propargyltitanium(III) complexes.....	64
4.3.1 Exo-allenyl bicyclic titanacyclobutenes	64

4.3.2 Macrobicyclic titanacyclobutenes	70
4.3.3 Demetallation of bicyclic titanacyclobutenes	83
4.3.4 Titanacyclobutenes from bis(bromopropargyl) malononitrile substrate.....	85
4.4 Future research and conclusion.....	88
Chapter 5: Intermolecular radical addition to titanium propargyl complexes	89
5.1 Introduction	89
5.2 Results	91
5.2.1 Synthesis and characterization of η^3 -propargyltitanium(III) complexes.....	91
5.2.2 Bimetallic titanacyclobutenes from epoxides	97
5.2.3 Demetallation of bimetallic titanacyclobutene complex	103
5.2.4 Synthesis of ester-functionalized titanacyclobutenes by intermolecular radical addition.....	104
5.2.5 Crystallographic properties of titanacyclobutenes	106
5.3 Future research and conclusion.....	111
Chapter 6: Experimental details.....	112
Appendix: Crystallographic data.....	168
References and notes	191

List of Tables

<i>Title</i>	<i>Page</i>
Table 1.1: Atom-transfer cyclizations of α -chloro alkenylesters	15
Table 3.1: ^1H and ^{13}C NMR assignments for bicyclic titanacyclobutene 131	55
Table 4.1: ^1H and ^{13}C NMR assignments for bicyclic titanacyclobutene 148f	68
Table 4.2: ^1H and ^{13}C NMR assignments for bicyclic titanacyclobutene 155a	74
Table 5.1: Select ^1H and ^{13}C NMR assignments for bimetallic titanacyclobutene 168	99
Table 5.2: Select data of crystallographically studied titanacyclobutenes	109

List of Figures

<i>Title</i>	<i>Page</i>
Figure 1.1: Steroidal radical precursors.....	9
Figure 1.2: Chair conformations of benzamide 23	11
Figure 1.3: Protoberberine 47 and isoindolo[1,2- <i>b</i>][3]benzazepine 48 alkaloid core..	19
Figure 1.4: Hydrogen-bonded stabilization of the <i>trans</i> -decalin form of benzamide 53	22
Figure 1.5: Brefeldin A.....	22
Figure 1.6: Furanocembranoids lophotoxin 73 and pukalide 74	26
Figure 1.7: Roseophilin	27
Figure 2.1: Walsh diagram of η^3 -propargyltitanium(III) complex.....	34
Figure 3.1: Target α,ω -alkylpropargyl dibromomalonates	42
Figure 3.2: Carbon and hydrogen labelling scheme for bicyclic titanacyclobutene 131	55
Figure 3.3: ORTEP diagram of bicyclic titanacyclobutene 129	56
Figure 4.1: α,ω -Bis(bromopropargyl) malonate 132	58
Figure 4.2: <i>Gem</i> -diester α,ω -bis(bromopropargyl) substrate 139	61
Figure 4.3: ORTEP diagram of tricyclic titanacyclobutene 149a	66
Figure 4.4: ORTEP diagram of bicyclic titanacyclobutene 148a	67
Figure 4.5: Carbon and hydrogen labelling scheme for bicyclic titanacyclobutene 148f	68
Figure 4.6: Bicyclic titanacyclobutene 154	72
Figure 4.7: Carbon and hydrogen labelling scheme for titanacyclobutene 155a	74

Figure 4.8: Pertinent HMBC and COSY correlations for titanacyclobutene 155a	75
Figure 4.9: ORTEP diagram of macrobicyclic titanacyclobutene 155a	76
Figure 4.10: ORTEP diagram of α,ω -bis(bromopropargyl) malonate 136d	78
Figure 4.11: ORTEP diagram of α,ω -bis(bromopropargyl) dimalonate 146d	79
Figure 4.12: Lowest-energy conformer calculated for bis(<i>gem-tert</i> -butyl) ester 146b	80
Figure 4.13: Energy profile for C6-C7 bond rotation of bis(<i>gem-tert</i> -butyl) ester 146b	81
Figure 5.1: ORTEP diagram of di(titanacyclobutene) dimer 162a	92
Figure 5.2: ORTEP diagram of titanacyclobutene 163	94
Figure 5.3: ORTEP diagram of η^3 -propargyltitanium(III) complex 161c	96
Figure 5.4: Carbon and hydrogen labelling scheme for bimetallic titanacyclobutene 168	99
Figure 5.5: ORTEP diagram of bimetallic titanacyclobutene 169a	102
Figure 5.6: ORTEP diagram of titanacyclobutene 175	105
Figure 5.7: Crystallographically characterized titanacyclobutenes.....	110

List of Abbreviations

Å	Angstrom
AIBN	2,2'-azobisisobutylnitrile
APT	attached proton test
BPO	benzoyl peroxide
bpy	2,2'-bipyridine
^t Bu	tert-butyl
^t BuCp	tert-butylcyclopentadienyl
cat.	catalytic
COSY	correlated spectroscopy
Cp	cyclopentadienyl
Cp*	pentamethylcyclopentadienyl
DCE	dichloroethane
DFT	density functional theory
DHP	dihydropyran
DMF	<i>N,N</i> -dimethylformamide
E	ester
EIMS	electron ionization mass spectrometry
ESMS	electrospray mass spectrometry
equiv.	equivalent
g	grams
h	hour(s)
HMBC	heteronuclear multiple bond correlation

HMQC	heteronuclear multiple quantum coherence
HSQC	heteronuclear single quantum correlation
Hz	hertz
<i>i</i>	iso
IR	infrared
<i>m</i> CPBA	<i>meta</i> -chloroperbenzoic acid
Me	methyl
mL	millilitre
M_n	number-average molecular weight
M_w/M_n	polydispersity
NMR	nuclear magnetic resonance
NOE	nuclear Overhauser effect
ppm	parts per million
Pr	propyl
PTS	<i>para</i> -toluenesulfonic acid
rt	room temperature
SOMO	singly-occupied molecular orbital
TBPO	<i>tert</i> -butyl peroxide
THF	tetrahydrofuran
THP	tetrahydropyranyl
TOCSY	total correlation spectroscopy
TTMS	tris(trimethylsilyl)silane
μ L	microlitre

Chapter 1: Introduction - Radical macrocyclization

1.1 Introduction

Free radical reactions have become an important and ubiquitous tool for synthetic organic chemists. It is, however, only relatively recently that chemists realized that the high reactivity of free radical intermediates could be synthetically useful, dispelling the prevailing attitude that they were *too* reactive to be controlled. Unlike their ionic counterparts, neutral radicals are less sensitive to solvent effects and many reactions even tolerate protic solvents. The fact that many functional groups also tolerate radical intermediates is quite advantageous, shortening syntheses by avoiding time-consuming protection and deprotection procedures. Radical cyclization reactions have been extensively used for the formation of five and six-membered rings; guidelines for successful syntheses have been discussed.¹ Only over the past 25 years has the possibility of larger-ring synthesis *via* radical methods been approached and analyzed.

This review covers all of the literature on radical macrocyclization reactions (ring sizes ≥ 10). There are few published reviews on this subject, some older^{2,3} as well as one much more recent account.⁴ However, the latter (written in Portuguese), includes only tin-related radical methods, a narrower scope than presented here. The scope of this review is limited to electronic ground-state reactions and, therefore, radical cyclizations by photo-excited states will not be discussed.⁵ As well, transannular cyclization reactions will be addressed only insofar as the resulting product is a macrocycle.^{3,6} Cyclization *via* diradicals will not be treated.⁷

Many recurring themes regarding radical macrocyclization will be evident throughout the discussion, but they bear summary in advance:

- Many macrocyclizations suffer low yields, principally from reduction of the acyclic radical intermediate *via* hydrogen atom abstraction. This reaction pathway is the direct result of the reduced rate of cyclization caused by the large entropy cost for macrocyclization when compared to five and six-membered congeners. The undesired reduction is especially prevalent with the use of aryl halides as radical precursors.

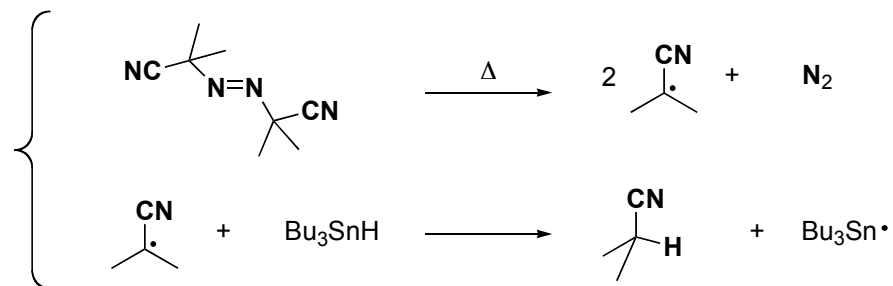
- The formation of smaller macrocycles, ring sizes of ten, eleven and sometimes twelve, are more difficult to achieve than larger macrocycles, where destabilizing transannular interactions in the transition state are less significant.
- In terms of regioselectivity, *endo*-cyclization is usually favoured over *exo*-cyclization. This appears to be quite general over the ring sizes reported, although in some cleverly designed cases, exclusive *exo*-cyclization is possible.
- Alkyl radicals are considered to be nucleophilic⁸ and thus the use of alkene or alkyne acceptors with electron-withdrawing substituents is generally favourable.
- Cyclizations are assisted by templating effects that stabilize reactive conformations favourable to cyclization. In some cases, seemingly minor structural nuances play a large role in determining successful cyclization.

1.2 General mechanism

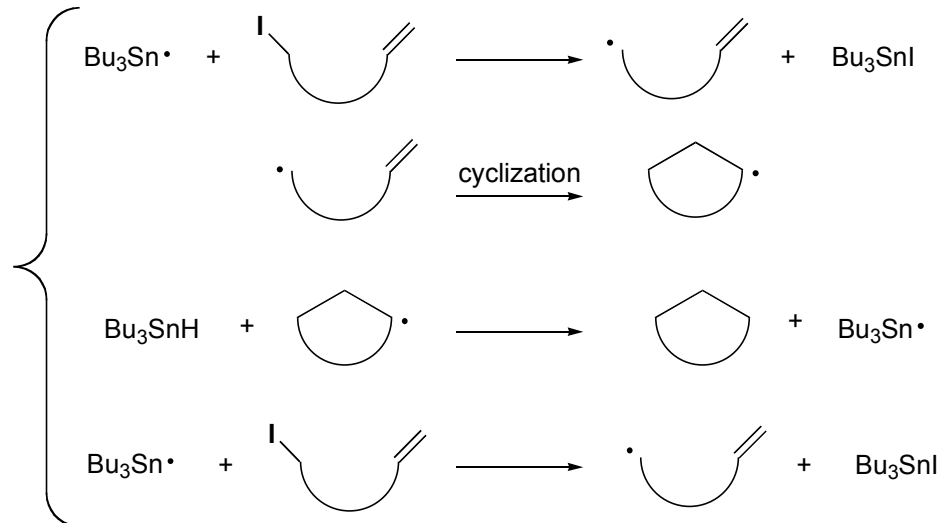
The general mechanism of radical cyclization involves several discrete steps characteristic of a radical chain reaction (Scheme 1.1). The first step is radical initiation. This is usually achieved by the reaction of tributylstannane and a catalytic amount of AIBN. Thermolysis of AIBN, normally in benzene at reflux, extrudes dinitrogen and results in two isobutyronitrile radicals. These radicals initiate the radical chain by hydrogen atom abstraction from the stannane, which then abstracts a halogen atom from the organic substrate. The acyclic organic radical intermediate reacts intramolecularly to afford the cyclic radical intermediate, which then abstracts hydrogen atom from the stannane donor. The newly formed stannane radical then repeats the cycle described above. Termination, or radical annihilation, occurs when two radicals combine or disproportionate.

Scheme 1.1

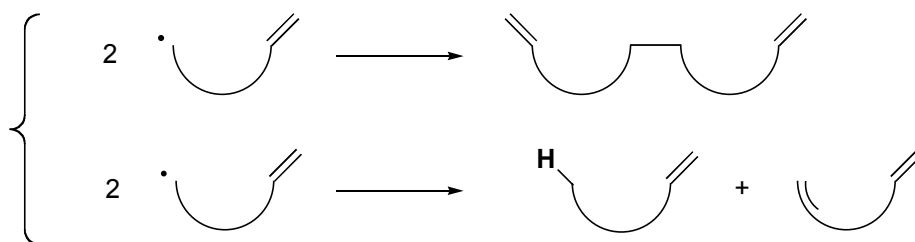
Initiation:



Propagation:



Termination:

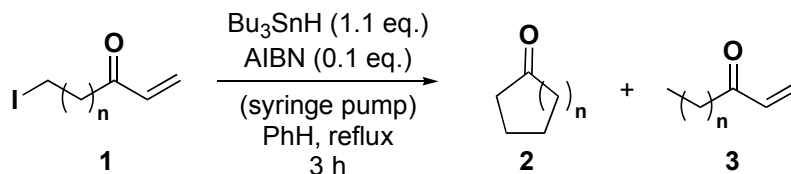


1.3 Historical perspective

In the late 1980's, Porter, *et al.*, began the first systematic studies on free radical macrocyclization and are now recognized as the pioneers of such cyclization chemistry.^{8,9,10,11} Porter found that the reactions of simple ω -halo- α,β -unsaturated ketones **1** with Bu_3SnH containing a catalytic amount of AIBN afforded the corresponding macrocyclic ketones, with the larger, more flexible rings isolated in higher

yield (Equation 1.1).⁸ The regioselectivity of macrocyclization results from the alkyl radical intermediate adding to the most electrophilic carbon, thus resulting in selective attack at the β -position of the enone to give the observed *endo*-cyclization product. The same trends were observed using iodo acrylates, synthesizing eleven- to twenty-membered ring lactones, again in an endocyclic fashion.⁹ High-dilution conditions were

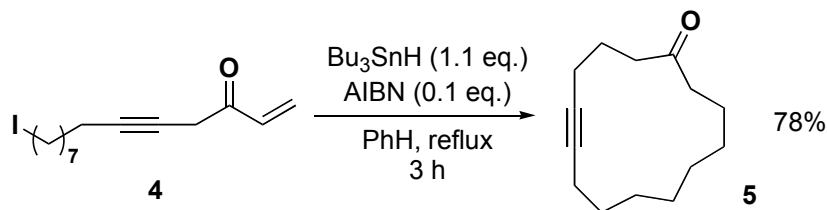
Equation 1.1



n	Ring size	Yield	
		Cyclic, 2	Acyclic, 3
6	10	15%	27%
10	14	63%	22%
14	18	54%	16%

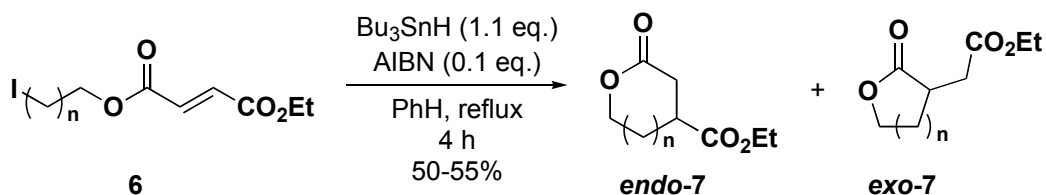
required, as is not unusual for intramolecular reactions forming large rings. Higher concentrations yield products from intermolecular reaction. Low concentration of Bu_3SnH is necessary to avoid direct reduction of the intermediate radical by hydrogen atom abstraction; this is achieved *via* the use of a syringe pump to deliver the reagent over several hours. Iodine is the halogen of choice, as bromine abstraction is more difficult and suppresses the yield of cyclic product. The addition of unsaturation within the substrate backbone results in better yields, producing the fourteen-membered ring alkyne **5** from alkynyl enone **4**, without the formation of bicyclic products from subsequent *5-exo*-cyclization of the intermediate α -keto radical (Equation 1.2). Presumably, the yield increase is due to both the decrease in transannular strain and the increased rigidity of the carbon backbone.

Equation 1.2



Poor control of regioselectivity was encountered in the cyclization of iodo alkyl fumarate substrates (Equation 1.3).⁹ Upon subjecting the halides to cyclization conditions, both *exo* and *endo* modes of ring closure were recovered from the reaction mixture. For the smaller rings (Entries 1 and 2), 12- and 13-*endo* cyclization dominates over the alternative 11- and 12-*exo* modes by a factor of five. However, as the carbon backbone increases in length, the selectivity for *endo* cyclization diminishes and a roughly 1 : 1 mixture of *endo* : *exo* isomers is obtained. This contrasts with the formation of smaller rings (*e.g.* five- and six-membered) where *exo*-closure is kinetically preferred. In an attempt to bias the macrocyclization to favour the *exo*-trajectory, β -alkyl

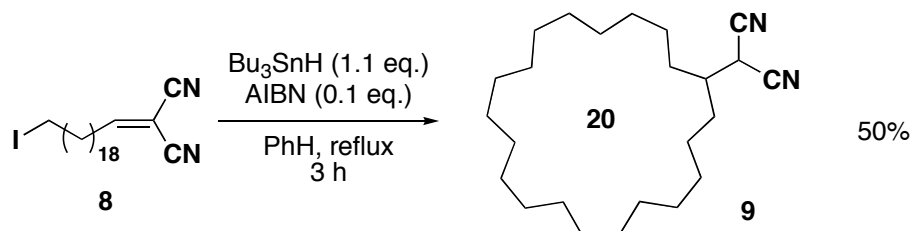
Equation 1.3



Entry	n	<i>endo</i> / <i>exo</i> ring size	<i>endo</i> / <i>exo</i> ratio
1	7	12 / 11	5 / 1
2	8	13 / 12	5 / 1
3	11	16 / 15	2.5 / 1
4	15	20 / 19	1.1 / 1

malononitrile derivative **8** was prepared and subjected to tin-mediated radical cyclization conditions, affording the twenty-membered macrocyclic product **9** (Equation 1.4). Ring sizes of sixteen and twelve were also synthesized with yields decreasing with decreasing ring size. In all cases, no *endo*-cyclization was observed. Several analogues were prepared including esters⁸ and nitro groups in place of nitrile. These reactions failed, however, resulting in either decomposition or simple reduction of acyclic radical

Equation 1.4



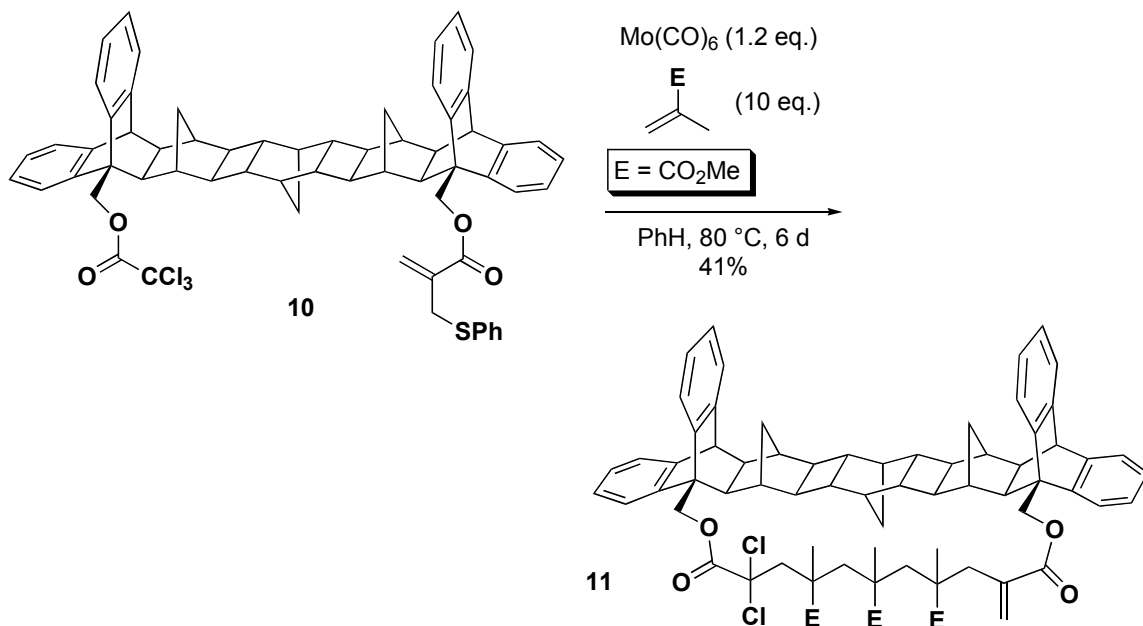
intermediates. The sterically accessible and electronically favoured radical attack on the β -carbon thus allows for *exo*-cyclization. In cases where the activated olefin is terminal, radical attack at the unsubstituted β -carbon gives the corresponding *endo*-cyclic product. When electronically unbiased, the regioselectivity for macrocyclization obeys Porter's rule that "*endocyclization modes are favored*".⁹ This rule will prove quite general for the examples presented from the literature.

1.4 Intermolecular reactions

1.4.1 Telomerization

Radical macrocyclization reactions have found some interesting application in template-controlled oligomerization studies.^{12,13,14} This process relies on a rigid template incorporating a 'start' point for initiating radical oligomerization. The termination step is achieved *via* a radical macrocyclization. The number of monomers incorporated into the product depends on the rigidity of the template and the distance between the radical initiation and termination moieties. Feldman, *et al.*, prepared the rigid polycyclic norbornane derivative **10** containing both α,α,α -trichloroester and allylic phenylsulfide acrylate functional groups to initiate the reaction and terminate the radical, respectively (Equation 1.5).¹² Molybdenum hexacarbonyl in benzene at reflux abstracts chlorine atom from the trichloroester. The captodative α -keto radical intermediate then reacts intermolecularly with the excess methacrylate. Intermolecular radical addition of methacrylate continues until radical macrocyclization *via* an $\text{S}_{\text{H}}2'$ type mechanism occurs. Under these conditions, 41% yield of the macrocyclic product **11** containing four methacrylate monomers was obtained. Unreacted starting material (11%) and

Equation 1.5

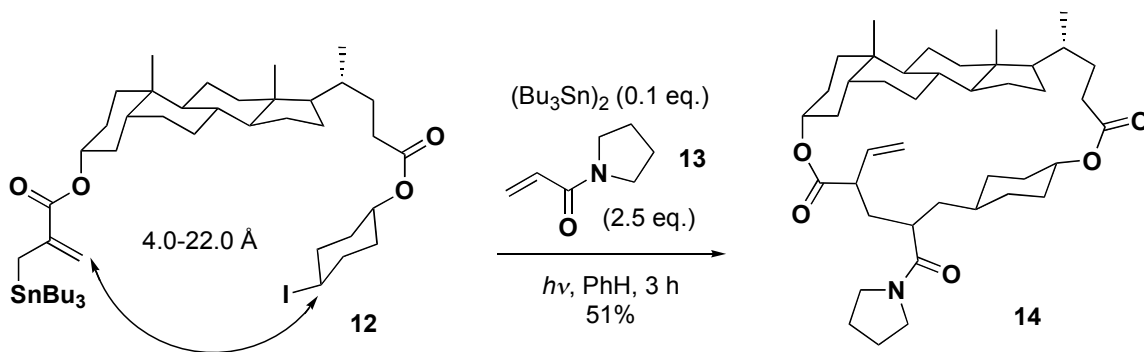


polymeric products from uncontrolled oligomerization (~26%) were also recovered from the reaction. This *26-endo-trig* radical cyclization is assisted by the inflexible template, reducing the occupied space of the radical tether, thus increasing its local concentration. There appears to be meager stereochemical control in this process with six of the possible eight stereoisomers formed in varying amounts.

Template-assisted cyclization chemistry was also applied to steroid derivatives.¹³ The authors were interested in radical oligomerization of acrylamide monomer units linking the radical initiation and termination sites on a range of iodo- and vinylstannane-functionalized steroids (Equation 1.6). The goal of these studies was to predict and synthesize monodisperse steroid macrocycles. To achieve this, both computational and experimental techniques were employed to determine the distance between radical initiation and termination moieties of steroid **12** (Equation 1.6). The calculated distance should control the number of monomer units oligomerized before termination by radical macrocyclization. In the calculation, the program treated the steroid backbone as rigid; only the appended substituents were allowed rotational freedom. The calculated straight-line distance between the iodocyclohexyl and olefin moieties of steroid derivative **12** varies from 4.0-22.0 Å depending on the conformation. The lower extreme (4 Å) is

approximately the size of the acrylamide monomer and thus it was predicted that the macrocyclic product would contain only one monomer. One potential experimental complication is competitive addition of the stannyl radical to the acrylamide, as opposed to iodine abstraction, since the acrylamide is present in a higher concentration. For this reason, the authors used the iodocyclohexyl initiator, as it was assumed to undergo abstraction at the diffusion limit. For comparative purposes, the rate of tributyl tin radical addition to methyl methacrylate is $1.2 \times 10^8 \text{ M}^{-1}\text{s}^{-1}$ at 25 °C, while iodine abstraction from methyl iodide is $4.3 \times 10^9 \text{ M}^{-1}\text{s}^{-1}$ at 25 °C.¹⁵ The steroidal template **12** in benzene was irradiated together with catalytic hexabutylditin and excess acrylamide derivative **13**. Indeed, a modest yield of macrocycle **14** was obtained, containing one acrylamide unit arising from a 25-*endo-trig* cyclization, very modestly confirming the hypothesis. Polymeric material was present but easily separated by chromatography. The strategy of using the stannylated precursor has the benefit of reducing the yield of intermediate radical reduction *via* hydrogen atom abstraction, which can be an issue for slow cyclizations in the presence of tributylstannane.¹⁶

Equation 1.6



Similar steroid-like precursors with greater minimum separation gave contrasting results (Figure 1.1). For example, α -**15** has a minimum calculated distance of 8.7 Å between the iodine and olefin moieties. Under similar conditions, the macrocyclic product isolated from reaction with methyl methacrylate contained three and four monomer units from 22 and 24-*endo-trig* cyclization, respectively, as well as significant amounts of polymeric material. When the minimum gap was slightly larger (11.6 Å) as calculated for the isomer β -**15**, only polymer products were recovered.

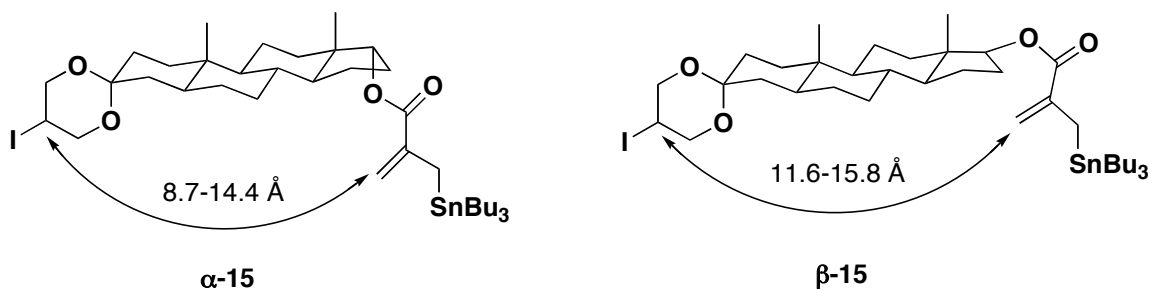


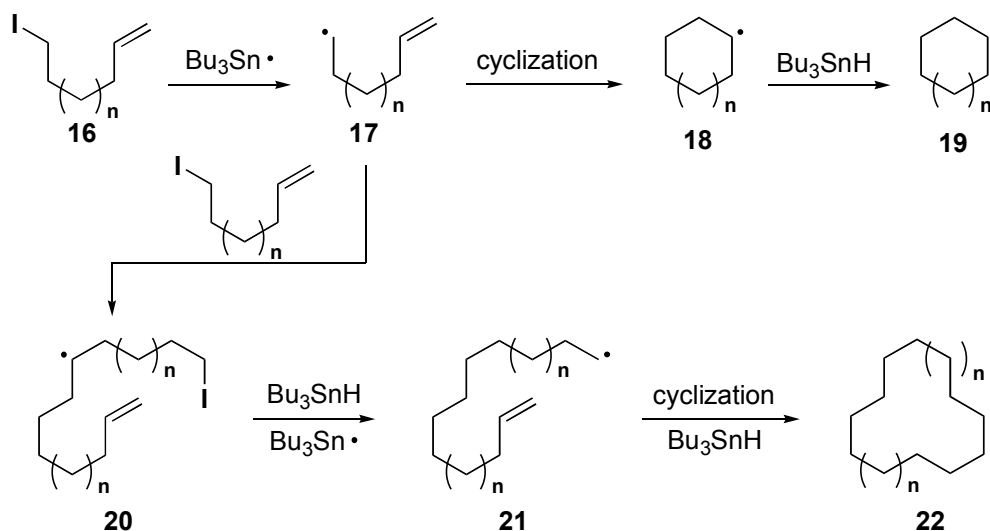
Figure 1.1: Steroidal radical precursors

These results indicate that as the gap between the radical initiator and terminus increases, the increasing conformational flexibility of the oligomerizing chain inhibits efficient radical termination by cyclization. Preparation of telomers with narrow dispersity favouring two monomer units has also been described by the same group.¹⁴

1.4.2 Dimerization and trimerization

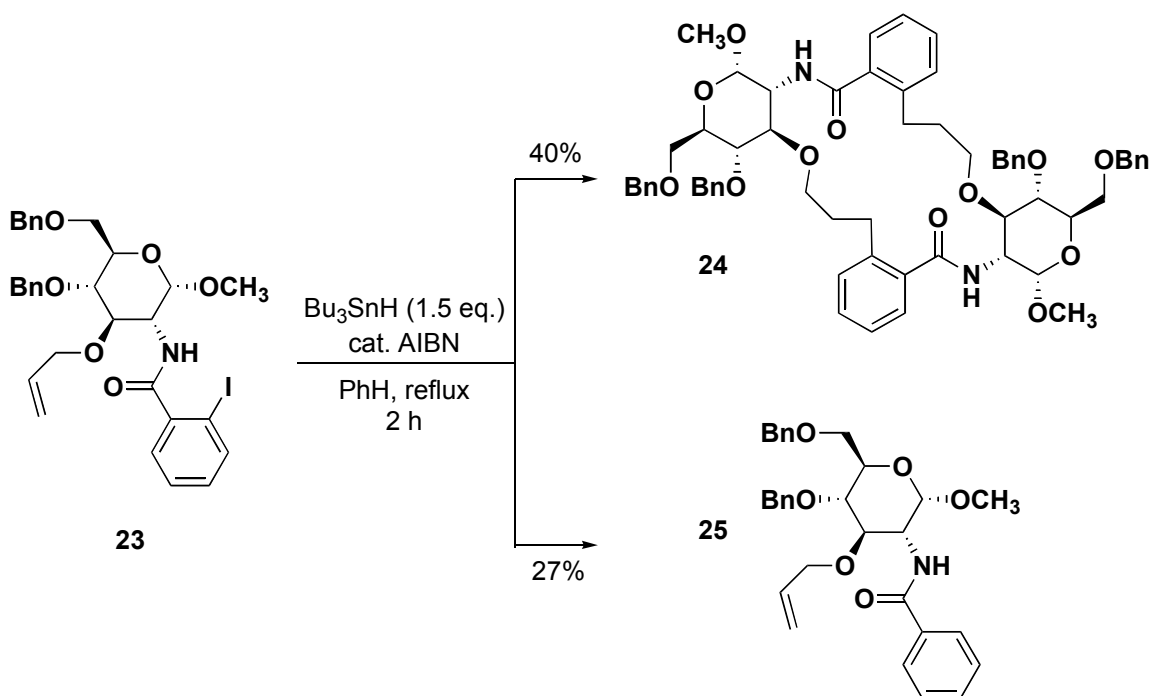
Radical dimerization reactions producing macrocycles are not very common when substrates and conditions are designed to favour intramolecular cyclization. The inclusion of a radicophilic group within the same substrate as the radical precursor will have an increased effective concentration compared to the same acceptor on another molecule. Therefore, for dimerization to occur, the intermediate radical **17** must be trapped by an acceptor intermolecularly faster than it undergoes cyclization (Scheme **1.2**). In other words, the cyclization must be unusually slow, typically a consequence of conformational restraint in the system. Along the reaction path, the coupled radical **20** intermediate could cyclize (**21** \rightarrow **22**), react intramolecularly again, forming oligomer or polymeric products, or abstract hydrogen in the presence of a suitable donor.

Scheme 1.2



In the pursuit of radical macrocyclization of *ortho*-iodobenzamides containing allyloxy side groups, Prado *et al.* found that benzamide substrate **23** undergoes radical dimerization to give macrolactam **24** via a 20-*endo-trig* cyclization in 40% yield, along with 27% reduction of the starting material (Equation 1.7). The monomer macrolactam

Equation 1.7



from competitive 10-*endo-trig* ring-closure was not observed, which was attributed to the general difficulty in forming smaller macrocycles. While this statement is certainly true, a simple conformational analysis of the sugar moiety provides further insight. The two chair conformations of iodobenzamide **23** are shown in Figure 1.2. The more stable conformer **23a** has the benzyloxy and methoxy groups in the equatorial position with the iodide and olefin *trans* diaxial. Ring-flip produces conformer **23b**, which contains three groups in the axial positions, increasing 1,3-diaxial strain, most notably between the methoxy and benzyloxy groups. The more stable conformation, however, should also cyclize most slowly because radical donor and acceptor are mutually *trans* diaxial. The slow rate of intramolecular radical cyclization thus promotes competitive radical dimerization-cyclization.

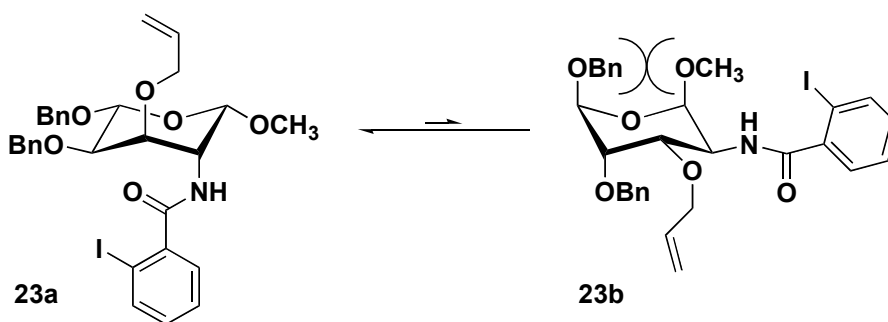
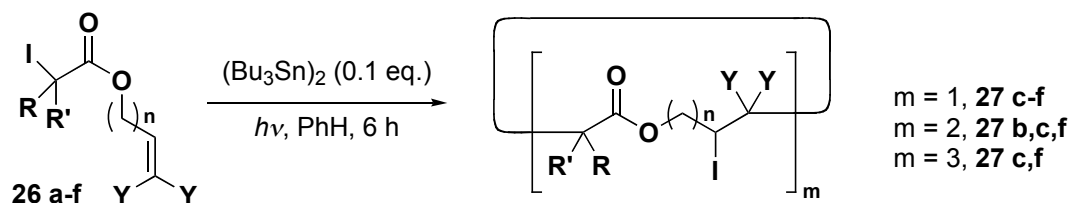


Figure 1.2: Chair conformations of benzamide **23**

Dimerized and even trimerized cyclic products are obtained upon treatment of α -halo alkenyl esters under atom transfer conditions.¹⁷ α -Halo alkenyl esters **26** were heated to reflux in benzene under high dilution and irradiated with a sun lamp in the presence of a catalytic amount of hexabutyldistannane (Scheme 1.3). The reactions produced five- and six-membered lactones from 5- and 6-*exo-trig* cyclization, respectively, but also unexpected cyclic dimer and trimer products. When the α,α -difluoro ester **26a** (Entry 1) was subjected to the reaction conditions, only starting

Scheme 1.3



Entry	Substrate ^a	Lactone yield		
		m = 1	m = 2	m = 3
1	26a , n = 1, Y = H, R = R' = F	-	-	-
2	26b , n = 1, Y = H, R = H, R' = F	-	56%	-
3	26c , n = 1, Y = H, R = R' = H	64%	22%	-
4	26d , n = 1, Y = CH ₃ , R = R' = H	68%	-	-
5	26e , n = 1, Y = CH ₃ , R = H, R' = F	62%	-	-
6	26f , n = 2, Y = H, R = R' = H	7%	66%	26%

^a[substrate] = 8 mM

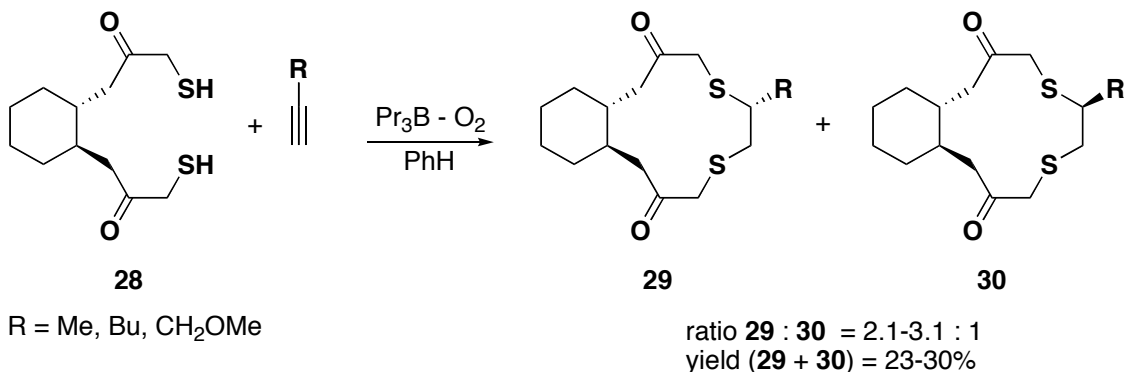
materials were recovered. The authors attribute the lack of reactivity to the stabilizing nature of fluorine substituents on radical centres adjacent to carbonyl functionality.¹⁸ The tetrasubstituted olefins (Entries 4 and 5) presumably undergo rapid 6-*exo-trig* cyclization to afford the tertiary radical intermediate, which then abstracts iodine radical to afford the corresponding iodo-lactone. The unhindered olefins on the other hand, undergo dimer and trimer cyclizations by intermolecular reaction (Entries 2, 3 and 6). The authors invoke a preference for the *s-trans* geometry of the ester¹⁹ over the *s-cis*, retarding cyclization and thus promoting intermolecular addition of the α -carbonyl radical to the alkene. Radical macrocyclization then provides the observed macrocyclic dimer. The trimer arises from a second intermolecular radical addition prior to cyclization. Similarly, dimerization of vinylstannyl selenoesters affording modest yields of dilactones has been observed by Baldwin, *et al.*, producing ring sizes from twelve to twenty-one.^{16b}

1.4.3 Other radical macrocyclization reactions

Crown thioethers have been prepared by homolytic radical cycloaddition between alkynes and dithiols with tripropylborane and oxygen as the radical initiator (Equation 1.8).²⁰ The *trans*-dithiol **28** provides modest 1,6-asymmetric induction in the cyclization

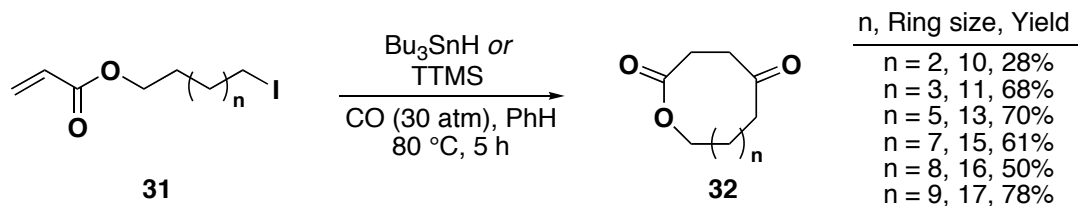
with isomer **29** favoured over **30** by as much as 3.1 : 1. Under similar reaction conditions, the *cis*-isomer of thiol **28** gave comparable yields but very little stereocontrol.

Equation 1.8



Interesting multicomponent radical macrocyclization methodology has been developed by the inclusion of carbon monoxide in the reaction medium.²¹ Under standard radical cyclization conditions but under thirty atmospheres of carbon monoxide, ω -acryloxy iodides **31** gave ten- to seventeen-membered 4-oxolactones **32** in modest to good yields (Equation 1.9). The carbon monoxide acts as both a radical acceptor to give an intermediate acyl radical,²² and donor, adding to the olefin in an *endo* fashion. The incorporation of a new oxygen-containing functional group into the molecule counters the reductive nature of the cyclization.

Equation 1.9



1.5 Atom-transfer reactions

Atom-transfer radical reactions are inherently advantageous compared to reductive methods: the former does not involve hydrogen atom abstraction as the termination step. Instead, the labile group (typically a halogen) abstracted to give the radical intermediate is simply ‘transferred back’ to the newly formed radical site after the

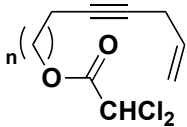
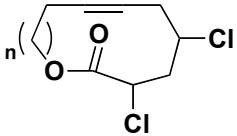
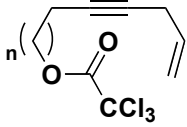
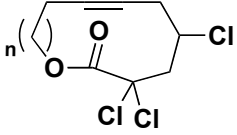
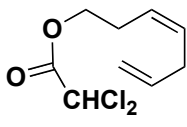
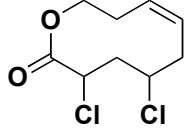
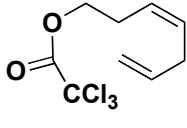
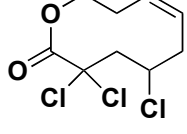
intervening cyclization is complete. Without the need for a hydrogen atom source, undesired reduction of the acyclic radical intermediate is avoided. Furthermore, atom transfer reagents need only be used catalytically since they are not consumed during the reaction.

1.5.1 Metal-catalyzed radical generation

Transition metals in atom-transfer chemistry have gathered some interest, in part to circumvent the use of organostannanes, which are highly toxic and often lead to purification difficulties. Various metals have been used,²³ but the most successful catalysts have been complexes of copper(I) chloride.²⁴

The synthesis of macrocyclic lactones from radical cyclization of α,α,α -trichloro and α,α -dichloro alkenylesters was achieved by sub-stoichiometric copper(I) chloride in the presence of 2,2'-bipyridine (bpy). Thus, heating α -halo alkenylesters **33 a-f** in the presence of 0.3 equivalents of copper(I) chloride and bpy gave the *endo*-selective macrocyclic chlorolactones (Table **1.1**). For cyclization, unsaturation in the

Table 1.1: Atom-transfer cyclizations of α -chloro alkenylesters

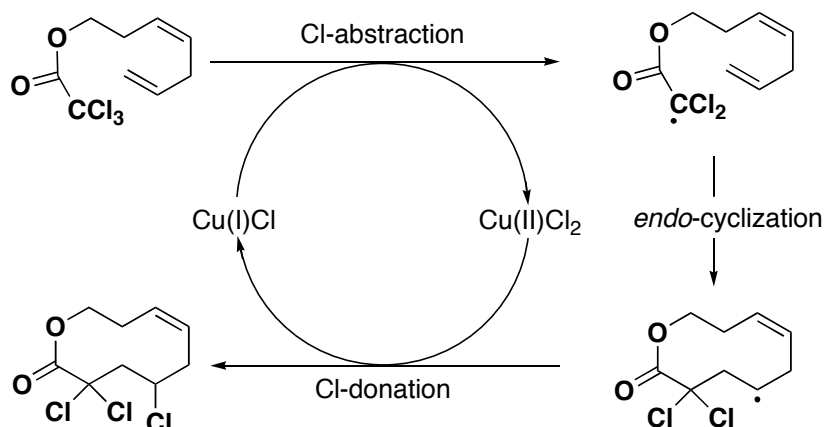
Substrate, conditions ^a		Product (% yield)	
 33a (n = 1), PhH, 80-160 °C 33b (n = 2), PhH, reflux, 18 h	 34a (no cyclization) 34b (51%)		
 33c (n = 1), DCE, 120 °C, 2 h 33d (n = 2), DCE, 175 °C, 3 h	 34c (36%) 34d (10%)		
 33e , PhH, 175 °C, 8 h	 34e (13%)		
 33f , DCE, reflux °C, 3 d	 34f (37%)		

^a 0.3 equiv. of Cu(bpy)Cl

substrate backbone was necessary; otherwise, only telomers were recovered from the reaction. Porter also observed that unsaturation in the chain provided increased yields of radical cyclization product (*vide supra*).¹⁰ This is an important consideration when designing substrates for cyclization.

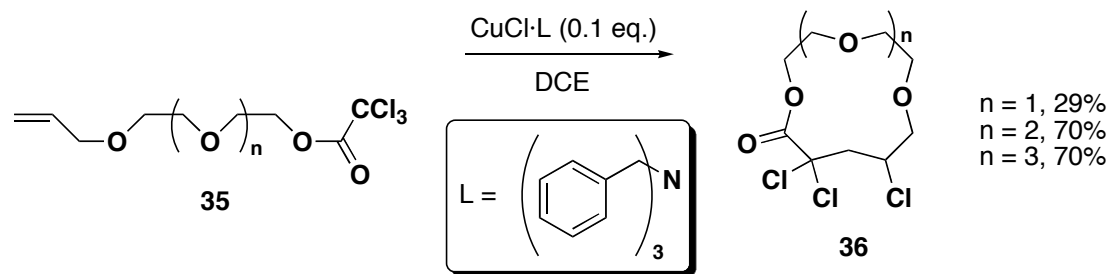
The mechanism of this atom transfer process relies upon the redox couple of Cu(I)/Cu(II). The proposed catalytic cycle is shown in Scheme 1.4. Copper(I) abstracts chlorine atom from the organic substrate to yield an intermediate α -carbonyl-stabilized radical which undergoes *endo*-cyclization. The cyclized alkyl radical intermediate reduces copper(II) by chlorine abstraction, regenerating the active catalyst and forming the organic product. In general, the low yields can be attributed to the difficulty usually encountered in making ten- and eleven-membered rings.

Scheme 1.4



This methodology was further modified by Verlhac, *et al.*, by using copper complexes of pyridine and tertiary amine derived ligands.²⁵ These ligands when combined with copper(I) chloride proved to be more soluble than $\text{Cu}(\text{bpy})\text{Cl}$, enabling catalyst loading as low as 10 mol%. With the catalysts developed, Verlhac prepared macrocyclic crown-type lactones **36** via *endo-cyclization* of α,α,α -trichloro alkenylesters **35**, synthesizing ring sizes twelve to eighteen in modest to good yield (Equation 1.10).

Equation 1.10

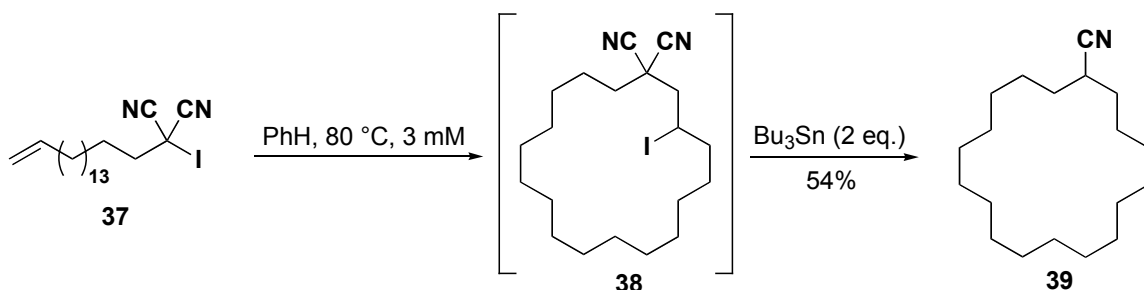


1.5.2 Other atom-transfer reagents

Other transfer reagents have been used to synthesize macrocycles. Hexabutyliditin has been employed in atom transfer macrocyclization of α -fluoro- α -iodo alkenyl esters, as discussed earlier.¹⁷ In Curran's atom transfer studies of iodomalonnitriles, thermolysis of **37** was used to cleave the carbon-iodine bond, which was followed by cyclization of the radical intermediate (Scheme 1.5).²⁶ The macrocyclic iodide **38**, from the 18-*endo-trig* cyclization, could not be isolated in pure form, due to the persistence of oligomeric

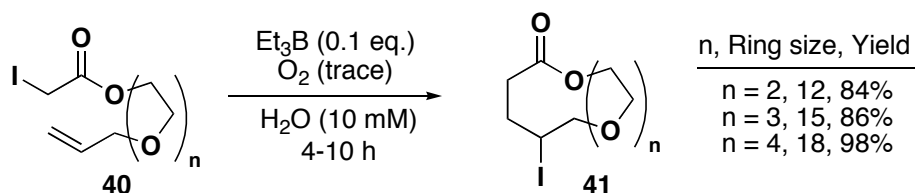
material, and was consequently reduced in the presence of excess tributylstannane. Much to their surprise, macrocyclic *mononitrile* **39** was isolated instead of the expected malononitrile, the first reported example of reductive decyanation of a malononitrile. Further studies proved the reaction to be general.²⁷ Although synthetically useful, only one other research group has published using this method in their synthesis of tricyclic cyano-substituted tetrahydroquinolines.²⁸

Scheme 1.5



Using water as a solvent for organic reactions has attracted much attention in an attempt to curb organic solvent usage, which constitutes the bulk of waste from reactions. Many important organic reactions have been reinvented using water as solvent.²⁹ This ‘green’ approach was taken by Oshima, *et al.*, in radical atom transfer chemistry. Oshima found that triethylborane/O₂ in water enabled the synthesis of macrocyclic iodo-lactones **41** in impressive yields *via* atom-transfer of α -iodo alkenyl esters **40** (Equation 1.11).³⁰ As is typically observed for macrocyclization, the more stable secondary radical intermediate is preferred and thus, only products from *endo*-cyclization were obtained.

Equation 1.11



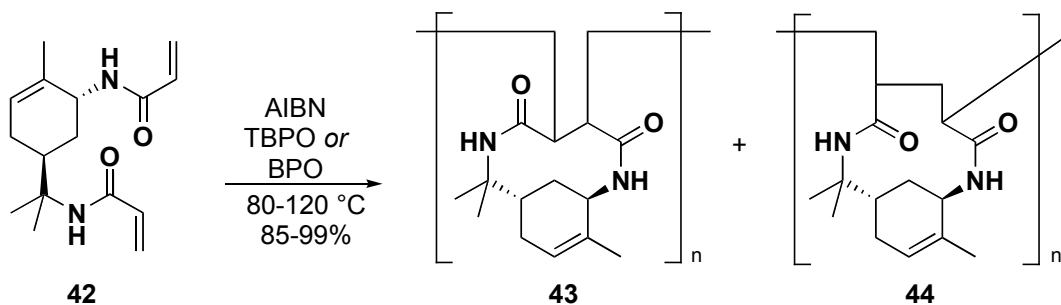
Under otherwise similar conditions, the reactions in benzene provided modest yields, countering the notion that radical reactions are generally not influenced by the reaction medium. The authors propose that hydrogen bonding to the carbonyl group

activates the α -carbonyl radical and the hydrophobic effect reduces the entropic barrier for cyclization. DFT calculations at the B3LYP level using the 6-31G* basis set showed that rotation of the *s-trans* ester rotamer to the *s-cis* form is more favourable in water than in benzene and the volume of the cyclization transition state decreases in water. Water favours conformers where the radical donor and acceptor are in closer proximity than in typical organic solvents, where extended, solvated conformers are preferred.

1.6 Polymers containing macrocycles

Cyclopolymerization to give macromolecules containing large-ring repeating units formed *during* the polymerization reaction may seem like a daunting task, as there is obviously a delicate balance between inter- and intramolecular reactions. There are several polar cyclopolymerization reactions reported and only a few radical methods have been developed.³¹ For example, the use of a chiral bisacrylamide **42** in radical polymerization by Endo, *et al.*, enabled the successful synthesis of ten- and eleven-membered ring-containing polymers (Equation 1.12) with number-average molecular weights (M_n) up to 11,400 although with high polydispersity ($M_w/M_n = 6.99$). It was difficult to analyze the ring size of the monomer subunits by NMR spectroscopy and the authors assume a mixture of ten- and eleven-membered rings are formed. As Porter demonstrated, the smaller macrocycles prefer to form *via endo*-cyclization, therefore it is

Equation 1.12

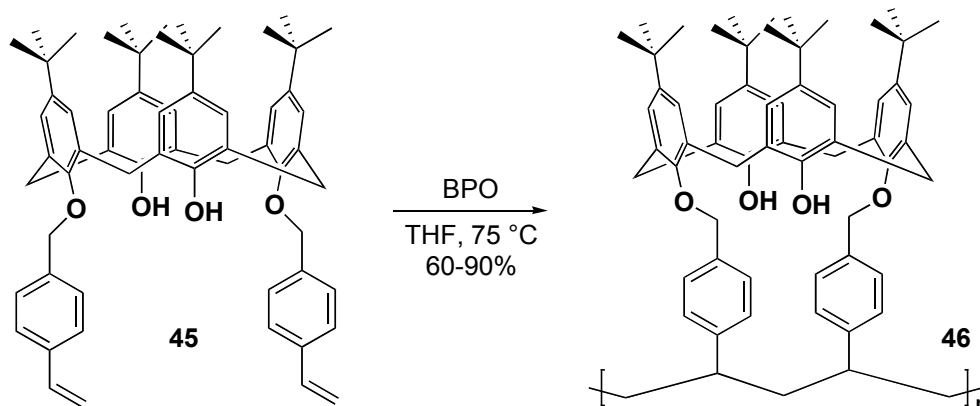


likely the polymer consists of mainly the eleven-membered ring subunit. Endo has also reported nineteen-membered ring synthesis in the radical cyclopolymerization reactions of urethane bis-methacrylates.³²

The rigidity and cone-shape of *O*-calix[4]arenes were exploited by Prata and coworkers in radical polymerization.³³ Tethering styrene moieties³⁴ onto opposite sides

of one face (**45**), followed by radical initiation gave the formal 24-*endo-trig* cyclopolymer **46** with M_n approaching 50,000 (Equation 1.13).

Equation 1.13



1.7 Natural product synthesis

Radical cyclization reactions in natural product synthesis has grown considerably over the past thirty years.³⁵ Stork in particular initiated this resurgence with his early contribution to five and six-membered ring synthesis *via* vinyl radical cyclizations.³⁶ As innumerable naturally occurring compounds have cyclic and polycyclic structures, radical pathways for the construction of these systems have been exploited by synthetic chemists.

1.7.1 Macrolactams

Protoberberine **47** and structurally similar isoindolo[1,2-*b*][3]benzazepine **48** alkaloids are isoquinolines characterized by a 10-membered-ring lactam core, with [6,6] and [7,5] ring fusions, respectively (Figure 1.3). These compounds are interesting from a pharmacological perspective, as the [3]benzazepine moiety possesses important biological activity.³⁷ The polycyclic cores are accessible from macrolactam intermediates, to which

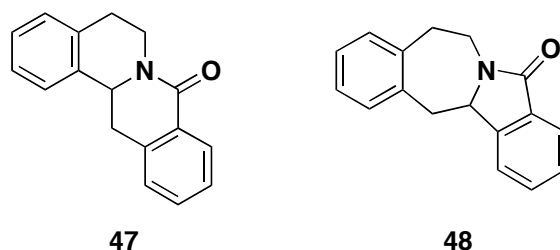
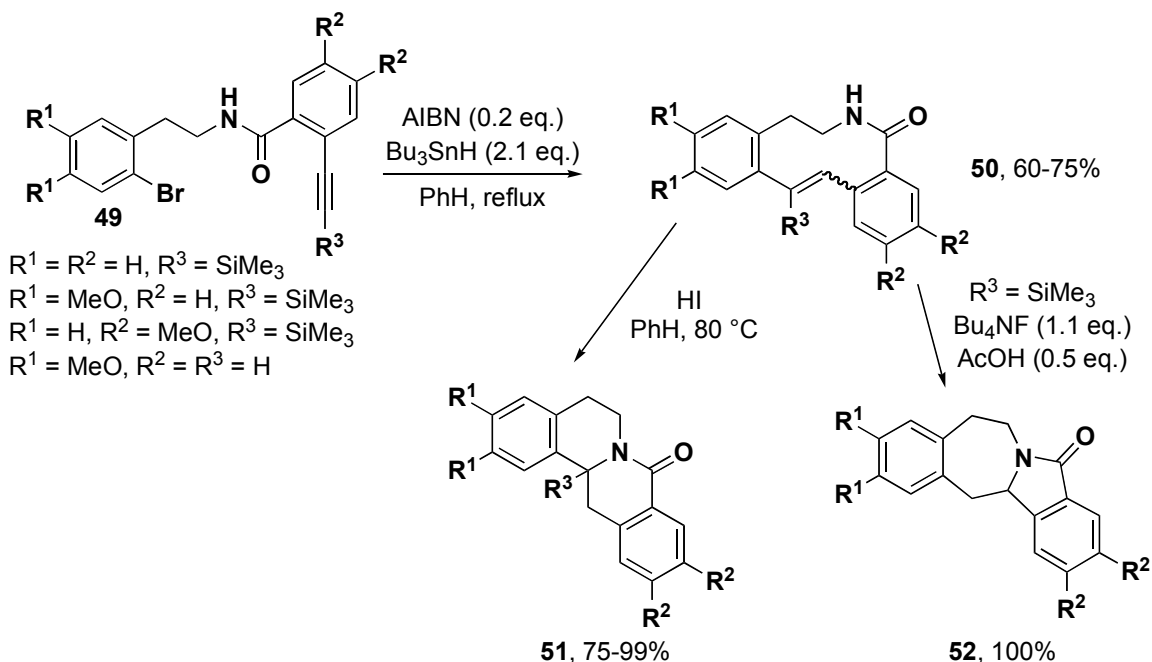


Figure 1.3: Protoberberine **47** and isoindolo[1,2-*b*][3]benzazepine **48** alkaloid core

the primary free radical route has been developed by Domínguez and coworkers.³⁸ After a palladium-catalyzed cyclization of alkynyl arylbromide **49** failed, Domínguez found that the 10-*endo-dig* cyclization of the aryl radical intermediate gave macrolactam **50** as a mixture of *E* and *Z* isomers (R = H, Scheme 1.6). When the trimethylsilyl derivative was subjected to similar reaction conditions, a single stereoisomer was obtained. Unfortunately, the stereochemistry could not be determined. The proto-desilylation conditions used in an attempt to determine the stereochemistry of the olefin led

Scheme 1.6

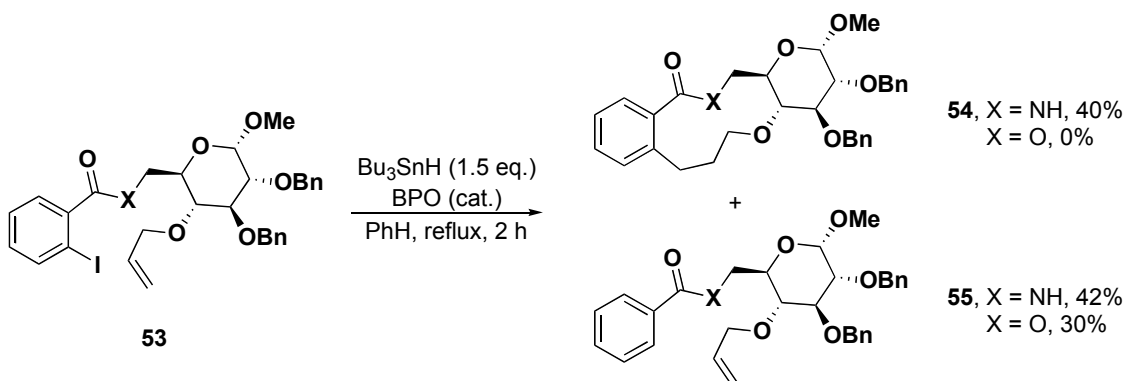


serendipitously to the formation of isoquinoline **51** by a 6-*exo-trig* transannular cyclization. Access to the [3]benzazepine backbone **52** was achieved under fluoride-

induced desilylation conditions, basic conditions or by treatment with the borane-dimethyl sulfide complex.

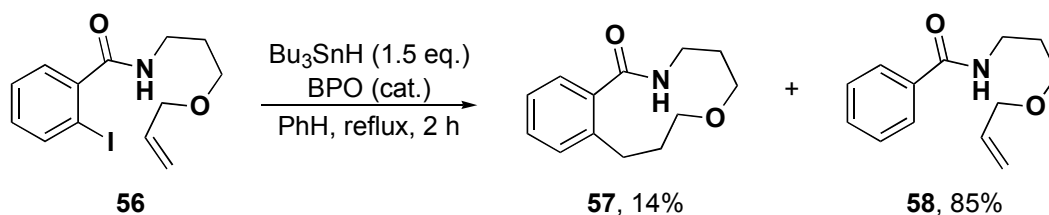
In ongoing work, Prado and coworkers have focused on methodologies for macrolactam synthesis with interesting successes and failures; one example of substrate dimerization was discussed previously.^{4,39} Using a carbohydrate template, a modest yield of macrolactam **54** was obtained by selective 11-*endo-trig* cyclization of allyloxy aryl iodide **53** (Equation 1.14). The ester analogue, however, did not cyclize under the

Equation 1.14



reaction conditions, with only a modest amount of acyclic material recovered. The effect of the carbohydrate template effect was evaluated by synthesizing the amide radical precursor without the appended sugar moiety. Under similar reaction conditions, only 14% of the macrolactam **57** was obtained, recovering 85% of the material as the reduced, acyclic alkene **58** (Equation 1.15). Clearly, both amide functional group and

Equation 1.15



glucopyranoside template influence the cyclization significantly. This can be understood by examining the proposed conformation of benzamide **X** (Figure 1.4). The most stable conformer has the aryl iodide and olefin acceptor as equatorial substituents with the anomeric methoxy group as the only axial substituent. The transition state for cyclization is favoured by intramolecular hydrogen bonding, forming a *trans*-decalin-like structure.

Therefore, both the presence of amide and sugar moiety work in conjunction to accelerate the rate of cyclization, reducing the conformational freedom of the radical donor and acceptor.

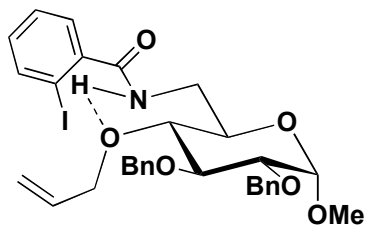


Figure 1.4: Hydrogen-bonded stabilization of the *trans*-decalin form of benzamide **53**

1.7.2 Macrolides

Brefeldin

Brefeldins are a subclass of macrolide esters. Brefeldin A (Figure 1.5) has interested scientists because it interferes with the protein transport mechanism in the Golgi apparatus, resulting in a protein build-up in the endoplasmic reticulum.⁴⁰

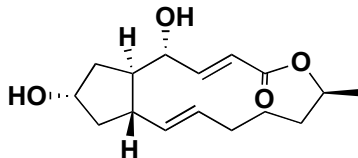
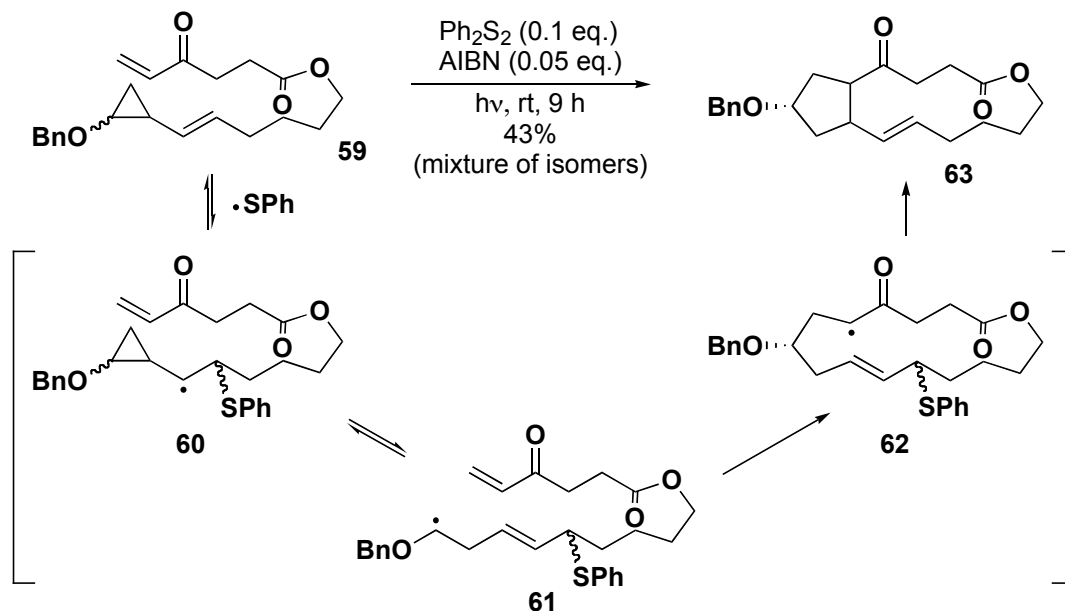


Figure 1.5: Brefeldin A

One synthetic route to the bredfeldin ring system has been achieved by Feldman, *et al.*, by using a vinylcyclopropane/alkene condensation reaction mediated by thiophenyl radical (Scheme 1.7).⁴¹ The addition of thiophenol radical to vinyl cyclopropane **59** presumably gives cyclopropylcarbinyl radical **60**. Rapid ring opening to give benzylic radical **61** followed by 16-*endo-trig* cyclization and 5-*exo-trig* transannular cyclization gives **63** as an unequal mixture of four diastereomers, the major one having the correct brefeldin stereochemistry.

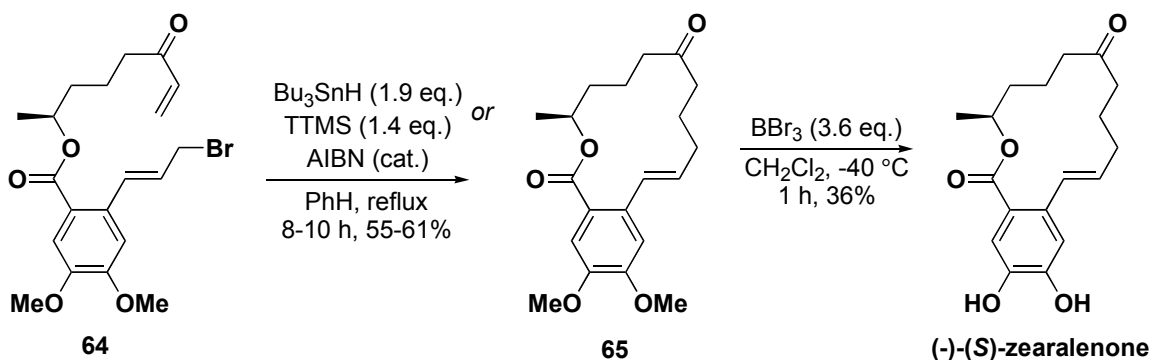
Scheme 1.7



(-)-(S)-Zearalenone

The fourteen-membered macrolide zearlanone is an oestrogenic mycotoxin produced by fusaria, which inhabit maize, barely, oats and wheat.⁴² Pattenden and coworkers have described the total synthesis of *(-)-(S)*-zearalenone, one of the first enantioselective syntheses at that time.^{43,44} Regioselective 14-*endo-trig* cyclization of the allylic radical, generated from cinnamyl bromide **64**, onto the appended enone allowed formation of the macrolactone core **65** (Scheme 1.8).⁴⁵ Although accessible geometrically, 12-*endo-trig* cyclization at the benzylic position was not observed. This selectivity can be attributed to the unfavourable rate of cyclization for the smaller macrocycles.

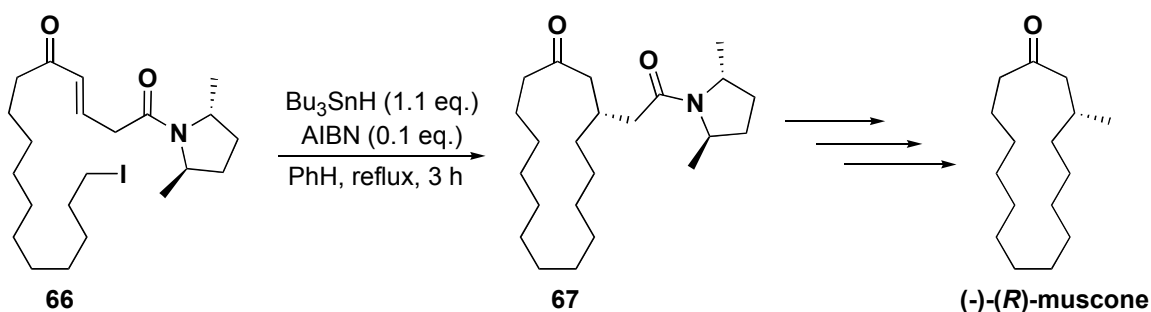
Scheme 1.8



(-)-(R)-Muscone

Muscone is found in the glands of musk deer and has been used in perfume and medicine for millennia.⁴⁶ Structurally, muscone is simply a cyclopentadecanone with an *R*-methyl substituent in the β -position. Numerous racemic and enantioselective syntheses of muscone have been published.^{47,48} The enantioselective radical approach taken by Porter was to form the macrocyclic framework by a 15-*endo-trig* free radical cyclization of ω -iodo- α,β -unsaturated keto-amide **66** (Scheme 1.9).¹¹ Under tin-mediated cyclization conditions, the chiral amide auxiliary induced formation of the *R*-enantiomer of the macrocycle **67** (93% e.e.). Reduction of the amide to the alcohol followed by deoxygenation under Barton conditions gave *(-)-(R)*-muscone.

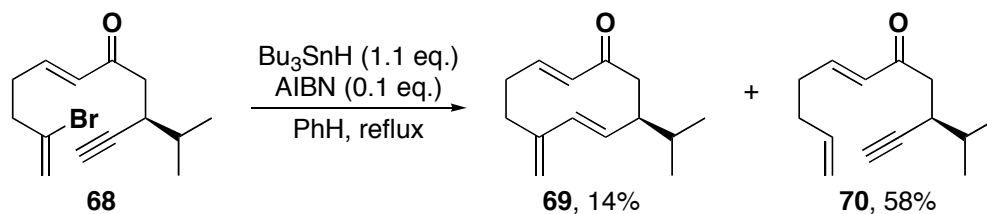
Scheme 1.9



Periplanones

Periplanones are derived from germacrenes, a class of sesquiterpenes found in both plants and animals.⁴⁹ Parsons has described a radical approach to the cyclodecene system through a 10-*endo-dig* cyclization of a vinyl radical onto an alkyne.⁵⁰ Under the reaction conditions, alkenyl vinyl bromide **68** cyclized to give triene **69** to in a mere 14% yield with 58% recovery of reduced acyclic substrate **70** (Equation 1.16). The highly reactive vinyl radical formed is apparently more quickly reduced by hydrogen abstraction from the stannane than it can undergo intramolecular cyclization.

Equation 1.16

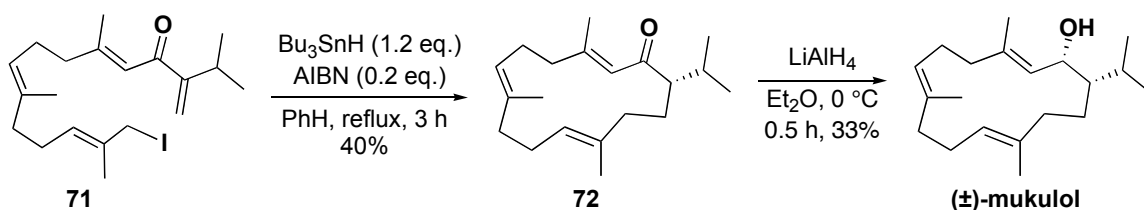


1.7.3 Cembranoids

(±)-Mukulol

Pattenden and coworkers⁵¹ have described the synthesis of (±)-mukulol, a member of the cembranoid family of naturally occurring compounds found in *Comiphora mukul*.⁵² The key step in the synthesis is the cyclization of the allylic radical derived from allylic iodide **71** onto the tethered enone (Scheme 1.10). This cyclization is quite impressive when one considers the large number of reaction pathways the resonance-stabilized allylic radical could take. Besides the desired 14-*endo-trig* cyclization, eleven alternative cyclizations are possible not including the possibility of transannular cyclizations from the intermediate α -keto radical. The 14-*endo-trig* addition is the only pathway observed with the reaction occurring on the most electrophilic and least substituted olefin. When the α -isopropyl group is replaced with hydrogen, a mixture of *E*- and *Z*-isomers are observed, resulting from double bond isomerization prior to cyclization.

Scheme 1.10



Furanocembranoids

Another subset of cembranoids, the furanocembranoids such as lophotoxin (**73**) and pukalide (**74**) (Figure 1.6), are neurotoxic substances, which bind to nicotinic acetylcholine receptors selectively and irreversibly.⁵³ Pattenden devised a free radical

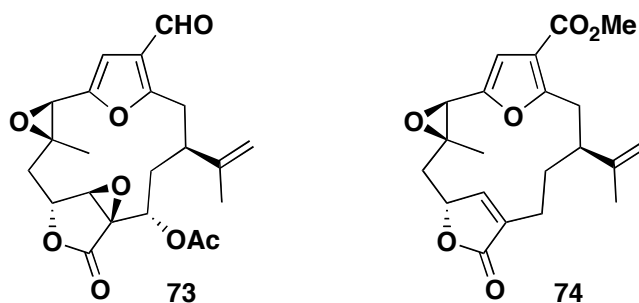
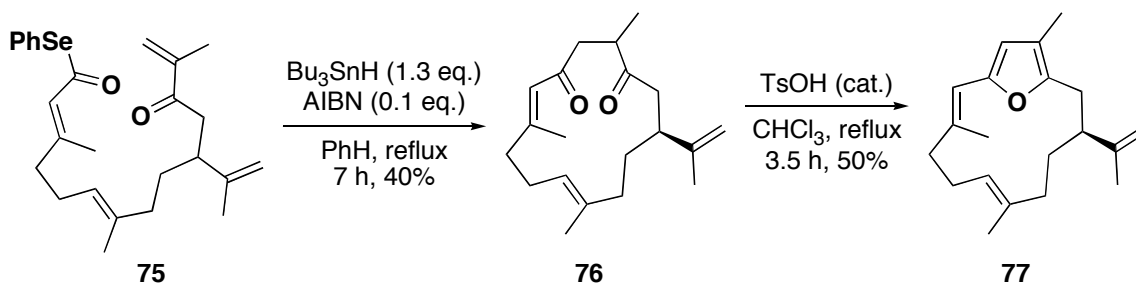


Figure 1.6: Furanocembranoids lophotoxin **73** and pukalide **74**

route to the fourteen-membered macrocyclic furan core, as illustrated in Scheme 1.11. Under tin-mediated cyclization conditions, bond homolysis of selenoester **75** provides an acyl radical intermediate which undergoes 14-*endo-trig* cyclization to give 1,4-dione **76** in modest yield. Cyclodehydration under catalytic acidic conditions provided macrocyclic furan **77**.

Scheme 1.11



Roseophilin

Roseophilin **X** (Figure 1.7) was first isolated from the culture broth of *Streptomyces griseoviridis* and showed cytotoxicity against K562 human erythroid leukemia cells.⁵⁴ A few total syntheses of this polycyclic natural compound have been reported.^{55,56,57}

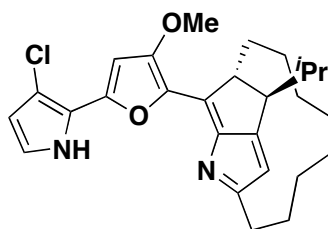
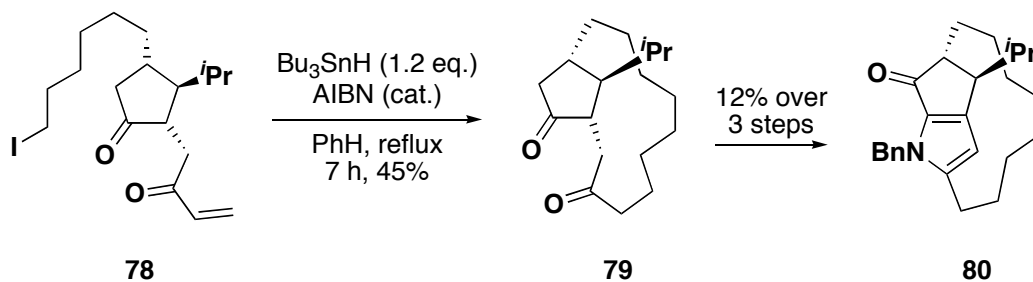


Figure 1.7: Roseophilin

Although they have not completed a total synthesis, Robertson, *et al.*, have devised a radical route to the tricyclic core (Scheme 1.12).⁵⁸ The crucial thirteen-membered ring was formed by *endo-trig* cyclization of iodo diketone **78**. Formation of the trimethylsilyl enol ether and oxidation with dimethyldioxirane, followed by Paal-Knorr condensation concomitant with oxidation of the alcohol, gave tricyclic imine **80**, an intermediate in Fürstner's roseophilin total synthesis.^{55a}

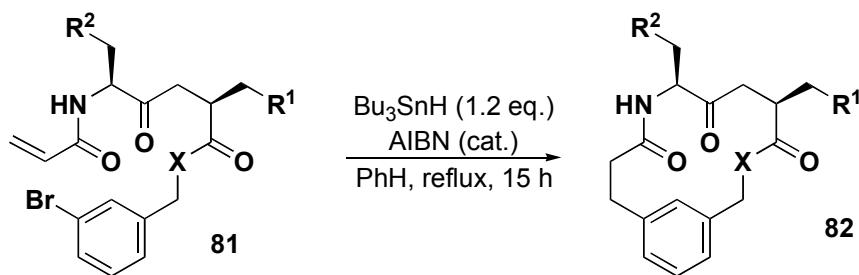
Scheme 1.12



1.7.4 Cyclic peptides

Not naturally occurring but nonetheless interesting from the perspective of peptidomimetics, small cyclic peptides have been synthesized by Iqbal, *et al.*, to pursue conformational and binding studies.⁵⁹ Under standard reductive tin-mediated radical conditions, macrocyclic peptides **82** were synthesized by a 14-*endo-trig* closure of the nucleophilic aryl radical derived from **81** onto the acrylamide moiety (Equation 1.17).

Equation 1.17



Entry	Substrate	Yield
1	X = NH; R ¹ = <i>i</i> Pr; R ² = Ph	47%
2	X = NH; R ¹ = H; R ² = <i>i</i> Pr	59%
3	X = O; R ¹ = <i>i</i> Pr; R ² = Ph	0%

The benzyl amide moiety is crucial for successful cyclization (Entries 1, 2). The authors propose that intramolecular (γ/β -turn) hydrogen bonding assists cyclization by substrate pre-organization. This hypothesis was also supported by detailed NMR studies. The ester analogue cannot hydrogen bond and no cyclic product is obtained (Entry 3). These results parallel those obtained by Prado (*vide supra*), where non-hydrogen bonded substrates also failed to cyclize.

1.8 Conclusion

In summary, the relatively new field of synthesizing macrocycles by radical methods has seen considerable exploitation over the past thirty years. The formation of large rings is important, particularly in natural product synthesis, where macrocycles are prevalent. Acceleration of the rate of radical cyclization is assisted by template effects; bringing the radical donor and acceptor into closer proximity through novel uses of steric, hydrogen bonding and hydrophobic effects. It should be stressed however, that this area remains in its infancy. General rules have been laid but many significant issues have yet to be resolved. One in particular regards controlling the regioselectivity — there is only one example of a radical macrocyclization reaction that completely favours *exo*-cyclization. As shown with Feldman's synthesis of the brefeldin core, stereoselectivity is especially difficult when multiple rings are formed in one step. Until these problems are fully addressed, the full potential of this powerful method of macrocyclization will remain untapped.

This thesis will present an alternative approach to the classical methods of radical macrocyclizations through the use of a transition-metal template. Chapter 2 will discuss previous explorations in this field, highlighting areas of weaknesses with proposed methods to circumvent these issues. Chapters 3 and 4 will explore these developments in the area of metal-templated intramolecular radical cyclization. Finally Chapter 5 will discuss metal-templated intermolecular radical reactions.

Chapter 2: Background – Titanacyclobutenes *via* radical methodology

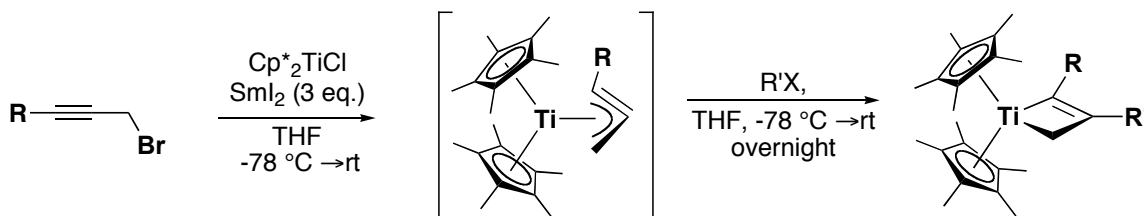
2.1 Introduction

The previous chapter dealt with the cyclization of organic radical intermediates formed by the reaction of an organic substrate with an odd-electron species, such as tributyltin radical. The ensuing cyclic radical intermediate then gives the product by abstracting either hydrogen or halogen atom or participating in further reaction, such as transannulation. The methodology developed in the Stryker lab for ring synthesis (including some macrocycles) that will be presented here is quite different. Namely, the reaction is complete after cyclization; there is no need for a hydrogen or halogen atom source because the product of cyclization is a closed-shell species. This is the result of a formal radical-radical annihilation in the ring-forming step. This also has logistical benefits; unlike tributyltin-mediated radical cyclizations, syringe-pump addition of reagents are not required. Furthermore, the methodology makes use of a transition metal, which is incorporated into the final product, thus expanding the potential reactivity profile for the functionalized compound. Key disadvantages, however, include the need for stoichiometric quantities of both transition-metal starting material and external reductant/radical generator.

2.2 Titanacyclobutenes from intermolecular radical addition

This novel ring-forming methodology is based on published work of titanacyclobutane⁶⁰ and titanacyclobutene⁶¹ synthesis from this group. In 1998, Ogoshi and Stryker found that organic free radicals add to the central carbon of η^3 -propargyltitanium(III)⁶² complexes to give titanacyclobutenes in excellent yield (Scheme 2.1). The organic radicals are generated using the one-electron reductant, samarium diiodide.⁶³ Recently, a small library of titanacyclobutenes, employing the unsubstituted titanocene reagent, has been reported.⁶⁴

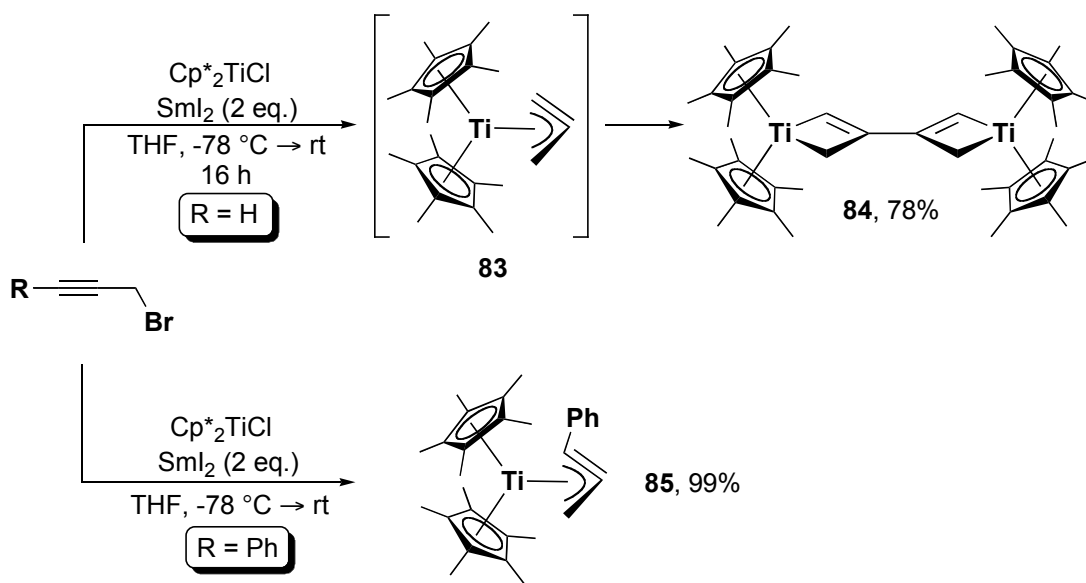
Scheme 2.1



Entry	R	R'X	Yield
1	H	PhCH ₂ Cl	94%
2	Me	PhC≡CCH ₂ Br	99%
3	Me	PhCH ₂ Cl	99%
4	Me	ⁱ PrI	99%
5	Ph	PhC≡CCH ₂ Br	93%
6	Ph	PhCH ₂ Cl	87%
7	Ph	ⁱ PrI	99%

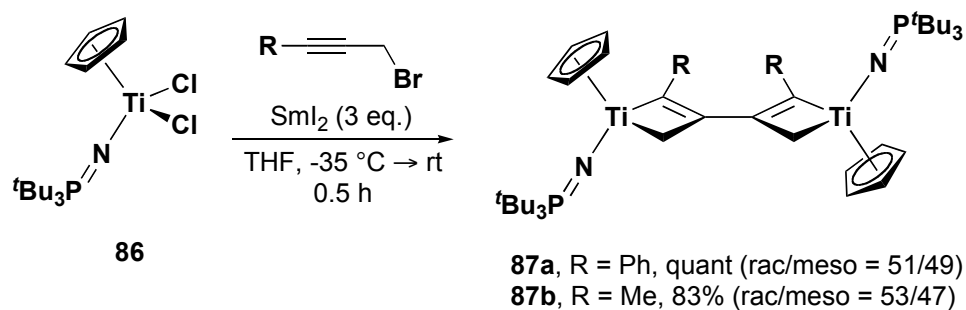
Although generally formed *in situ*, some of the intermediate η^3 -propargyltitanium(III) complexes can be isolated in very good yield (R = Ph, Scheme 2.2). The exception, however, is the unsubstituted propargyl complex (R = H), which dimerizes in solution to give di(titanacyclobutene) dimer **84**, presumably from central-carbon radical-radical combination of the propargyl moieties.

Scheme 2.2



In previous work, dimerization was not observed in the bis(cyclopentadienyl) titanocene series, which was attributed to a decreased in electron donating ability compared to the more electron-rich alkyl substituted ancillary ligands. However, Morita showed that the replacement of one of the cyclopentadienyl ligands with the strongly electron donating *tert*-butyl phosphinimide⁶⁵ ligand results in dimerization of the intermediate η^3 -propargyltitanium(III) complexes to give the α -methyl- and phenyl-substituted dititanacyclobutenes (Equation 2.1).⁶⁶

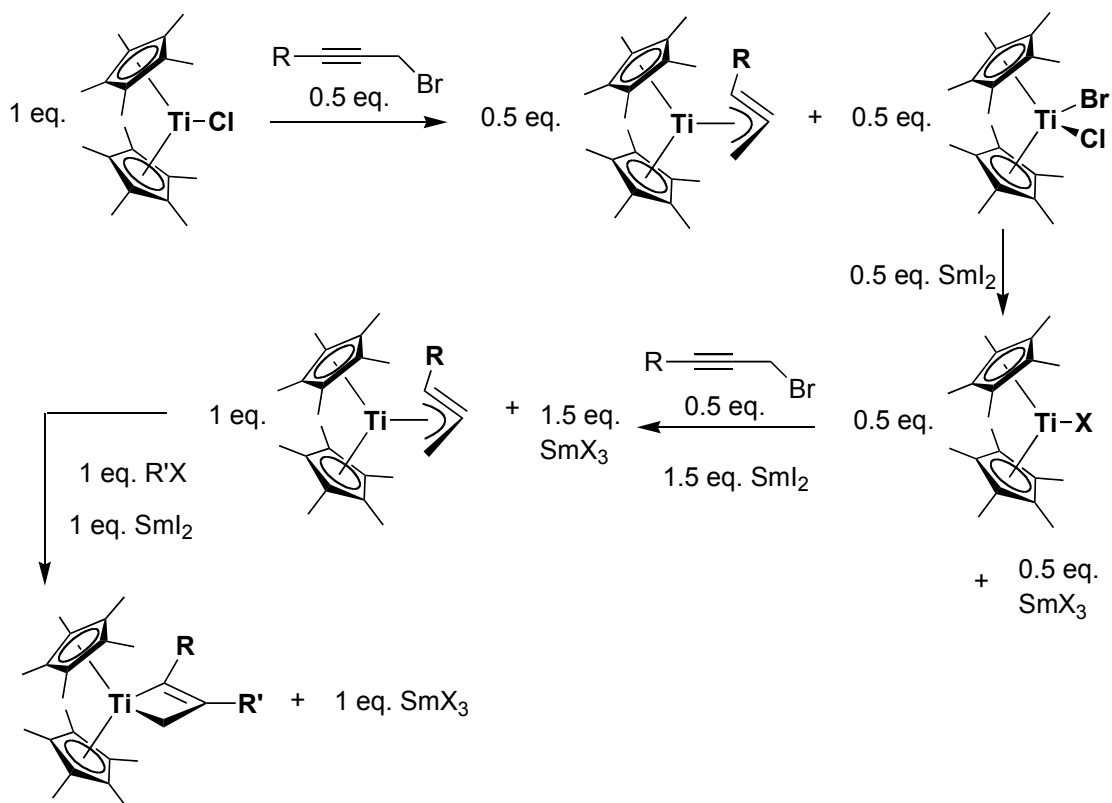
Equation 2.1



2.3 Mechanism and frontier orbital analysis

The proposed mechanism for titanacyclobutene formation is shown in Scheme 2.3.⁶¹ Abstraction of halogen atom by either the titanium or samarium species (or mediated by pre-coordination of the alkyne to titanium in concert with samarium acting as the reducing agent) results in the formation of a titanium(IV) dihalide and a η^3 -propargyltitanium(III) complex. The d^0 complex can be reduced by an equivalent of samarium diiodide to regenerate the titanium(III) halide. An organic radical (formed by halide abstraction by samarium diiodide or titanium(III)) then adds to the central carbon of the titanium(III) complex resulting in the titanacyclobutene product.

Scheme 2.3



The regioselectivity of attack at the central carbon can be understood by examining the frontier molecular orbital diagram of the η^3 -propargyltitanium(III) complex. (Figure 2.1).⁶⁷ Combining orbitals of proper symmetry from the titanocene cation and propargyl anion fragments leads to the frontier atomic orbitals of the propargyl complex. The singly-occupied molecular orbital (SOMO) has significant metal-character and therefore kinetic attack at the metal by an incoming organic radical is anticipated. However, titanium is a small atom and is sterically shielded by the cyclopentadienyl ligands, therefore, the alternative attack is at the central carbon of the propargyl ligand, due its contribution to the SOMO.

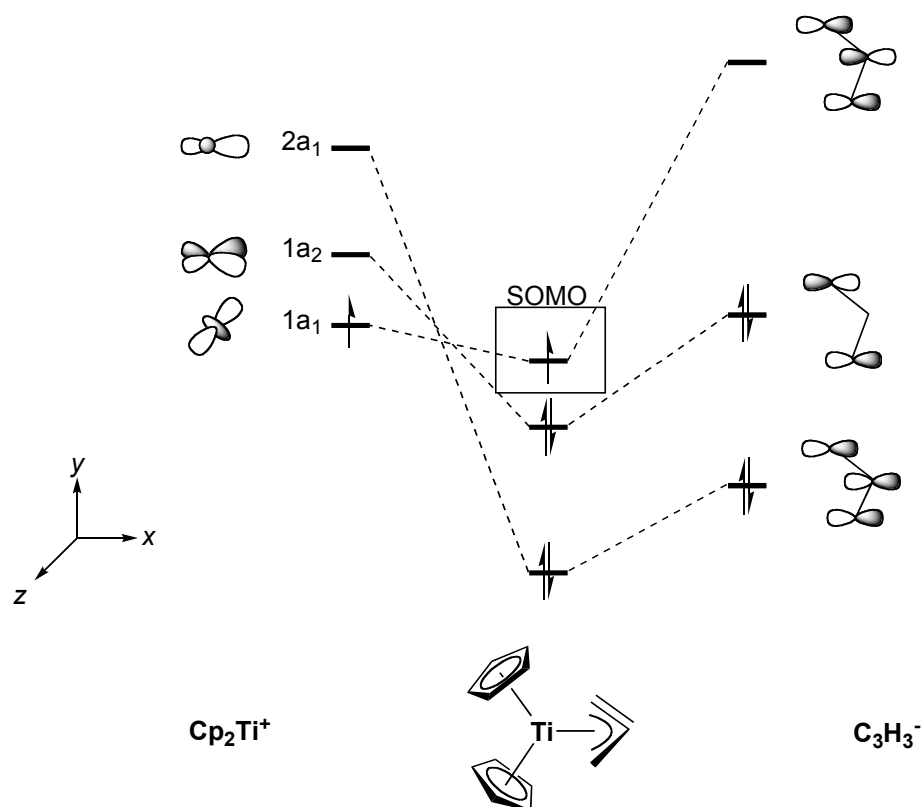
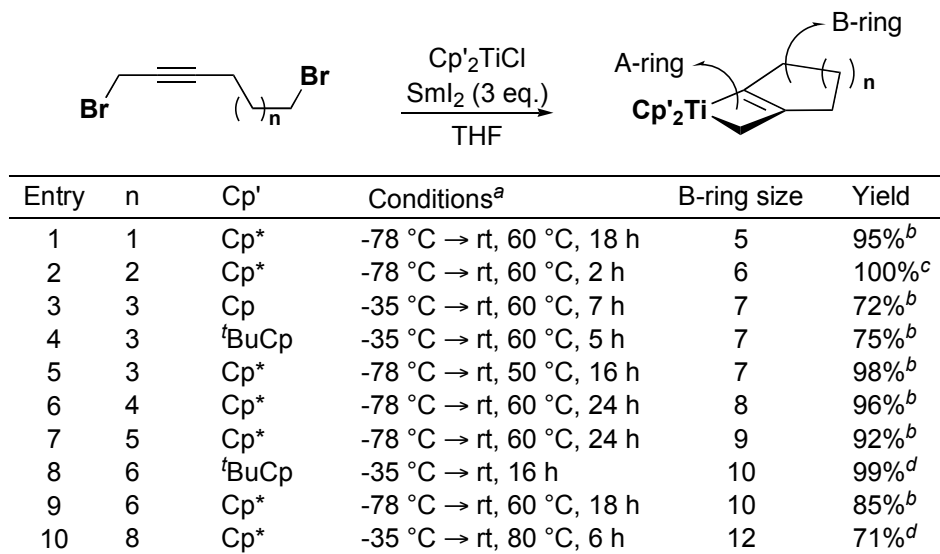


Figure 2.1: Walsh diagram of η^3 -propargyltitanium(III) complex

2.4 Bicyclic titanacyclobutenes from intramolecular radical addition

The intermolecular addition of free radicals to η^3 -propargyltitanium(III) complexes was adapted to the intramolecular variant. Thus, using the unsubstituted, *tert*-butyl-substituted and pentamethyl-substituted cyclopentadienyl ancillary ligands, an array of bicyclic titanacyclobutenes were prepared *via* central-carbon radical addition of titanium-propargyl generated from α,ω -alkylpropargyl dibromides (Scheme 2.4).^{61,68} The scope is general, forming appended fused rings sizes from five to, perhaps, twelve. The yields, although reported good to excellent, should be taken with caution as isolation of pure material is seldom achieved. This is because the bicyclic titanacycles are very lipophilic and often are isolated as oils. As such, they are difficult to purify and therefore most characterization data excludes elemental analysis. The NMR spectra of the larger bicycles are broad, making these analyses limited. However, this broad range of attainable ring sizes is limited to the substituted ancillary ligands; the unsubstituted

Scheme 2.4



^a Cp'₂TiCl and Sml₂ combined prior to addition of substrate

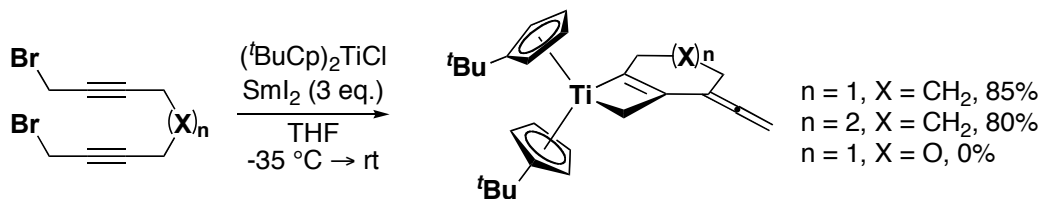
^b Reference 68a; ^c Reference 61; ^d Reference 68b

cyclopentadienyl titanocene reagent does not allow access to B-ring sizes greater than seven. The absence of cyclization can be attributed to both electronic and steric factors. Electronically, alkyl substitution increases the electron density of the cyclopentadienyl ligands, which is partially donated to the metal centre. This in turn, increases the SOMO character of the propargyl ligand central-carbon, facilitating radical attack at that position. Sterically, substitution increases the bulk of the ligand and therefore, reduces the conformational flexibility of the appended radical tether, increasing the probability of radical addition to the central carbon of the propargyl ligand. This is not unlike the templating effects discussed with the purely organic radical cyclizations and may be categorized as organometallic Thorpe-Ingold effect.⁶⁹ Therefore, the less bulky, less electron-rich unsubstituted cyclopentadienyl ligands lead to a decreased rate of radical cyclization, allowing competing intermolecular and decomposition pathways to dominate. Titanacyclobutane synthesis to yield bicyclic rings was found to be very limited in ring-size scope, even with the pentamethylcyclopentadienyl ligands.^{68a,70}

The intramolecular central-carbon radical alkylation methodology was further applied to more elaborate organic substrates. With more functionality incorporated into the organic substrate, the synthetic utility of the product increases. Thus, by using bis-

propargyl bromide substrates, bis(*tert*-butylcyclopentadienyl)titanacyclobutene complexes were prepared with an allenyl functional group incorporated into the B-ring (Equation 2.2).^{68b} Although the yields of the bicyclic titanacycles were good, the scope

Equation 2.2

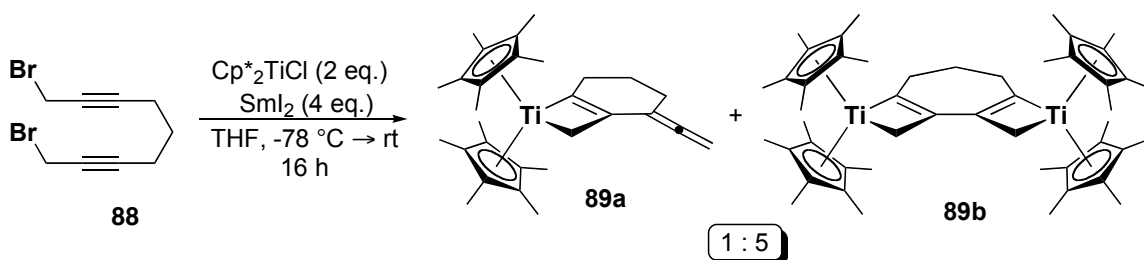


was limited to the formation of six- and seven-membered B-rings and only with the *tert*-butyl- and pentamethylcyclopentadienyl ligands. An attempt to prepare the eight-membered analogue failed. The five-membered B-ring titanacyclobutene, although claimed,^{68b} is suspect as the spectroscopy is both incomplete and inconsistent with the proposed product. One attempted synthesis of a titanacyclobutene containing a heteroatom ($X = \text{O}$) substituted into the B-ring failed.

2.5 Di(titanacyclobutenes) via propargyl-propargyl radical coupling

When the electron-rich pentamethylcyclopentadienyl ancillary ligands are used, η^3 -propargyltitanium(III) dimerization is observed in competition with intramolecular cyclization (Equation 2.3).^{68b} The formation of the tricyclic di(titanacyclobutene) **89b** is

Equation 2.3

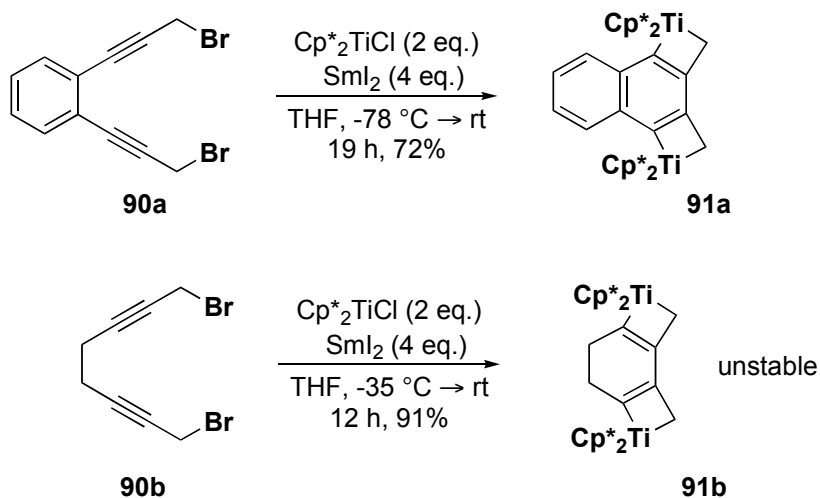


favoured under conditions where excess titanium and samarium diiodide are present. Under similar reaction conditions in the presence of four equivalents of titanocene reagent and six equivalents of samarium diiodide, the tricyclic complex **89b** is the sole

titanium product in 77% yield. Increasing the initial reaction temperature from -78 °C to -35 °C decreases the ratio of di- to mono-titanacyclobutene.

By using an aromatic template to anchor two propargyl bromides close to each other, (**90a**, Scheme 2.5) access to a naphthalene substituted di(titanacyclobutene) **91a** could be achieved in good yield.⁶¹ This is contrasted against the parent bis-propargyl bromide substrate **91a** where under similar reaction conditions, the isolated dititanacyclobutene proved to be unstable in solution even at -35 °C.^{68b} The nature of the stability of **91a** compared to the instability of **91b** is unknown but the aromatic nature of the former may play an important role.

Scheme 2.5



2.6 Conclusion

Intramolecular radical cyclization *via* the intermediate η^3 -propargyltitanium(III) template has been shown to furnish bicyclic titanacyclobutenes from propargyl halide precursors. However, just as this method has advantages with regard to classic radical cyclization, the drawbacks regarding this radical ring-forming methodology remain numerous:

- The necessity of using a substituted titanocene strating material. These are more cumbersome to prepare (and more expensive) than titanocene monochloride, which is readily achieved by reduction of the commercially available titanocene dichloride.

- Limited functionality scope. Allene is the only successful functional group that has been incorporated into B-ring bicyclic titanacyclobutenes. Previous attempts to include an oxygen atom have failed.
- Maximum B-ring size of twelve. Even with the η^3 -propargyltitanium(III) template, the flexibility of the α,ω -alkylpropargyl dibromides do not allow the formation of very large rings. This can be attributed directly to a decrease in the rate of organic free radical addition to the η^3 -propargyl intermediate with an increase in the tether length.

Chapter 3: Bicyclic titanacyclobutenes from α,ω -alkylpropargyl dibromide malonates

3.1 Introduction

To access macrocycles *via* radical cyclization, any means that reduce the activation energy for the reaction will increase the rate of radical cyclization. The bicyclic titanacyclobutene syntheses described in Chapter 2, impose conformational restriction by means of an intermediate η^3 -propargyltitanium(III) template. This allows for the formation of up to twelve-membered macrocycles, at least using the bulky pentamethylcyclopentadienyl ligands to assist sterically and electronically. To access these and even larger macrocycles using this free radical methodology, further enhancement of the templating-effect is required.

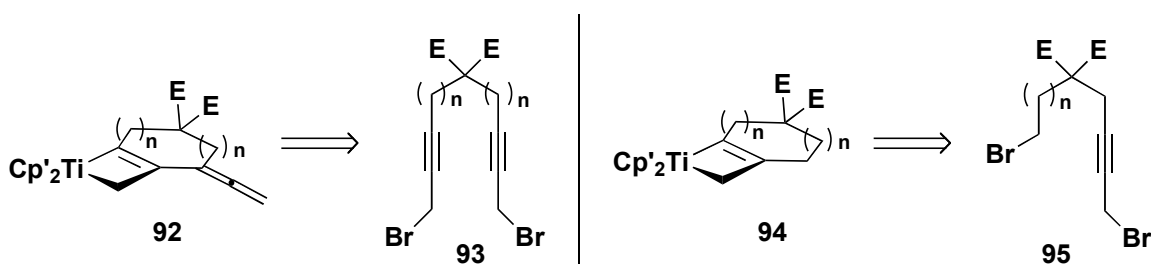
Installation of a *gem*-diester group into the organic substrate accomplishes this through a Thorpe-Ingold effect.⁶⁹ The term “Thorpe-Ingold” is used loosely as this specifically infers to the enhanced rate of ring closure due to a decreased internal angle at the site of *gem*-substitution, the latter caused by steric compression. It has been argued that although steric compression is important when considering small ring formation, the small change in bond angle does not account for the significant rate enhancements for large ring cyclizations.⁷¹ Although it may be more appropriate to refer to the ring closure acceleration phenomenon as the *gem*-dialkyl effect, the Thorpe-Ingold effect is important in a historical context and therefore this term will be used. While not causing significant steric compression, *gem*-disubstitution reduces the number of low-energy conformers of the radical intermediate compared to the unsubstituted analogue. This, in turn, reduces the number of unproductive rotamers (those which do not lead to cyclization) and thus will increase the rate of cyclization. The inclusion of *gem*-diester functionality also has synthetic benefits, increasing the utility of the bicyclic titanacyclobutene product for further chemical manipulation.

Considering the main function of the *gem*-diester group is to create a sterically-sensitive environment, a di-*tert*-butyl malonate derivative was preferred in the organic substrate, for two reasons: 1) The *tert*-butyl esters are sterically bulkier than the more commonly used methyl and ethyl esters and 2) the unit incorporates a better

spectroscopic handle. In the ^1H NMR spectrum, in the absence of a stereogenic centre, the *tert*-butyl groups appear as an eighteen hydrogen singlet. This serves as a quick indicator to the number of products containing the *tert*-butyl group, should mixtures arise. Non- C_2 symmetric diethylmalonate derivatives will necessarily have diastereotopic methylene groups, even if the molecule is achiral, while the methyl signals that appear sufficiently upfield might be obscured by other aliphatic hydrogen signals. Although most of the substrates were synthesized using di-*tert*-butyl malonate as the starting material, some were prepared using the readily available (and much less expensive) diethylmalonate.

The titanacyclobutene structural classes synthesized from the *gem*-diester-bearing substrates are shown in Scheme 3.1. Both the allenyl- (92) and non-allenyl (94) titanacyclobutenes generated from bis- and mono-propargyl dibromides, 93 and 95, respectively are desired to demonstrate generality and compatibility of the potentially reactive ester functionality.

Scheme 3.1



3.2 Project goals

The goals of this project were initially set to address some of the issues surrounding previous titanacyclobutene syntheses. Issues surrounding macrocyclizations could be investigated by the inclusion of a *gem*-diester group into the organic substrates. A second goal is to expand the scope of organic radicals used for central-carbon alkylation of η^3 -propargyltitanium(III) complexes. By using electrophilic one-electron reductants and epoxides, the intermediate β -alkoxy alkyl radical would lead to titanacyclobutene complexes with oxygen functionality substituted in the addend. These

explorations should increase the synthetic utility of titanacyclobutenes in particular for large-ring formation.

3.3 Results: α,ω -alkylpropargyl dibromide substrate synthesis

3.3.1 Introduction

The maximum B-ring size claimed from titanium-induced radical cyclization of α,ω -alkylpropargyl dibromide substrates is twelve (Entry **X**, Scheme **X**). Therefore, it seemed reasonable to construct the analogous substrate containing the *gem*-diester group. This allows a direct comparison to be made to confirm whether indeed the *gem*-disubstitution provides a substantial Thorpe-Ingold effect and whether the presence of the oxygen-containing functional groups proves to be compatible with the reaction conditions. Also of interest are titanacyclobutenes containing a six-membered B-ring since six-membered rings are commonly encountered in organic synthesis. In the titanium-mediated intramolecular radical cyclization chemistry developed in the Stryker group, only radicals derived from primary halides have been previously used for the addition to the η^3 -propargyltitanium(III) intermediate. Therefore, secondary and tertiary halide-containing substrates were considered important to probe how the alkyl radical stability and substitution affect the radical cyclization step. The targeted α -propargyl- ω -bromoalkyl compounds **96-100** are summarized in Figure **3.1**.

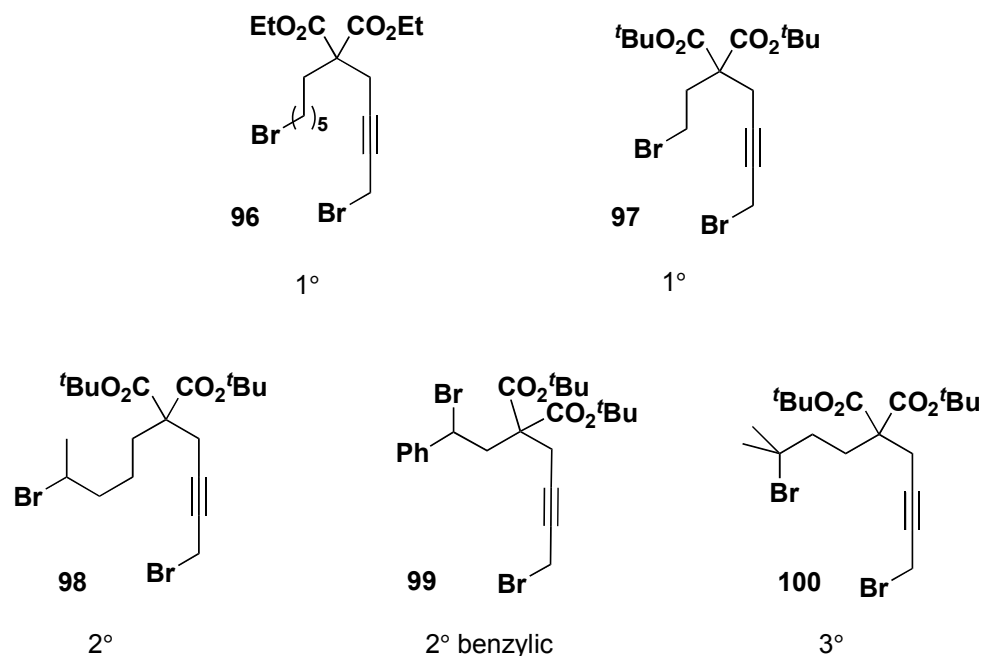
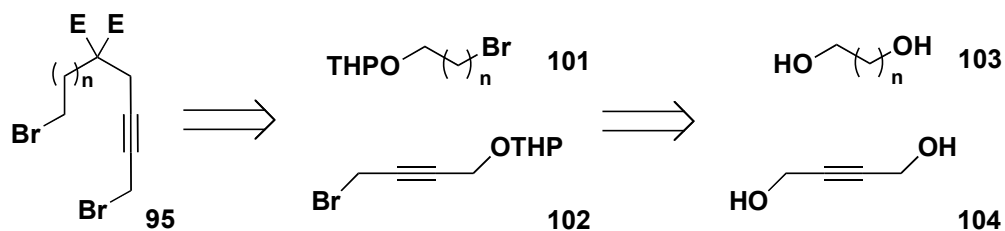


Figure 3.1: Target α,ω -alkylpropargyl dibromomalonates

To synthesize α,ω -alkylpropargyl dibromide compounds containing *gem*-di-ester functionality, the retrosynthetic analysis envisioned was straightforward, as shown in Scheme 3.2. α,ω -alkylpropargyl dibromide esters of the type **95** are made from two consecutive alkylations using bromides **101** and **102**. Each of these bromides is synthesized from THP-protection and bromination of readily available diols, **103** and **104**, respectively.

Scheme 3.2

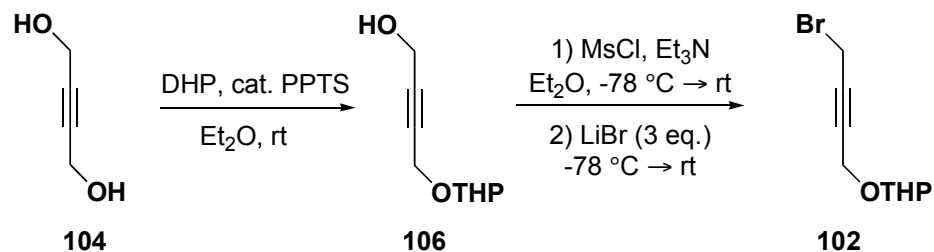


3.3.2 Synthesis of organic substrates bearing a primary halide

To synthesize a 12-membered B-ring titanacyclobutene, the appropriate value of n for the primary halide alkylating agent **101** is five. Therefore, 2-(6-bromohexyloxy)-tetrahydro-2*H*-pyran (**105**) was prepared, following the procedure reported by Godfroid *et al.*⁷² mono-bromination of 1,6-hexanediol using aqueous hydrobromic acid followed by protection of the alcohol with dihydropyran catalyzed by concentrated hydrochloric acid.

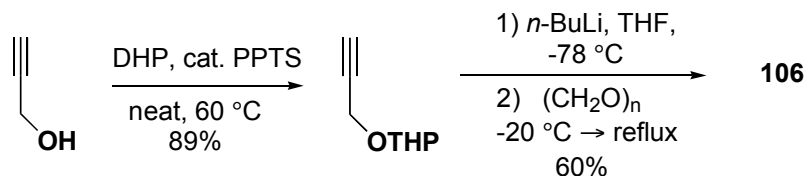
The THP-protected butynyl bromide **102**⁷³ was synthesized by non-selective mono-protection of 2-butyne-1,4-diol with dihydropyran and catalytic *para*-toluenesulfonic acid (PPTS) followed by bromination of the propargylic alcohol *via* mesylation and displacement with excess lithium bromide (Scheme 3.3). Although this

Scheme 3.3



synthetic route does furnish the desired compound, there is a drawback associated with the protection step. Isolation of pure alcohol **106** on large-scale proved to be difficult. Vacuum distillation is not efficient as the starting diol, product, and doubly THP-protected side product distill at very similar temperatures. Column chromatography does provide separation but is quite inconvenient when purifying tens of grams of material. Another approach was taken to circumvent this problem (Scheme 3.4). Protection of propargyl alcohol⁷⁴ was accomplished in high yield followed by addition of the corresponding lithium acetylide to excess paraformaldehyde.⁷⁵ This is a much more efficient route to alcohol **106** as simple distillation can be used for purification.

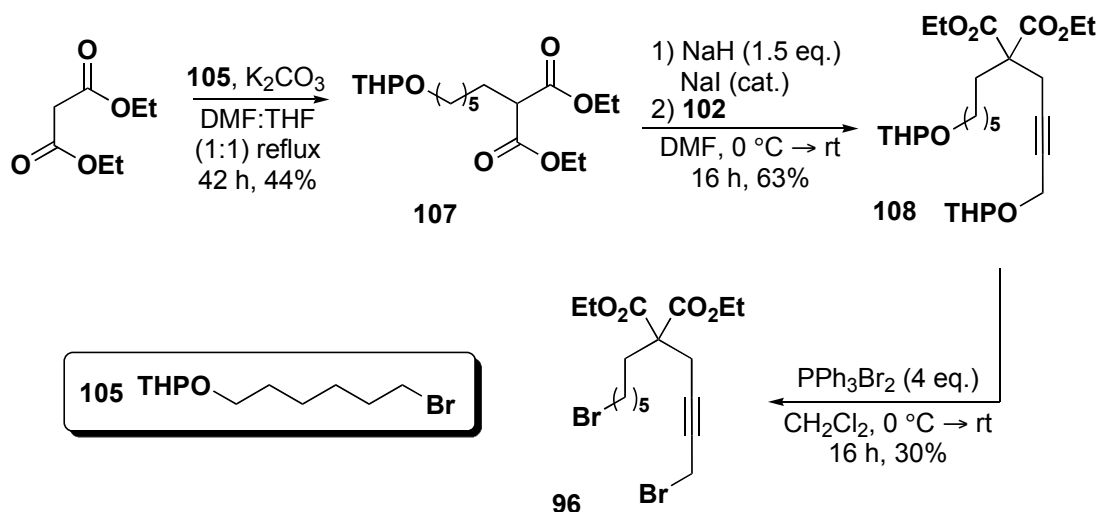
Scheme 3.4



Alkylation of the saturated alkylbromide **105** was performed first (Scheme 3.5). This was selected because alkylation of a propargylic bromide by a bulky mono-substituted malonate anion occurs more readily than that of an unactivated primary bromide, without the possibility of competitive elimination. Thus, following a literature procedure, a THF/DMF solution of bromide **105** was added to diethylmalonate and a stoichiometric amount of potassium carbonate.⁷⁶ After workup and vacuum distillation, the previously reported monoalkylated product **107** was isolated in 44% yield. The second alkylation was carried out under milder conditions using propargyl bromide **102**, affording the disubstituted malonate derivative **108** in 63% yield. Finally, a one-pot

and

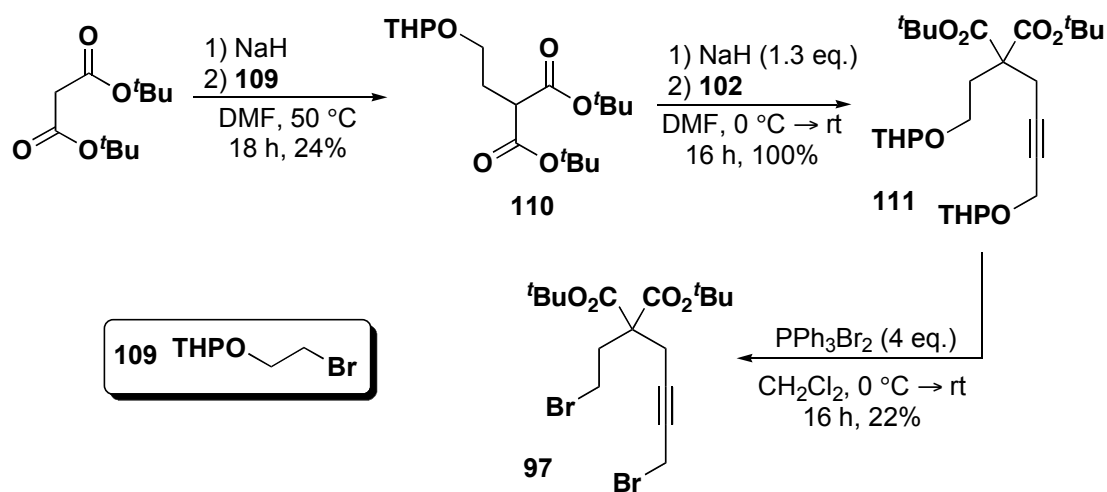
Scheme 3.5



bromination was conducted using two equivalents of triphenylphosphine dibromide,⁷⁶ leading to the α,ω -alkylpropargyl dibromide **109** in 30% yield.

The shorter chain analogue of **97** was synthesized using di-*tert*-butyl malonate as the starting material (Scheme 3.6). Thus, the first alkylation step using THP-protected bromoethanol **109**,⁷⁷ afforded the monoalkylated malonate **110**. Alkylation using propargyl halide **102** under mild conditions gave a quantitative yield of dialkylated malonate **111** with no need for formal purification. One-step deprotection and bromination with triphenylphosphine dibromide provided the dibromide **97** as a white solid in a poor 22% yield.

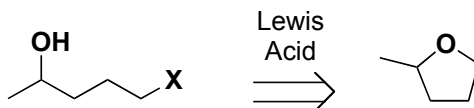
Scheme 3.6



3.3.3 Synthesis of organic substrates bearing a secondary or tertiary halide

To synthesize the necessary alkylating agent for the secondary halide substrate, attention was turned to ring opening of 2-methyltetrahydrofuran induced by Lewis acids such as (MeO)₂BBr⁷⁸, BF₃•Et₂O,⁷⁹ and AlCl₃ (Equation 3.1).⁸⁰ However, some of these

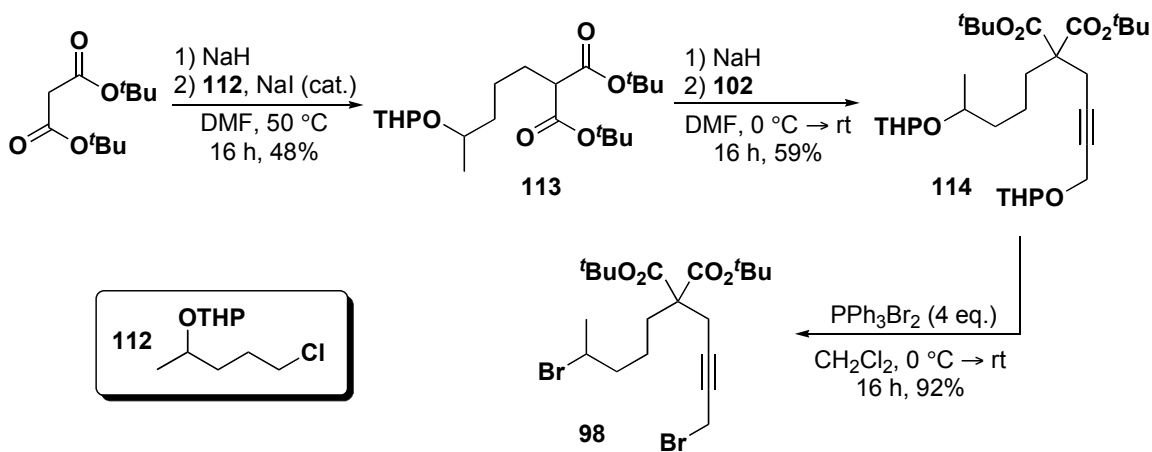
Equation 3.1



methods are inconvenient. The boron reagent, (MeO)₂BBr, is prepared *in situ* from (MeO)₃B and hazardous BBr₃. The preparation to make the iodoalcohol using aluminum

trichloride is not atom economical in the least: five equivalents of both the aluminum reagent and sodium iodide are required for good yields. The reaction was instead accomplished by using stoichiometric trimethylsilyl chloride and sodium iodide.⁸¹ The reaction proceeded smoothly to give 5-iodo-2-pentanol in very good yield, requiring no purification. However, the thermal instability of this compound was quite evident. Attempted protection of the alcohol with dihydropyran and catalytic hydrochloric acid gave a dark-brown crude product mixture, which upon distillation or column chromatography resulted only in decomposition. The compound was finally synthesized by sodium borohydride reduction of commercial 5-chloro-2-pentanone⁸² followed by the standard THP protection of the alcohol to give the alkylating agent **112** as a mixture of diastereomers. Alkylation of the chloride **112** using di-*tert*-butyl malonate gave 48% yield of the mono-alkylated product **113** as a mixture of diastereomers (Scheme 3.7).

Scheme 3.7

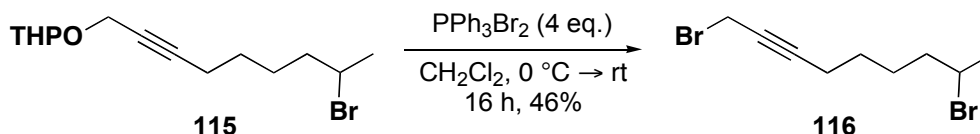


The second alkylation step with propargylic bromide **102** proceeded to give the doubly-protected malonate derivative **114**, which was then converted under standard bromination conditions to afford dibromide **98** in a pleasing 92% yield. The reason for the superior yield compared to the other bromination steps performed (Schemes 3.5 and 3.6) is probably more a function of the experimenter than of the substrate itself.

An α,ω -alkylpropargyl dibromide substrate without the appended *gem*-diester group was prepared for comparison. Fortunately, the immediate precursor **115** had been

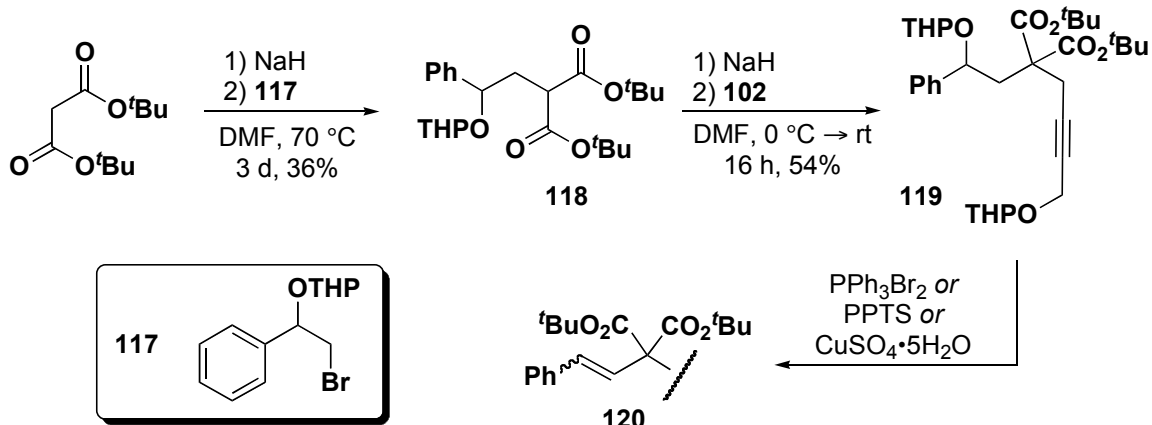
synthesized by a previous member of the group.⁸³ Thus, alkynyl bromide **115** was subjected to the bromination conditions to furnish the secondary bromide **116** in modest yield (Equation 3.2).

Equation 3.2



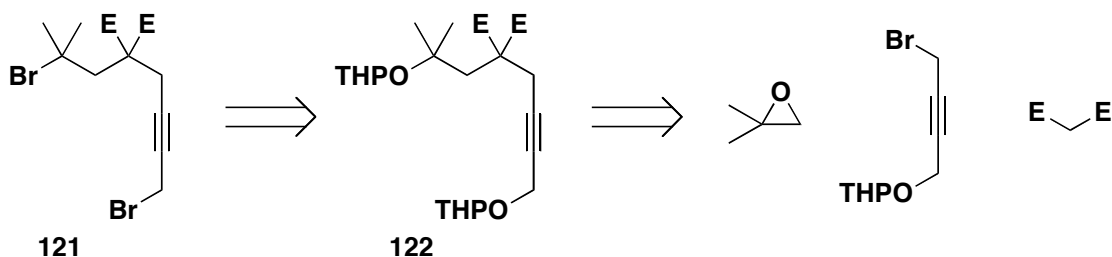
The synthesis of benzylic halide analogue of **98** was attempted by initial alkylation of di-*tert*-butyl malonate with benzylic bromide **117**,⁸⁴ which was prepared by hydrobromination of styrene with NBS in water, followed by THP-protection.⁸⁵ (Scheme 3.8). Harsh conditions are required for the reaction to proceed, probably due to the steric hinderance of the THP and phenyl groups. Unfortunately, the harsh conditions also results in competitive E_2 -elimination of the bromide, producing 2-(1-phenylvinyl)oxy)-tetrahydro-2*H*-pyran as the side product. This was followed by a second alkylation step with propargylic bromide **102** to furnish the ester derivative **119** in modest yield. The usual one-pot deprotection and bromination with triphenylphosphine dibromide failed, however, resulting exclusively in elimination to give the styrenyl malonate derivative (**120**). Attempts to deprotect the acetal with catalytic PPTS or catalytic cupric sulfate pentahydrate⁸⁶ also resulted in the formation of the unsaturated elimination product, along with other decomposition products.

Scheme 3.8



Despite the instability of the benzylic halide derivative, the analogous compound containing a tertiary halide was targeted based on the following retrosynthetic analysis (Scheme 3.9). Tertiary halide **121** could, in principle, be made from bromination of the THP-protected alcohol **122**, which in turn could be synthesized from ring-opening of isobutylene oxide using the appropriate malonate anion.

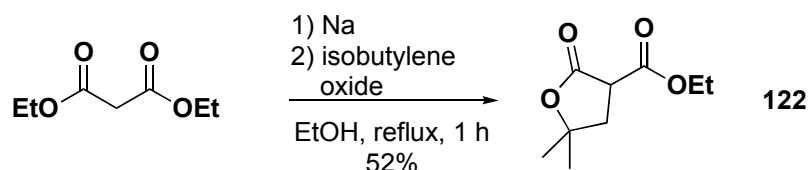
Scheme 3.9



All attempts to synthesize tertiary alcohols *via* this method failed. The reaction between sodium diethylmalonate and isobutylene oxide leads to γ -lactone **122**⁸⁷ in modest yield (Equation 3.3). The reactions between epoxides such as oxirane and cyclohexene oxide with malonate anions also form γ -lactones under alkylation conditions.⁸⁸ An exception to this was observed with cyclopentene oxide, which does not lactonize and good yields of the *trans* secondary alcohol are obtained. The reason for this is attributed to the high level of strain that would be present in the ring system with two

five-membered fused rings in a *trans*-relationship. The *gem*-dimethyl and *gem*-diester groups in the formation of **122** presumably both increase the rate of lactonization through the restricted rotamer effect and provide stability to the five-membered ring. Under hydrolysis conditions, an increase in the number of substituents on a γ -butyrolactone results in the equilibrium shifted toward to the cyclic form.⁸⁹ The analogous reaction

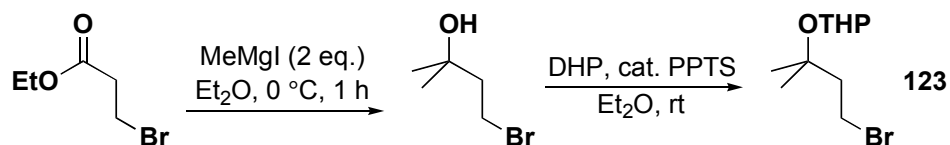
Equation 3.3



with di-*tert*-butyl malonate only gave a small amount of the lactone with unreacted malonate recovered. The slow alkylation and lactonization in this case could be attributed to the bulky *tert*-butyl groups sterically hindering the approach of the congested disubstituted epoxide.

The tertiary alkylating agent **123** was finally realized by a β -bromoester-derived tertiary alcohol (Scheme 3.10). The compound was synthesized by addition of two equivalents of methyl Grignard to ethyl 3-bromopropanoate⁹⁰ followed by protection of the alcohol as the tetrahydropyranyl acetal.⁹¹

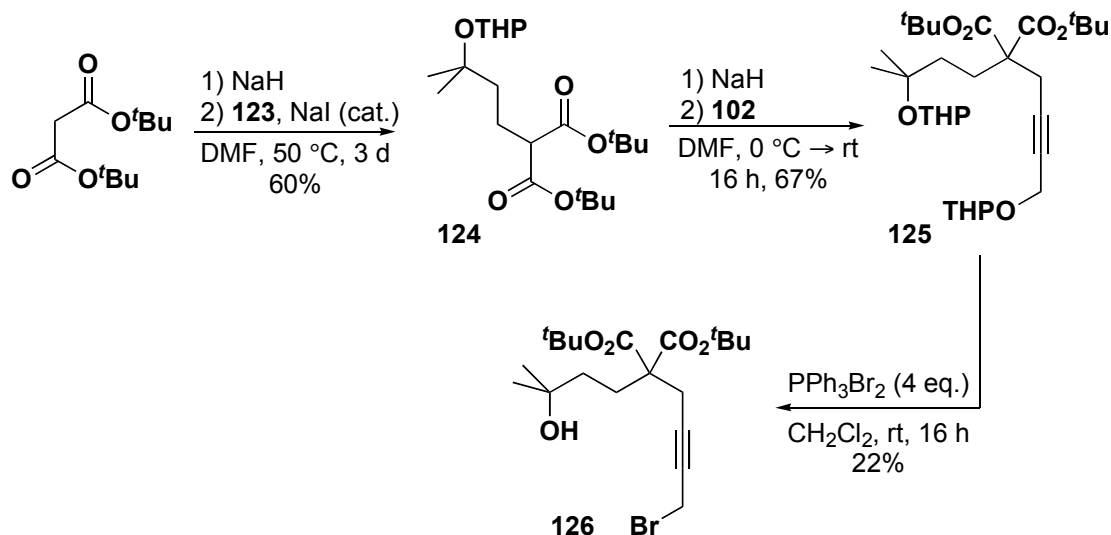
Scheme 3.10



The first alkylation step using this reagent proceeded to the desired malonate derivative **124** (Scheme 3.11). Forcing reaction conditions reflect the hindered approach for nucleophilic substitution. The butynyl unit was then installed to give the halide

precursor **125** in a respectable overall yield. An attempt to use the one-pot deprotection and bromination protocol using triphenylphosphine dibromide again failed, giving instead α -bromo- ω -alcohol **126**, which was isolated in poor yield. Indeed, Mioskowski, *et al.*, note

Scheme 3.11



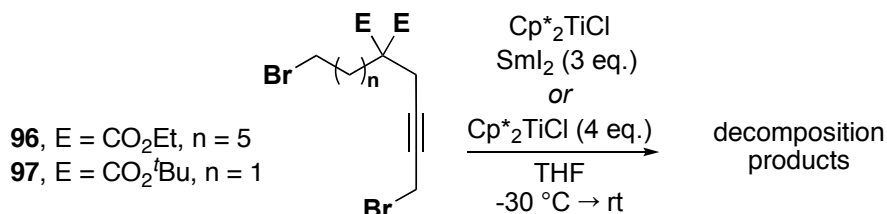
that the use of triphenylphosphine dibromide at low temperature is effective at hydrolyzing acetals at secondary or tertiary centres to their corresponding alcohols.⁹² At slightly higher temperature, the former are transformed into bromides whereas the latter remain as the alcohol, presumably from the difficulty of S_N2 displacement of the pentavalent phosphorus species by the bromide anion. In hindsight, a more reasonable approach to the dibromide may have been acetal deprotection with pyridinium *para*-toluenesulfonate followed by bromination with phosphorus tribromide under buffered conditions.

3.4 Results: Intramolecular addition of radicals to η^3 -propargyltitanium(III) complexes

3.4.1 Intramolecular addition with primary radicals

The primary α,ω -dibromides **96** and **97** were subjected to standard conditions for titanium-mediated radical cyclization. Thus, each dibromide **96** and **97** was combined with bis(pentamethylcyclopentadienyl)titanium chloride and samarium diiodide at low temperature (Equation 3.4). The colour of each reaction mixture eventually changed from dark-blue to red, accompanied by a yellow precipitate. Trituration of the crude residue with hexanes provided a dark-red oil; ^1H NMR spectroscopy, however, showed only decomposition products. The same results were obtained when all of the samarium

Equation 3.4

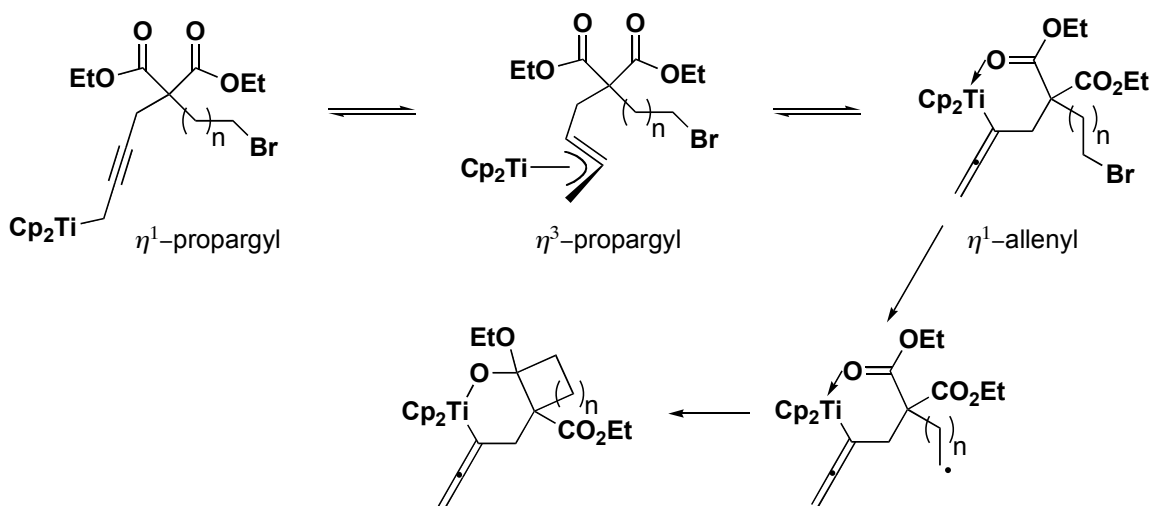


diodide was replaced by bis(pentamethylcyclopentadienyl)titanium chloride as the reductant. The reactions of the unsubstituted and 1,1'-bis(*tert*-butyl)-substituted titanocene monochlorides with the same substrates also fail.

These results contrast dramatically with those obtained from the ester-free substrates for which the synthesis of the twelve-membered bicyclic titanacyclobutene complex was possible (Scheme 2.4). The geminal di-ester moiety must be responsible for the lack of controlled reactivity. It is clear that whatever the diversive pathway(s) are, the reactions must be quite rapid, since even the six-membered ring cyclization product, from substrate **97**, is inaccessible. Decomposition of the titanacyclobutene product induced *intermolecularly* by the esters is ruled out by control reactions. One possible rationalization arises from the functional array present in the propargyltitanium intermediate. The propargyl ligand bound to the titanium(III) centre has three possible hapticities: η^3 -propargyl, η^1 -allenyl and η^1 -propargyl (Scheme 3.12). Both the η^1 -allenyl and η^1 -propargyl complexes leave an open coordination site on the metal centre. The former can coordinate to the oxophilic titanium centre *via* the lone pair on the carbonyl

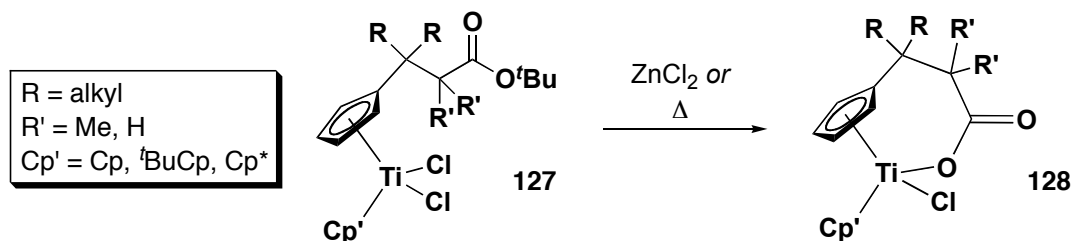
oxygen, forming a six-membered ring chelate. This favourable interaction decreases the population of the η^3 -propargyl form, the only tautomer that leads to free radical alkylation at the propargyl central carbon. There may be some precedent for this

Scheme 3.12



proposed binding; Gansäuer, *et al.*, recently provided a modular synthetic route to prepare substituted titanocenes, with one of the key steps in the synthesis involving an ester cleavage.⁹³ The cleavage of *tert*-butyl ester in titanocenedichloride complex **127** is promoted by the titanium itself, added ZnCl_2 , or heating in toluene (Equation 3.5). Alternatively, an intramolecular samarium-mediated Barbier reaction may take place between the primary halide and the ester.⁹⁴ Another possibility is radical addition to the ester. Although esters are considered inert toward radical addition, Fernández-Mateos, *et al.*, showed that intramolecular radical cyclization of α,ω -epoxyesters occurs in the presence of titanocene monochloride.⁹⁵

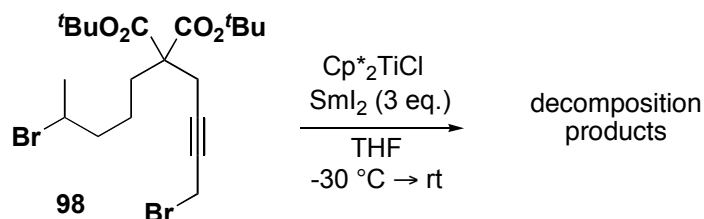
Equation 3.5



3.4.2 Intramolecular addition with secondary radicals

To increase the rate of cyclization, the nature of the radical used for the addition onto the η^3 -propargyltitanium(III) complex was changed. A more stabilized radical is expected to form more rapidly by reduction of the bromide with samarium diiodide and persists longer in solution. Thus, the secondary propargylic dibromide **98** was treated with bis(pentamethylcyclopentadienyl)titanium chloride and samarium diiodide, again resulting only in decomposition products (Equation 3.6). The failure to obtain controlled reactivity may also be the result of titanium-carbonyl binding and subsequent radical addition.

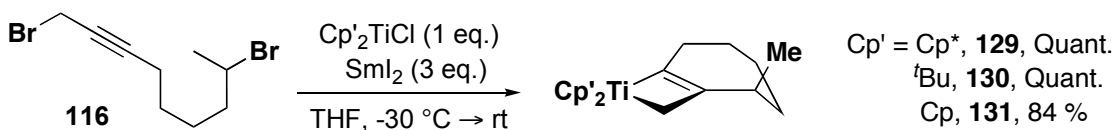
Equation 3.6



The only success obtained from this series of compounds came from a substrate lacking the *gem*-diester group. The secondary propargyl dibromide **116** reacts with the unsubstituted, the *tert*-butyl-substituted, and pentamethyl-substituted titanocene chlorides in the presence of samarium diiodide (Equation 3.7). Each of these reactions resulted in the formation of the seven-membered bicyclic titanacyclobutene complexes **129-131**, isolated as red oils or solids in good to quantitative yields. Spectroscopically, the reactions were clean, allowing complete characterization through NMR spectroscopy,

MS and IR spectroscopy. Elemental analysis of titanacyclobutene complex **131** provided the correct composition while titanacycles **129** and **130** could not be obtained in pure form.

Equation 3.7



The structures of titanacyclobutene complexes **129**, **130**, and **131** were confidently elucidated by NMR analysis. The unsubstituted titanacyclobutene complex **131** is a representative example (see Figure 3.2 for the atom numbering scheme). In the ¹H NMR spectrum, the chemically inequivalent cyclopentadienyl hydrogens (H_{10a,b}) appear as a singlet at δ 5.52 due to accidental overlap. The inequivalent α-methylene hydrogens (H_{8a,b}) on the titanacyclobutene moiety resonate at δ 3.44 and 3.19, respectively, and show relatively small geminal coupling ($J = 11.4$ Hz) and fine coupling ($J = 1.3$ - 3.0 Hz) through the alkene to only one of the allylic methylene protons (H_{6a}). These allylic protons are located at δ 2.56 and 2.41 and show a typical geminal coupling constant of 16 Hz as well as multiple couplings, most of which cannot be extracted from the complex and broadened multiplets. The methine proton (H₂) is found at δ 2.31 and is coupled to the neighbouring methylene (H₃) with both relatively large and small coupling constants ($J = 13.0$ and 3.6 Hz) consistent with the methine proton occupying a pseudo-axial position. Also coupled is the appended methyl group (H₉); a doublet ($J = 7.2$ Hz) upfield at δ 0.94. The remaining three methylene (H₃₋₅) groups located in the B-ring appear as complex multiplets between δ 1.63-1.37. The ¹³C NMR spectrum confirms the presence of a titanacyclobutene core by displaying characteristic resonances at δ 217.1, 95.0 and 80.1, corresponding to the α-*sp*² carbon, β-carbon, and α-*sp*³ carbon, respectively. These values are consistent with previously reported titanacyclobutene complexes.^{61,96} Although the ¹H NMR spectrum showed accidental overlap of the cyclopentadienyl ligands, in the carbon spectrum, each ligand appears separately, at δ 110.4 and 110.1 (C_{10a,b}). The rest of the assignments are based on two-dimensional NMR

techniques, HMQC and HMBC, which give direct ($^1J_{CH}$) and longer range ($^2J_{CH}$ and $^3J_{CH}$) hydrogen-carbon coupling information (Table 3.1). Single-crystals of titanacyclobutene complex **129** were obtained by recrystallization from pentane at -30 °C followed by X-ray crystallography to confirm the proposed structure (Figure 3.3).

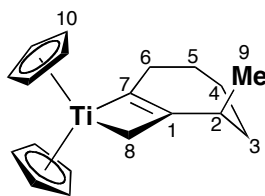


Figure 3.2: Carbon and hydrogen labelling scheme for bicyclic titanacyclobutene **131**

Table 3.1: ^1H and ^{13}C NMR assignments for bicyclic titanacyclobutene **131**

$^1\text{H}^a$	$^{13}\text{C}^b$
-	C ₁ , δ 95.0
H ₂ , δ 2.31 (dq, $J = 13.0$ Hz, $J = 7.2$ Hz, $J = 3.6$ Hz, 1H)	C ₂ , δ 36.8/36.9 ^c
H ₃ , δ 1.45 (m, 2H)	C ₃ , δ 34.1
H ₄ , δ 1.37 (m, 2H)	C ₄ , δ 28.8
H ₅ , δ 1.63 (m, 2H)	C ₅ , δ 26.4
H _{6a} , δ 2.56 (m, $J = 16.1$ Hz (d), 1H); H _{6b} , δ 2.41 (ddq, $J = 16.0$ Hz, $J = 10.2$ Hz, $J = 2.4$ Hz, 1H)	C ₆ , δ 36.8/36.9 ^c
-	C ₇ , δ 217.1
H _{8a} , δ 3.44 (br d, $J = 11.4$ Hz, 1H); H _{8b} , δ 3.19 (dt, $J = 11.4$ Hz, $J = 2.0$ Hz, 1H)	C ₈ , δ 80.1
H ₉ , δ 0.94 (d, $J = 7.2$ Hz, 3H)	C ₉ , δ 17.5
H _{10a} , δ 5.52 (s, 5H)	C _{10a} , δ 110.4
H _{10b} , δ 5.52 (s, 5H)	C _{10b} , δ 110.1

^a C₆D₆, 400 MHz; ^b C₆D₆, 100 MHz; ^c unable to resolve signals

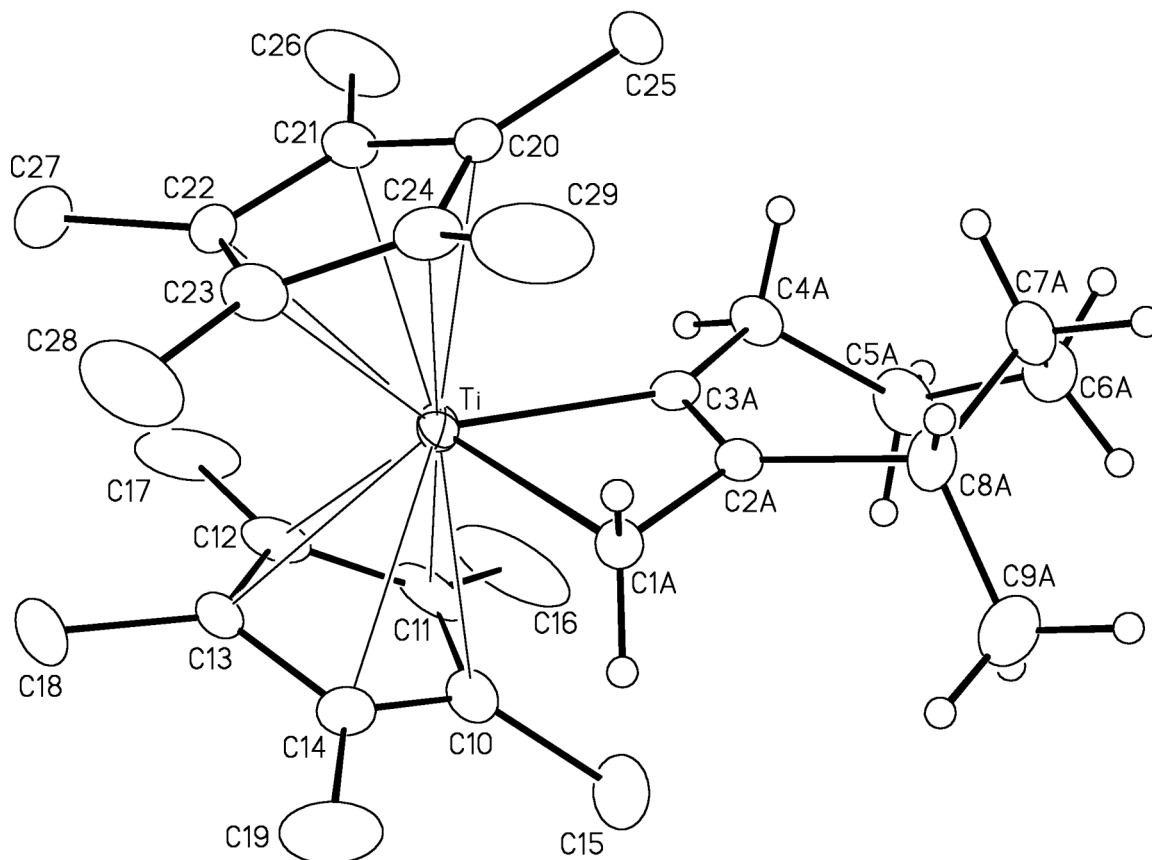


Figure 3.3: Perspective view of the $[\text{Cp}^*_2\text{Ti}(2\text{-methanidyl-3-methylcyclohept-1-enyl})]$ **129** (Report JMS0859) molecule showing the atom labelling scheme. Non-hydrogen atoms are represented by Gaussian ellipsoids at the 20% probability level. Hydrogen atoms are shown with arbitrarily small thermal parameters for the 2-methanidyl-3-methylcyclohept-1-enyl group, and are not shown for the pentamethylcyclopentadienyl groups. $R_I = 0.0573$, $R(w) = 0.1592$.

3.5 Future research and conclusion

α,ω -Alkylpropargyl dibromide malonate substrates **96**, **97** and **98** fail to undergo radical cyclization under the conditions employed. The failure may be due to the ester functionality interacting with the oxophilic titanium, resulting in competitive decomposition pathways. Increasing the stability of the alkyl radical used for central-carbon alkylation did not alleviate the problem. If the proposed attack (radical or nucleophilic) on the chelated carbonyl carbon of the ester is correct, this could be tested by including double bonds in the organic substrate to make this mode of decomposition unfavourable.

Under similar reaction conditions, organic substrates *without* ester functionality allowed access to bicyclic titanacyclobutene complexes. The bicyclic compounds (**129**, **130**, and **131**) synthesized are the first examples using a secondary halide for intramolecular central-carbon alkylation. A systematic study of cyclizations employing different organic radicals (2°, 3°, benzylic, allylic) and rigidifying elements as a function of ring size is now needed to examine the criteria required to efficiently synthesize macrocycles. There is much room for improvement as the largest bicyclic titanacyclobutene complex synthesized using the unsubstituted titanocene reagent is a seven-membered ring.

Chapter 4: Bicyclic titanacyclobutenes from α,ω -bis(bromopropargyl) malonates

4.1 Introduction

Much of the bicyclic titanacyclobutene chemistry explored by previous members of the group utilized α,ω -alkylpropargyl dibromide substrates. Mechanistically, the bicyclic titanacyclobutene complexes are formed by the intramolecular addition of an *alkyl* radical to the η^3 -propargyltitanium(III) intermediate. Tiege adapted this methodology and began investigating intramolecular *propargyl/allenyl* radical addition from α,ω -bis(bromopropargyl) substrates to synthesize bicyclic allenyl-titanacyclobutene complexes (Equation 2.2). With this methodology, ring sizes of up to eight are accessible. One attempt to access larger ring sizes through *gem*-diester α,ω -bis(bromopropargyl) substrate **132** (Figure 4.1) resulted only in decomposition. The failure to obtain the anticipated ten-membered bicyclic titanacyclobutene complex was disappointing: under the conditions used, any Thorpe-Ingold effect from the malonate moiety appeared to be insufficient to enhance the rate of radical cyclization.

4.2 Results: α,ω -bis(bromopropargyl) malonate synthesis

To reinvestigate the reactivity of these substrates several *gem*-diester α,ω -

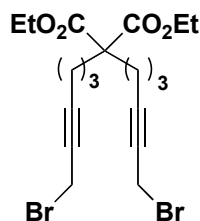
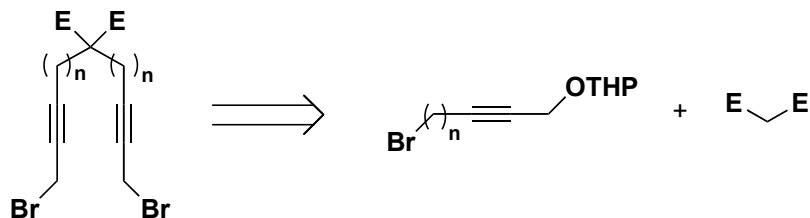


Figure 4.1: α,ω -Bis(bromopropargyl) malonate **132**

bis(bromopropargyl) malonates were synthesized. The synthetic approach to that used for the substrates was similar to the α,ω -alkylpropargyl dibromide syntheses (Scheme 3.2). A cursory retrosynthetic analysis shows that the desired substrates can be prepared

simply by double alkylation of the malonate using two equivalents of the appropriate propargyl bromide.

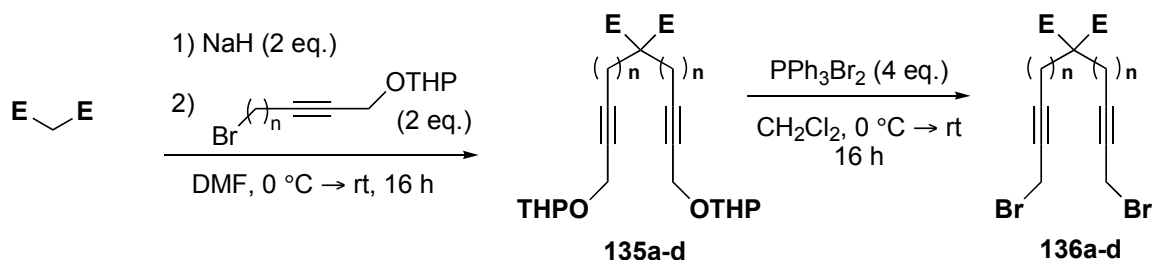
Equation 4.1



Preparation of butynyl bromide **102** ($n = 1$) has already been described (Scheme **3.3**). The next higher homologue **133** ($n = 2$) was made by ring-opening of ethylene oxide using the lithium acetylide of THP-protected propargyl alcohol followed by bromination with PBr_3 .⁷⁶ For the bromide **134** ($n = 3$), a synthesized sample was obtained from a previous member of the group.⁹⁷

α,ω -Bis(bromopropargyl) malonates **135a-d** were easily synthesized under alkylation conditions (Table **4.1**). Conveniently, for $n = 1$ and 3, it was possible to install both propargyl moieties in a one-pot procedure using two equivalents of sodium hydride and propargyl bromide. Similar reaction conditions were found unsuitable for bromide **133** where $n = 2$ (*vide infra*). For the short chain alkylations, di-*tert*-butyl malonate, diethyl malonate and malononitrile derivatives were prepared to investigate the tolerance of these functional groups under the reaction conditions.

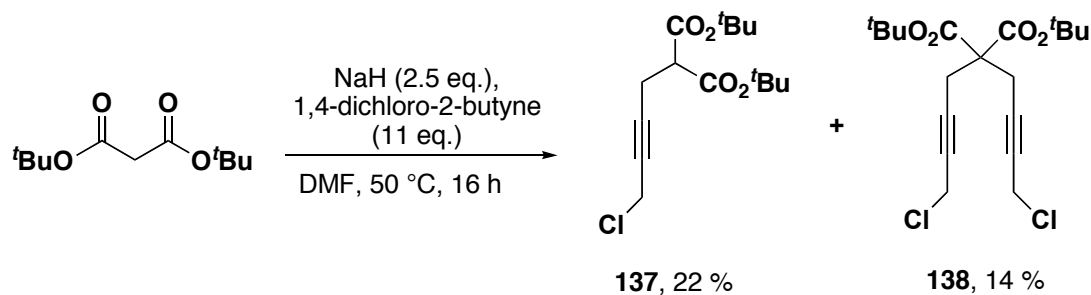
Scheme 4.1



Entry	E	Bromide, n	135a-d Yield	136a-d Yield
1	CN	102 , 1	135a , 69%	136a , 77%
2	CO ₂ Et	102 , 1	135b , 38%	136b , 91%
3	CO ₂ ^t Bu	102 , 1	135c , 82%	136c , 100%
4	CO ₂ ^t Bu	134 , 3	135d , 82%	136d , 43%

In attempt to shorten the synthesis, propargyl chloride **138** analogous to **136c** was synthesized (in poor unoptimized yield) from a one step reaction: double alkylation of *tert*-butyl malonate using excess of the commercially available 1,4-dichloro-2-butyne (Equation 4.2).

Equation 4.2



Although the yield was very poor, separation of the two products was easily achieved by fractional distillation under reduced pressure.

The one-pot approach to synthesize α,ω -bis(bromopropargyl) substrates **136a-d** was not successful for the synthesis of dialkylated malonate **139** (Figure 4.2). The

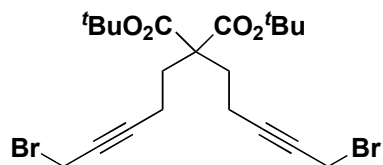
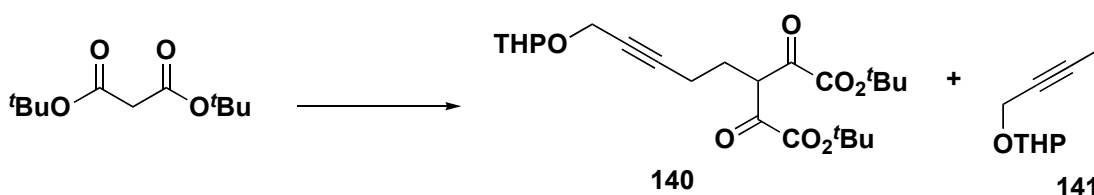


Figure 4.2: Gem-diester α,ω -bis(bromopropargyl) substrate **139**

reaction of di-*tert*-butyl malonate anion and pentynyl bromide **133** did not produce the anticipated dialkylated malonate **139**, but rather gave enyne **140**, mono-alkylated malonate **141** (Equation 4.3, Entry 1) as well as recovered starting material. Although the elimination product could be the result of sodium hydride reacting directly with

Equation 4.3

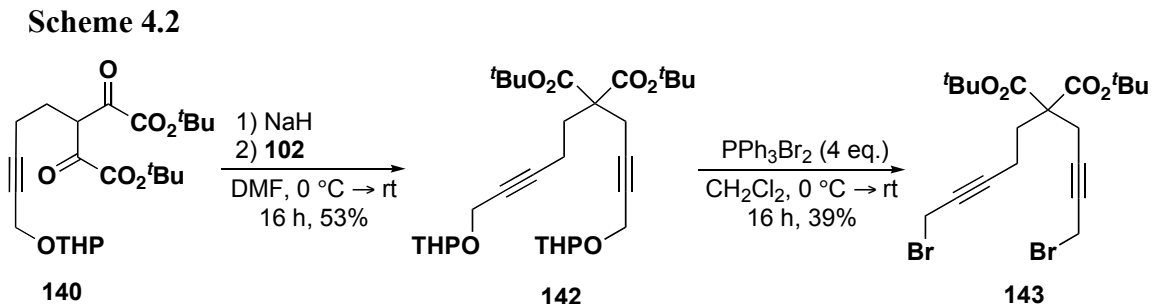


Entry	Conditions	Yield	
		140	141
1	NaH (2 eq.); 133 (2 eq.), DMF 0 °C → 50 °C, 16 h	35% ^a	50% ^b
2	NaH (0.8 eq.); 133 (0.7 eq.), DMF 0 °C → rt, 16 h	66% ^a	0%

^a isolated yield; ^b estimated from ¹H NMR integration

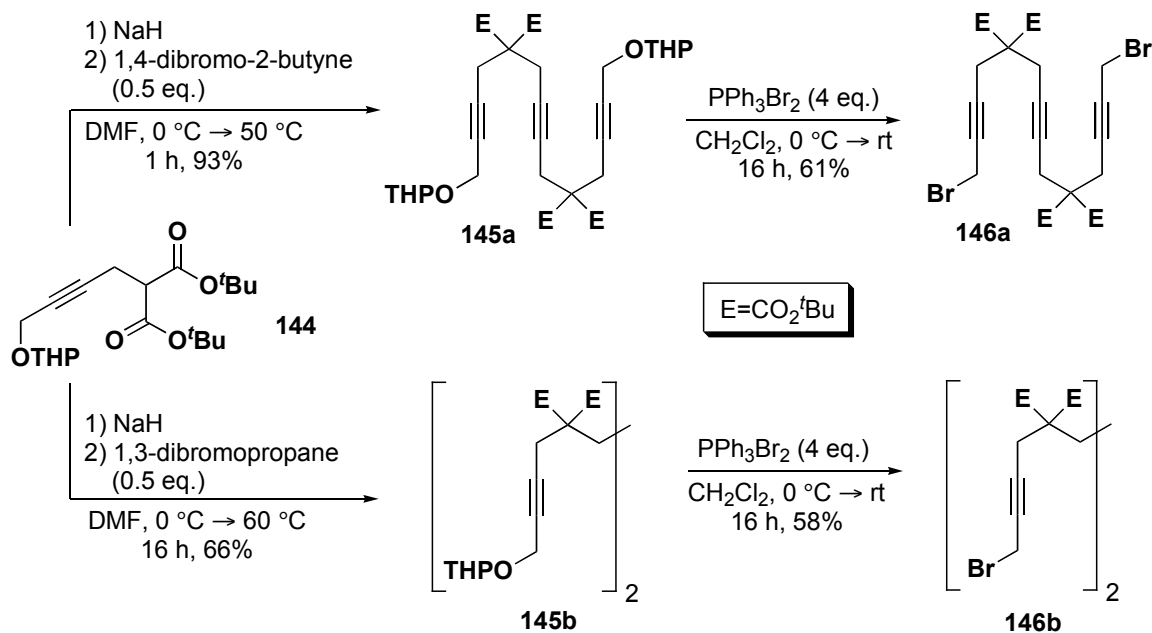
homo-propargylic bromide **133**, reaction conditions optimized for mono-alkylation worked rather well, affording 66% yield of alkynyl malonate **140** (Entry 2). Interestingly, however, the reaction of the pre-formed sodium salt of mono-alkylated di-*tert*-butyl malonate **140** with pentynyl bromide **133** resulted only in elimination. This experiment suggests that the enolate of **140** is basic enough to induce E₂-elimination to occur. This is rationalized by the increasing basicity and decrease in nucleophilicity of dialkyl malonate anions with increasing size of the ester alkoxy groups and α -position substituent.⁹⁸ Similar cases where elimination competes under malonate alkylation conditions have been observed.⁹⁹ Realizing these difficulties, the alkylation of malonate **140** with propargyl bromide **102** then provided the unsymmetrical dialkylated malonate

142 in modest yield (Scheme 4.2). Under the standard deprotection and bromination conditions, dibromide **143** was obtained in acceptable yield.



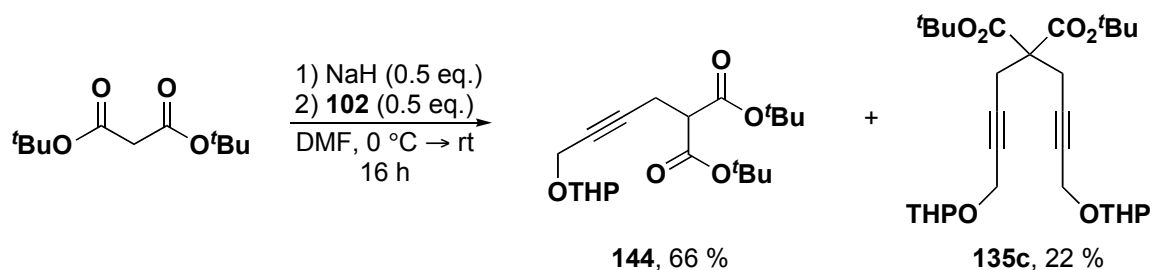
To explore the effect of two *gem*-diester groups in the α,ω -bis(bromopropargyl) substrate radical cyclization, two symmetrical substrates, **146a** and **146b**, were synthesized (Scheme 4.3). Each was prepared *via* the alkylation of **144** with half an equivalent of 1,4-dibromo-2-butyne or 1,3-dibromopropane, to give bis(*gem*-diester) substrates **145a** and **145b**, respectively. Accompanying **145b**, the E_2 -elimination product (*ca.* 4%) and starting material (*ca.* 4%) were also isolated. After deprotection and bromination, the dibromides **146a** and **146b** were obtained as white, solids in modest yield. Crystallization of **146b** by evaporation from dichloromethane provided single-crystals suitable for X-ray analysis (Figure X, *vide infra*). The alkynyl

Scheme 4.3



malonate starting material **144** used for this synthesis itself was prepared under normal alkylation reactions conditions (Equation 4.4), using two equivalents of di-*tert*-butyl malonate to minimize the formation of the dialkylated product **147**. However, even under these reaction conditions a 3 : 1 mixture of mono- : di-alkylated products was obtained, indicating the *facile* nature of the second alkylation step.

Equation 4.4

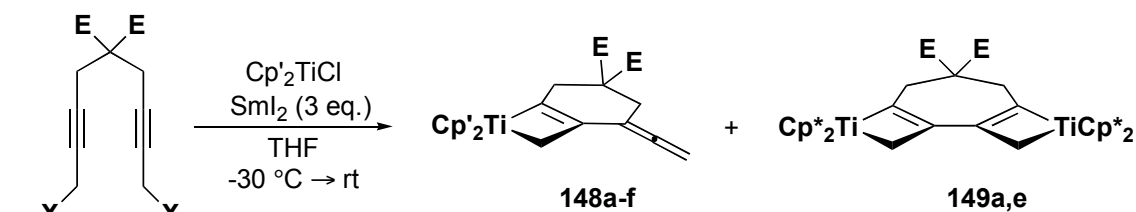


4.3 Results: Intramolecular addition of radicals to η^3 -propargyltitanium(III) complexes

4.3.1 *Exo-allenyl bicyclic titanacyclobutenes*

With the cyclization precursors in hand, six-membered *exo*-allenyl bicyclic titanacyclobutenes were prepared in good yield by treatment of halides **136b**, **136c** and **138** with the substituted titanocene complex and samarium diiodide (Scheme 4.4). The unsubstituted titanocene, however, reacts to give only decomposition products. Interestingly, when decamethyltitanocene chloride is used, tricyclic di(titanacyclobutene)

Scheme 4.4



136b, E = CO₂Et, X = Br

138, E = CO₂^tBu, X = Cl

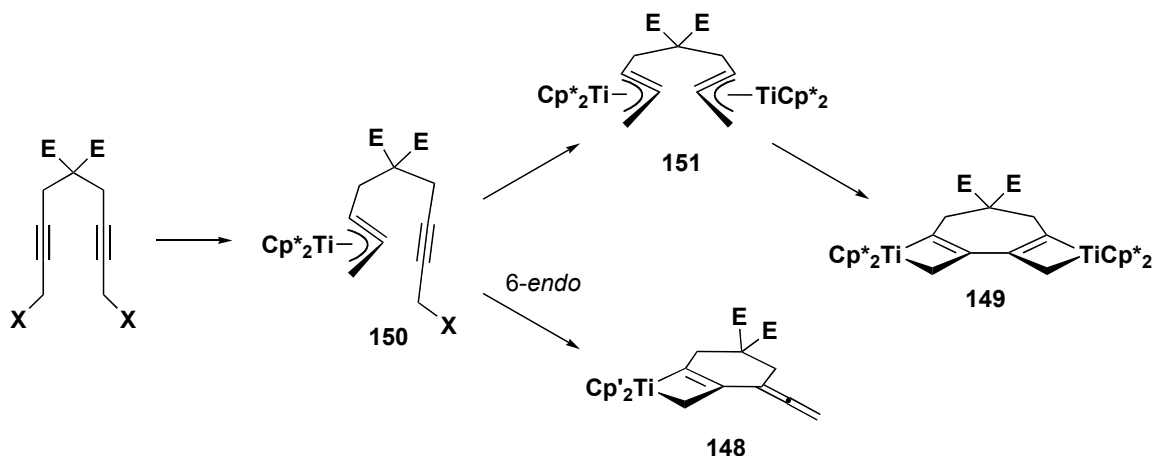
136c, E = CO₂^tBu, X = Br

Entry	Substrate	Cp'	Product, Yield
1	136b	Cp*	148a , 67%; 149a , 10%
2	136b	^t BuCp	148b , 73%
3	138	Cp	148c , trace
4	138	^t BuCp	148d , 74%
5	138	Cp*	148e , 78%; 149e , 8%
6	136c	Cp	0%
7	136c	^t BuCp	148f , 81%

complexes **149a** and **149e** were isolated as minor byproducts (Entries 1 and 5). Due to the tendency of the lipophilic titanacyclobutene products to be isolated as oils, crystallization as a means of purification was difficult.

A mechanism accounting for the formation of both observed modes of reactivity is shown in Scheme 4.5. The allenyl-substituted titanacyclobutene complex arises from 6-*endo* cyclization of the radical derived from η^3 -propargyltitanium(III) intermediate **150**. If persistent enough in solution, intermediate **150** can react with another equivalent of the

Scheme 4.5



titanium reagent and two equivalents of samarium diiodide to produce the bis- η^3 -propargyltitanium(III) complex **151**. The observed competitive pseudo-dimerization product **149** presumably is formed by the radical-radical coupling of intermediate **151**. In one case single-crystals of both bicyclic- and tricyclic titanacyclobutene complexes **148a** and **149a** were obtained by fractional crystallization from pentane at low temperature. Crystal structures were obtained by X-ray analysis and are represented in Figures **4.3** and **4.4**, respectively.

The failure of the unsubstituted titanocene chloride to promote the radical cyclization (Entries 3 and 6, Scheme **4.4**) parallels the results reported by Tiege for reactions of α,ω -bis(bromopropargyl) substrates (Equation **2.2**). The reason for this may be a favourable change in hapticity of the propargyl ligand, from η^3 - to η^1 -coordination due to the more weakly donating cyclopentadienyl ligands compared to the more electron-rich *tert*-butyl- and pentamethylcyclopentadienyl ligands. Although some iridium η^1 -allenyl complexes are susceptible to nucleophilic attack at the central carbon, prior coordination of the incoming nucleophile to the metal is necessary.¹⁰⁰

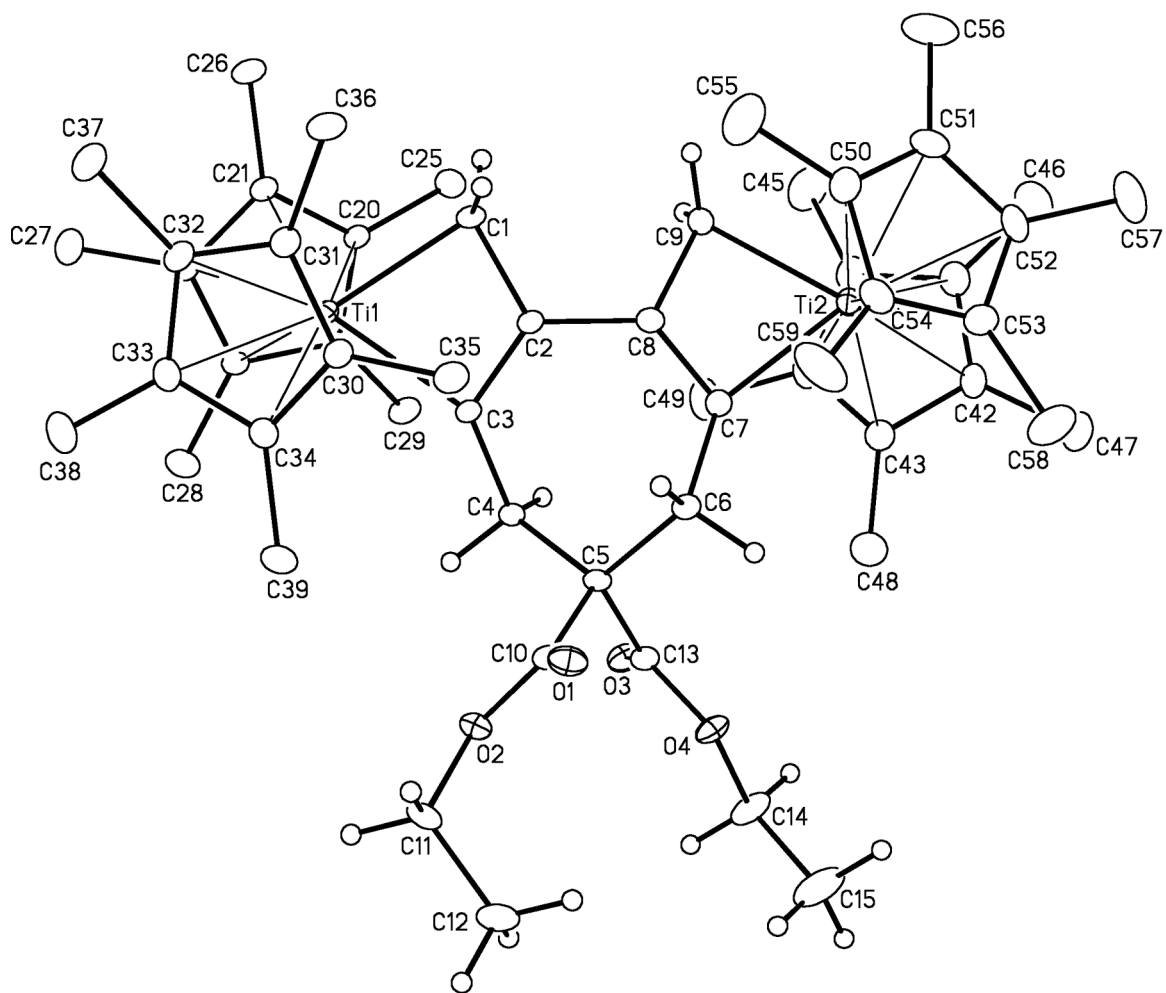


Figure 4.3: Perspective view of $[(Cp^*_2Ti)_2\{2,3\text{-dimethanidyl-6,6-bis(ethoxycarbonyl)cyclohepta-1,3-diene-1,4-diyl}\}]$ **19a** showing the atom labelling scheme. Non-hydrogen atoms are represented by Gaussian ellipsoids at the 20% probability level. Hydrogen atoms are shown with arbitrarily small thermal parameters, and are not shown for the pentamethylcyclopentadienyl groups. $R_1 = 0.0601$, $R(w) = 0.1757$.

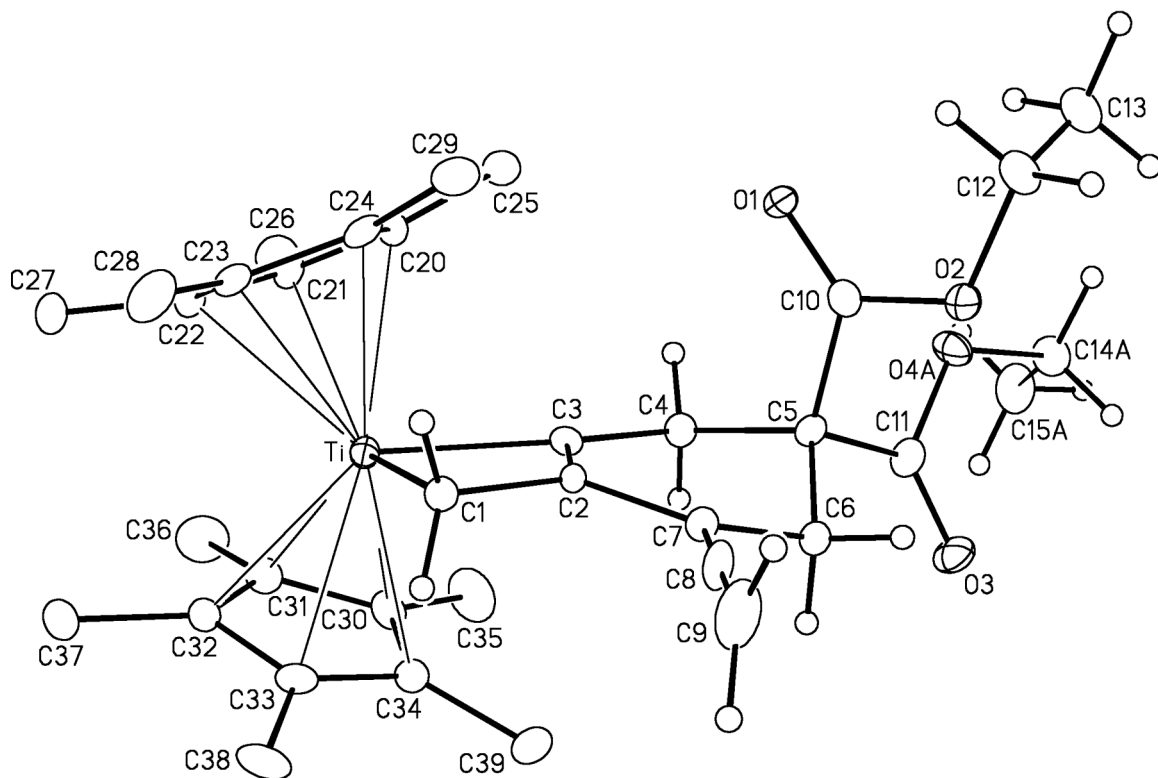


Figure 4.4: Perspective view of $[\text{Cp}^*_2\text{Ti}\{3\text{-ethenylidene-5,5-bis(ethoxycarbonyl)-2-methanidylcyclohex-1-enyl}\}]$ **148a** showing the atom labelling scheme. Non-hydrogen atoms are represented by Gaussian ellipsoids at the 20% probability level. Only one orientation of the disordered ethoxy (O4A, C14A, C15A) group is shown for clarity. Hydrogen atoms are shown with arbitrarily small thermal parameters for the 3-ethenylidene-5,5-bis(ethoxycarbonyl)-2-methanidylcyclohex-1-enyl group, and are not shown for the pentamethylcyclopentadienyl groups. $R_I = 0.0541$, $R(w) = 0.1060$.

The six-membered bicyclic titanacyclobutene complexes were characterized unambiguously by IR and NMR spectroscopy. In the ^{13}C NMR spectrum, typical resonances for titanacyclobutene core are seen at δ 213.3, 94.1 and 65.2. The equivalent allene protons are seen at δ 4.95 as a broad singlet. The allene moiety is further identified by its characteristic *sp*-carbon chemical shift at δ 210.8 and an intense IR stretching frequency at 1935 cm^{-1} . The remaining carbon assignments are based on extensive HMQC and HMBC analysis and are summarized **148f** in Table **4.1**. The compounds' mass spectrum was analyzed using high-resolution electrospray rather than

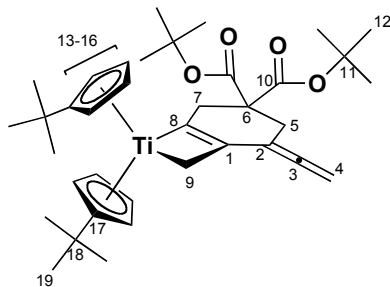


Figure 4.5: Carbon and hydrogen labelling scheme for bicyclic titanacyclobutene **148f**

Table 4.1: ^1H and ^{13}C NMR assignments for bicyclic titanacyclobutene **148f**

$^1\text{H}^a$	$^{13}\text{C}^b$	$^1\text{H}^a$	$^{13}\text{C}^b$
-	C ₁ , δ 65.2	-	C ₁₁ , δ 80.5
-	C ₂ , δ 98.0	H ₁₂ , δ 1.42 (s, 18H)	C ₁₂ , δ 27.9
-	C ₃ , δ 210.8	H ₁₃ , δ 6.19 (q, $J \sim 3$ Hz)	C ₁₃ , δ 111.5
H ₄ , δ 4.96 (br s, 2H)	C ₄ , δ 76.8	H ₁₄ , δ 5.63 (q, $J \sim 3$ Hz)	C ₁₄ , δ 110.6
H ₅ , δ 3.10 (s, 2H)	C ₅ , δ 34.2	H ₁₅ , δ 5.58 (q, $J \sim 3$ Hz)	C ₁₅ , δ 111.1
-	C ₆ , δ 56.8	H ₁₆ , δ 5.53 (q, $J \sim 3$ Hz)	C ₁₆ , δ 108.6
H ₇ , δ 3.42 (br s, 2H)	C ₇ , δ 41.6	-	C ₁₇ , δ 140.0
-	C ₈ , δ 213.3	-	C ₁₈ , δ 32.8
H ₉ , δ 3.09 (br s, 2H)	C ₉ , δ 65.2	H ₁₉ , δ 1.20 (s, 18H)	C ₁₉ , δ 31.6
-	C ₁₀ , δ 170.7		

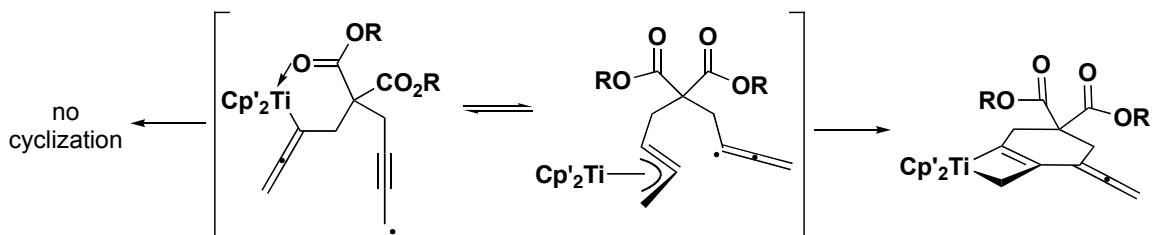
^a C₆D₆, 400 MHz; ^b C₆D₆, 100 MHz

electron impact (EI) due to the sensitivity of *tert*-butyl ester groups toward fragmentation. At the high temperature required EI, thermolysis of the *tert*-butyl esters occurs, liberating isobutylene.¹⁰¹ The detected molecular ion mass (as the sodium adduct) is consistent with the calculated value (m/z 631.32373 and 631.32406, respectively).

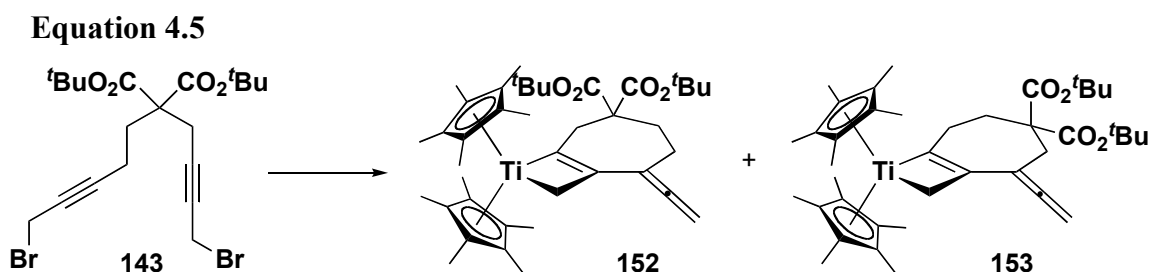
It is interesting that the ester functionality in the α,ω -bis(bromopropargyl) malonate substrates is tolerated: no significant quantities of decomposition products are detected in the crude NMR spectra. Using the same argument as depicted in Scheme 4.6,

chelation of the carbonyl oxygen in the η^1 -allenyltitanium complex could lead to a six-membered ring by competitive addition to the ester. However, attack at this chelated ester by the presumably linear propargyl radical is not possible geometrically (Scheme 4.6).

Scheme 4.6



Under the standard radical cyclization condition, unsymmetrical α,ω -bis(bromopropargyl) malonate **143** was expected to give roughly an equal mixture of two bicyclic titanacyclobutene products, structural isomers arising from initial formation of an η^3 -propargyl complex on either of the two ends and subsequent trapping from the allenyl radical derived from the other end. As predicted, a 2 : 3 ratio of the two bicyclic titanacyclobutene products **152** and **153** are obtained from the reaction of α,ω -bis(bromopropargyl) malonate **143**, bis(pentamethylcyclopentadienyl)titanium chloride and samarium diiodide (Equation 4.5). No tricyclic product from bis[η^3 -



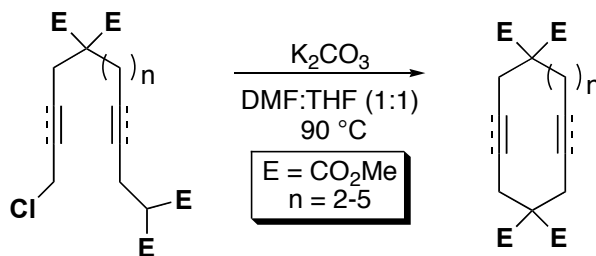
Entry	conditions	yield	
		152	153
1	Cp* ₂ TiCl, Sml ₂ (3 eq.), THF -30 °C → rt, 16 h	14%	21%
2	Cp* ₂ TiCl, (2 eq.), Sml ₂ (4 eq.), THF -78 °C → rt, 16 h	0%	63%

propargyltitanium(III)] coupling was observed. The reaction was repeated, but at lower temperature and using *two* equivalents of bis(pentamethylcyclopentadienyl) titanium chloride to bias the reaction toward formation of the di(titanacyclobutene) product (Equation 4.5). Surprisingly, not only was the di(titanacyclobutene) complex was not observed, a single bicyclic titanacyclobutene was formed, with no evidence for an isomeric product (Entry 2). It appears that the η^3 -propargyltitanium(III) intermediate preferentially forms at the least hindered of the two propargyl functions. The absence of the di(titanacyclobutene) product under what should have been favourable conditions is indicative of an enhanced rate of cyclization of the η^3 -propargyltitanium(III) intermediate, presumably an effect of the *gem*-diester group. Unfortunately, not enough material was obtained to fully characterize the seven-membered product or to further investigate the reactivity of unsymmetrical bromide **143** with other titanocene reagents.

4.3.2 Macrobicyclic titanacyclobutenes

The inclusion of more than one restricting element in a cyclization substrate was explored by Deslongchamps, *et al.*, in the syntheses of ten- to fourteen-membered macrocycles (Equation 4.6).^{76,102} The authors used a combination of *gem*-diester functionality and sites of unsaturation (*cis* or *trans* alkenes and alkyne moieties) within

Equation 4.6

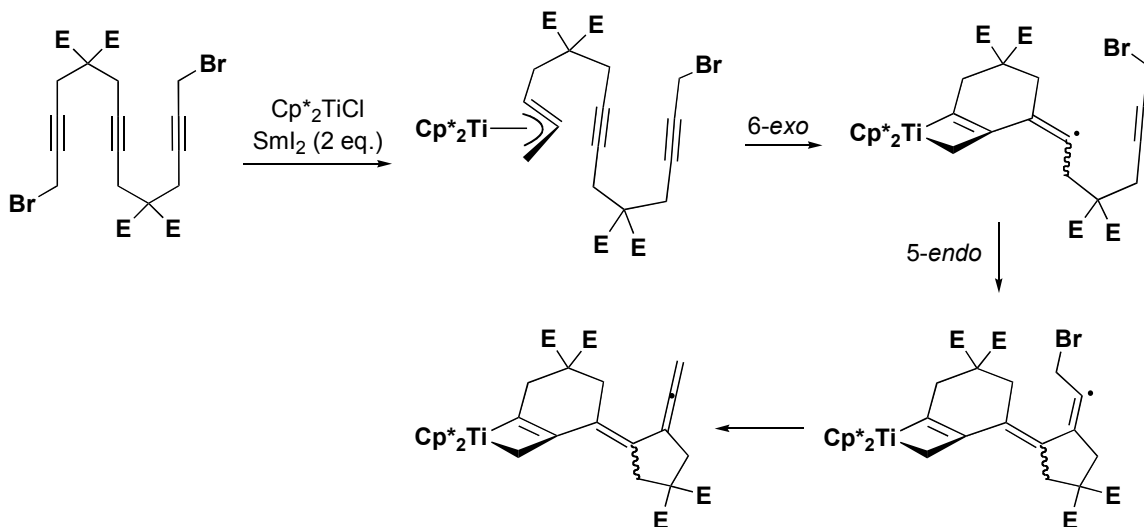


the substrates. The combination of these two structural elements places significant constraint on the number of low-energy rotamers of the substrate therefore lowering the entropy for cyclization. The unsaturation also lowers the number of transannular

interactions, decreasing the enthalpy component for cyclization. As a result, under malonate alkylation conditions, the macrocycles were formed in modest to good yield without resorting to high-dilution techniques.

We were interested in how such results might translate to the titanium-mediated radical cyclization methodology. Thus, the reactivity of α,ω -bis(bromopropargyl) dimalonates **146a** and **146b** were examined. Since the substrates differ only by one carbon in the backbone, the latter is expected to cyclize faster due to the conformationally more restricted alkyne moiety. However, when α,ω -bis(bromopropargyl) dimalonates **146a** and **146b** were treated with the parent, 1,1'-bis(*tert*-butyl), or decamethyltitanocenes and samarium diiodide, only decomposition products were obtained. Treatment of **146a** with decamethyltitanocene and isopropyl iodide or with excess decamethyltitanocene also failed. Decomposition may be the result of the isolated alkyne, which may act as a competitive radical acceptor (Scheme 4.7). 6-*Exo* ring-closure of the η^3 -propargyltitanium complex onto the alkyne results in a highly reactive vinyl radical. The σ -radical could then cyclize onto the alkyne by 5-*exo-dig* ring-closure, the preferred mode of cyclization.¹⁰³

Scheme 4.7



Remarkably, however, when α,ω -bis(bromopropargyl) malonate **136d** (Entry 4, Scheme 4.1) was subjected to the standard radical cyclization conditions, a single product

was isolated. The product was predicted to be the 10-membered bicyclic titanacyclobutene **154** with an exocyclic allene substituent (Figure 4.6). However, it was

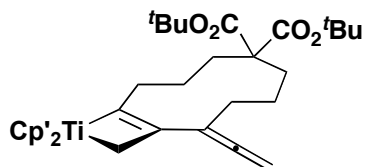
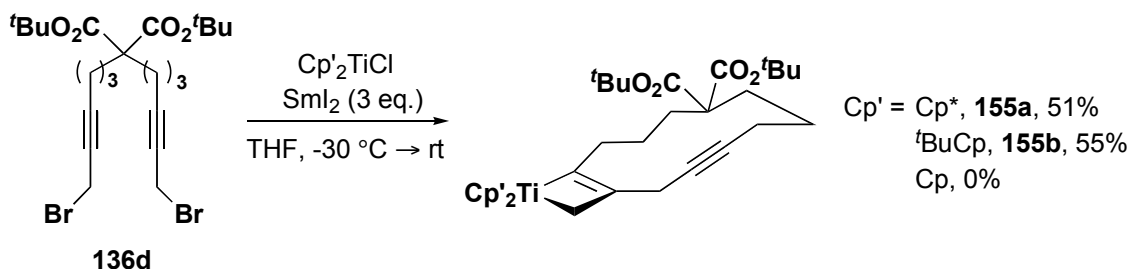


Figure 4.6: Bicyclic titanacyclobutene **154**

clear upon spectroscopic analysis that the predicted ten-membered complex **154** was not obtained. Instead, the twelve-membered cycloalkyne titanacyclobutene **155** was obtained in modest yield (Equation 4.7).

Equation 4.7



Confirmation of the presence of the alkyne could not be obtained from the IR spectrum, as the stretch was too weak to be observed. This is reasonable considering the isolated and nearly symmetrical nature of the bond: such a stretch would not change the bond dipole to a great degree. Raman spectroscopy was considered a logical alternative, but the scattering wavelength of the laser was unsuitable for analysis of the intensely red-coloured solution. Therefore, extensive analyses of the 1D and 2D NMR spectra were undertaken. The numbering system for the carbons and hydrogen atoms is shown in Figure 4.7. In the ¹H NMR spectrum, the most downfield signal is assigned to the methylene H₁, a broad singlet at δ 3.16. In the COSY spectrum, long-range coupling is observed across the alkyne to H₄ a very broad multiplet at δ 2.09. Following the ¹H-¹H COSY correlations, H₄ is vicinally coupled to H₅, a signal at δ 1.49. Unfortunately, this

signal is obscured by intense peaks from the pentamethylcyclopentadienyl ring and *tert*-butyl esters, as well as a trace of unknown decomposition products. To alleviate this problem, a 1D TOCSY experiment was performed. The 1D TOCSY method provides a ^1H NMR spectrum of hydrogen atoms within the same spin system. Thus, the signal at H_6 , a triplet ($J = 6.8$ Hz) at δ 2.39, which is correlated to H_5 in the COSY spectrum, was irradiated to observe the multiplicity of H_5 . Once H_6 is irradiated, H_5 appears as a quintet with $J = 6.3$ Hz. These signals from H_1 - H_6 conclude the first isolated spin system. The next through-correlated spin system begins with the methylene in the titanacyclobutene ring, H_{13} , which appears as a broad singlet at δ 2.16. This signal is long-range coupled to H_{10} , a triplet ($J = 7.6$ Hz). This triplet is coupled to a broad multiplet, H_9 , at δ 1.86, which is coupled to the second order methylene in the α -position of the malonate moiety, H_8 , at δ 2.31. Finally, the methyl signals of the ancillary ligands are an intense singlet at δ 1.70 and the *tert*-butyl groups of the malonate are an eighteen hydrogen singlet at δ 1.41.

The carbon assignments were made using the complementary heteronuclear correlations experiments, HMQC and HMBC. Table 4.2 summarizes the assignments from this analysis, while Figure 4.8 displays the pertinent correlations in the HMBC and COSY spectra used to determine the connectivity. The only signals that cannot be unambiguously assigned are the two *sp*-hybridized carbons of the alkyne unit. This is for obvious reasons: HMQC spectroscopy is useless as there are no attached hydrogens and HMBC correlations to the methylene groups (H_1 , H_2) on either side of the alkyne are observed to *both* carbons of the alkyne by two and three-bond coupling. Electrospray mass spectrometry was used to determine the mass of titanacycle **155a**, but only a low-resolution value could be obtained due to the weak signal of the sodium adduct. The low-resolution value ($m/z = 715.4$), however, agrees with the calculated value of 715.4.

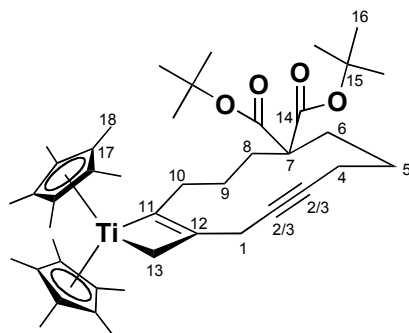


Figure 4.7: Carbon and hydrogen labelling scheme for titanacyclobutene **155a**

Table 4.2: ^1H and ^{13}C NMR assignments for bicyclic titanacyclobutene **155a**

$^1\text{H}^a$	$^{13}\text{C}^b$	$^1\text{H}^a$	$^{13}\text{C}^b$
$\text{H}_1, \delta 3.16$ (br s, 2H)	$\text{C}_1, \delta 24.0$	-	$\text{C}_{11}, \delta 211.7$
-	$\text{C}_{2,3}, \delta 80.2, 81.3^c$	-	$\text{C}_{12}, \delta 102.5$
$\text{H}_4, \delta 2.09$ (br m, 2H)	$\text{C}_4, \delta 20.2$	$\text{H}_{13}, \delta 2.16$ (br s, 2H)	$\text{C}_{13}, \delta 79.2$
$\text{H}_5, \delta 1.49$ (p, $J = 6.3$ Hz, 2H)	$\text{C}_5, \delta 23.1$	-	$\text{C}_{14}, \delta 171.1$
$\text{H}_6, \delta 2.39$ (t, $J = 6.8$ Hz, 2H)	$\text{C}_6, \delta 28.9$	-	$\text{C}_{15}, \delta 79.9$
-	$\text{C}_7, \delta 58.7$	$\text{H}_{16}, \delta 1.41$ (s, 18H)	$\text{C}_{16}, \delta 28.0$
$\text{H}_8, \delta 2.31$ (2^{nd} order m, 2H)	$\text{C}_8, \delta 32.6$	-	$\text{C}_{17}, \delta 118.5$
$\text{H}_9, \delta 1.86$ (m, 2H)	$\text{C}_9, \delta 26.1$	$\text{H}_{18}, \delta 1.70$ (s, 30H)	$\text{C}_{18}, \delta 12.1$
$\text{H}_{10}, \delta 2.61$ (t, $J = 7.6$ Hz, 2H)	$\text{C}_{10}, \delta 35.5$		

^a C_6D_6 , 400 MHz; ^b C_6D_6 , 100 MHz; ambiguous assignments

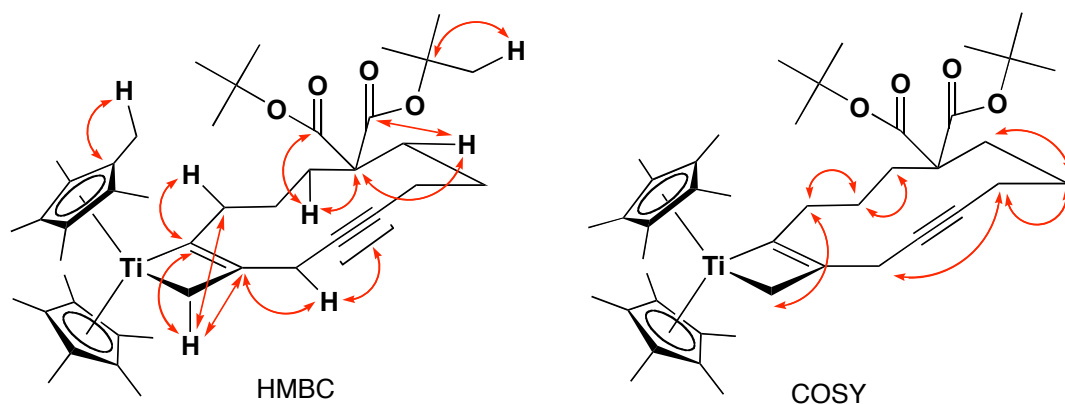


Figure 4.8: Pertinent HMBC and COSY correlations for titanacyclobutene **155a**

The possibility that the product is the ten-membered allenyl titanacyclobutene **154** is thus refuted by a few simple arguments. The IR spectrum has no intense signal (*ca.* $\sim 1950\text{ cm}^{-1}$) corresponding to an allene stretch. Furthermore, the absence of resonances at $\sim \delta 5$ in the ^1H NMR spectrum and $\sim \delta 210$ in the ^{13}C NMR spectrum together indicate the absence of a terminal allene. Fortunately and unambiguously, a single-crystal of complex **155a** was obtained by crystallization of from pentane at $-30\text{ }^\circ\text{C}$. Crystallographic analysis of this material confirms the proposed macrocyclic cycloalkyne structure (Figure 4.9).

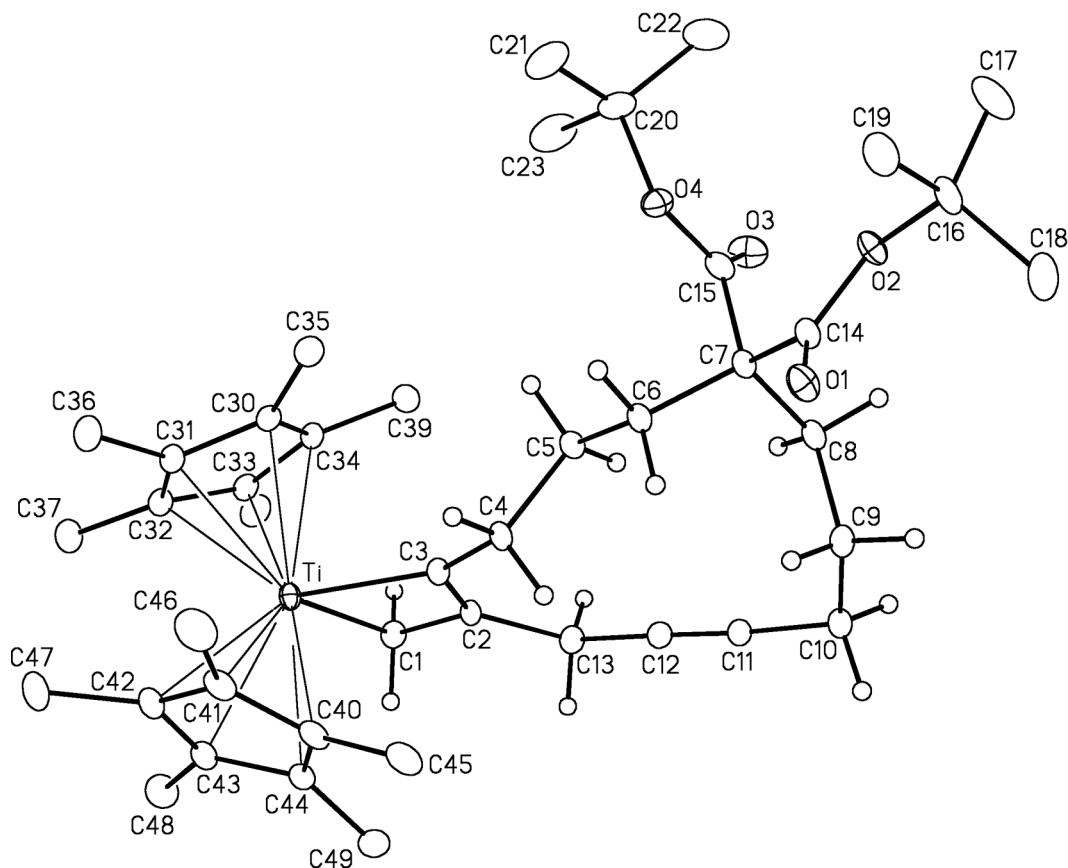
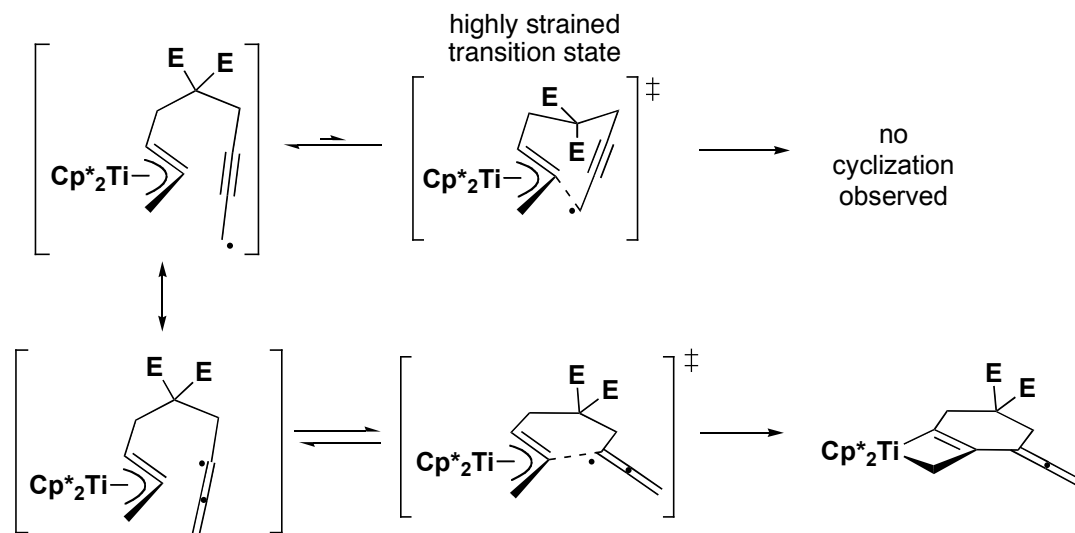


Figure 4.9: Perspective view of $[\text{Cp}^*_2\text{Ti}\{9,9\text{-bis}(t\text{-butoxycarbonyl})\text{-}2\text{-methanidylcyclododec-1-en-4-yn-1-yl}\}]$ **155a** showing the atom labelling scheme. Non-hydrogen atoms are represented by Gaussian ellipsoids at the 20% probability level. Hydrogen atoms are shown with arbitrarily small thermal parameters for the methylene groups, and are not shown for the *t*-butyl and Cp* methyl groups. $R_I = 0.0614$, $R(w) = 0.1938$.

The reason for the reaction favoring 12-membered ring-closure favouring over 10-membered is not entirely clear. However, as noted by Porter, the smaller of the macrocycles (*esp.* ten- and eleven-membered rings) are generally more difficult to form. Therefore, the transition state for the observed twelve-membered titanacyclobutene product **155** may simply be more favourable energetically. This is the opposite selectivity than that observed in the formation of the six-membered titanacyclobutene **148** where the transition state geometry required for competitive cyclooctyne formation would be highly strained (Scheme 4.8).

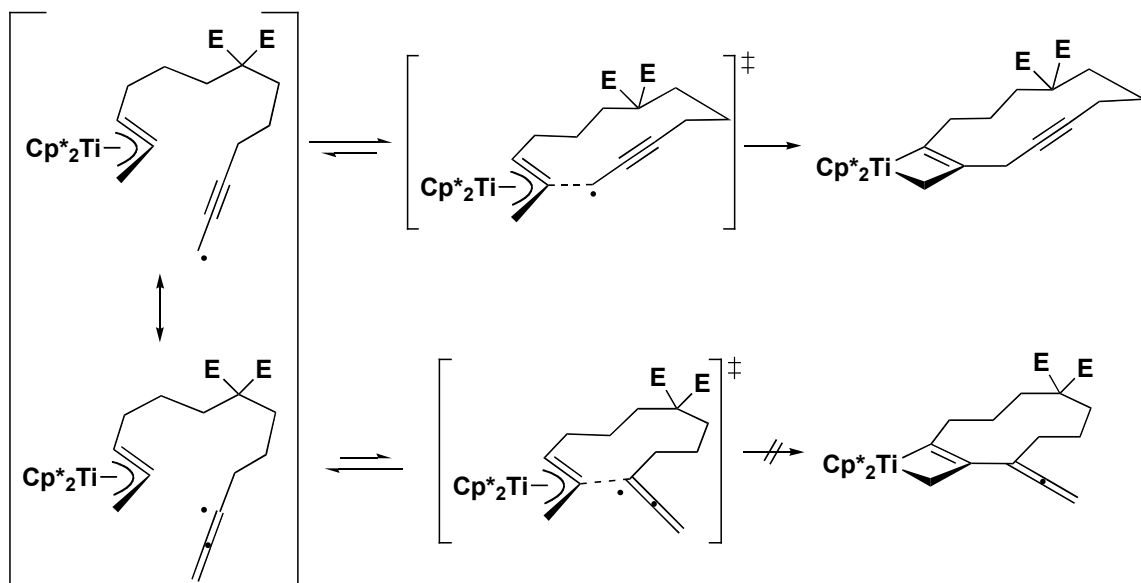
Examination of the nature of the organic free radical provides further insight.

Scheme 4.8



Photochemical hydrogen atom abstraction from allene in the presence of methyl radicals yield a very high ratio of 1-butyne to 1,2-butadiene, indicating the reactive radical is dominantly propargyl in nature.¹⁰⁴ The natural reactivity pattern thus appears to be addition as a propargyl rather than allenyl moiety *unless* the transition state is geometrically unfavourable, as is the case *en route* to the cyclooctyne bicyclic titanacyclobutene (Scheme 4.9).

Scheme 4.9



It is clear, however, the geminal *tert*-butyl ester groups in α,ω -bis(bromopropargyl) dimalonate **136d** facilitate the radical cyclization, while the two *gem-tert*-butyl esters in extended substrate **146b** are actually *hinder* the cyclization. One rationale to explain this phenomenon is found by examining the crystal structures of both of the organic substrates, as well as performing some molecular mechanics calculations. It is recognized that the solid state structure does not necessarily reflect that of the solution state. The crystal structure does generally represent one low-energy conformation (a local, if not global minimum) and therefore, extrapolation to the relative ground state conformations seems reasonable. The crystal structure diagrams of α,ω -bis(bromopropargyl) malonates **136d** and **146b** were obtained by X-ray analysis and are shown in Figures 4.10 and 4.11, respectively.

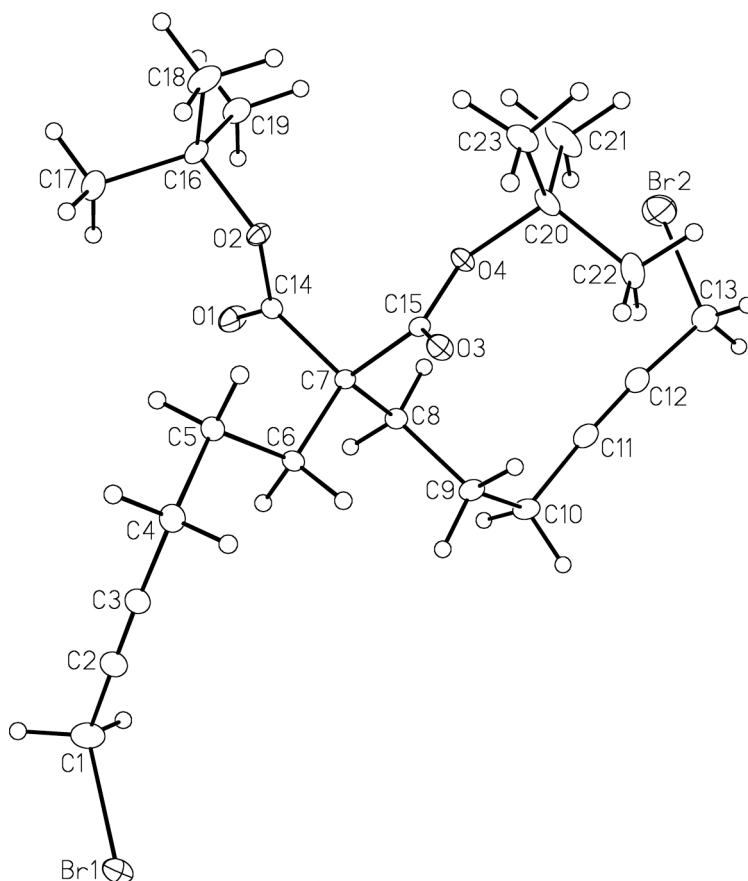


Figure 4.10: Perspective view of di-*tert*-butyl bis(6-bromohex-4-yn-1-yl)propanedioate **136d** showing the atom labelling scheme. Non-hydrogen atoms are represented by Gaussian ellipsoids at the 20% probability level. Hydrogen atoms are shown with arbitrarily small thermal parameters. $R_I = 0.0342$, $R(w) = 0.0836$.

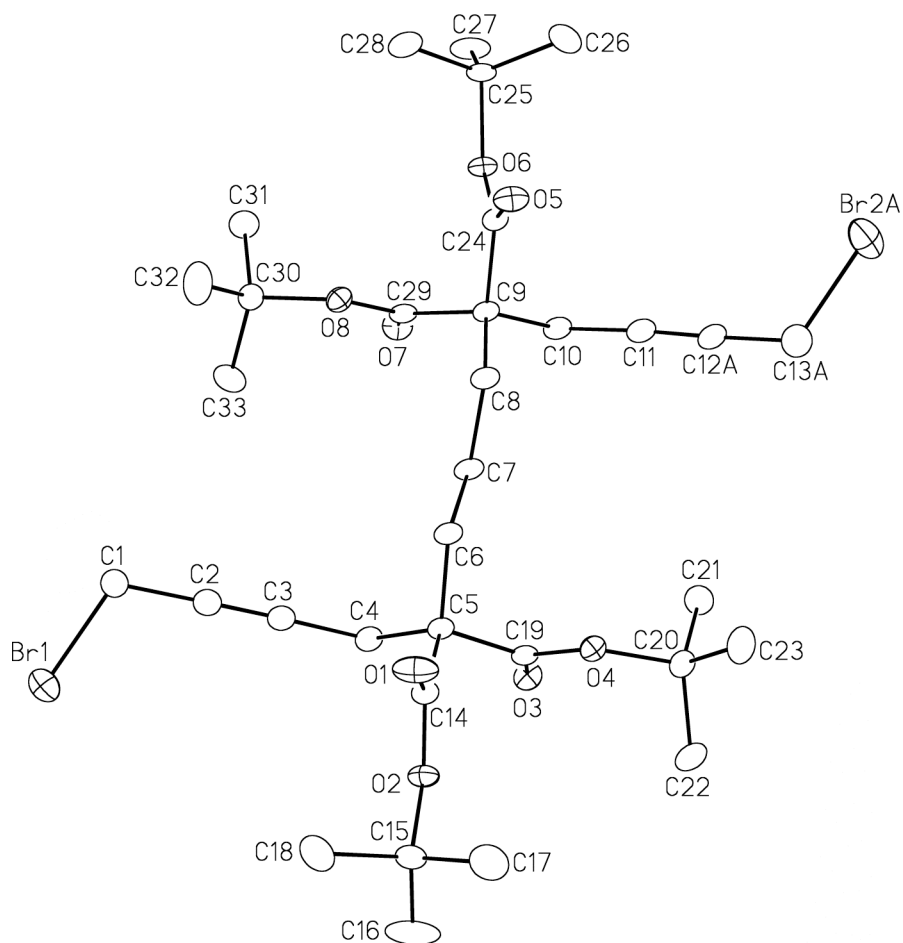


Figure 4.11: Perspective view of tetra-*tert*-butyl 1,13-dibromotrideca-2,11-diyne-5,5,9,9-tetracarboxylate **146b** showing the atom labelling scheme. Only the major (75%) orientation of the disordered C-CH₂Br group (C12A, C13A, Br2A) is shown. Non-hydrogen atoms are represented by Gaussian ellipsoids at the 20% probability level. Hydrogen atoms are not shown. $R_I = 0.0397$, $R(w) = 0.1074$.

For the malonate derivative **136d**, a simple bond rotation about one of the unconstrained linear chains (*e.g.* C8-C9) allows both propargyl ends to become in close contact, facilitating the titanium-induced radical cyclization. From the crystal structure of the bis(*gem-tert*-butyl) ester compound **146b**, the bromine atoms are considerably more distanced from each other, possibly due to steric interactions of the two malonate groups in alternative conformations. Molecular mechanics force field (MMFF) calculations were used to find the global minimum conformations of substrate **146b**. A systematic method was employed to calculate molecular conformations, an alternative method using the Monte-Carlo algorithm continually failed. The number of molecular conformations was

restricted by the fold number of each rotatable bond. The fold number is the number of conformational minima between two groups bonded together. For example, an sp^3 - sp^3 carbon-carbon bond has a fold number of three because there are generally three well-defined minima upon a complete 360° rotation of this bond. After each rotation, the energy of the molecule is re-minimized. The lowest-energy conformer obtained from this process is shown in Figure 4.12.

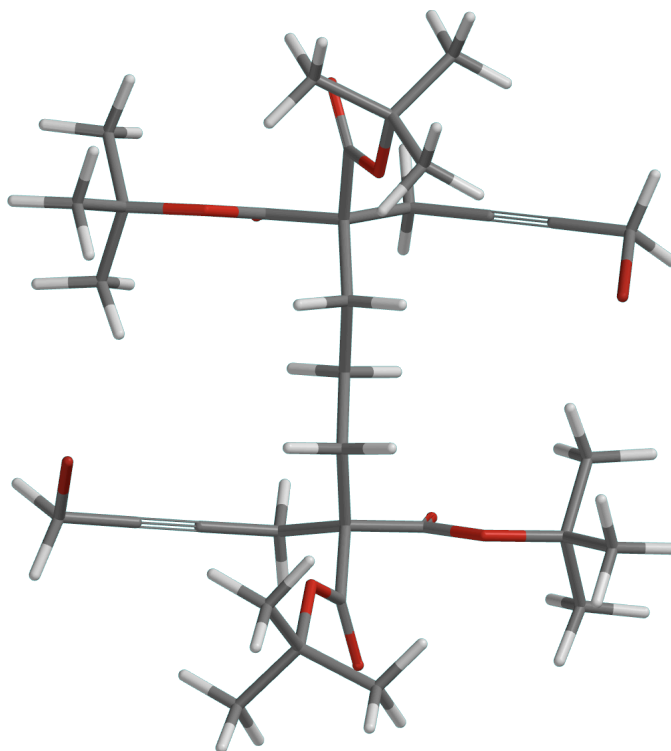


Figure 4.12: Lowest-energy conformer calculated for bis(*gem-tert*-butyl) ester **146b**

The low-energy conformation is strikingly similar to that obtained from the X-ray analysis, suggesting that the crystal structure is close to the true global minimum. For radical cyclization to occur, the two propargyl moieties must be on the ‘same side’ of the molecule. Therefore, further calculations were performed to examine the energy requirements to obtain such a conformation. The simplest way of achieving this is by rotating the C6-C7 bond of the minimized structure. Beginning with this minimized conformation, a full 360° rotation in 1° increments was performed on the C6-C7 bond, minimizing and calculating the energy for each increment. The energy profile for the C6-C7 bond rotation is shown in Figure 4.13. The graph shows minima at 90° and near 270° ,

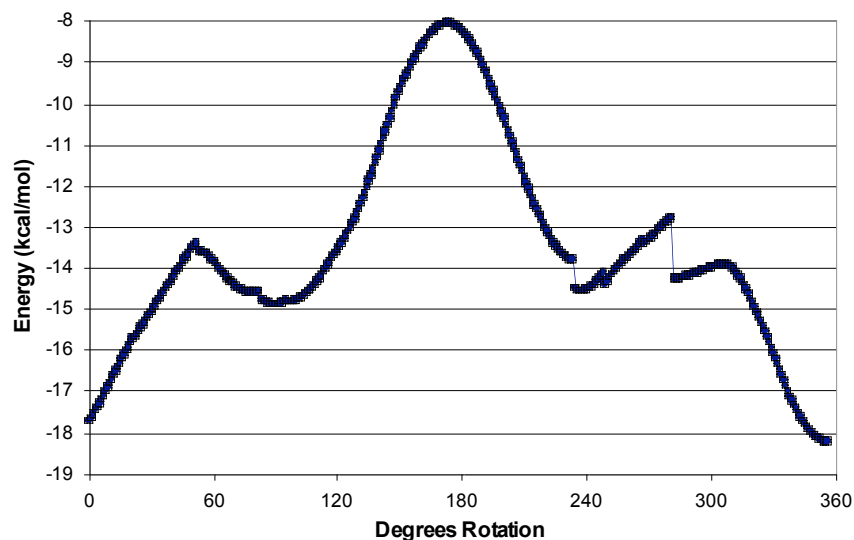


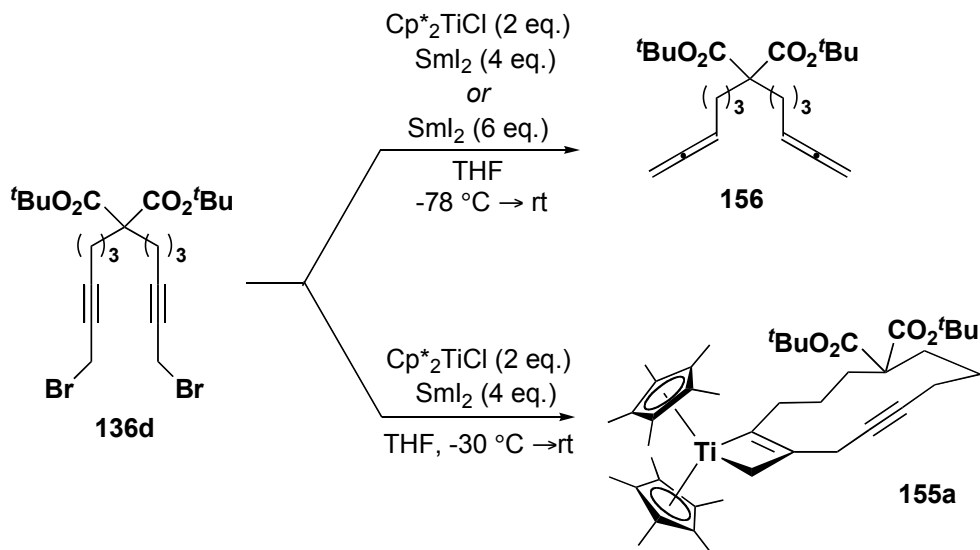
Figure 4.13: Energy profile for C6-C7 bond rotation of bis(*gem-tert-butyl*) ester **146b**

although there are two unaccountably discontinuous points in that region. At approximately 180°, an energy *maximum* is observed, 10.2 kcal/mol higher than the ground state energy, presumably from eclipsing the bulky *tert-butyl* esters. This barrier is about the same as for chair-chair interconversion of cyclohexane. The lifetime of this conformer is at best fleeting and at the reaction temperature for cyclization (-30 °C), the barrier for rotation is relatively high. The calculations thus concur that bis(*gem-tert-butyl*) ester **146b** is an unfavourable substrate for radical cyclization, consistent with experimental observation.

The balance between bicyclic titanacyclobutene or tricyclic di(titanacyclobutene) formation was previously probed by Tiege. His results show that increasing the stoichiometry of the titanocene and lowering the reaction temperature favours the formation of di(titanacyclobutene) product (Equation 2.3). Consequently, the synthesis of an analogous di(titanacyclobutene) complex was attempted using the α,ω -bis(bromopropargyl) malonate **136d** as the substrate. Disappointingly, none of the desired di(titanacyclobutene) complex was obtained, nor was the bicyclic allenyl titanacyclobutene. Instead, only the product **156** corresponding to the reduction of the propargyl bromide functionality to allene was observed (Scheme 4.10). The same

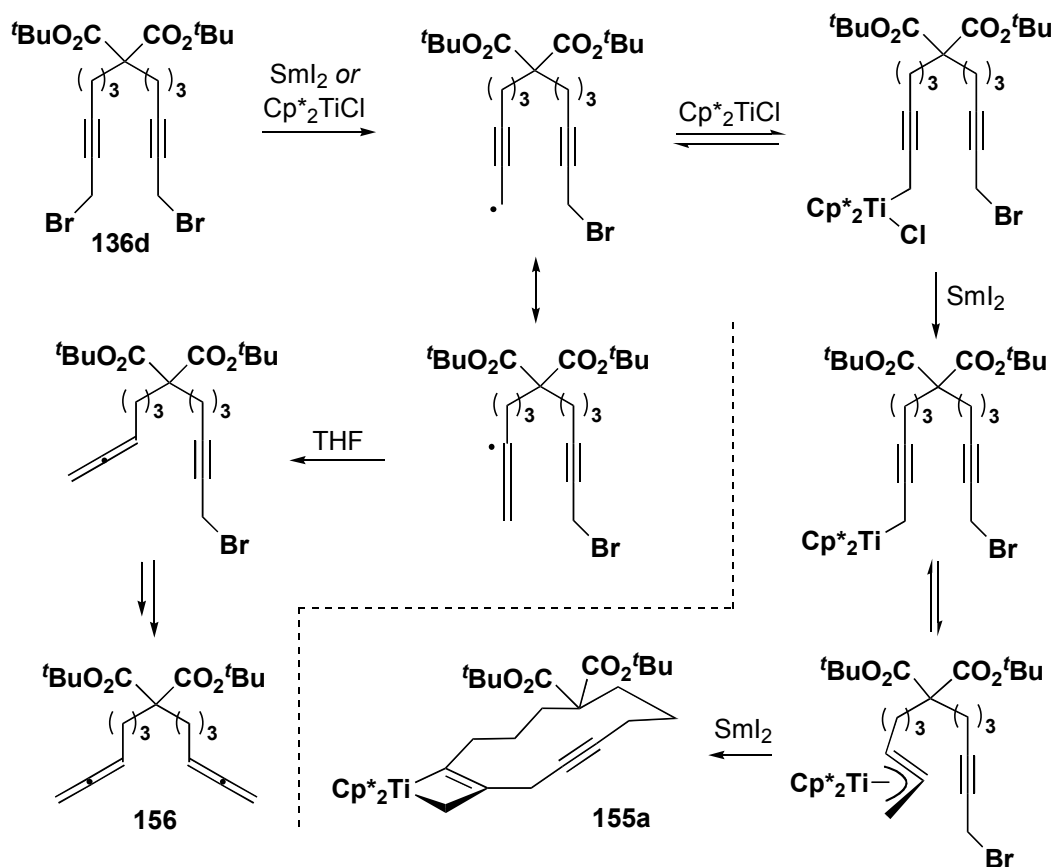
reduction product is obtained from the reaction using samarium diiodide in the absence of the

Scheme 4.10



titanocene reagent. When slightly higher reaction temperatures ($-30\text{ }^\circ\text{C}$) are employed, the twelve-membered bicyclic titanacyclobutene complex **155a** is observed to the exclusion of both di(titanacyclobutene) and reduction product. A proposed mechanism for the formation of the products is depicted in Scheme 4.11. The intermediate propargyl/allenyl radical follows one of two main pathways, trapping with the titanocene reagent or abstraction of hydrogen atom from THF. If reduction of the titanium(IV) intermediate is slow at $-78\text{ }^\circ\text{C}$, the pathway for the bis-allene product dominates. The absence of di(titanacyclobutene) complex from α,ω -bis(bromopropargyl) malonate **136d** in the presence of two equivalents of titanocene reagent may indicate that the radical cyclization step is significantly more rapid than the formation of the η^3 -propargyltitanium(III) intermediate. Qualitatively, this is reasonable as even at $-30\text{ }^\circ\text{C}$ the colour change of the reaction from dark-blue to red (indicating the

Scheme 4.11



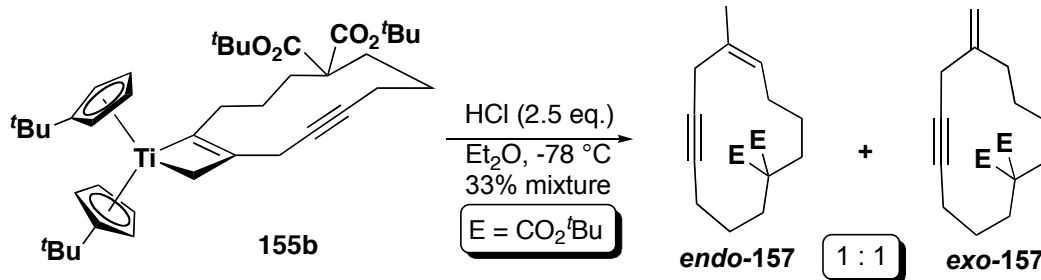
formation of a titanium(IV) complex) is almost instantaneous. This would also suggest, under these reaction conditions, radical cyclization forming a twelve-membered ring is kinetically faster than forming a seven-membered ring from an unsubstituted substrate, which can be interpreted as a consequence of an enhanced Thorpe-Ingold effect from the *gem*-diester moiety in the former.

4.3.3 Demetallation of bicyclic titanacyclobutenes

Titanacyclobutenes can react in a variety of ways but the simplest of these is protonolysis with a strong acid to liberate the organic fragment from the transition-metal. Thus, treatment of the twelve-membered bicyclic titanacyclobutene complex **155b** with anhydrous hydrogen chloride in diethyl ether gave an inseparable mixture of two constitutional isomers *endo*-**157** and *exo*-**157** in a near 1 : 1 ratio (Equation 4.8). One

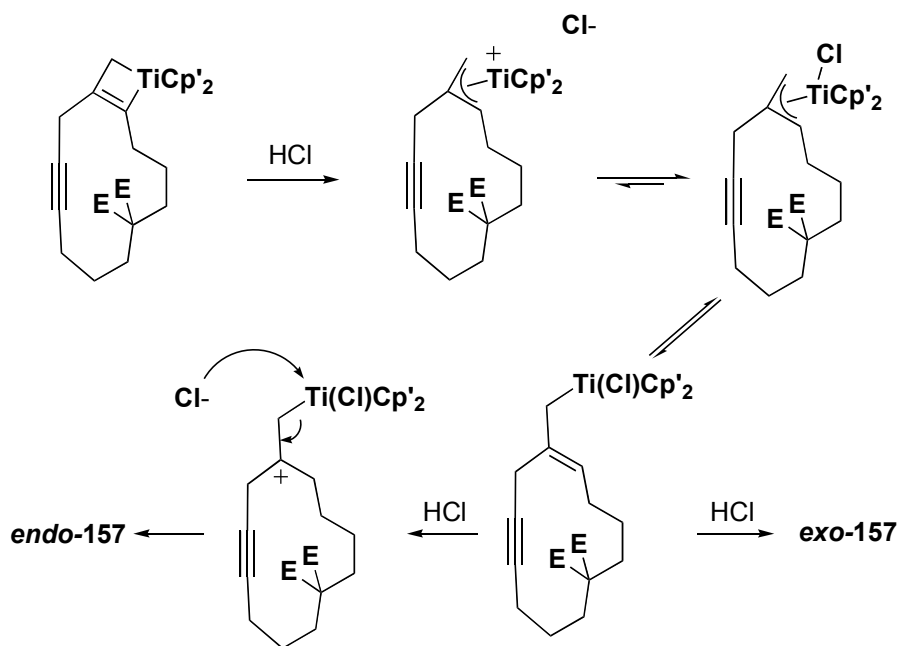
product corresponds to the twelve-membered carbocycle with an endocyclic double bond while the other is of the exocyclic alkene isomer. The rationale for the formation of the

Equation 4.8



isomeric products is outlined in Scheme 4.12. Protonation of the titanacyclobutene complex with HCl forms a tertiary carbocation. This is a canonical form of a cationic titanium-allyl complex. Inner sphere coordination of chloride gives a neutral η^3 -allyltitanium(IV) complex. A change in hapticity to the η^1 -form leads to two η^1 -isomers; with either the alkene di- or trisubstituted. The disubstituted *exo*-methylene isomer must be the least stable, a consequence of the weaker 2°-carbon metal bond and the thermodynamic instability of a less substituted olefin. Protonation of the double bond gives a tertiary carbocation, which can eliminate the titanium(IV) moiety to give the exocyclic double bond product. Alternatively, direct protonation of the titanium-alkyl bond produces the free endocyclic double bond macrocycle.

Scheme 4.12

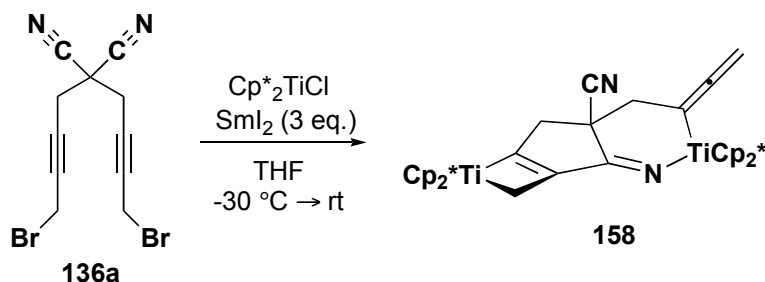


4.3.4 Titanacyclobutenes from bis-(bromopropargyl) malononitrile substrate

To investigate the scope of functional group tolerance in the titanium-mediated radical cyclization, a single α,ω -bis(bromopropargyl) substrate containing a *gem*-dicyano group was prepared (Scheme 4.1). The linear and compact nature of the nitrile groups would not be anticipated to provide much enhancement in the rate of cyclization. Curiously, when α,ω -bis(bromopropargyl) malononitrile **136a** was treated with decamethyltitanocene and samarium diiodide, the solution immediately became very dark, almost black, in place of the usual dark-red colour. A small amount of the crude product was analyzed by ^1H NMR spectroscopy, which revealed signals suggestive of a titanacyclobutene complex. Purification of the crude material by trituration with pentane left behind a light-red solid. The IR spectrum of this solid suggested the presence of both nitrile and allene, based upon stretches at 2218 and 1908 cm^{-1} , respectively. Four pentamethylcyclopentadienyl peaks of equal intensity at δ 2.08, 1.85, 1.79 and 1.64 indicated that two titanium centres were present and the compound lacked symmetry. Therefore, a stereogenic centre must also be present. Analysis of the ^1H and COSY

NMR spectra led to the tentatively proposed tricyclic titanacyclobutene structure **158** shown in Equation 4.9. In support of this assignment, the allene protons appear more

Equation 4.9

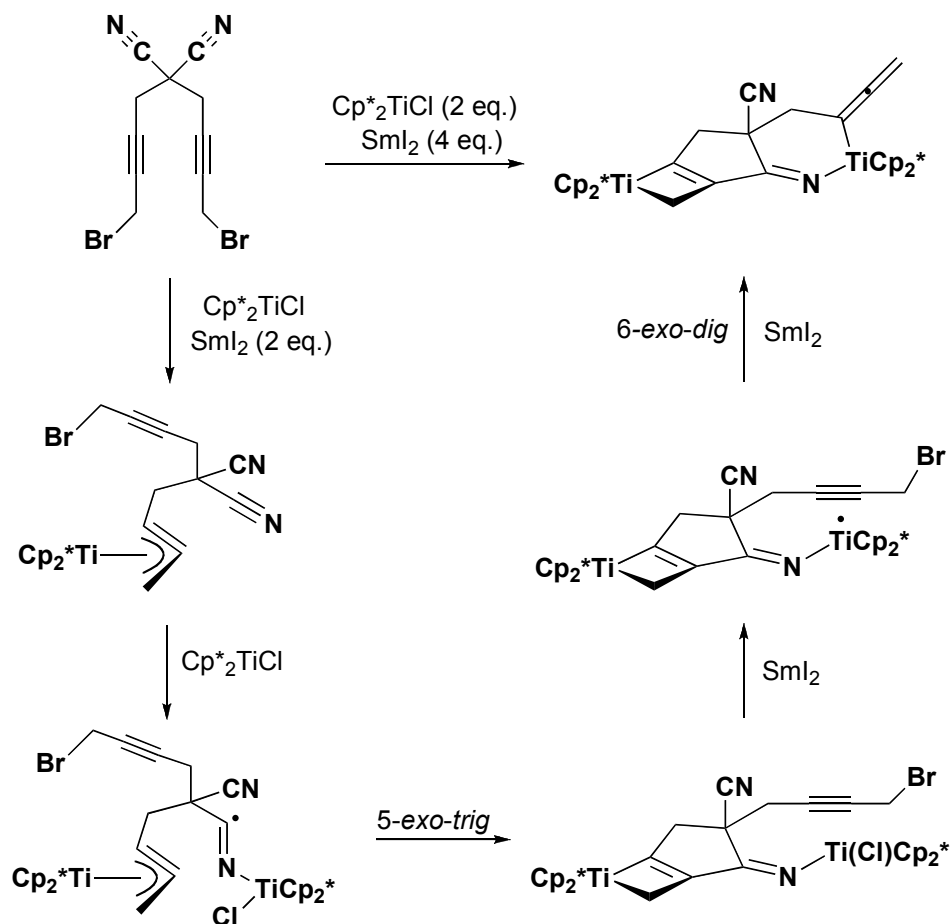


upfield than usual at δ 3.98 as two mutually coupled doublet of doublets. The 8.0 Hz geminal coupling constant for these protons is consistent with the typical value of 9.0 Hz.¹⁰⁵ The COSY spectrum shows a correlation to a single proton at δ 2.15 with a doublet ($J = 14$ Hz) of triplet splitting pattern. The other proton for this methylene pair resonates at δ 2.90 as a doublet ($J = 14.0$ Hz). The absence of coupling from this proton to the allene protons is quite interesting and is presumably a conformational effect of the six-membered ring. Due to the quaternary centre adjacent to this methylene and the ring fusion to a flat five-membered ring inhibits any ring flipping. The diastereotopic methylene protons in the five-membered ring resonate at δ 3.37 and 2.75, as a doublet of doublet and doublet of triplets, respectively, with one large geminal coupling (16.7 Hz) and smaller long-range couplings (2-4 Hz). The methylene unit in the metallacyclobutene moiety appears to be obscured by the pentamethylcyclopentadienyl resonances.

A plausible reaction mechanism accounting for the proposed product is shown in Scheme 4.13. A propargyltitanium(III) complex is initially formed by the reaction of one of the propargyl bromide moieties with bis(pentamethylcyclopentadienyl)titanium chloride and samarium diiodide. Another equivalent of bis(pentamethylcyclopentadienyl) titanium chloride is consumed by coordination of the nitrile which transfers single electron density to the π^* orbital of the nitrile, creating a

functional unit σ -radical character on the carbon adjacent to nitrogen. Fernandez-Matéos¹⁰⁶ and Gansäuer¹⁰⁷ have employed nitriles as radical traps for titanium-mediated epoxide opening reactions. This work suggests that the titanium plays a dual role, both generating the organic radical from the epoxide and activating the acceptor nitrile. Radical-radical annihilation by ring-closure forms the five-membered ring fused to the titanacyclobutene. Reduction of the titanium(IV) by samarium diiodide gives an odd-electron species. Bromine abstraction from the remaining propargyl functionality forms a six-membered ring by radical-radical annihilation with titanium(III). Both ring-closures are favourable from an orbital trajectory perspective.

Scheme 4.13



4.4 Future research and conclusion

Bicyclic titanacyclobutene complexes are accessible from α,ω -bis(bromopropargyl) substrates containing a *gem*-diester group in the carbon backbone. Unlike the α,ω -alkylpropargyl dibromomalonate substrates, the esters are tolerated in the reaction, demonstrating enhanced scope for this radical cyclization methodology. Depending on the ring size, exclusive formation of either allenyl or alkynyl bicyclic titanacyclobutene complexes are obtained. Where strain from the triple bond is minimal, the alkynyl-substituted product is preferred. When the propargyl substrate is unsymmetrical, chemoselectivity can be achieved by reducing the reaction temperature, at the intermediate η^3 -propargyltitanium(III) complex forming with the least hindered propargyl bromide. Further examples are needed to demonstrate generality of this selectivity.

The investigation of radical macrocyclization using the η^3 -propargyltitanium(III) template should be continued with the α,ω -bis(bromopropargyl) malonate series, in particular, to determine the limit of ring-sizes accessible and the ‘crossover’ point, where bicyclic cycloalkynyl systems are formed preferentially over the isomeric cycloallenyl complexes. Other rigidifying elements, such as double or triple bonds, which cannot participate in the intramolecular cyclization, should also be examined.

Preliminary results from the malononitrile indicate that alkylation with the nitrile substrates should be explored further, with both intra- and intermolecular variants of radical addition. Simple hydrolysis of the intramolecular radical cyclization products could provide synthetically useful α,β -unsaturated cyclic ketones. Alternatively, elaboration of the complex by insertion carbonyls or isonitriles could lead to expanded contexts for synthetic applications.

Chapter 5: Intermolecular radical addition to titanium propargyl complexes

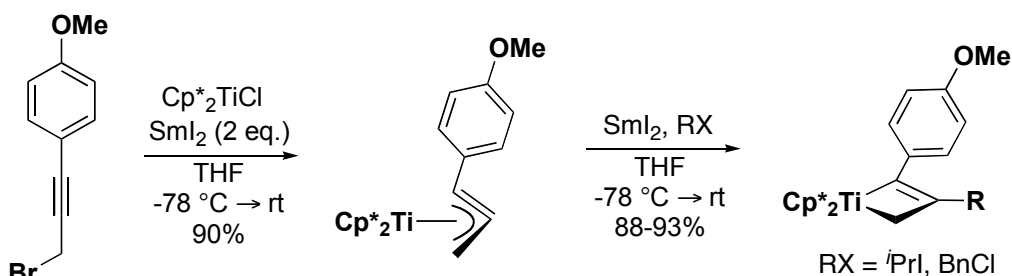
5.1 Introduction

Much of the research in central-carbon radical alkylation of propargyltitanium(III) complexes has been devoted halides as the radical precursors. This section will describe an alternative source of free radicals, epoxides. These radical precursors have advantages compared to alkyl halide analogues. First is atom economy. To obtain a radical from an alkyl halide, abstraction of the halide is necessary (unless under radical atom-transfer conditions) and thus a functional group is lost. In the case of epoxides, carbon-oxygen bond homolysis leads to a radical with no loss of atoms, and thus the oxygen functionality remains intact for further manipulation.

The use of bis(cyclopentadienyl)titanium chloride for reductive epoxide opening has grown tremendously since its introduction by Nugent and RajanBabu in the late 1980's.¹⁰⁸ Several reviews covering the use of this reagent have been written.¹⁰⁹ The general mechanism involves coordination of the oxygen atom to the Lewis acidic titanium(III) centre followed by a one electron transfer, creating a β -titanoxyethyl radical. This contrasts with pinacol coupling reactions of carbonyls where α -alkoxide radicals are the reactive intermediates. Trapping the carbon-centered radical with another equivalent of bis(cyclopentadienyl)titanium chloride gives the bimetallic species which can undergo 1,2-elimination, effectively deoxygenating the epoxide,¹¹⁰ yielding the alkene. Alternatively, addition of hydrogen atom donor such as 1,4-cyclohexadiene or γ -terpinene followed by protonolysis with collidine hydrochloride yields the corresponding alcohol. Synthetically useful intermolecular reactions are also possible, using activated olefins as radical acceptors.¹¹¹ If a suitable acceptor is present in the epoxide-containing substrate, intramolecular radical cyclization can occur. The latter has found use for key transformations in the synthesis of 12,6- and 12,8-eudesmanolides, a subclass of sesquiterpenoids,¹¹² and in the enantioselective synthesis of the odorant compound (-)- α -ambrinol, found in the intestinal tract of certain whales.¹¹³ A short review has been written, collecting examples of titanocene-mediated radical epoxide cyclizations in natural product synthesis.¹¹⁴

It is desirable to use η^3 -propargyltitanium(III) complexes as the radical trap in titanium-mediated epoxide opening. This effects the direct incorporation of an oxygen atom into the titanacyclobutene cyclization product, a seemingly simple task that has been very difficult accomplish. Prior investigation of haloethers to generate α -alkoxyalkyl radicals led either to decomposition or radical fragmentation to yield non-oxygenated titanacyclobutene products. The use of α,ω -bis(bromopropargyl) ethers in the intramolecular radical cyclization chemistry also failed (*vide supra*). Remote oxygenation was, however, not a problem as illustrated in Scheme 5.1.¹¹⁵

Scheme 5.1

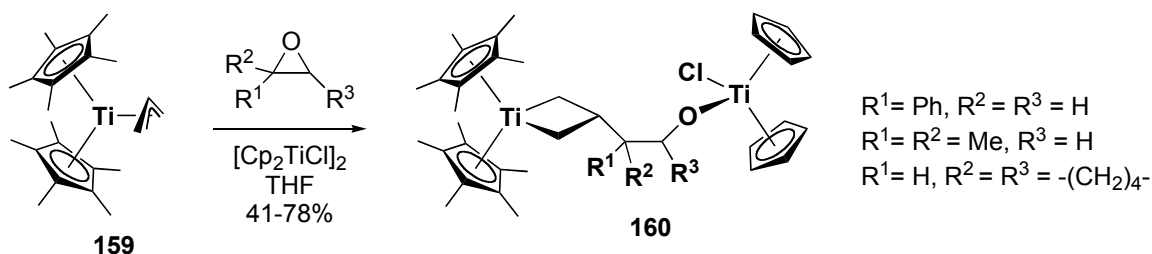


The initial goal of this investigation was to use a one-pot procedure to generate a β -titanoxyethyl radical and trap this intermediate by reaction with a η^3 -propargyltitanium(III) source. The advantage of such a system is that the reagent that generates the radical intermediate is incorporated in the final product. Thus, isolation of the product away from spent reagents is much simpler, although at the cost of using another equivalent of the titanocene reagent. The bimetallic product can in principle be manipulated further, its chemistry potentially enriched from the presence of two transition metal centres.

The use of alkyl-substituted titanocenes although some have been employed in mechanistic studies, regiodivergent synthesis, and cases where the unsubstituted titanocene reagent leads to decomposition.^{116,122} Titanium reagents other than a titanocene chloride, however, have not been investigated for this reaction manifold. Casty, *et al.*, have reported the reaction of bis(pentamethylcyclopentadienyl)- η^3 -allyltitanium(III) complex **159** with epoxides in the presence of

bis(cyclopentadienyl)titanium chloride to generate the β -alkoxyalkyl titanacyclobutene complexes (Scheme 5.2).^{60a,117} The allyl complex itself is unreactive toward epoxides,

Scheme 5.2



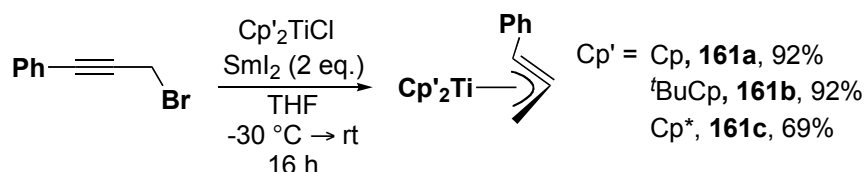
presumably due to the steric bulk around the titanium centre. Demetallation by acidolysis gave the corresponding alcohols in modest yields.

5.2 Results

5.2.1 Synthesis and characterization of η^3 -propargyltitanium(III) complexes

The intermediate η^3 -phenylpropargyltitanium(III) complex **161a** as well as substituted analogues **161b** and **161c** can be synthesized by addition of phenyl propargyl bromide to bis(cyclopentadienyl)titanium chloride and samarium diiodide (Equation 5.1).⁶¹ The crude complexes are obtained in good to high yield as a green oil or solid for the unsubstituted and *tert*-butyl-substituted ligands, while the pentamethylcyclopentadienyl complex **161c** is a dark, almost black-purple, colour.

Equation 5.1



Recrystallization of the green titanocene propargyl complex **161a** in toluene at $-30\text{ }^{\circ}\text{C}$ surprisingly gave purple single-crystals, which were characterized by X-ray crystallography to be the di(titanacyclobutene) dimer **162a** (Figure 5.1).

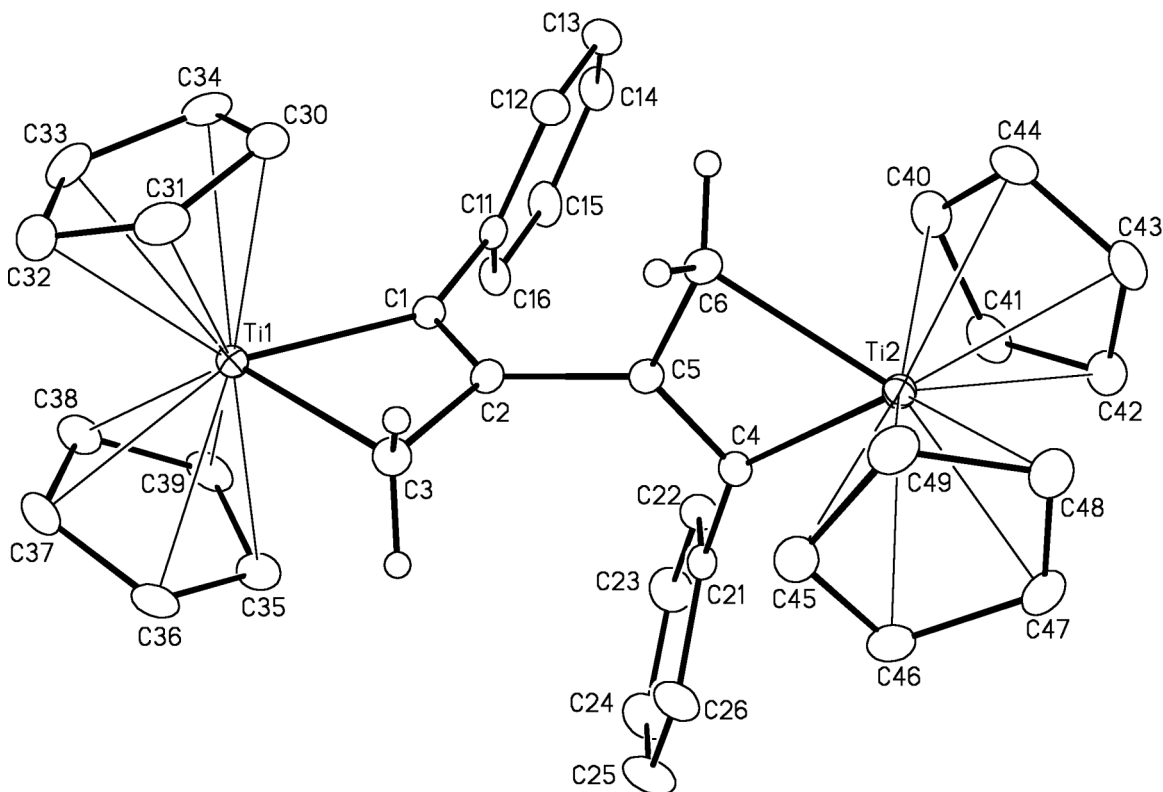
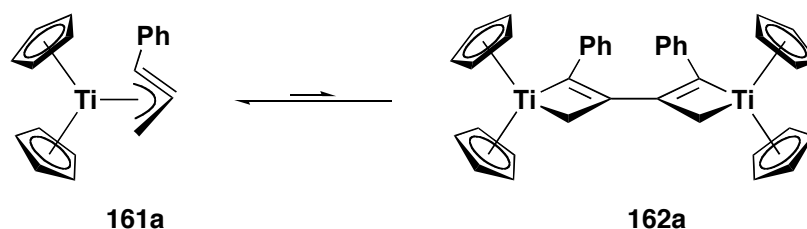


Figure 5.1: Perspective view of $[\text{Cp}_2\text{Ti}\{\text{PhC}=\text{C}(\text{CH}_2)\text{C}(\text{CH}_2)=\text{CPh}\}\text{TiCp}_2]$ **162a** showing the atom labelling scheme. Non-hydrogen atoms are represented by Gaussian ellipsoids at the 20% probability level. Hydrogen atoms are shown with arbitrarily small thermal parameters for the methylene groups, and are not shown for the cyclopentadienyl and phenyl groups. $R_I = 0.0349$, $R(w) = 0.1014$.

Low temperature NMR studies of the paramagnetic monomeric **161a** in toluene- d^8 suggest that some titanacyclobutene complex is present in solution. Although the ^1H NMR spectrum remains broad between $-80\text{ }^{\circ}\text{C}$ and room temperature, the ^{13}C NMR spectrum shows at $-80\text{ }^{\circ}\text{C}$ characteristic resonances consistent with a titanacyclobutene complex. The sp^2 α -carbon, β -carbon and α -methylene carbons of the titanacyclobutene core resonate at typical values (δ 214.1, 90.4 and 78.8, respectively). The *ipso* carbon of the phenyl ring is seen at δ 145.8, while the other phenyl peaks are unobserved, probably

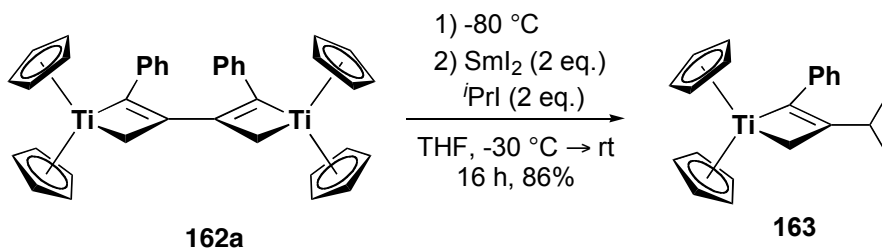
from obstruction by the intense toluene carbon signals. The cyclopentadienyl carbons are seen as an intense peak at δ 110.4. Warming the solution to -20 °C, however, results in the disappearance of these signals, while re-cooling the sample leads to their reappearance. This strongly suggests that there is an equilibrium between the monomeric propargyltitanium(III) complex and the dimeric titanium(IV) metallacyclobutene complex in solution, entropically favouring the monomer at high temperature (Equation 5.2).

Equation 5.2



To further confirm this equilibrium hypothesis, the diamagnetic material used for the low-temperature NMR experiments was subjected to central-carbon radical alkylation conditions through the addition of isopropyl iodide and samarium diiodide to the titanium(III)/(IV) mixture (Equation 5.3). The known α -phenyl- β -isopropyl

Equation 5.3



titanacyclobutene complex **163** was isolated in 86% yield as a red solid, with no other products detected by ^1H NMR spectroscopy, consistent only with the equilibrium hypothesis. Single crystals were grown from a cool pentane solution suitable for X-ray analysis. A representation of the solid-state structure is shown in Figure 5.2.

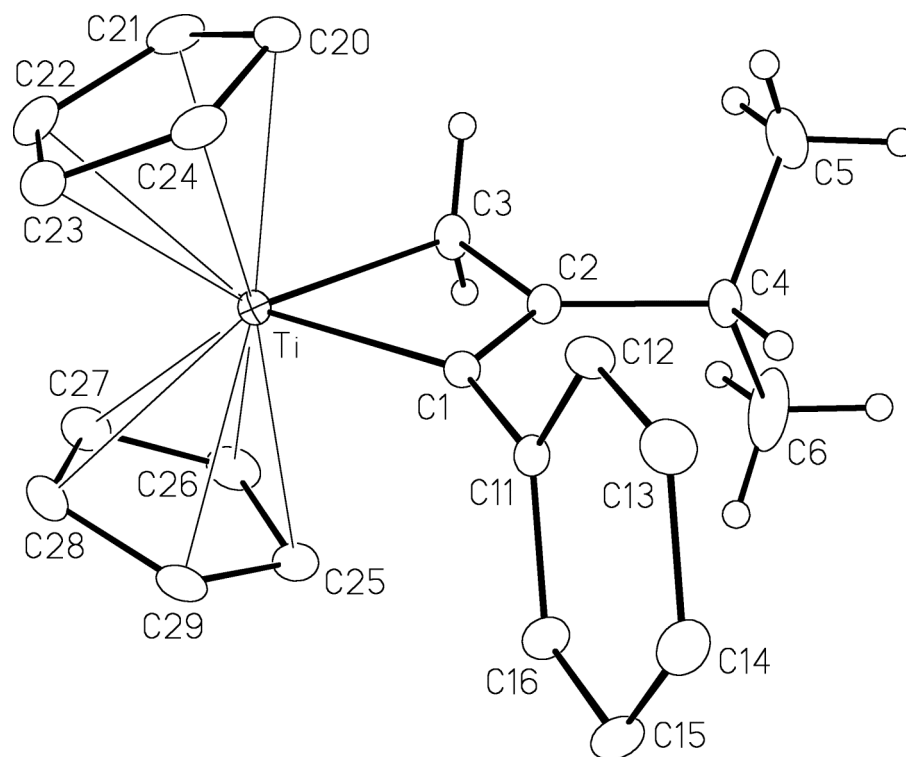


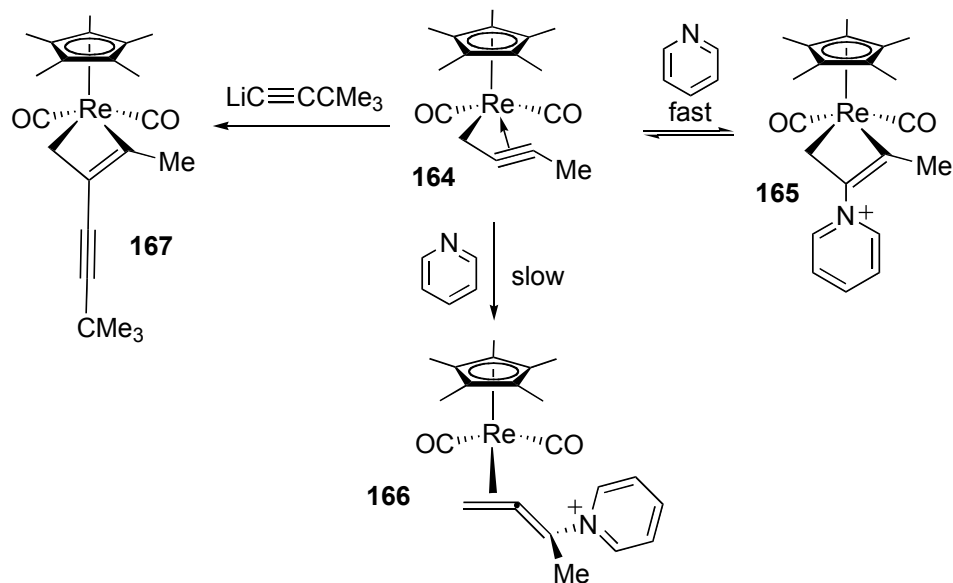
Figure 5.2: Perspective view of $[(\eta^5\text{-C}_5\text{H}_5)_2\text{Ti}\{\eta^2\text{-PhC}=\text{C}(\text{iPr})\text{CH}_2\}]$ **163** showing the atom labelling scheme. Non-hydrogen atoms are represented by Gaussian ellipsoids at the 20% probability level. Hydrogen atoms of the methylene and isopropyl groups are shown with arbitrarily small thermal parameters, while phenyl and cyclopentadienyl hydrogens are not shown. $R_I = 0.0333$, $R(w) = 0.0917$.

When the crystallization of propargyltitanium complex **161a** takes place from a concentrated pentane solution, green crystals form relatively quickly over a few days. Over the span of a couple of weeks, the initially-formed crystals are slowly replaced by newly-formed purple crystals. This implies that the η^3 -propargyltitanium(III) complex crystallizes first, slowly redissolves, equilibrates, and crystallizes again as the dimer complex. Isolated crystals of the dimer remain purple in colour for weeks, even at room temperature. However, when exposed to solvent, the purple solid dissolves and the solution rapidly becomes green, indicating the equilibrium shift from the dimer to monomer at higher dilution.

The hypothesis that addition to η^3 -propargyl-transition-metal complexes can be reversible has been explored with rhenia¹¹⁸ and platinumacyclobutenes^{100b} prepared the

reversible addition of nitrogen or phosphorus nucleophiles. For example, Casey, *et al.*, have found that the kinetic product of addition of pyridine to η^3 -propargylrhenium complex **164** at low temperature is the metallocyclobutene complex **165** from nucleophilic attack at the central-carbon (Scheme 5.3).^{118c} Upon warming, dissociation of pyridine is followed by irreversible addition to form the thermodynamically more

Scheme 5.3



stable η^2 -allene complex **166**. Addition of carbon nucleophiles such as lithium acetylide however, proceeds irreversibly to give the η^3 -propargyl complex, affording the rhenacyclobutene complex **167**. Therefore, the equilibrium between di(titanacyclobutene) and η^3 -propargyltitanium complexes is possibly the first example of reversible addition of carbon nucleophiles to η^3 -propargyl complexes.

The *tert*-butyl-substituted titanium complex **161b** also displayed monomer to dimer equilibrium. In solution at room temperature, the complex is dark-green, consistent with the monomeric titanium(III) complex. When cooled to $-30\text{ }^\circ\text{C}$, the colour becomes dark-purple, returning quickly to green if allowed to warm back to ambient temperature. The permethylated analogue **161c** is more difficult to assess by colour alone because it appears dark-purple both at room temperature and $-30\text{ }^\circ\text{C}$. However, crystallization from pentane at $-30\text{ }^\circ\text{C}$ afforded very small, flat, dark crystals. X-ray

crystallographic analysis revealed that co-crystallization of two species had occurred, one being the β -(phenylpropargyl)-substituted metallacycle **175** (*vide infra*) and the other, the monomeric η^3 -propargyltitanium(III) complex **161c** (Figure 5.3). The titanacyclobutene coproduct presumably arises from a competitive radical alkylation during the synthesis of the propargyl complex. This side reaction was also observed by Ogoshi in his original preparation of the 3,3'-bi(titanacyclobutene) complex from the unsubstituted propargyl.¹¹⁹

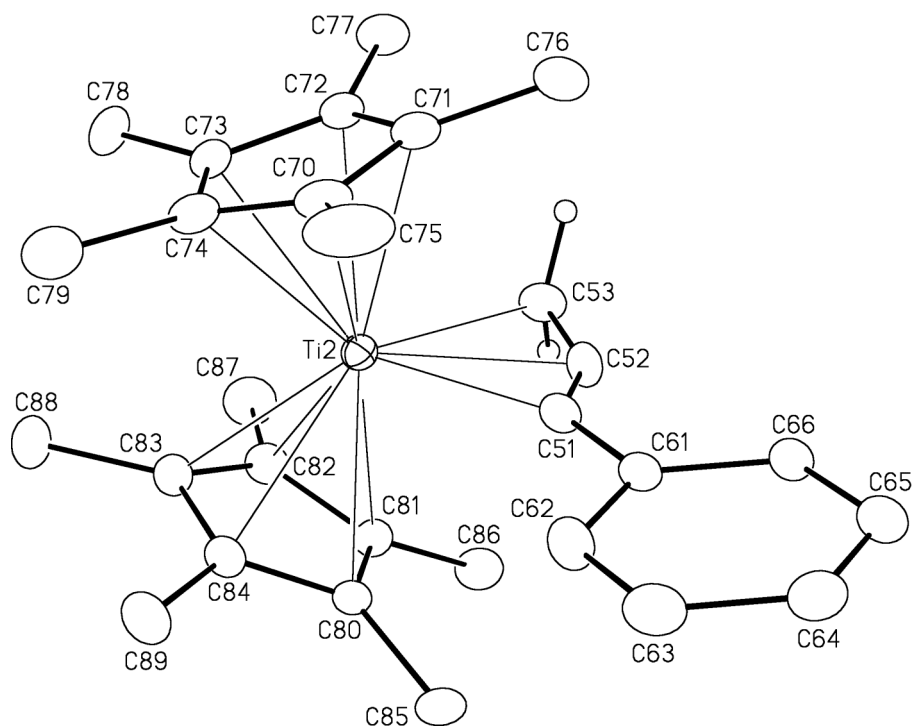


Figure 5.3: Perspective view of $[(\eta^5\text{-C}_5\text{Me}_5)_2\text{Ti}\{\eta^3\text{-PhCCCH}_2\}]$ **161c** showing the atom labelling scheme. Non-hydrogen atoms are represented by Gaussian ellipsoids at the 20% probability level. Hydrogen atoms are shown with arbitrarily small thermal parameters for the methylene group, and are not shown for the methyl and phenyl groups. $R_1 = 0.0622$, $R(w) = 0.1843$.

The η^3 -propargyltitanium(III) complex **161c**, which appears to be the first η^3 -propargyltitanium(III) complex characterized crystallographically, has a C51-C52-C53 bond angle of 149.6° for the carbon atoms bound to titanium. This is consistent with other reported η^3 -propargyl-transition-metal complexes, which shown values ranging from $145 \sim 155^\circ$, with one anomalous zirconium complex described as ‘nearly linear’.¹²⁰ The carbon-carbon bond lengths are also consistent with hybridization halfway between

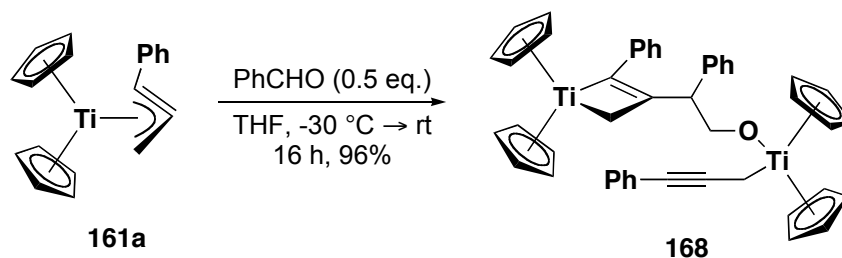
propargyl and allenyl. The central carbon bonded to the terminal methylene (C52-C53) has a length of 1.376 Å, between that of a double and single bond while the C51-C52 bond length, 1.250 Å, is between that of a triple and double bond. The backbone of the η^3 -propargyl moiety is more or less coplanar with the titanium centre (least-squares planes atom deviations: Ti2 -0.0053, C51 0.019, C52 -0.030, C53 0.017 Å), contrasting the corresponding η^3 -allyl complexes which are side-on bonded to the metal.¹²¹

It is interesting that the phenylpropargyltitanocene complex **161c** crystallizes as the dimer, while the permethylatedcyclopentadienyl analogue **161a** crystallizes as the monomer. This counters the previous notion that dimerization is favoured only for electron-rich cyclopentadienyl ligands. This observation could thus be a steric effect, since the pentamethylcyclopentadienyl ligands are much bulkier than the unsubstituted analogue. However, because Ogoshi did isolate the di(titanacyclobutene) of the unsubstituted propargyl ligand, steric interactions between the ancillary ligands are probably not as important as the repulsion between the ligand and the α -substituent on the titanacycle. As seen in the solid-state structure of dimer **161a**, the α -phenyl group is perpendicular to the cyclopentadienyl ligands, even though this breaks conjugation with the double bond in the titanacyclobutene core. The permethylated η^3 -phenylpropargyl complex probably does not dimerize to any great extent because such a conformation would force the phenyl group into the methyl groups on both ligands. The equilibrium described in Equation 5.2 presumably lies heavily to the left.

5.2.2 Bimetallic titanacyclobutenes from epoxides

To test the reactivity of η^3 -propargyltitanium(III) complexes toward reductive epoxide opening, styrene oxide was added to two equivalents of [bis(cyclopentadienyl)- η^3 -3-phenylpropargyl]titanium **161a** (Equation 5.4). The green colour of the titanium(III) complex was replaced by dark-red over the course of several hours at room temperature, providing the spectroscopically clean bimetallic titanacyclobutene **168** in 96% yield.

Equation 5.4



The structure of complex **168** was confirmed by extensive NMR analysis; the carbon and hydrogen numbering scheme is detailed in Figure 5.4. The ^1H NMR spectrum shows four cyclopentadienyl singlets; the inequivalence of the cyclopentadienyl ligands arises from the benzylic stereogenic centre. The titanacyclobutene moiety was confirmed by diagnostic signals in the ^{13}C NMR spectrum: δ 211.2, 97.0 and 69.5 for the titanium-vinyl carbon, central carbon and sp^3 carbon of the metallacycle, respectively. The carbon and hydrogen assignments for complex X are summarized in Table X excluding the phenyl signals. The η^1 -phenylpropargyl moiety was characterized by signals at δ 86.4 and 80.6 in the ^{13}C NMR spectrum and, in the IR spectrum, a strong absorption at 2176 cm^{-1} corresponding to the carbon-carbon alkyne stretch. The stretch is quite intense due to the large change in dipole moment induced by the electropositive titanium. EI mass spectrometry does not provide the molecular ion, but rather fragmentation of the molecule occurs and an m/z peak corresponding to the titanium-propargyl portion is observed (Scheme 5.4). The molecular radical cation can undergo carbon-carbon bond homolysis to give the observed cationic titanium propargyl complex. The neutral radical portion of the molecule is benzylic radical. The observed signal may also be from residual starting titanium reagent.

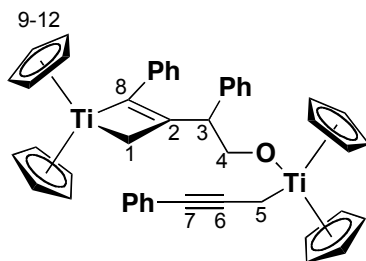


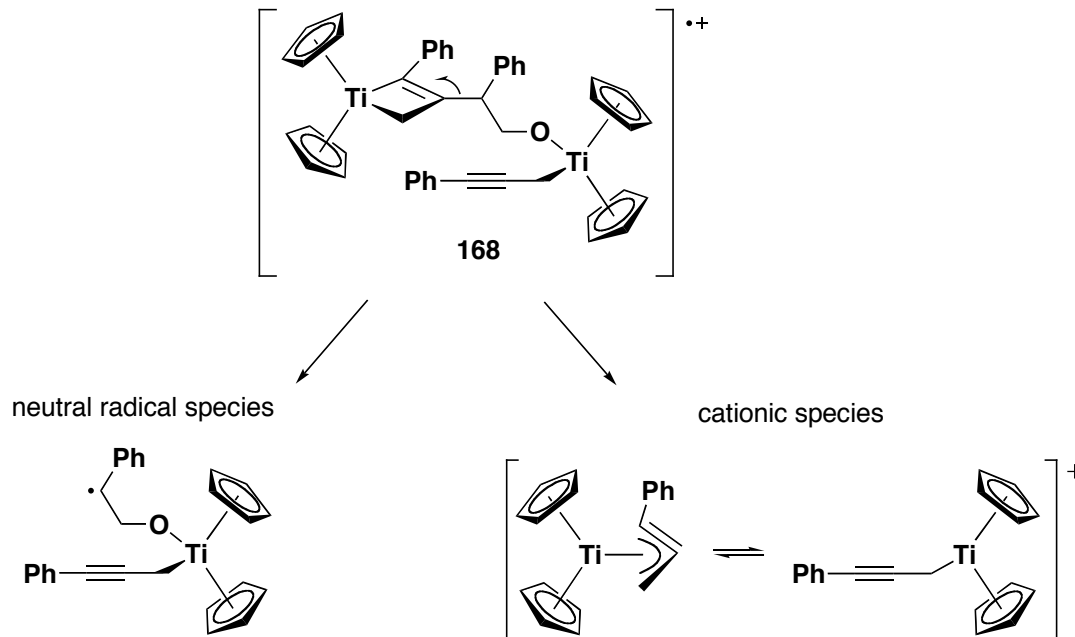
Figure 5.4: Carbon and hydrogen labelling scheme for bimetallic titanacyclobutene **168**

Table 5.1: Select ^1H and ^{13}C NMR assignments for bimetallic titanacyclobutene **168**^a

$^1\text{H}^b$	$^{13}\text{C}^c$
H _{1a} , δ 3.11 (d, J = 11.7 Hz, 1H)	C ₁ , δ 69.5
H _{1b} , δ 2.84 (d, J = 11.7 Hz, 1H)	C ₂ , δ 97.0
-	C ₃ , δ 48.8
H ₃ , δ 3.78 (dd, J = 9.7 Hz, J = 6.0 Hz, 1H)	C ₄ , δ 80.6
H _{4a} , δ 4.65 (dd, J = 11.2 Hz, J = 9.7 Hz, 1H)	C ₅ , δ 26.5
H _{4b} , δ 4.44 (dd, J = 11.2 Hz, J = 6.0 Hz, 1H)	C ₆ , δ 80.6
H _{5a} , δ 2.06 (d, J = 12.5 Hz, 1H)	C ₇ , δ 86.4
H _{5b} , δ 1.91 (d, J = 12.5 Hz, 1H)	C ₈ , δ 211.2
-	C ₉ , δ 113.0
-	C ₁₀ , δ 112.2
-	C ₁₁ , δ 113.2
H ₉ , δ 5.68	C ₁₂ , δ 111.5
H ₁₀ , δ 5.61	
H ₁₁ , δ 5.56	
H ₁₂ , δ 5.42	

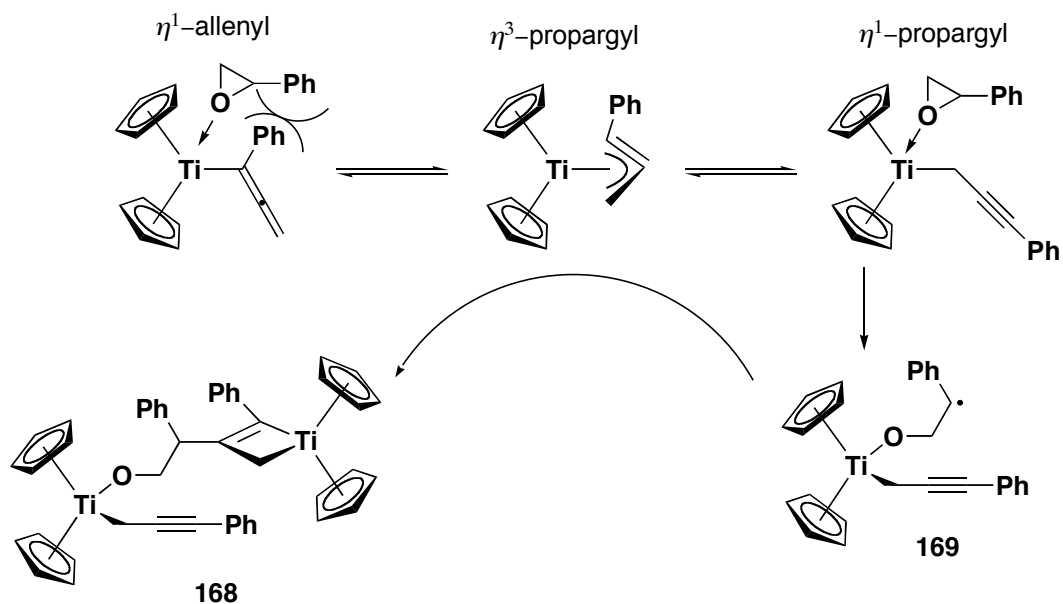
^a assignments for Ph signals not included; ^b C₆D₆, 300 MHz; ^c C₆D₆, 100 MHz

Scheme 5.4



A plausible mechanism for the product formation is shown in Scheme 5.5. The η^3 -propargyltitanium intermediate **161a**, in addition to being in equilibrium with the dimer **162a**, is in equilibrium with the η^1 -isomer, where the odd-electron is metal- rather than ligand-centered. The η^1 -propargyl structure is probably the only reactive odd-electron complex present, considering that the η^1 -allenyl resonance form is much more sterically hindered at the metal centre. Coordination and single-electron transfer to the epoxide gives a stabilized secondary benzylic β -titanoxy radical **169**, which then adds to the central carbon of the remaining η^3 -propargyl titanium complex **161a** to give the observed product **168**. Under similar reaction conditions but using isobutylene oxide or cyclohexene oxide, no colour change of the green solution is observed even after several days at room temperature. The stabilized nature of the benzylic radical intermediate clearly accounts for the ease with which single-electron transfer occurs, although the tertiary β -alkoxy radical formed from isobutylene oxide would be qualitatively only slightly less stable. A steric argument is equally plausible for isobutylene oxide.¹²² Gansäuer found that unsubstituted, monosubstituted and *cis*-1,2-disubstituted epoxides

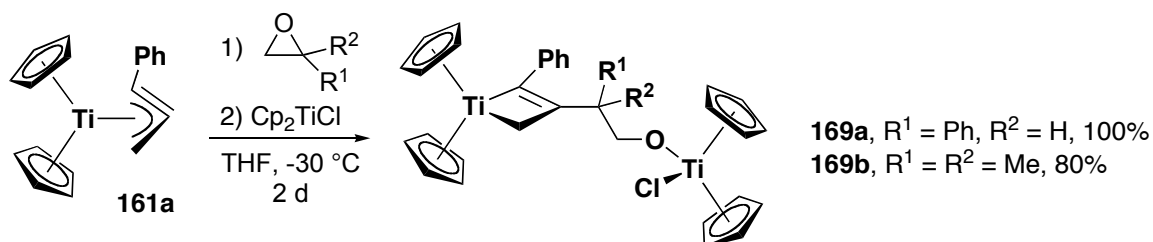
Scheme 5.5



bind to titanocene monochloride more strongly than THF, and can therefore, thermodynamically displace solvent from the coordination sphere¹²³ However, 1,1-disubstitued and trisubstitued epoxides bind less favourably than THF, although they still undergo rapid ring-opening. The η^1 -propargyltitanium(III) complex appears to be more sterically restrictive than the chloride complex, which is entirely unsurprising.

The use of bis(cyclopentadienyl)titanium chloride as the epoxide opening reagent was then examined (Equation 5.5). This system has the advantage of consuming only one equivalent of the propargyltitanium(III) complex, a valuable material. Unfortunately, the propargyltitanium(III) complex must be pre-synthesized and not generated *in situ* from the corresponding halide and samarium diiodide. This is because samarium diiodide is a strong reducing agent, capable of epoxide deoxygenation¹²⁴ and other epoxide chemistry.¹²⁵ Isolation of the propargyltitanium(III) complex is desirable to avoid potential side reactions with residual samarium diiodide.

Equation 5.5



The structures of **169a** and **169b** were elucidated by NMR spectral analysis providing data very similar to bimetallic complex **168** but lacking the η^1 -propargyl moiety. Single-crystals of **169a** were grown from a benzene / pentane solution at low temperature. A representation of the solved X-ray structure is shown in Figure 5.5, confirming the spectroscopic assignment.

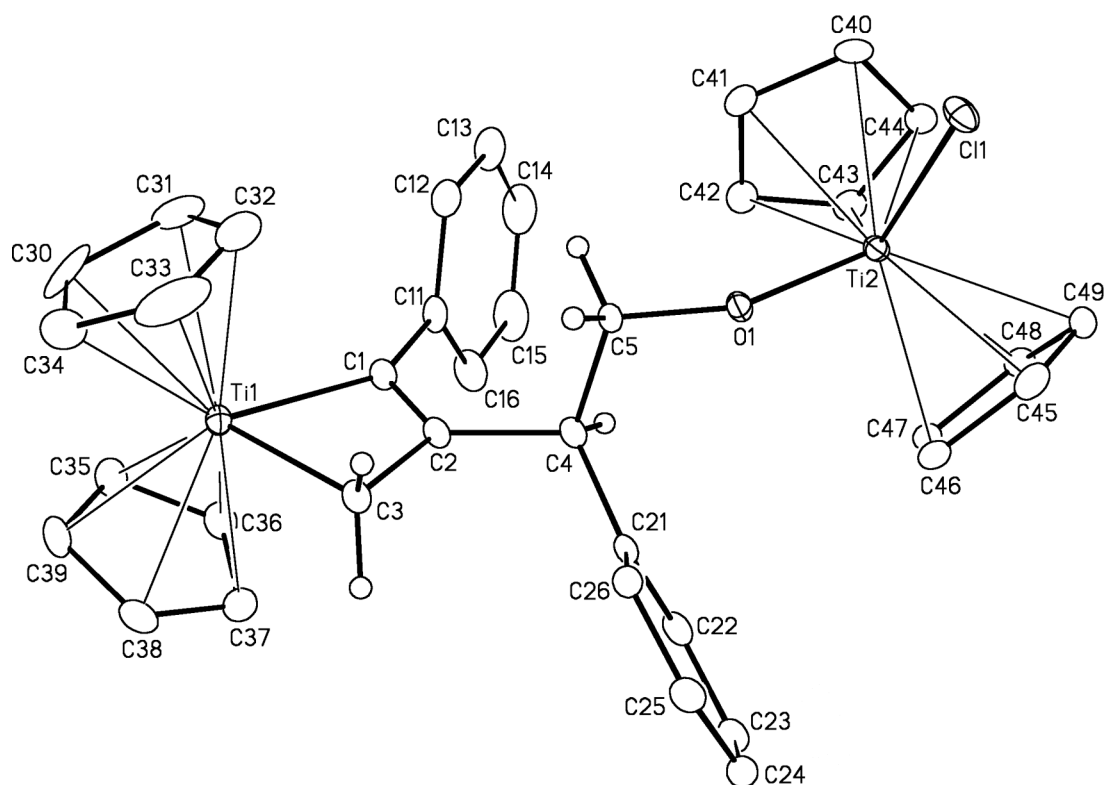
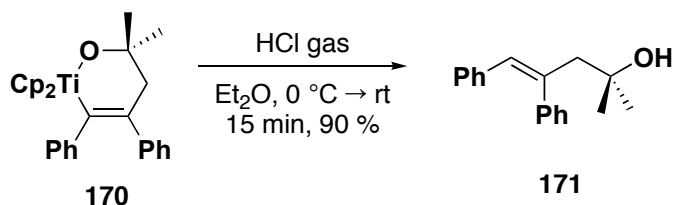


Figure 5.5: Perspective view of one of two crystallographically independent $[\text{Cp}_2\text{Ti}\{\text{PhC}=\text{C}(\text{CHPhCH}_2\text{OTiClCp}_2)\text{CH}_2\}]$ **169a** molecules (molecule A) showing the atom labelling scheme. Non-hydrogen atoms are represented by Gaussian ellipsoids at the 20% probability level. Hydrogen atoms are shown with arbitrarily small thermal parameters and are not shown for the cyclopentadienyl or phenyl groups. $R_I = 0.0422$, $R(w) = 0.1091$.

5.2.3. Demetallation of bimetallic titanacyclobutene complex

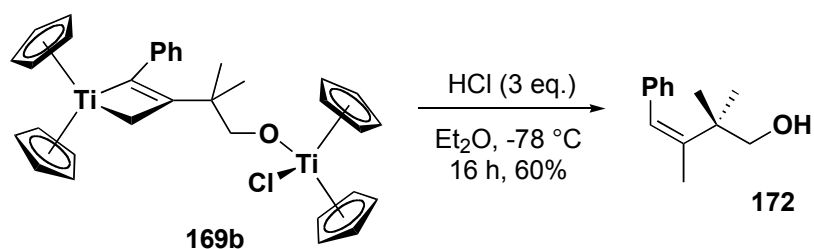
Grubbs demonstrated that insertion of carbonyls into the titanium-alkyl bond of diphenyl-substituted titanacyclobutene give six-membered titanaoxocyclohexenes.¹²⁶ Acidolysis of titanaoxocyclohexene complex **170** (obtained from the insertion of acetone) with anhydrous HCl gas affords the corresponding homoallylic alcohol **171** (Equation 5.6). Secondary and tertiary alcohols are obtained from protonolysis of aldehyde and ketone insertion complexes, while primary alcohols are inaccessible due to competing insertion of formaldehyde into the titanium-vinyl bond.¹²⁷

Equation 5.6



Protonolysis of titanacyclobutenes from β -alkoxyalkyl radical addition to η^3 -propargyltitanium(III) complexes also affords homoallylic alcohols. Upon treatment with two equivalents of hydrochloric acid in diethyl ether, bimetallic titanacyclobutene complex **169b** undergoes protonolysis to afford the isomerically pure homoallylic primary alcohol **172** (Equation 5.7). The stereochemistry of the double bond was verified by NOE experiments, with irradiation of the allylic methyl resulting in an enhancement of 2.8% of the vinyl hydrogen signal. Conversely, irradiation of the vinyl hydrogen only resulted in

Equation 5.7

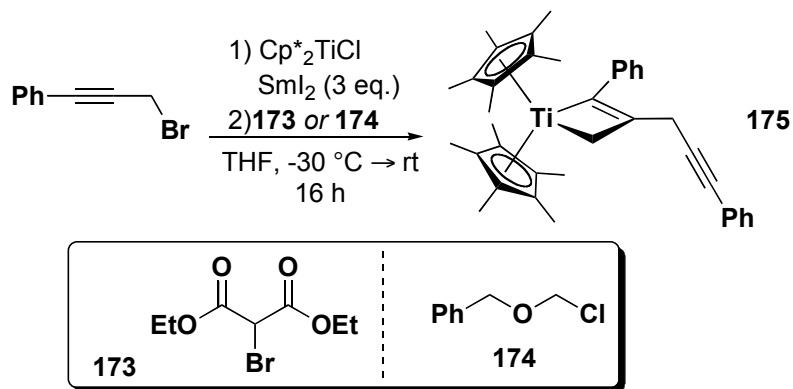


enhancement of the allylic methyl signal by 4.6%. This stereoselective homoallylic alcohol synthesis provides a simple two-step route to this class of useful trisubstituted olefin synthons.

5.2.4 Synthesis of ester-functionalized titanacyclobutenes by intermolecular radical addition

In an attempt to expand the scope of substrates used for radical addition, bromodiethyl malonate was evaluated as the free radical precursor. Iodomalonates have been used in radical atom-transfer chemistry using tin-based reagents¹²⁸ and the diethyl malonyl radical is proposed as an intermediate in the Mn(OAc)₃-assisted addition of alkylidenecyclopropanes to diethyl malonate.¹²⁹ The addition of this resonance-stabilized radical would provide an efficient route titanacyclobutenes with oxygen-containing β -substituents. The η^3 -propargyltitanium(III) complex was thus generated *in situ* by the standard method followed by the addition of bromodiethyl malonate. Surprisingly, the resulting dark solid was the known β -phenylpropargyl titanacyclobutene complex **175**,⁶¹ and not the anticipated β -malonate complex (Equation 5.8). The structure was confirmed by single-crystal X-ray diffraction, giving the same complex characterized previously in

Equation 5.8



the co-crystallite containing the η^3 -propargyltitanium(III) complex **161c** (Figure 5.6). The ¹H NMR spectrum of the titanacyclobutene **175** also agreed with that of the known compound.

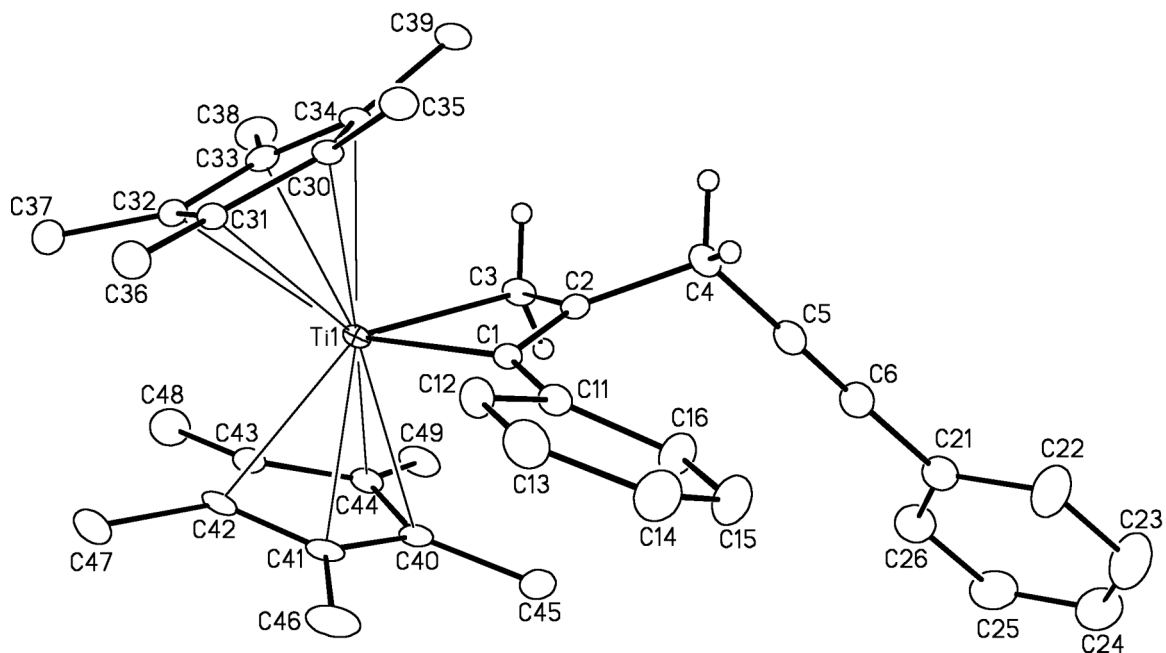
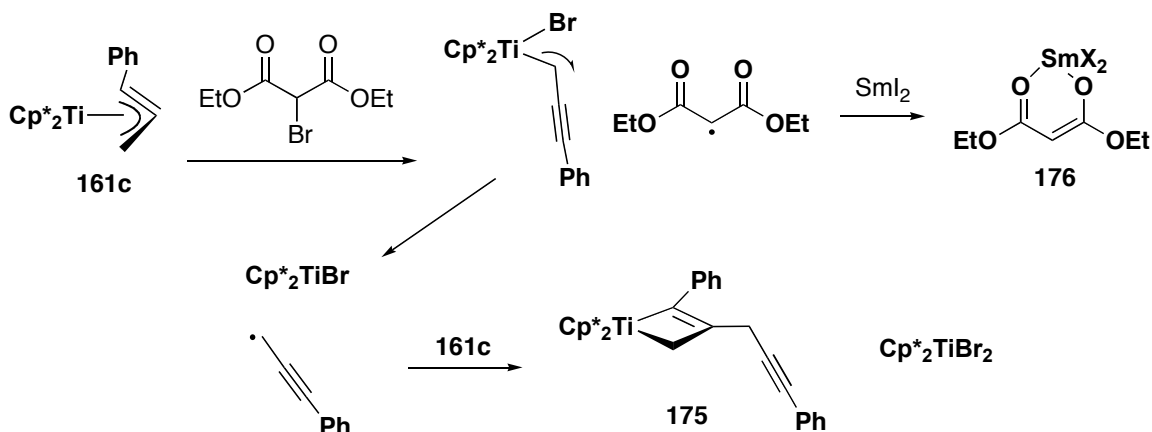


Figure 5.6: Perspective view of $[(\eta^5\text{-C}_5\text{Me}_5)_2\text{Ti}\{\eta^2\text{-PhC}=\text{C}(\text{CH}_2\text{C}\equiv\text{CPh})\text{CH}_2\}]$ **175** showing the atom labelling scheme. Non-hydrogen atoms are represented by Gaussian ellipsoids at the 20% probability level. Hydrogen atoms are shown with arbitrarily small thermal parameters for the methylene groups, and are not shown for the methyl and phenyl groups. $R_1 = 0.0622$, $R(w) = 0.1843$.

The same product was observed when 1,2-dibromoethyl ethyl ether **174** was used to generate the free organic radical (Equation 5.8). The problem presumably arises from the *facile* over-reduction of the malonate to the anion induced by the samarium diiodide. Scheme 5.6 shows a proposed rationale, in which the initial step is formation of the malonate radical by bromine abstraction from η^1 -propargyltitanium(III). The electrophilic malonate radical could easily be reduced by samarium diiodide to form the

Scheme 5.6



chelated samarium enolate species **176**.¹³⁰ The titanium(IV) propargyl complex is then left to disproportionate. Since only nucleophilic radicals have been demonstrated to undergo radical addition to η^3 -propargyltitanium(III) complexes, the SOMO of the electrophilic malonate radical may also be too stable to interact favourably with the singly-occupied orbital on the propargyltitanium(III) moiety.

5.2.5 Crystallographic properties of titanacyclobutenes

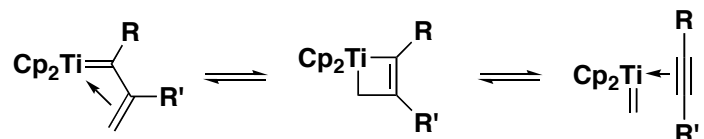
X-ray crystallography is a very powerful tool in organometallic chemistry. In addition to connectivity, crystal structures provide vital information on bonding, which in contrast to the majority of organic molecules is not always clear-cut. The assignment of paramagnetic transition-metal structures, for which NMR spectroscopy is less diagnostic, is perhaps most important. A range of crystal structures of titanacyclobutene complexes have been reported, both from the Stryker group and elsewhere,¹³¹ included as proof of structural assignments and in some instances, comparative trends. Table 5.2 provides relevant bond lengths and angles for the titanacyclobutene core of all of the crystallographically characterized titanacyclobutenes. The numbering system for the atoms is located above the table, while the titanacyclobutene structures are summarized in Figure 5.7. The titanium- sp^2 carbon bond (Ti-C1) has an average length of 2.10 ± 0.05 Å.¹³² This is slightly shorter than the titanium- sp^3 carbon (Ti-C3), which on average is 2.13 ± 0.04 Å. The C1-C2 bond and is 1.34 ± 0.01 Å, consistent with a formal double bond. The C2-C3 bond length is 1.53 ± 0.02 Å, for the sp^3 - sp^2 bond. The C2-C4 bond

length ($1.52 \pm 0.04 \text{ \AA}$) is very dependant on the β -substituent on the titanacyclobutene. Since bond length is related to homolytic bond strength, the C2-C4 length is reflective of the stability of both the η^3 -propargyltitanium(III) complex and the radical used for central-carbon alkylation. Comparing bis(cyclopentadienyl)titanacyclobutenes within the α -phenyl series (Entries 11-19), a clear trend of increasing C2-C4 bond length with increasing radical stability is seen in the order *tert*-butyl > benzyl > *iso*-propyl ~ methallyl ~ cyclohexyl ~ η^3 -propargyltitanium(III) > phenyl. From this order, the stability of the η^3 -propargyltitanium(III) complex is comparable to an allylic or secondary organic radical. Compared with the other crystallographically characterized di(titanacyclobutenes) (Entries 3 and 10), the order of η^3 -propargyltitanium(III) complex stability as a function of the ancillary ligands is Cp₂ ~ Cp(N=P^tBu₃) > Cp*₂, consistent with the increasing electron-donating ability of the ancillary ligands destabilizing the η^3 -propargyl complex by enhancing the central-carbon contribution to the SOMO, promoting dimerization in the absence of overriding steric effects. Furthermore, the angle intersected by two the titanacyclobutene planes for compounds **162a**, **87a** and **149a** is 81.3°, 67.4° and 32.8° consistent with the electron-rich pentamethylcyclopentadienyl ligands promoting a more conjugated structure (although **149a** is constrained by ring fusion). Even in the near planar form, the β - β carbon-carbon bond of di(titanacyclobutene) complex **149a** is longer than expected for a conjugated diene (1.455 Å) for a typical organic molecule.¹³³

For bond homolysis of the β -carbon and β -substituent to occur, a thermodynamically viable pathway must exist. Upon bond homolysis, there is a formal reduction of titanium(IV) to titanium(III). Therefore, electron-donation from the ligands to the titanium atom would presumably assist this transformation. There is evidence for agostic (C-C)→M interactions in electron-deficient, early-metal metallacyclobutanes¹³⁴ and in titanacyclobutenes.¹³⁵ Electron density studies of the titanacyclobutanes show that this agostic interaction presumably contributes to the 3-4 valence electrons located about the titanium atom.^{134b} π -Donation from the carbon-carbon double bond in titanacyclobutenes is suspected but the observed changes in the C=C bond length are comparable to the error in measurement,¹³⁵ therefore it is useful to examine the NMR

characteristics. The ^{13}C NMR chemical shifts of the titanacyclobutene core (*ca.* δ 210, 100, and 75 for C1, C2, and C3, respectively) suggest contribution from the canonical structures shown in Scheme 5.7. The retro [2+2] and electrocyclic ring-opening contributors explain that the unusually deshielded sp^3 carbon is due to a decrease in p -character.

Scheme 5.7



The non-trivial electron density donated to the titanium atom by the ancillary ligands and C-C / C=C agostic interactions presumably allow back-donation to an appropriate acceptor. Indeed, the titanium-vinylalkylidene canonical structure can be thought to arise from the α - sp^2 carbon acting as a π acceptor, much like CO. The canted nature of the titanacyclobutene C=C presumably disfavours the alkene acting as a δ -acid. The distance between Ti-C2 is comparable to the distance between the cyclopentadienyl carbons and titanium (*ca.* 2.50 and 2.45 Å, respectively), therefore it is interesting to know if the titanium(IV)/(III) equilibrium is at least partially assisted by donation from the titanium atom to the σ^* orbital of the C2-C4 bond.

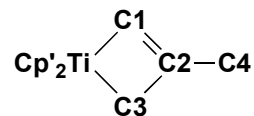


Table 5.2: Select data of crystallographically studied titanacyclobutenes

Entry	Compound	Bond lengths (Å)					Bond Angle (deg)			
		Ti-C1	Ti-C3	C1-C2	C2-C3	C2-C4	Ti-C1-C2	Ti-C3-C2	C1-C2-C3	C1-Ti-C3
1	155a	2.123(3)	2.135(4)	1.335(5)	1.520(5)	1.513(5)	90.2(2)	85.1(2)	115.0(3)	68.93(14)
2	148a	2.114(4)	2.159(4)	1.335(6)	1.510(5)	1.492(6)	89.4(3)	83.4(3)	117.5(4)	69.44(16)
3	149a	2.127(3)	2.134(3)	1.346(5)	1.502(5)	1.504(5)	89.2(2)	85.1(2)	116.0(3)	69.14(13)
4	129	2.061(9)	2.275(4)	1.32(2)	1.500(12)	1.576(9)	93.4(8)	80.7(4)	117.9(7)	67.7(4)
5	175	2.1324(14)	2.1573(14)	1.345(2)	1.5085(19)	1.5353(19)	89.27(9)	84.30(8)	116.34(12)	68.88(5)
6	177^f	2.109(3)	2.104(3)	1.365(4)	1.434(4)	1.528(4)	89.4(2)	87.8(2)	114.8(2)	68.0(1)
7	178^f	2.173(6)	2.102(6)	1.352(8)	1.502(7)	1.511(8)	87.4(4)	86.5(3)	116.7(5)	69.3(2)
8	179^j	2.088(7)	2.152(6)	1.322(9)	1.503(9)	1.535(9)	90.3(5)	83.3(4)	117.1(6)	69.3(3)
9	180^a	2.093(3)	2.144(3)	1.338(4)	1.516(4)	1.537(5)	88.8(2)	82.50(17)	117.6(3)	70.41(12)
10	87a^{h,a}	2.055(3)	2.077(3)	1.351(4)	1.541(4)	1.517(4)	85.51(19)	80.33(17)	119.4(3)	74.41(12)
11	162a^h	2.1013(18)	2.1239(19)	1.337(2)	1.528(2)	1.520(2)	86.39(12)	81.17(10)	120.12(16)	72.01(7)
12	163	2.0844(15)	2.1183(16)	1.335(2)	1.528(2)	1.531(2)	87.99(9)	82.11(9)	118.27(13)	71.62(6)
13	169a	2.094(3)	2.123(3)	1.337(4)	1.526(4)	1.537(4)	88.50(19)	82.82(17)	117.6(3)	71.07(11)
14	181^{b,g}	2.100(2)	2.139(2)	1.338(3)	1.532(3)	1.526(3)	89.00(14)	82.83(12)	117.39(18)	70.75(8)
15	182^b	2.0969(14)	2.1263(17)	1.337(2)	1.538(2)	1.553(2)	90.30(9)	84.11(9)	115.30(14)	70.29(6)
16	183^{b,g}	2.0909(16)	2.1205(18)	1.340(2)	1.536(2)	1.523(2)	88.30(11)	82.45(10)	117.62(15)	71.57(6)
17	184^c	2.104(4)	2.122(5)	1.344(6)	1.537(6)	1.489(6)	91.8(3)	86.0(3)	112.8(4)	69.3(2)
18	186^d	2.050(4)	2.083(5)	1.340(5)	1.556(5)	1.8829(2) ^k	85.0(2)	78.9(2)	120.9(3)	75.2(2)
19	187^e	2.100(3)	2.130(3)	1.339(4)	1.543(4)	1.499(4)	88.7(2)	82.62(18)	117.3(3)	71.22(12)
20	185^{d,i}	2.099(3)	2.064(4)	1.335(5)	1.598(5)	1.891(1) ^k	83.4(2)	78.9(2)	121.6(3)	76.0(2)

^a Reference 66; ^b Reference 64; ^c Reference 131a; ^d Reference 131b; ^e Reference 131c; ^f Reference 131d; ^g Two independent solutions available, only one is shown; ^h Only one set of values are shown; ⁱ Average value of two independent solutions; ^j Reference 61; ^k C2-Si bond length

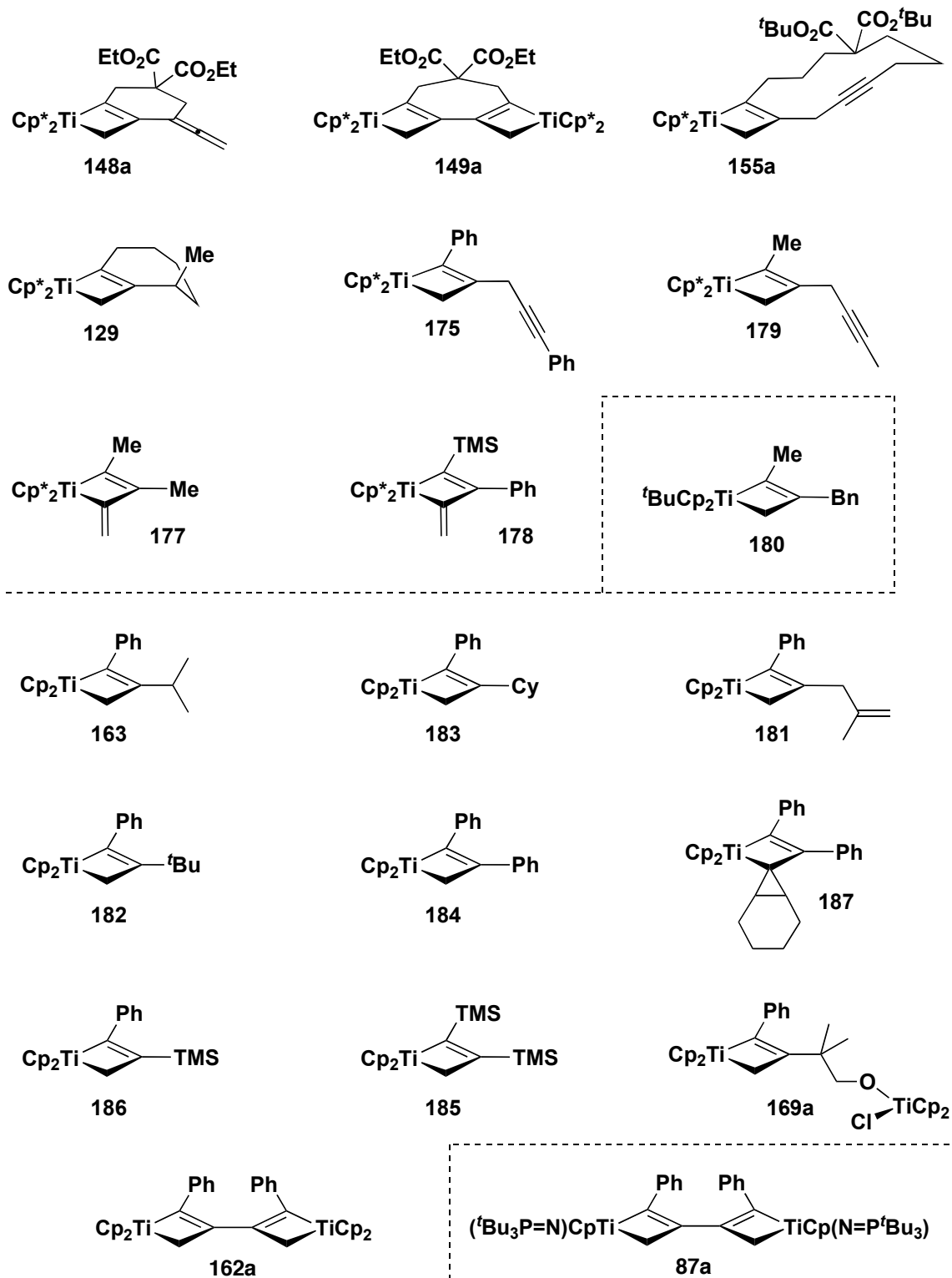


Figure 5.7: Crystallographically characterized titanacyclobutenes

5.3 Future research and conclusion

The incorporation of oxygen atoms into titanacyclobutene complexes is achieved by the use of epoxides as radical precursors. Although titanocene monochloride promotes ring-opening of isobutylene oxide and styrene oxide, producing an alkoxyalkyl radical intermediate, only the latter undergoes ring-opening by this reagent, presumably a result of steric effects. An example of demetallation by protonolysis produces the corresponding homoallylic alcohol, complementary to Grubb's method. An attempt to alkylate η^3 -propargyltitanium complex using an electrophilic malonate radical failed, possibly due to the incompatibility of the reagent with samarium diiodide. Future research using carbonyls or oxetanes to generate α - and γ -alkoxyalkyl radicals, respectively, may allow access to a wider variety of oxygen-functionalized titanacyclobutene complexes. The use of α -epoxy- ω -propargylbromo substrates in intramolecular radical cyclization is also an area which should be explored.

Equilibrium between η^3 -propargyltitanium(III) complexes and their respective dimers is observed for the unsubstituted and *tert*-butyl-substituted bis(cyclopentadienyl) phenylpropargyltitanium complexes. This was concluded by X-ray analysis, low-temperature NMR, as well as qualitative observations of colour change. The isolated α -phenyl di(titanacyclobutene) dimer **162a** disproves the conviction that only the electron-rich pentamethylcyclopentadienyl analogues dimerize. In this case, the bulky nature of the former, forces the equilibrium to favour the η^3 -propargyltitanium(III) complex.

A collection of crystallographically analyzed titanacyclobutene complexes shows a correlation between the β -substituent bond length and the stability of the radicals formed from bond homolysis. The trend shows the stability of the η^3 -propargyltitanium(III) complex to be similar to that of an allylic or secondary organic radical. With respect to the ancillary ligands, the electron-rich pentamethyl-substituted cyclopentadienyl ligands destabilize the η^3 -propargyltitanium(III) form, reflected in the shorter bond length between titanacyclobutene moieties.

Chapter 6: Experimental details

General methods and instrumentation:

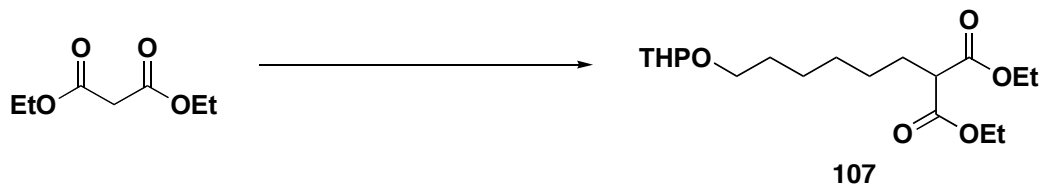
All air-sensitive manipulations were conducted under a nitrogen atmosphere using standard Schlenk techniques or drybox techniques. Flash column chromatography separations were performed using Silicycle flash silica gel (40-63 μm). Celite filtrations were performed using a plug of Celite 545 filter aid over dried Kim-Wipe packed into disposable glass pipettes. Infrared (IR) spectra were recorded on a Nicolet Magna IR 750 spectrophotometer equipped with a Nic-Plan FTIR Microscope and are reported in reciprocal wave numbers (cm^{-1}). Nuclear magnetic resonance (NMR) spectra were recorded on Varian Unity-Inova 400 (^1H , 400 MHz; ^{13}C , 100 MHz) spectrometers, a Varian Mercury 400 (^1H , 400 MHz; ^{13}C , 100 MHz) spectrometer, or a Varian Inova (^1H , 300 MHz) spectrometer. Chemical shifts are reported in parts per million (ppm, δ) relative to TMS (^1H , ^{13}C) and unless stated otherwise, NMR spectra were obtained at 26.5 $^\circ\text{C}$. Coupling constants reported as J refer to J_{HH} are given in hertz (Hz). Coupling constants are reported to 0.1 Hz, which is within the limits of instrumental precision, but these values are normally accurate only to within ± 0.5 Hz. Multiplicities are reported as observed. High-resolution electron impact mass spectra were obtained by the 154 Mass Spectrometry Facility on a Kratos MS-50G spectrometer with an ionization energy of 70 eV and GC-MS was performed on an Agilent Technologies 7890 GC with a 5975C electron impact MS detector. Electrospray mass spectra were obtained on a Applied BioSystems Mariner BioSpectrometry Workstation. Combustion analyses were performed by the University of Alberta Microanalysis Laboratory with a Carlo Erba Instruments CHSN-O EA1108 Elemental Analyzer. All air-sensitive compounds (~ 2 mg) were wrapped in pre-weighed aluminum foil boats and kept in nitrogen-filled one-dram vials immediately prior to analysis. X-Ray structural data were collected on a Bruker Platform diffractometer with a SMART 1000 CCD area detector at -80 $^\circ\text{C}$. Data collection, structural solutions, and further refinements were performed by Dr. Robert McDonald and Dr. Michael J. Ferguson of the X-Ray Crystallography Laboratory. Computational analyses were performed using the Spartan 8 software, with much assistance from Kai Ylijoki.

Reagents and materials:

Benzene, hexanes, pentane, tetrahydrofuran and diethyl ether were purified by distillation from sodium or potassium benzophenone ketyl under a nitrogen atmosphere while dichloromethane and acetonitrile were dried over calcium hydride under air. Dimethylformamide was distilled over calcium hydride under reduced pressure to avoid decomposition.

The following compounds were made by literature procedures: diethyl 2-(6-(tetrahydro-2*H*-pyran-2-yloxy)hexyl)malonate,⁷⁶ 2-(4-bromobut-2-ynyloxy)-tetrahydro-2*H*-pyran,^{73,74,75} 5-(tetrahydro-2*H*-pyran-2-yloxy)pent-3-yn-1-ol,⁷⁶ [Cp₂TiCl]₂,¹³⁶ isobutylene oxide,¹³⁷ styrene oxide,¹³⁸ diethylbromomalonate.¹³⁹

Diethyl 2-(6-(tetrahydro-2H-pyran-2-yloxy)hexyl)malonate (107)⁷⁶



In a round bottom flask, a mixture of THF and DMF (7 : 9, 400 mL), 6-bromo-1-(tetrahydropyran-2'-yloxy)hexane (14.98 g, 56.5 mmol), potassium carbonate (7.83 g, 56.7 mmol) and diethyl malonate (9.06 g, 56.6 mmol) was added. The mixture was stirred vigorously at reflux for 45 h then diluted with diethyl ether and hexanes, washed with saturated sodium bicarbonate and extracted into diethyl ether/hexanes. The organic layer was dried over magnesium sulfate, and the solvent was removed *in vacuo*. The crude residue was purified by short-path distillation under reduced pressure (152 °C, ~0.01 mm Hg) to afford malonate **107** as a colourless liquid (9.35 g, 48%). Spectroscopic data for **X**: **IR** (neat, cm⁻¹): 2939 (s), 2863 (m), 1751 (s), 1734 (s), 1466 (m), 1369 (m), 1343 (m), 1260 (m), 1201 (m), 1153 (s), 1121 (m), 1078 (m), 1034 (s), 987 (w), 906 (w), 869 (w), 814 (w); **¹H NMR** (400 MHz, CDCl₃): δ 4.52 (m, 1H, OCHO), 4.14 (overlapping quartets, *J* = 7.1 Hz, 4H, CH₂CH₃), 3.81 (ddd, *J* = 10.9 Hz, *J* = 7.7 Hz, *J* = 3.7 Hz, 1H, CHHO (THP)), 3.67 (dt, *J* = 9.6 Hz, *J* = 6.8 Hz, 1H, THPOCHH), 3.44 (m, 1H, CHHO (THP)), 3.32 (dt, *J* = 9.6 Hz, *J* = 6.6 Hz, 1H, THPOCHH), 3.26 (t, *J* = 7.6 Hz, 1H, CH(C=O)₂), 1.89-1.25 (m, 16H, CH₂), 1.22 (t, *J* = 7.1 Hz, 6H, CH₂CH₃); **¹³C{¹H} NMR** (100 MHz, CDCl₃): δ 169.4 (C=O), 98.8, 67.4, 62.2, 61.1, 52.0, 30.7, 29.6, 29.0, 28.6, 27.2, 25.9, 25.4, 19.6, 14.0; **¹H-¹H COSY** (400 MHz, CDCl₃): δ 4.14 ↔ δ 1.22; δ 3.81 ↔ δ 3.44; δ 3.67 ↔ δ 3.44; **HMQC** (400 MHz, CDCl₃): δ 4.52 ↔ δ 98.8; δ 4.14 ↔ δ 61.1; δ 3.81 ↔ δ 62.2; δ 3.67 ↔ δ 67.4; δ 3.44 ↔ δ 62.2; δ 3.32 ↔ δ 67.4; δ 3.26 ↔ δ 52.0; δ 1.22 ↔ δ 14.0; **EIMS** *m/z* calculated for C₁₈H₃₂O₆ (M)⁺: 344.21988; found: 344.21925; **Analysis** calculated for C₁₈H₃₂O₆: C, 62.77%; H, 9.45%; found: C, 62.40%; H, 9.42%.

Diethyl 2-(4-bromobut-2-ynyl)-2-(6-bromohexyl)malonate (**96**)

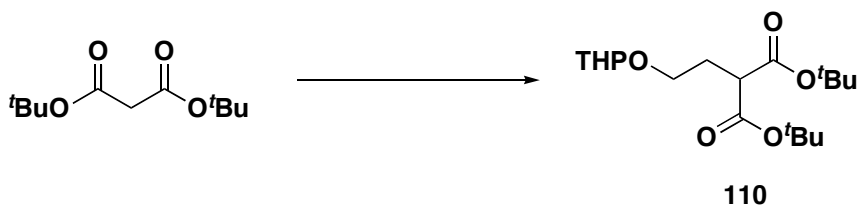


To a cool (0 °C) suspension of sodium hydride (60% by mass, 468 mg, 11.7 mmol) in a round bottom flask was added THF (10 mL) and diethyl 2-(6-(tetrahydro-2H-pyran-2-yloxy)hexyl)malonate (2.46 g, 7.14 mmol) dropwise and stirred until H₂ ceased to evolve. This solution was then transferred by canula to a mixture of 2-(4-bromobut-2-ynyloxy)-tetrahydro-2H-pyran (1.71 g, 7.35 mmol) and a catalytic amount of sodium iodide (~100 mg, 0.7 mmol) in THF (10 mL). The mixture was stirred overnight at room temperature and the reaction was quenched with saturated ammonium chloride, diluted with water and extracted with diethyl ether. The organic layer was dried over magnesium sulfate and solvents were evaporated *in vacuo* to give 2.68 g of orange crude material. Purification by column chromatography (3 : 1 hexanes: ethyl acetate; R_f 0.31) gave diethyl 2-(4-(tetrahydro-2H-pyran-2-yloxy)but-2-ynyl)-2-(6-(tetrahydro-2H-pyran-2-yloxy)hexyl)malonate **108** as a colourless oil (2.25 g, 63%). Spectroscopic data for **108**: IR (neat film, cm⁻¹): 2939 (s), 2866 (m), 1735 (s), 1443 (w), 1367 (w), 1323 (w), 1265 (m), 1201 (m), 1120 (m), 1078 (m), 1055 (m), 1025 (s), 946 (w), 903 (w), 870 (w), 815 (w); ESMS *m/z* calculated for C₂₇H₄₄O₈Na (M+Na)⁺: 519.29284; found: 519.29295. The material was used directly in the next step without further characterization.

In a round bottom flask, to a cold (0 °C) solution of triphenylphosphine (3.17 g, 12.1 mmol) in dichloromethane (15 mL) was added bromine (1.95 g, 12.2 mmol) dropwise resulting in a white, creamy suspension. To this was added a solution of diethyl 2-(4-(tetrahydro-2H-pyran-2-yloxy)but-2-ynyl)-2-(6-(tetrahydro-2H-pyran-2-yloxy)hexyl)malonate (1.561 mg, 3.14 mmol) in dichloromethane (15 mL) at 0 °C. The mixture was stirred overnight at room temperature after which the volatiles were removed *in vacuo*. The resulting crude material was stirred in diethyl ether and filtered. The

filtrate was concentrated and purified by flash silica gel chromatography (7 : 1 hexanes:ethyl acetate; R_f 0.24) to afford the desired dibromide **96** as an orange liquid (433.1 mg, 30%). Spectroscopic data for **96**: IR (neat, cm^{-1}): 2979 (s), 2937 (s), 2860 (m), 2237 (w), 1731 (s), 1465 (m), 1445 (m), 1389 (w), 1367 (m), 1298 (s), 1262 (s), 1210 (s), 1147 (s), 1097 (s), 1074 (m), 1034 (s), 987 (w), 967 (m), 915 (w), 903 (w), 862 (m), 817 (w), 780 (w), 726 (w); $^1\text{H NMR}$ (400 MHz, CDCl_3): δ 4.20 (apparent qd, $J = 7.1$ Hz, $J = 1.6$ Hz, 4H, CH_2CH_3), 3.86 (t, $J = 2.3$ Hz, 2H, $\equiv\text{CCH}_2\text{Br}$), 3.40 (t, $J = 6.8$ Hz, 2H, $\text{CH}_2\text{CH}_2\text{Br}$), 2.87 (t, $J = 2.3$ Hz, 2H, $\text{CH}_2\text{C}\equiv\text{CCH}_2\text{Br}$), 2.01 (m, 2H, $\text{CH}_2\text{CH}_2\text{Br}$), 1.85 (quintet, $J = 7.1$ Hz, 2H, $\text{CH}_2\text{CH}_2\text{CH}_2\text{Br}$), 1.50-1.33 (m, 4H, CH_2), 1.26 (t, $J = 7.1$ Hz, 6H, CH_2CH_3), 1.20 (m, 2H, CH_2); $^{13}\text{C}\{^1\text{H}\}$ NMR (100 MHz, CDCl_3) δ 170.2, 129.9, 82.5, 78.1, 61.6, 56.8, 33.8, 32.6, 31.8, 28.8, 27.8, 23.6, 23.2, 14.8, 14.1; EIMS m/z calculated for $\text{C}_{17}\text{H}_{27}\text{O}_4^{81}\text{Br}_2$ ($\text{M}+\text{H}$) $^+$: 457.02353; found: 457.02469. Analysis calculated for $\text{C}_{19}\text{H}_{26}\text{O}_4\text{Br}_2$: C, 47.72%; H, 5.48%; found: C, 48.94%; H, 5.66%.

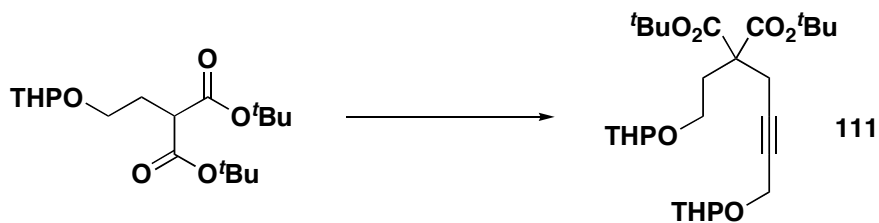
Di-*tert*-butyl 2-(2-(tetrahydro-2*H*-pyran-2-yloxy)ethyl)malonate (**110**)



In a round bottom flask, to a cold (0 °C) suspension of sodium hydride (60% in mineral oil, 0.39 g, 9.8 mmol) in dimethylformamide (45 mL) was added di-*tert*-butyl malonate (2.05 g, 9.48 mmol) dropwise and stirred until H_2 ceased to evolve. This solution was then transferred by canula to a flask containing 2-bromo-1-(tetrahydropyran-2'-yloxy)ethane (1.98 g, 9.47 mmol). After heating at 50 °C for 18 h, the reaction was quenched with saturated ammonium chloride, diluted with water and extracted with hexanes: diethyl ether (1 : 1 v/v). The organic layer was dried over magnesium sulfate and solvents were evaporated *in vacuo* to give the crude product. Purification by flash silica gel chromatography (6 : 1 hexanes:ethyl acetate; R_f 0.33) gave the title compound

110 as a colourless oil (0.77 g, 24%). Spectroscopic data for **110**: **IR** (cast film, cm^{-1}): 2977 (m), 2940 (m), 2873 (w), 1745 (s), 1729 (s), 1479 (w), 1455 (w), 1393 (w), 1369 (m), 1344 (w), 1258 (m), 1201 (w), 1139 (s), 1077 (w), 1064 (m), 1036 (m), 1021 (w), 976 (w), 895 (w), 869 (w), 848 (w), 816 (w); **$^1\text{H NMR}$** (400 MHz, CDCl_3): δ 4.58 (t, $J = 3.4$ Hz, 1H, OCHO), 3.84 (ddd, $J = 11.5$ Hz, $J = 8.3$ Hz, $J = 2.9$ Hz, 1H, CHHO (THP)), 3.77 (dt, $J = 9.9$ Hz, $J = 6.2$ Hz, 1H, THPOCHH), 3.49 (m, 1H, CHHO (THP)), 3.41 (dt, $J = 9.9$ Hz, $J = 6.2$ Hz, 1H, THPOCHH), 2.11 (q, $J = 6.8$ Hz, 2H, $\text{CH}_2\text{C}(\text{C}=\text{O})_2$), 1.88-1.48 (m, 6H), 1.46 (s, 18H, $\text{C}(\text{CH}_3)_3$); **ESMS** m/z calculated for $\text{C}_{18}\text{H}_{32}\text{O}_6\text{Na}$ ($\text{M}+\text{Na}$) $^+$: 367.20911; found: 367.20900.

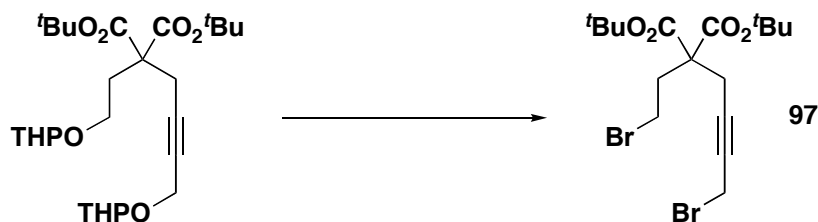
Di-tert-butyl 2-(4-(tetrahydro-2H-pyran-2-yloxy)but-2-ynyl)-2-(2-(tetrahydro-2H-pyran-2-yloxy)ethyl)malonate (111)



In a round bottom flask, to a cold (0 °C) suspension of sodium hydride (60% in mineral oil, 0.13 g, 3.3 mmol) in dimethylformamide (10 mL) was added di-tert-butyl 2-(2-(tetrahydro-2H-pyran-2-yloxy)ethyl)malonate (0.77 g, 2.2 mmol) and 2-(4-bromobut-2-ynyloxy)-tetrahydro-2H-pyran (0.54 g, 2.3 mmol) dropwise. The reaction was stirred overnight at room temperature then diluted with water and extracted with petroleum ether. The organic layer was dried over magnesium sulfate and the solvents were evaporated *in vacuo* to afford the spectroscopically pure title compound in a mixture of diastereomers as a yellow, viscous oil (1.11 g, 100%). Isolation of each diastereomer was not attempted as the removal of the THP protecting groups later in the synthesis results in an achiral molecule. Spectroscopic data for **111**: **IR** (cast film, cm^{-1}): 2941 (m), 2871 (w), 1731 (s), 1455 (w), 1392 (w), 1369 (m), 1290 (w), 1252 (w), 1202 (w), 1148 (s), 1079 (m), 1055 (w), 1025 (s), 976 (w), 904 (w), 870 (w), 848 (w), 816 (w), 732 (w);

^1H NMR (400 MHz, CDCl_3): δ 4.48 (t, $J = 3.4$ Hz, 1H, OCHO), 4.55 (t, $J = 3.4$ Hz, 1H, OCHO), 4.20 (2nd order m, 2H, $\equiv\text{CCH}_2\text{O}$), 3.81 (m, 2H, CH_2O (THP)), 3.77 (dt, $J = 10.3$ Hz, $J = 6.8$ Hz, 1H, $\text{CH}_2\text{CH}_2\text{O}$), 3.49 (m, 2H, CHHO (THP)), 3.40 (dt, $J = 10.3$ Hz, $J = 6.8$ Hz, 1H, $\text{CH}_2\text{CH}_2\text{O}$), 2.83 (br. s, 2H, $\text{CH}_2\text{C}\equiv\text{CCH}_2\text{O}$), 2.29 (t, $J = 6.9$ Hz, 2H, $\text{CH}_2\text{CH}_2\text{O}$), 1.85-1.47 (m, 12H, CH_2 (THP)), 1.44 (s, 18H, $\text{C}(\text{CH}_3)_3$); **$^{13}\text{C}\{^1\text{H}\}$ NMR** (100 MHz, CDCl_3): δ 169.3, 98.7, 96.5, 81.5, 78.6, 63.3, 62.1, 56.5, 54.2, 31.3, 30.4, 30.3, 27.8, 25.5, 25.4, 23.3, 19.3, 19.2; **ESMS** m/z calculated for $\text{C}_{27}\text{H}_{44}\text{O}_8\text{Na}$ ($\text{M}+\text{Na}$)⁺: 519.29284; found: 519.29222; **Analysis** calculated for $\text{C}_{27}\text{H}_{44}\text{O}_8$: C, 65.30%; H, 8.93%; found: C, 65.82%; H, 8.92%.

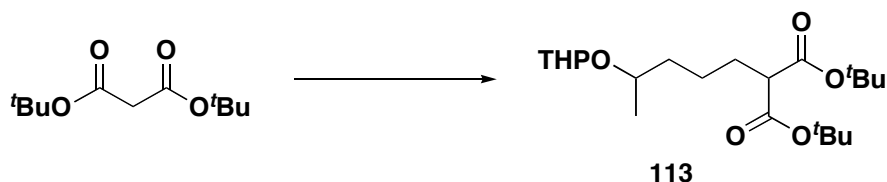
Di-*tert*-butyl 2-(4-bromobut-2-ynyl)-2-(2-bromoethyl)malonate (97)



In a round bottom flask, to a cold (0 °C) solution of triphenylphosphine (1.82 g, 6.94 mmol) in dichloromethane (10 mL) was added bromine (1.05 g, 6.57 mmol) dropwise resulting in a white, creamy suspension. To this was added a solution of di-*tert*-butyl 2-(4-(tetrahydro-2*H*-pyran-2-yl)oxy)but-2-ynyl)-2-(2-(tetrahydro-2*H*-pyran-2-yl)oxy)ethylmalonate (0.84 g, 1.69 mmol) in dichloromethane (5 mL) at 0 °C. The mixture was stirred overnight at room temperature. Volatiles were removed *in vacuo* and the product was extracted into hexanes. Evaporation of solvent *in vacuo* left behind a crude oil which was purified by flash silica gel chromatography (10 : 1 hexanes : ethyl acetate; R_f 0.22) to give dibromide **97** as a white, crystalline solid (0.17 g, 22%). Spectroscopic data for **97**: **IR** (cast film, cm^{-1}): 2978 (m), 2933 (w), 2237 (w), 1728 (s), 1477 (w), 1456 (w), 1427 (w), 1394 (w), 1370 (m), 1304 (m), 1275 (m), 1253 (m), 1223 (m), 1163 (s), 1143 (s), 1081 (w), 1051 (w), 1035 (w), 846 (m), 731 (w); **^1H NMR** (400 MHz, CDCl_3): δ 3.87 (t, $J = 3.3$ Hz, 2H, $\equiv\text{CCH}_2\text{Br}$), 3.38 (2nd order m, 2H, $\text{CH}_2\text{CH}_2\text{Br}$),

2.79 (t, $J = 2.3$ Hz, 2H, $\text{CH}_2\text{C}\equiv\text{CCH}_2\text{Br}$), 2.52 (2nd order m, 2H, $\text{CH}_2\text{CH}_2\text{Br}$), 1.49 (s, 18H, $\text{C}(\text{CH}_3)_3$); $^{13}\text{C}\{^1\text{H}\}$ NMR (100 MHz, CDCl_3): δ 168.4 (C=O), 82.4 ($\text{C}(\text{CH}_3)_3$), 82.1 ($\text{C}\equiv\text{C}$), 78.5 ($\text{C}\equiv\text{C}$), 58.0 ($\text{C}(\text{C}=\text{O})_2$), 36.0 ($\text{CH}_2\text{CH}_2\text{Br}$), 27.8 ($\text{C}(\text{CH}_3)_3$), 27.1 ($\text{CH}_2\text{CH}_2\text{Br}$), 23.8 ($\text{CH}_2\text{C}\equiv\text{CCH}_2\text{Br}$), 14.5 ($\equiv\text{CCH}_2\text{Br}$); HMBC (400 MHz, CDCl_3): δ 3.87 \leftrightarrow δ 82; 78.5, 58.0, 23.8; δ 3.38 \leftrightarrow δ 58.0, 36.0; δ 2.79 \leftrightarrow δ 168.4, 82, 78.5, 58.0, 36.0, 14.5; δ 2.52 \leftrightarrow δ 168.4, 58.0, 27.1, 23.8; δ 1.49 \leftrightarrow δ 82; ESMS m/z calculated for $\text{C}_{17}\text{H}_{26}\text{O}_4\text{Br}_2\text{Na}$ ($\text{M}+\text{Na}$)⁺: 475.00900; found: 475.00886; Analysis calculated for $\text{C}_{17}\text{H}_{26}\text{O}_4\text{Br}_2$: C, 44.96%; H, 5.77%; found: C, 45.27%; H, 5.58%.

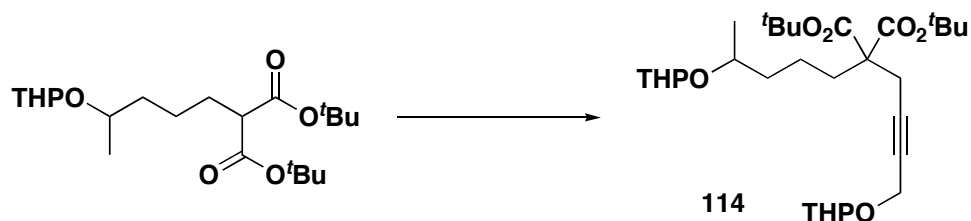
Di-*tert*-butyl 2-(4-(tetrahydro-2*H*-pyran-2-yloxy)pentyl)malonate (**113**)



In a round bottom flask, to a cold (0 °C) suspension of sodium hydride (60% in mineral oil, 0.95 g, 24 mmol) in dimethylformamide (125 mL) was added di-*tert*-butyl malonate (8.3 mL, 37 mmol) dropwise and stirred until H_2 ceased to evolve. To this solution was then added 2-(5-chloropentan-2-yloxy)-tetrahydro-2*H*-pyran (90% pure by ^1H NMR, 3.82 g, ~17 mmol) and a catalytic amount of sodium iodide (~200 mg, 1 mmol) at 0 °C. After stirring overnight at 50 °C, the reaction was quenched with saturated ammonium chloride then extracted with 1 : 1 petroleum ether : ether. The organic layer was dried over magnesium sulfate and solvents were evaporated *in vacuo* to give the crude product. Purification by vacuum distillation (b.p 124-132 °C, 1 mm Hg) afforded the monoalkylated compound **113** as a clear, colourless, viscous oil present as an equal mixture of diastereomers (3.45 g, 48%). Isolation of each diastereomer was not attempted as the removal of the THP protecting groups later in the synthesis results in a single stereogenic centre. Spectroscopic data for **113**: IR (neat, cm^{-1}): 2976 (m), 2936 (m), 2871 (w), 1746 (s), 1729 (s), 1457 (w), 1393 (w), 1369 (m), 1342 (w), 1322 (w), 1289 (w), 1252 (m), 1201 (w), 1139 (s), 1077 (w), 1033 (w), 1023 (m), 994 (w), 943 (w), 903 (w),

870 (w), 849 (w), 814 (w), 745 (w); $^1\text{H NMR}$ (300 MHz, CDCl_3 ; reported as a mixture of diastereomers): δ 4.68 (m, 1H, OCHO), 4.60 (m, 1H, OCHO), 3.94-3.82 (m, 2H, CHHO (THP)), 3.72 (overlapping sextets, $J = 6.1$ Hz, 2H, CH_3CH), 3.46 (m, 2H, CHHO (THP)), 3.11 (overlapping triplets, $J = 7.6$ Hz, 2 H, $\text{CH}(\text{C}=\text{O})_2$), 1.80 (br. quintet, $J = 7.6$ Hz, 4H, $\text{CH}_2\text{CH}(\text{C}=\text{O})_2$), 1.72-1.46 (m, 12H, CH_2 (THP)), 1.44 (s, 36H, $\text{C}(\text{CH}_3)_3$), 1.42-1.28 (m, 4H, $\text{OCHCH}_2\text{CH}_2$), 1.20 (t, $J = 6.3$ Hz, 3H, CH_3CH), 1.08 (t, $J = 6.1$ Hz, 3H, CH_3CH); $^{13}\text{C}\{^1\text{H}\}$ NMR (100 MHz, CDCl_3 reported as a mixture of diastereomers): δ 168.9, 168.8, 98.7, 95.5, 81.17, 81.16, 81.10, 81.08, 73.6, 70.7, 62.8, 62.3, 53.92, 53.89, 37.1, 36.1, 31.2, 31.1, 28.63, 28.62, 27.89, 27.87, 27.86, 25.53, 25.47, 23.5, 23.1, 21.5, 20.0, 19.6, 19.0; $^1\text{H}-^1\text{H COSY}$ (300 MHz, CDCl_3): δ 3.94-3.82 \leftrightarrow δ 3.46; δ 3.72 \leftrightarrow δ 1.20, 1.08; δ 3.11 \leftrightarrow δ 1.80; δ 1.80 \leftrightarrow δ 1.42-1.28; **ESMS** m/z calculated for $\text{C}_{21}\text{H}_{38}\text{O}_6\text{Na}$ ($\text{M}+\text{Na}$) $^+$: 409.25606; found: 409.25668; **Analysis** calculated for $\text{C}_{21}\text{H}_{38}\text{O}_6$: C, 65.26%; H, 9.91%; found: C, 66.04%; H, 9.93%.

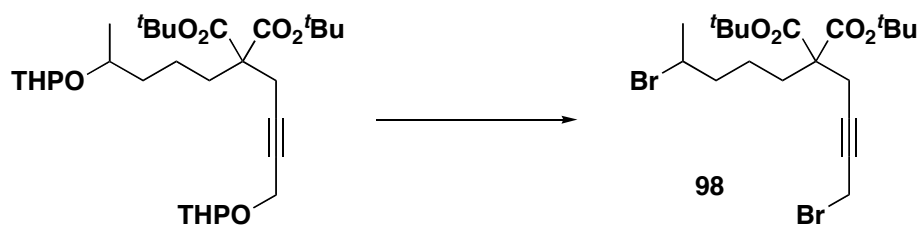
Di-*tert*-butyl 2-(4-(tetrahydro-2*H*-pyran-2-yloxy)but-2-ynyl)-2-(4-(tetrahydro-2*H*-pyran-2-yloxy)pentyl)malonate (114)



In a round bottom flask, to a cold (0 °C) suspension of sodium hydride (60% in mineral oil, 0.36 g, 9.0 mmol) in dimethylformamide (50 mL) was added di-*tert*-butyl 2-(4-(tetrahydro-2*H*-pyran-2-yloxy)pentyl)malonate (2.90 g, 7.50 mmol) dropwise and stirred until H_2 ceased to evolve. To this solution was then dropwise added 2-(4-bromobut-2-ynyloxy)-tetrahydro-2*H*-pyran (1.80 g, 7.72 mmol) at 0 °C. After stirring overnight at room temperature, the reaction was quenched with water and extracted with hexanes. The organic layer was dried over magnesium sulfate and solvents were evaporated *in vacuo* to give ~4.5 g of yellow, crude product. Purification by flash silica gel chromatography (3 : 1 petroleum ether : diethyl ether; R_f 0.26) gave the dialkylated

malonate **114** as a very viscous, colourless oil (2.39 g, 59%). Isolation of each diastereomer was not attempted as the removal of the THP protecting groups later in the synthesis results in a single stereogenic centre. Spectroscopic data for **114**: **IR** (cast film, cm^{-1}): 2940 (s), 2871 (m), 1730 (s), 1455 (w), 1393 (w), 1369 (m), 1322 (w), 1300 (w), 1258 (m), 1201 (m), 1150 (s), 1119 (s), 1078 (m), 1054 (w), 1024 (s), 999 (m), 945 (w), 903 (w), 871 (w), 849 (w), 815 (w), 728 (w); **^1H NMR** (400 MHz, CDCl_3 ; select diagnostic signals): δ 4.77 (t, $J = 3.4$ Hz, OCHO), 4.19 (leaning dt, $J = 15.5$ Hz, 1.1 Hz, $\equiv\text{CCH}_2\text{O}$), 2.74 (q, $J = 3.8$ Hz, $\text{CH}_2\text{C}\equiv\text{CCH}_2\text{O}$), 1.44 (s, $\text{C}(\text{CH}_3)_3$), 1.20 (d, $J = 6.8$ Hz, CHCH_3); **$^{13}\text{C}\{^1\text{H}\}$ NMR** (100 MHz, CDCl_3 , reported as mixture of diastereomers): δ 169.55, 169.51, 98.9, 96.5, 95.4, 81.42, 81.38, 81.35, 81.34, 81.31, 78.52, 75.46, 73.7, 70.7, 62.8, 62.3, 62.1, 57.8, 57.7, 54.3, 54.2, 37.8, 36.8, 31.8, 31.7, 31.21, 31.15, 30.3, 27.8, 25.54, 25.48, 25.4, 22.91, 22.90, 21.6, 20.2, 20.1, 19.8, 19.6, 19.21, 19.19, 18.9; **ESMS** m/z calculated for $\text{C}_{30}\text{H}_{50}\text{O}_8\text{Na}$ ($\text{M}+\text{Na}$) $^+$: 561.33979; found 561.34039; **Analysis** calculated for $\text{C}_{30}\text{H}_{50}\text{O}_8$: C, 66.89%; H, 9.35%; found: C, 66.80%; H, 9.51%.

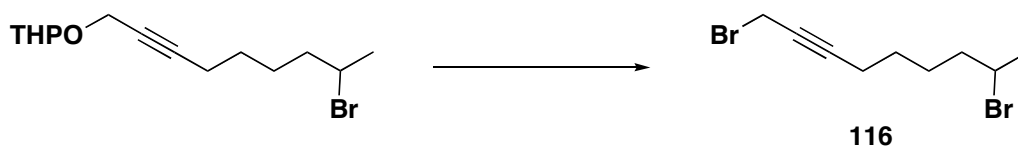
Di-*tert*-butyl 2-(4-bromobut-2-ynyl)-2-(4-(bromopentyl)malonate (**98**)



In a round bottom flask, to a cold (0 °C) solution of triphenylphosphine (4.01 g, 15.3 mmol) in dichloromethane (150 mL) was added bromine (0.77 mL, 15 mmol) dropwise resulting in a white, creamy suspension. To this was added a solution of di-*tert*-butyl 2-(4-(tetrahydro-2*H*-pyran-2-yloxy)but-2-ynyl)-2-(4-(tetrahydro-2*H*-pyran-2-yloxy)pentyl)malonate (1.91 g, 3.55 mmol) in dichloromethane (15 mL) at 0 °C. The mixture was stirred overnight at room temperature. The organic layer was successively washed with aqueous sodium bisulfite and sodium bicarbonate. The product was then extracted into dichloromethane and the organic layer was dried over magnesium sulfate. Volatiles were removed *in vacuo* leaving behind ~6.2 g of a yellow solid containing

abundant amounts triphenylphosphine oxide. Purification by flash silica gel chromatography (dichloromethane; R_f 0.69) provided dibromide **98** as a pale, yellow liquid (1.62 g, 92%). Spectroscopic data for **98**: **IR** (neat film, cm^{-1}): 2978 (s), 2933 (m), 2237 (w), 1729 (s), 1624 (w), 1477 (m), 1456 (m), 1428 (m), 1393 (m), 1369 (s), 1301 (m), 1277 (s), 1258 (s), 1215 (s), 1165 (s), 1073 (m), 962 (w), 848 (m), 747 (w), 726 (m); **^1H NMR** (300 MHz, CDCl_3): δ 4.15 (qt, $J = 5.0$ Hz, $J = 6.6$ Hz, 1H, CH_3CHBr), 3.87 (t, $J = 2.3$ Hz, 2H, $\equiv\text{CCH}_2\text{Br}$), 2.79 (t, $J = 2.3$ Hz, 2H, $\text{CH}_2\text{C}\equiv\text{CCH}_2\text{Br}$), 2.02-1.79 (m, 2H, $\text{CH}_2\text{C}(\text{C}=\text{O})_2$), 1.90-1.74 (m, 2H, CHCH_2CH_2), 1.70 (d, $J = 6.6$ Hz, 3H, CH_3CH), 1.46 (s, 16H, $\text{C}(\text{CH}_3)_3$), 1.44-1.28 (m, 2H, CHCH_2CH_2); **$^{13}\text{C}\{^1\text{H}\}$ NMR** (100 MHz, CDCl_3): δ 169.21 ($\text{C}=\text{O}$), 169.20 ($\text{C}=\text{O}$), 82.8 ($\text{C}\equiv\text{C}$), 81.73 ($\text{OC}(\text{CH}_3)_3$), 81.70 ($\text{OC}(\text{CH}_3)_3$), 77.9 ($\text{C}\equiv\text{C}$), 57.6 ($\text{C}(\text{C}=\text{O})$), 51.0 (CH_3CHBr), 41.1 (CHCH_2CH_2), 31.0 ($\text{CH}_2\text{C}(\text{C}=\text{O})_2$), 27.8 ($\text{C}(\text{CH}_3)_3$), 26.4 (CH_3CH), 23.1 ($\text{CH}_2\text{C}\equiv\text{CCH}_2\text{Br}$), 22.2 (CHCH_2CH_2), 14.9 ($\equiv\text{CCH}_2\text{Br}$); **$^1\text{H}-^1\text{H}$ COSY** (300 MHz, CDCl_3): δ 4.15 \leftrightarrow δ 1.90-1.74, 1.70; δ 3.87 \leftrightarrow δ 2.79; δ 2.02-1.76 \leftrightarrow δ 1.44-1.28; **HMQC** (300 MHz, CDCl_3): δ 4.15 \leftrightarrow δ 51.0; δ 3.87 \leftrightarrow δ 14.9; δ 2.79 \leftrightarrow δ 23.1; δ 2.02-1.79 \leftrightarrow δ 31.0; δ 1.90-1.74 \leftrightarrow δ 41.1; δ 1.70 \leftrightarrow δ 51.0; δ 1.46 \leftrightarrow δ 27.8; **HMBC** (400 MHz, CDCl_3): δ 4.15 \leftrightarrow δ 41.1, 26.4, 22.2; δ 3.87 \leftrightarrow δ 81.7, 77.9, 57.6, 23.1; δ 2.79 \leftrightarrow δ 169.2, 81.7, 77.9, 31.0, 14.9; δ 2.02-1.74 \leftrightarrow δ 169.2, 57.6, 41.1, 23.1, 22.2; δ 1.90-1.74 \leftrightarrow δ 51.0, 31.0, 26.4, 22.2; δ 1.70 \leftrightarrow δ 51.0, 41.1; δ 1.46 \leftrightarrow δ 81.7; δ 1.44-1.28 \leftrightarrow δ 51.0, 41.1, 31.0; **ESMS** m/z calculated for $\text{C}_{20}\text{H}_{32}\text{Br}_2\text{O}_4\text{Na}$ ($\text{M}+\text{Na}$) $^+$: 517.05595; found 517.05576; **Analysis** calculated for $\text{C}_{20}\text{H}_{32}\text{Br}_2\text{O}_4$: C, 48.40%; H, 6.50%; found: C, 48.46%; H, 6.15%.

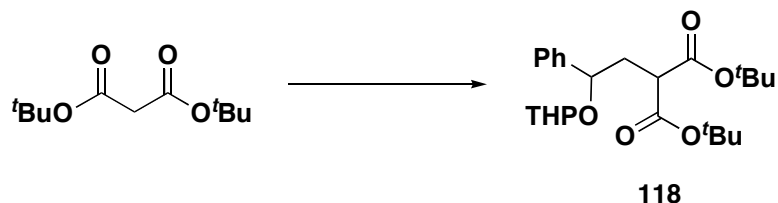
1,8-Dibromo-2-nonyne (116)



In a round bottom flask, to a cold (0 °C) solution of triphenylphosphine (3.46 g, 13.2 mmol) in dichloromethane (60 mL) was added bromine (0.68 ml, 0.13 mmol) dropwise resulting in a white, creamy suspension. To this was added a solution of 2-(8-

bromonon-2-ynoxy)-tetrahydro-2H-pyran (1.94 g, 6.40 mmol) in dichloromethane (10 mL) at 0 °C. The mixture was stirred for three hours and allowed to warm to room temperature. The solution was successively washed with sodium bisulfite and potassium carbonate. The organic layer was dried over magnesium sulfate and the volatiles were removed *in vacuo* leaving behind a yellow solid containing abundant amounts of triphenylphosphine oxide. The solid was triturated several times with portions of petroleum ether. Removal of the solvent *in vacuo* followed by flash silica gel chromatography (6 : 1 petroleum ether : dichloromethane; R_f 0.46) provided dibromide **116** as a colourless liquid (0.84 g, 46%). Spectroscopic data for **116**: **IR** (cast film, cm^{-1}): 2940 (s), 2862 (m), 2835 (w), 2310 (w), 2233 (m), 1452 (m), 1428 (m), 1379 (m), 1352 (w), 1330 (w), 1261 (w), 1211 (s), 1153 (w), 1119 (w), 1105 (w), 1060 (w), 975 (w), 896 (w), 864 (w), 728 (w); **^1H NMR** (400 MHz, CDCl_3): δ 4.12 (dq, $J = 8.0$ Hz, $J = 6.7$ Hz, $J = 5.3$ Hz, 1H, CH_3CH), 3.91 (t, $J = 2.4$ Hz, 2H, $\equiv\text{CCH}_2\text{Br}$), 2.26 (2nd order m, 2H, $\text{CH}_2\text{C}\equiv\text{CCH}_2\text{Br}$), 1.80 (m, 2H, CH_3CHCH_2), 1.70 (d, $J = 6.7$ Hz, 3H, CH_3CH), 1.65-1.48 (m, 4H, CH_2); **$^{13}\text{C}\{^1\text{H}\}$ NMR** (100 MHz, CDCl_3): δ 87.6 ($\text{C}\equiv\text{C}$), 75.7 ($\text{C}\equiv\text{C}$), 51.3 (CH_3CH), 40.5 (CH_3CHCH_2), 27.7 (CH_2), 26.9 (CH_2), 26.4 (CH_3CH), 18.8 ($\text{CH}_2\text{C}\equiv\text{CCH}_2\text{Br}$), 15.6 ($\equiv\text{CCH}_2\text{Br}$); **^1H - ^1H COSY** (400 MHz, CDCl_3): δ 4.12 \leftrightarrow δ 1.80, 1.70; δ 3.91 \leftrightarrow δ 2.26; δ 2.26 \leftrightarrow δ 1.65-1.48; δ 1.80 \leftrightarrow δ 1.65-1.48; **HMQC** (400 MHz, CDCl_3): δ 4.12 \leftrightarrow δ 51.3; δ 3.91 \leftrightarrow δ 15.6; δ 2.26 \leftrightarrow δ 18.8; δ 1.80 \leftrightarrow δ 40.5; δ 1.70 \leftrightarrow δ 26.4; EIMS failed to give $(\text{M})^+$ but rather detected the cation with a loss of bromine. **EIMS** m/z calculated for $\text{C}_9\text{H}_{14}\text{Br}$ ($\text{M}-\text{Br}$)⁺: 203.02583; found 203.02577; **Analysis** calculated for $\text{C}_9\text{H}_{14}\text{Br}_2$: C, 38.33%; H, 5.00%; found: C, 38.16%; H, 4.96%.

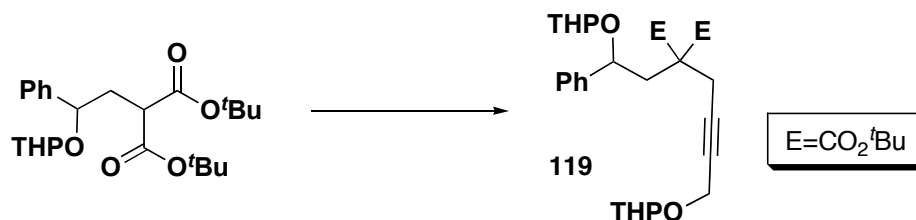
Di-tert-butyl 2-(2-phenyl-2-(tetrahydro-2H-pyran-2-yloxy)ethyl)malonate (118)



In a round bottom flask, to a cold (0 °C) suspension of sodium hydride (60% in mineral oil, 0.51 g, 13 mmol) in dimethylformamide (15 mL) was added di-*tert*-butyl malonate (2.28 g, 10.5 mmol) and 2-(2-bromo-1-phenylethoxy)-tetrahydro-2*H*-pyran (3.00 g, 10.5 mmol) at 0 °C. The reaction was heated to 70 °C for three days after which saturated NH₄Cl was added and extracted into hexanes. The organic layer was dried over magnesium sulfate and solvents were evaporated *in vacuo* to give the crude product. Purification by flash silica gel chromatography (12 : 1 hexanes : ethyl acetate; R_f 0.08) gave the title compound as a viscous oil (1.59 g, 36%) in a diastereotopic ratio of 5 : 3. Isolation of each diastereomer was not attempted as the removal of the THP protecting groups later in the synthesis results in a single stereogenic centre. Also, a significant amount of elimination product (*ca.* 11%) was recovered. Spectroscopic data for **118**: **IR** (cast film, cm⁻¹): 2978 (m), 2940 (m), 1743 (s), 1728 (s), 1455 (m), 1393 (m), 1369 (s), 1345 (w), 1259 (m), 1202 (w), 1140 (s), 1078 (m), 1024 (m), 986 (m), 907 (w), 871 (w), 848 (w), 702 (w); **¹H NMR** (400 MHz, CDCl₃, major isomer): δ 7.40-7.20 (m, 5H, PhH), δ 4.79 (t, *J* = 3.3 Hz, 1H, OCHO), 4.58 (dd, *J* = 5.5 Hz, *J* = 8.2 Hz, 1H, PhCH), 1.47 (s, 9H, C(CH₃)₃); 1.44 (s, 9H, C(CH₃)₃); **ESMS** *m/z* calculated for C₂₄H₃₆O₆Na (M+Na)⁺: 443.24041; found: 443.24029; **Analysis** calculated for C₂₄H₃₆O₆: C, 68.54%; H, 8.63%; found: C, 68.58%; H, 8.57%. Spectroscopic data for **2-(1-phenylvinyl)oxy-tetrahydro-2H-pyran**: **IR** (cast film, cm⁻¹): 3084 (w), 3057 (w), 2944 (s), 2874 (m), 2852 (w), 1621 (m), 1575 (m), 1494 (m), 1468 (w), 1443 (m), 1388 (w), 1353 (w), 1314 (m), 1299 (m), 1282 (s), 1259 (m), 1203 (m), 1183 (m), 1149 (w), 1125 (s), 1109 (m), 1077 (m), 1039 (s), 1023 (s), 985 (s), 952 (m), 898 (m), 881 (m), 820 (m), 769 (m), 695 (m); **¹H NMR** (400 MHz, CDCl₃): δ 7.69 (dd, *J* = 8.4 Hz, *J* = 1.8 Hz, 2H, *o*-PhH), 7.37 (m, 3H, *m/p*PhH), 5.43 (t, *J* = 3.1 Hz, 1H, OCHO), 4.87 (d, *J* = 2.3 Hz, 1H, =CHH), 4.65 (d, *J* =

2.3 Hz, 1H, =CHH), 3.96 (ddd, $J = 11.4$ Hz, $J = 9.7$ Hz, $J = 3.0$ Hz, 1H, CHHO), 3.67 (ddd, $J = 11.4$ Hz, $J = 5.5$ Hz, $J = 1.5$ Hz, 1H, CHHO), 2.10-1.80 (6H, CH₂ (THP)); ¹³C{¹H} NMR (100 MHz, CDCl₃): δ 157.3 (=COTHP), 136.4 (*ipso*-Ar), 128.3 (*p*-Ar), 128.0 (*m*-Ar), 125.3 (*o*-Ar), 95.7 (OCHO), 86.4 (=CH₂), 61.8 (CH₂O), 30.2 (CH₂ (THP)), 25.2 (CH₂ (THP)), 18.8 (CH₂ (THP)); **HMQC** (400 MHz, CDCl₃): δ 7.69 ↔ δ 125.3; δ 7.37 ↔ δ 128.3, 128.0; δ 5.43 ↔ δ 95.7; δ 4.87 ↔ δ 86.4; δ 4.65 ↔ δ 86.4; δ 3.96 ↔ δ 61.8; δ 3.67 ↔ δ 61.8; **ESMS** m/z calculated for C₁₃H₁₆O₂Na (M+Na)⁺: 227.10425; found: 227.10422.

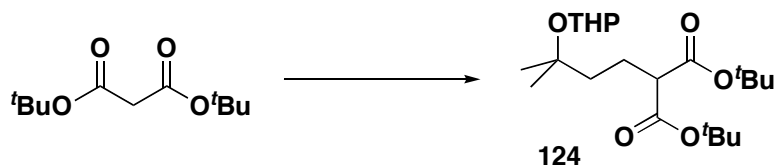
Di-*tert*-butyl 2-(2-phenyl-2-(tetrahydro-2*H*-pyran-2-yloxy)ethyl)-2-(4-(tetrahydro-2*H*-pyran-2-yloxy)but-2-ynyl)malonate (119)



In a round bottom flask, to a cold (0 °C) suspension of sodium hydride (60% in mineral oil, 0.14 g, 3.5 mmol) in dimethylformamide (5 mL) was added a premixed solution of di-*tert*-butyl 2-(2-phenyl-2-(tetrahydro-2*H*-pyran-2-yloxy)ethyl)malonate (1.17 g, 2.78 mmol) and 2-(4-bromobut-2-ynyloxy)-tetrahydro-2*H*-pyran (0.71 g, 3.1 mmol) in dimethylformamide (5 mL). After stirring overnight at room temperature, saturated ammonium chloride was added and the product was extracted into hexanes. The organic layer was dried over magnesium sulfate and the solvents were evaporated *in vacuo*. The crude material was filtered through a short plug of silica to remove inorganic salts to give the crude product as a yellow, viscous oil. Purification by flash silica gel chromatography (5 : 1 hexanes : ethyl acetate; R_f 0.19) gave the title compound as an undetermined mixture of diastereomers as a highly viscous colourless oil which became a wax after sitting for several weeks (864 mg, 54%). Isolation of each diastereomer was not attempted as the removal of the THP protecting groups later in the synthesis results in a

single stereogenic centre. Spectroscopic data for **119**: **IR** (film, cm^{-1}): 2941 (m), 2870 (w), 1731 (s), 1455 (w), 1441 (w), 1393 (w), 1369 (m), 1291 (m), 1250 (w), 1202 (m), 1144 (s), 1120 (w), 1078 (m), 1065 (w), 1024 (s), 974 (w), 946 (w), 903 (w), 871 (w), 847 (w), 816 (w), 761 (w), 744 (w), 701 (w); **^1H NMR** (400 MHz, CDCl_3 ; select diagnostic signals): δ 4.72 (t, $J = 3.4$ Hz, OCHO), 4.50 (dd, $J = 4.2$ Hz, $J = 9.8$ Hz, PhCH), 2.74 (dt, $J = 17.2$ Hz, $J = 2.2$ Hz, $\text{CH}_2\text{C}\equiv\text{CCH}_2\text{O}$), 2.52 (leaning dd, $J = 15.2$ Hz, $J = 9.9$ Hz, PhCHCHH), 2.34 (leaning ddd, $J = 15.2$ Hz, $J = 4.2$ Hz, $J = 2.4$ Hz, PhCHCHH), 1.43 (s, $\text{C}(\text{CH}_3)_3$); **$^{13}\text{C}\{^1\text{H}\}$ NMR** (100 MHz, CDCl_3 , reported as mixture of diastereomers): δ 169.13, 143.8, 141.9, 128.2, 127.9, 127.5, 127.1, 127.0, 126.5, 99.9, 96.38, 95.4, 81.5, 81.4, 81.3, 80.9, 78.8, 78.0, 73.5, 65.7, 62.9, 62.0, 61.9, 56.5, 54.2, 54.1, 39.2, 39.0, 30.4, 30.2, 30.0, 27.8, 27.7, 25.3, 25.2, 22.9, 22.3, 19.7, 19.1, 15.2; **ESMS** m/z calculated for $\text{C}_{33}\text{H}_{48}\text{O}_8\text{Na}$ ($\text{M}+\text{Na}$) $^+$: 595.32414; found: 595.32367; **Analysis** calculated for $\text{C}_{33}\text{H}_{48}\text{O}_8$: C, 69.20%; H, 8.45%; found: C, 68.98%; H, 8.48%.

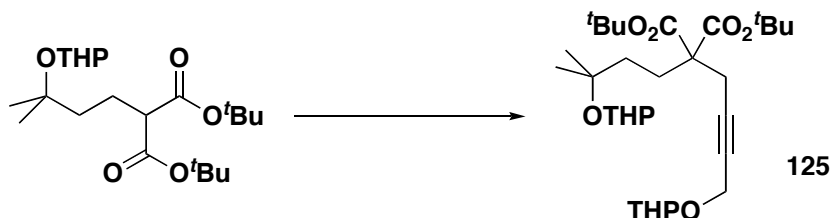
Di-*tert*-butyl 2-(3-methyl-3-(tetrahydro-2*H*-pyran-2-yloxy)butyl)malonate (**124**)



In a round bottom flask, to a cold (0 °C) suspension of sodium hydride (60% in mineral oil, 0.37 g, 9.3 mmol) in dimethylformamide (15 mL) was added di-*tert*-butyl malonate (2.58 g, 11.9 mmol) dropwise and stirred until H_2 ceased to evolve. This solution was then transferred by canula to a flask containing 2-(4-bromo-2-methylbutan-2-yloxy)-tetrahydro-2*H*-pyran (1.51 g, 6.01 mmol) and a catalytic amount of sodium iodide (~30 mg) at 0 °C. After stirring for 3 days at 50 °C, thin-layer chromatography confirmed complete consumption of the bromide and the reaction was quenched with saturated ammonium chloride then extracted with diethyl ether. The organic layer was dried over magnesium sulfate and solvents were evaporated *in vacuo* to give the crude product. Purification by flash silica gel chromatography (7 : 1 hexanes : ethyl acetate; R_f

0.24) gave the desired monoalkylated product **124** contaminated with ~9 mol% di-*tert*-butyl malonate. The starting material was removed by evaporation *in vacuo* by use of a diffusion pump ($\sim 5 \times 10^{-5}$ torr) to afford the title compound **124** as a colourless, viscous oil (1.39 g, 60%). Spectroscopic data for **124**: IR (neat, cm^{-1}): 2977 (s), 2941 (s), 2872 (m), 1729 (s), 1455 (m), 1393 (m), 1369 (m), 1349 (m), 1252 (s), 1199 (m), 1133 (s), 1108 (m), 1077 (m), 1024 (s), 997 (m), 850 (m), 817 (w), 746 (w); $^1\text{H NMR}$ (400 MHz, CDCl_3): δ 4.72 (m, 1H, OCHO), 3.93 (ddd, $J = 9.5$ Hz, $J = 5.3$ Hz, $J = 3.6$ Hz, 1H, CHHO), 3.43 (m, 1H, CHHO), 3.07 (t, $J = 7.5$ Hz, 1H, $\text{CH}(\text{C}=\text{O})_2$), 1.90-1.45 (m, 10H), 1.45 (s, 18H, $\text{C}(\text{CH}_3)_3$), 1.22 (s, 3H, $\text{CH}_3(\text{CH}_3)\text{CCH}_2$), 1.20 (s, 3H, $\text{CH}_3(\text{CH}_3)\text{CCH}_2$); $^{13}\text{C}\{^1\text{H}\}$ NMR (100 MHz, CDCl_3): δ 168.9 (C=O), 93.7 (OCHO), 81.2 ($\text{OC}(\text{CH}_3)_3$), 75.7 (THPOC), 63.4 (CH_2O), 54.2 ($\text{C}(\text{C}=\text{O})_2$), 39.3, 32.4, 27.9 ($\text{C}(\text{CH}_3)_3$), 26.8, 25.9 ($\text{CH}_3(\text{CH}_3)\text{CCH}_2$), 25.5 ($\text{CH}_3(\text{CH}_3)\text{CCH}_2$), 23.4, 20.6; $^1\text{H}-^1\text{H COSY}$ (400 MHz, CDCl_3): δ 3.93 \leftrightarrow δ 3.43; **HMQC** (400 MHz, CDCl_3): δ 4.72 \leftrightarrow δ 93.7; δ 3.93 \leftrightarrow δ 63.4; δ 3.43 \leftrightarrow δ 63.4; δ 3.07 \leftrightarrow δ 54.2; δ 1.45 \leftrightarrow δ 27.9; δ 1.22 \leftrightarrow δ 25.9; δ 1.20 \leftrightarrow δ 25.5; **ESMS** m/z calculated for $\text{C}_{21}\text{H}_{38}\text{O}_6\text{Na}$ ($\text{M}+\text{Na}$) $^+$: 409.25606; found: 409.25588; **Analysis** calculated for $\text{C}_{21}\text{H}_{38}\text{O}_6$: C, 65.26%; H, 9.91%; found: C, 64.70%; H, 9.87%.

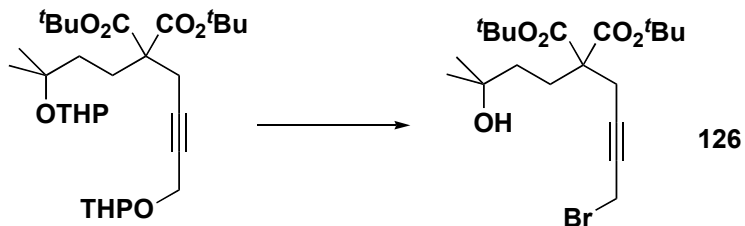
Di-*tert*-butyl 2-(3-methyl-3-(tetrahydro-2*H*-pyran-2-yloxy)butyl)-2-(4-(tetrahydro-2*H*-pyran-2-yloxy)but-2-ynyl)malonate (125)



In a round bottom flask, to a cold (0 °C) suspension of sodium hydride (60% in mineral oil, 0.17 g, 4.3 mmol) in dimethylformamide (10 mL) was added di-*tert*-butyl 2-(3-methyl-3-(tetrahydro-2*H*-pyran-2-yloxy)butyl)malonate (1.38 g, 3.57 mmol) dropwise and stirred until H_2 ceased to evolve. This solution was then transferred by canula to a flask containing 2-(4-bromobut-2-ynyl)-tetrahydro-2*H*-pyran (0.85 g, 3.7 mmol) at 0

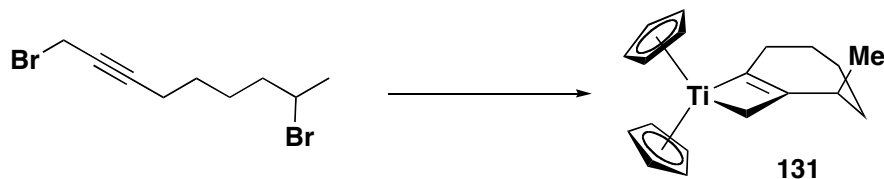
°C. After stirring overnight at room temperature, the reaction was quenched with saturated ammonium chloride and extracted with hexanes: diethyl ether (1 : 1 v/v). The organic layer was dried over magnesium sulfate and solvents were evaporated *in vacuo* to give the crude product. Purification by flash silica gel chromatography (4 : 1 hexanes : ethyl acetate; R_f 0.33) gave the dialkylated malonate **125** as a viscous, colourless oil (1.09 g, 57%). Spectroscopic data for **125**: **IR** (neat, cm^{-1}): 2975 (m), 2941 (s), 2871 (m), 1730 (s), 1455 (m), 1392 (m), 1369 (m), 1293 (m), 1250 (m), 1201 (w), 1161 (s), 1078 (m), 1024 (s), 990 (m), 945 (w), 903 (w), 870 (w), 849 (m), 816 (w), 730 (w); **^1H NMR** (300 MHz, CDCl_3): δ 4.78 (t, $J = 3.6$ Hz, 1H, OCHO), 4.75 (dd, $J = 3.1$ Hz, $J = 2.1$ Hz, 1H, OCHO), 4.20 (apparent q, $J = 2.5$ Hz, 2H, $\equiv\text{CCH}_2\text{O}$), 3.94 (ddd, $J = 9.7$ Hz, $J = 5.1$ Hz, $J = 3.3$ Hz, 1H, CHHO), 3.81 (ddd, $J = 11.7$ Hz, $J = 8.5$ Hz, $J = 3.5$ Hz, 1H, CHHO), 3.52 (m, 1H, CHHO), 3.45 (m, 1H, CHHO) 2.75 (t, $J = 2.2$ Hz, 2H, $\text{CH}_2\text{C}\equiv\text{CCH}_2\text{O}$), 2.01 (2nd order m, 2H), 1.90-1.46 (m, 12H, CH_2 (THP)), 1.45 (s, 16H, $\text{C}(\text{CH}_3)_3$), 1.36 (2nd order m, 2H), 1.23 (s, 3H, $\text{CH}_3(\text{CH}_3)\text{CCH}_2$), 1.22 (s, 3H, $\text{CH}_3(\text{CH}_3)\text{CCH}_2$); **$^{13}\text{C}\{^1\text{H}\}$ NMR** (100 MHz, CDCl_3): δ 169.5, 96.5, 93.5, 81.3, 81.2, 78.6, 75.6, 62.8, 62.1, 57.4, 54.2, 35.8, 32.3, 30.3, 27.8, 26.9, 26.2, 25.9, 25.5, 25.4, 22.7, 20.4, 19.2; **^1H - ^1H COSY** (400 MHz, CDCl_3): δ 4.20 \leftrightarrow δ 2.75; δ 3.94 \leftrightarrow δ 3.45; δ 3.81 \leftrightarrow δ 3.52; δ 2.01 \leftrightarrow δ 1.36; **HMQC** (400 MHz, CDCl_3): δ 4.78 \leftrightarrow δ 96.5; δ 4.75 \leftrightarrow δ 93.5; δ 4.20 \leftrightarrow δ 54.2; δ 2.75 \leftrightarrow δ 22.7; δ 1.45 \leftrightarrow δ 27.8; **ESMS** m/z calculated for $\text{C}_{30}\text{H}_{50}\text{O}_8\text{Na}$ ($\text{M}+\text{Na}$)⁺: 561.33979; found: 561.33982; **Analysis** calculated for $\text{C}_{30}\text{H}_{50}\text{O}_8$: C, 66.89%; H, 9.35%; found: C, 66.69 %; H, 9.37 %.

Di-tert-butyl 2-(4-bromobut-2-ynyl)-2-(3-hydroxy-3-methylbutyl)malonate (126)



In a round bottom flask, to a cold (0 °C) solution of triphenylphosphine (2.14 g, 8.16 mmol) in dichloromethane (50 mL) was added carbon tetrabromide (2.66 g, 8.02 mmol) dropwise resulting in a white, creamy suspension. To this was added a solution di-tert-butyl 2-(3-methyl-3-(tetrahydro-2*H*-pyran-2-yloxy)butyl)-2-(4-(tetrahydro-2*H*-pyran-2-yloxy)but-2-ynyl)malonate (0.86 g, 1.60 mmol) in dichloromethane (15 mL) at 0 °C. The mixture was stirred overnight at room temperature. The organic layer was successively washed with aqueous sodium bisulfite and sodium bicarbonate. The product was then extracted into dichloromethane and the organic layer was dried over magnesium sulfate. Volatiles were removed *in vacuo*. Purification by flash silica gel chromatography (3: 1 hexanes: ethyl acetate; R_f 0.18) provided the bromoalcohol **126** as a viscous, yellow-orange oil (151.3 mg, 22%). Spectroscopic data for **126**: IR (cast film, cm^{-1}): 3467 (br. w), 2976 (m), 2933 (m), 2237 (w), 1727 (s), 1454 (w), 1427 (w), 1393 (w), 1369 (m), 1294 (m), 1250 (w), 1218 (m), 1160 (s), 1141 (s), 1060 (m), 1022 (m), 909 (w), 847 (m), 748 (w), 728 (w); $^1\text{H NMR}$ (400 MHz, CDCl_3): δ 3.83 (apparent q, $J = 2.2$ Hz, 2H, $\equiv\text{CCH}_2\text{Br}$), 2.73 (apparent q, $J = 2.2$ Hz, 2H, $\text{CH}_2\text{C}\equiv\text{CCH}_2\text{Br}$), 1.96 (AA' MM', 2H), 1.62 (br. s, 1H, OH), 1.41 (s, 16H, $\text{C}(\text{CH}_3)_3$), 1.31 (AA' MM', 2H), 1.20 (s, 6H, $(\text{CH}_3)_2\text{CCH}_2$); $^{13}\text{C}\{^1\text{H}\}$ NMR (100 MHz, CDCl_3): δ 169.3 (C=O), 82.7 ($\text{C}\equiv\text{C}$), 81.7 ($\text{OC}(\text{CH}_3)_3$), 77.9 ($\text{C}\equiv\text{C}$), 70.5 ($(\text{CH}_3)_2\text{CCH}_2$), 57.3 ($\text{C}(\text{C}=\text{O})_2$), 37.6 (OCCH_2CH_2 or OCCH_2CH_2), 29.0 ($(\text{CH}_3)_2\text{CCH}_2$), 27.8 ($\text{C}(\text{CH}_3)_3$), 26.7 (OCCH_2CH_2 or OCCH_2CH_2), 22.9 ($\text{CH}_2\text{C}\equiv\text{CCH}_2\text{Br}$), 14.9 ($\text{CH}_2\text{C}\equiv\text{CCH}_2\text{Br}$); ESMS m/z calculated for $\text{C}_{20}\text{H}_{33}\text{BrO}_5\text{Na}$ ($\text{M}+\text{Na}$) $^+$: 457.2; found: 457.2.

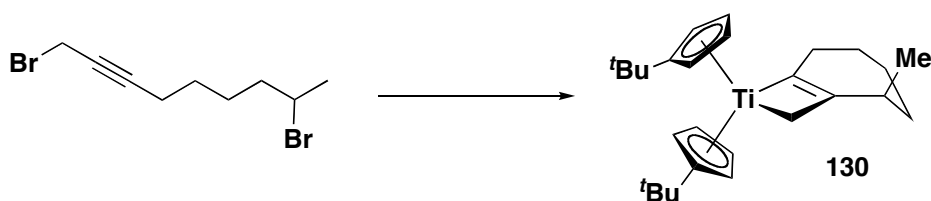
[Cp₂Ti(2-methanidyl-3-methylcyclohept-1-enyl)] (131)



In the drybox, a mixture of [Cp₂TiCl]₂ (15.2 mg, 35.6 μmol) and SmI₂ (150.7 mg, 248 μmol) in 2 mL THF was cooled to -30 °C. In a separate vessel, a solution of 1,8-dibromo-2-nonyne (19.5 mg, 68.9 μmol) in 1 mL THF was prepared and also cooled to -30 °C. The solutions were combined at -30 °C and allowed to stir at room temperature. Within minutes, the blue colour of the solution became green. The mixture was stirred overnight, after which the solution had become red and there was a yellow precipitate. The volatiles were removed *in vacuo* and the residue was triturated with pentane and filtered through Celite to remove the grey-green powder. Evaporation of the solvent provided the bicyclic titanacycle **131** as spectrally homogenous red oil (17.5 mg, 84%). No further purification was attempted. Spectroscopic data for **131**: **IR** (neat film, cm⁻¹): 2914 (s), 2852 (s), 1805 (w), 1710 (w), 1614 (w), 1444 (m), 1369 (w), 1315 (w), 1261 (w), 1207 (w), 1168 (w), 1142 (w), 1078 (w), 1018 (m), 805 (s); **¹H NMR** (400 MHz, C₆D₆): δ 5.52 (s, 10H, CpH), 3.44 (br. d, *J* = 11.4 Hz, 1H, TiCHH), 3.19 (dt, *J* = 11.4 Hz, *J* = 2.0 Hz, 1H, TiCHH), 2.56 (m, extracted coupling *J* = 16.1 Hz, 1H, TiCCHH), 2.41 (ddq, *J* = 16.0 Hz, *J* = 10.2 Hz, *J* = 2.4 Hz, 1H, TiCCHH), 2.31 (ddq, *J* = 13.0 Hz, *J* = 7.2 Hz, *J* = 3.6 Hz, 1H, CHCH₃), 1.63 (m, 2H), 1.45 (m, 2H, CH₂CHCH₃), 1.37 (m, 2H), 0.94 (d, *J* = 7.2 Hz, 3H, CHCH₃); **¹³C{¹H} NMR** (100 MHz, C₆D₆): δ 217.1 (TiC=C), 110.4 (C₅H₅), 110.1 (C₅H₅), 95.0 (TiC=C), 80.1 (TiCH₂), 36.9 (TiCCH₂ or CHCH₃), 36.8 (TiCCH₂ or CHCH₃), 34.1 (CH₂CHCH₃), 28.8, 26.4, 17.5 (CHCH₃); **¹H-¹H COSY** (400 MHz, C₆D₆): δ 3.44 ↔ δ 3.19, 2.56; δ 3.19 ↔ δ 2.56; δ 2.56 ↔ δ 2.41, 1.63 ; δ 2.31 ↔ δ 0.94; **HMQC** (400 MHz, C₆D₆): δ 5.52 ↔ δ 110.4, δ 110.1; δ 3.44 ↔ δ 80.1; δ 3.19 ↔ δ 80.1; δ 2.56, δ 2.56 ↔ δ 36.8/36.9¹⁴⁰; δ 2.41 ↔ δ 36.8/36.9¹⁴⁰; δ 2.31 ↔ δ 36.8/36.9¹⁴⁰; δ 1.63 ↔ δ 26.4; δ 1.45 ↔ δ 34.1; δ 1.37 ↔ δ 28.8; δ 0.94 ↔ δ 17.5; **HMBC** (400 MHz,

C_6D_6): δ 3.44, δ 3.19 \leftrightarrow δ 217.1, 95.0, 36.8/36.9¹⁴⁰; δ 2.56 \leftrightarrow δ 26.4; δ 2.41 \leftrightarrow δ 217.1, 95.0; δ 1.63 \leftrightarrow δ 36.8/36.9¹⁴⁰, 34.1, 28.8; δ 1.45 \leftrightarrow δ 36.8/36.9¹⁴⁰, 28.8, 26.4; δ 1.37 \leftrightarrow δ 36.8/36.9¹⁴⁰; δ 0.94 \leftrightarrow δ 95.0, 36.8/36.9¹⁴⁰, 34.1; **EIMS** m/z calculated for $C_{19}H_{24}Ti$ (M)⁺: 300.13574; found: 300.13545; **Analysis** calculated for $C_{19}H_{24}Ti$: C, 76.00%; H, 8.06%; found: C, 75.59%; H, 8.04%.

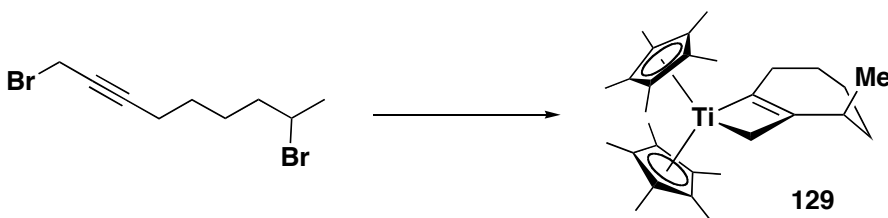
[^tBuCp₂Ti(2-methanidyl-3-methylcyclohept-1-enyl)] (130)



In the drybox, a mixture of [^tBuCp₂TiCl]₂ (19.3 mg, 29.7 μ mol) and SmI₂ (119.2 mg, 196.4 μ mol) in 2 mL THF was cooled to -30 °C. In a separate vessel, a solution of 1,8-dibromo-2-nonyne (16.6 mg, 58.7 μ mol) in 1 mL THF was prepared and also cooled to -30 °C. The solutions were combined at -30° C and allowed to stir at room temperature. Within minutes, the blue colour of the solution became green. The mixture was stirred overnight, after which the solution had become red and there was a yellow precipitate. The volatiles were removed *in vacuo* and the residue was triturated with pentane and filtered through Celite to remove the greenish powder. Evaporation of the solvent provided the bicyclic titanacycle **130** as spectrally homogenous dark-red oil (quantitative). No further purification was attempted. Spectroscopic data for **130**: **IR** (neat film, cm⁻¹): 2958 (s), 2925 (s), 2861 (m), 1489 (w), 1460 (m), 1361 (m), 1279 (w), 1201 (w), 1161 (w), 1044 (w), 1024 (w), 854 (w), 795 (s), 734 (m), 687 (w); **¹H NMR** (400 MHz, C₆D₆): δ 5.95 (apparent q, J = 2.7 Hz, 1H, ^tBuCpH), 5.86 (apparent q, 2.7 Hz, 1H, ^tBuCpH), 5.56 (apparent q, J = 2.6 Hz, 1H, ^tBuCpH), 5.52 (apparent q, J = 2.7 Hz, 1H, ^tBuCpH), 5.43 (apparent q, 2.5 Hz, 1H, ^tBuCpH), 5.40 (apparent p, J = 2.7 Hz, 2H, ^tBuCpH), 5.36 (apparent q, J = 2.4 Hz, 1H, ^tBuCpH), 3.38 (d, J = 11.6 Hz, 1H, TiCHH), 3.14 (d, J = 11.7 Hz, 1H, TiCHH), 2.64 (br dd, J = 15.9 Hz, 1H, TiCCHH), 2.51 (ddd, J =

16.0 Hz, $J = 9.7$ Hz, $J = 1.8$ Hz, 1H, TiCCHH), 2.33 (m, 1H, CHCH₃), 1.77-1.45 (m, 6H), 1.17 (s, 9H, C(CH₃)₃), 1.16 (s, 9H, C(CH₃)₃), 1.02 (d, $J = 7.2$ Hz, 3H, CHCH₃); ¹³C{¹H} NMR (100 MHz, C₆D₆): δ 214.2 (TiC=C), 139.04 (*ipso*-^tBuCp), 139.00 (*ipso*-^tBuCp), 110.4 (^tBuCp), 110.13 (^tBuCp), 110.09 (^tBuCp), 110.0 (^tBuCp), 109.6 (^tBuCp), 109.5 (^tBuCp), 107.0 (^tBuCp), 106.4 (^tBuCp), 99.7 (TiC=C), 76.2 (TiCH₂), 37.4 (TiCCH₂ or CHCH₃), 37.3 (TiCCH₂ or CHCH₃), 33.9, 32.80, 32.76, 31.8 (C(CH₃)₃), 31.7 (C(CH₃)₃), 29.1, 26.7, 17.9 (CHCH₃); ¹H-¹H COSY (400 MHz, C₆D₆): δ 3.38 ↔ δ 3.14, δ 2.51; δ 3.14 ↔ δ 2.51; δ 2.33 ↔ δ 1.02; **HMQC** (400 MHz, C₆D₆): δ 3.38 ↔ δ 76.2; δ 3.14 ↔ δ 76.2; δ 2.64 ↔ δ 37.4/37.3¹⁴⁰; δ 2.51 ↔ δ 37.4/37.3¹⁴⁰; δ 2.33 ↔ δ 37.4/37.3¹⁴⁰; δ 1.17 ↔ δ 31.8/31.7¹⁴⁰; δ 1.16 ↔ δ 31.8/31.7¹⁴⁰; δ 1.02 ↔ δ 17.9; **HMBC** (400 MHz, C₆D₆): δ 3.38 ↔ δ 214.2, 99.7, 37.4/37.3¹⁴⁰; δ 3.14 ↔ δ 214.2, 99.7, 37.4/37.3¹⁴⁰; δ 1.17 ↔ δ 139.04/139.00¹⁴⁰; δ 1.16 ↔ δ 139.04/139.00¹⁴⁰; δ 1.02 ↔ δ 99.7; **EIMS** m/z calculated for C₂₇H₄₀Ti (M)⁺: 412.26096; found: 412.25984; **Analysis** calculated for C₂₇H₄₀Ti: C, 78.62%; H, 9.77%; found: C, 75.54%; H, 9.73%.

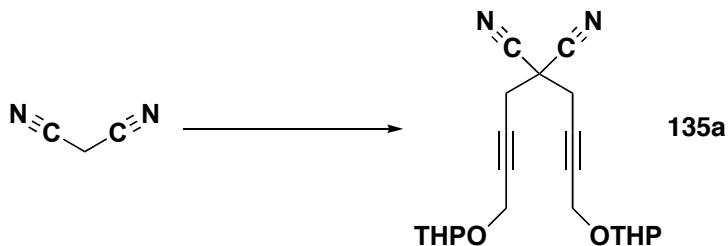
[Cp*₂Ti(2-methanidyl-3-methylcyclohept-1-enyl)] (129)



In the drybox, a mixture of Cp*₂TiCl (21.7 mg, 61.3 μmol) and SmI₂ (128.5 mg, 211.7 μmol) in 2 mL THF was cooled to -30 °C. In a separate vessel, a solution of 1,8-dibromo-2-nonyne (17.2 mg, 60.8 μmol) in 1 mL THF was prepared and also cooled to -30 °C. The solutions were combined at -30° C and allowed to stir at room temperature. Within minutes, the blue colour of the solution became green. The mixture was stirred overnight, after which the solution had become red and there was a yellow precipitate. The volatiles were removed *in vacuo* and the residue was triturated with pentane and

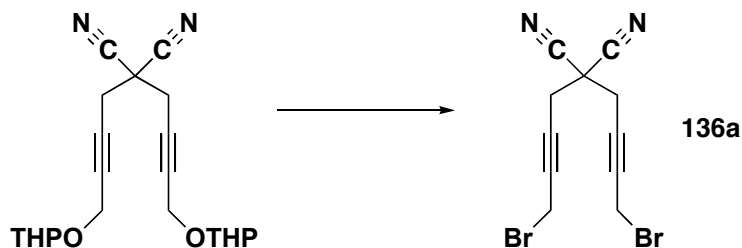
filtered through Celite to remove the greyish powder. Evaporation of the solvent provided the bicyclic titanacycle **129** as a spectrally homogenous red solid (quantitative). No further purification was attempted. Single-crystals were obtained by recrystallization from pentane at -30 °C. Spectroscopic data for **129**: **IR** (neat film, cm^{-1}): 2918 (s), 2860 (s), 2720 (w), 1495 (w), 1440 (m), 1376 (s), 1295 (w), 1263 (w), 1207 (w), 1081 (w), 1020 (w), 949 (w), 806 (w); **^1H NMR** (400 MHz, C_6D_6): δ 2.44 (m, 1H, CHCH_3), 2.43 (m, 1H, TiCCHH), 2.37 (d, $J = 12$ Hz, 1H, TiCHH), 2.32 (m, 1H, TiCCHH), 2.01 (d, $J = 12$ Hz, 1H, TiCHH), 1.89-1.72 (m, 4H, $\text{TiCCH}_2\text{CH}_2\text{CH}_2$), 1.73 (s, 15H, $(\text{CH}_3)_5\text{C}_5$), 1.71 (s, 15H, $(\text{CH}_3)_5\text{C}_5$), 1.60 (m, 2H, CHCH_2), 1.23 (d, $J = 7.2$ Hz, 3H, CHCH_3); **$^{13}\text{C}\{^1\text{H}\}$ NMR** (100 MHz, C_6D_6): δ 209.6 ($\text{TiC}=\text{C}$), 117.84 ($(\text{CH}_3)_5\text{C}_5$), 117.76 ($(\text{CH}_3)_5\text{C}_5$), 108.7 ($\text{TiC}=\text{C}$), 78.0 (TiCH_2), 38.7 (CHCH_3), 36.3 ($\text{TiCCH}_2\text{CH}_2$), 34.4 (TiCCH_2), 29.9 (CHCH_2), 27.8 (CHCH_2CH_2), 20.9 (CHCH_3), 12.1 ($(\text{CH}_3)_5\text{C}_5$), 12.0 ($(\text{CH}_3)_5\text{C}_5$); **^1H - ^1H COSY** (400 MHz, C_6D_6): δ 2.44 \leftrightarrow δ 1.23; δ 2.43 \leftrightarrow δ 2.32, 1.60 \leftrightarrow δ 2.01; δ 2.32 \leftrightarrow δ 1.60; **HMQC** (400 MHz, C_6D_6): δ 2.43 \leftrightarrow δ 38.7, 34.4; δ 2.37 \leftrightarrow δ 78.0; δ 2.32 \leftrightarrow δ 34.4; δ 2.01 \leftrightarrow δ 78.0; δ 1.73 \leftrightarrow δ 12.1; δ 1.71 \leftrightarrow δ 12.0; δ 1.60 \leftrightarrow δ 29.9; δ 1.23 \leftrightarrow δ 20.9; **HMBC** (400 MHz, C_6D_6): δ 2.44 \leftrightarrow δ 214.2, 108.7, 27.8, 20.9; δ 2.37 \leftrightarrow δ 214.2, 108.7; δ 2.32 \leftrightarrow δ 214.2, 108.7; δ 2.01 \leftrightarrow δ 214.2, 108.7, 38.7; 1.73 \leftrightarrow δ 118; δ 1.71 \leftrightarrow δ 118; δ 1.60 \leftrightarrow δ 27.8; δ 1.23 \leftrightarrow δ 108.7, 38.7, 36.3; **EIMS** m/z calculated for $\text{C}_{29}\text{H}_{44}\text{Ti}$ (M) $^+$: 440.29224; found: 440.29183; **Analysis** calculated for $\text{C}_{29}\text{H}_{44}\text{Ti}$: C, 78.62%; H, 9.77%; found: C, 77.55%; H, 10.15%.

2,2-Bis(4-(tetrahydro-2H-pyran-2-yloxy)but-2-ynyl)malononitrile (**135a**)



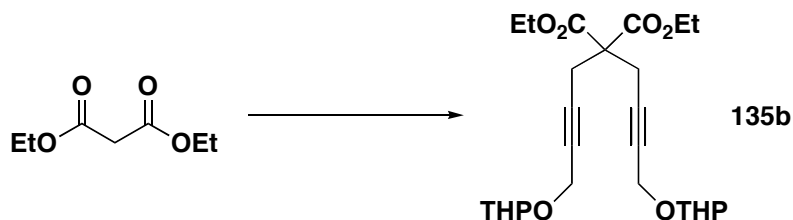
In a round bottom flask, to a cold (0 °C) suspension of sodium hydride (60% in mineral oil, 0.45 g, 11 mmol) in dimethylformamide (20 mL) was added malononitrile (0.33 g, 5.0 mmol) and 2-(4-bromobut-2-ynyloxy)-tetrahydro-2H-pyran (2.38 g, 10.2 mmol) dropwise. The reaction was stirred overnight then diluted with water and extracted with hexanes. The organic layer was dried over magnesium sulfate and the volatiles were evaporated *in vacuo* to give the crude material. The dimethylformamide was removed by distillation and the residue was purified by flash silica gel chromatography (2 : 1 hexanes : ethyl acetate; R_f 0.35) to provide the malononitrile compound **135a** as a very pale yellow, viscous oil (1.28 g, 69%). The material was used without further purification. Spectroscopic data for **135a**: **IR** (neat film, cm^{-1}): 2946 (s), 2870 (m), 2254 (w), 1442 (m), 1390 (w), 1346 (m), 1324 (w), 1265 (m), 1202 (m), 1183 (m), 1120 (s), 1078 (s), 1056 (s), 1027 (s), 970 (w), 944 (m), 903 (m), 871 (m), 815 (m), 698 (w); **^1H NMR** (300 MHz, CDCl_3): δ 4.68 (t, $J = 3.2$ Hz, 2H, OCHO), 4.19 (ABX₂, 4H, $\equiv\text{CCH}_2\text{O}$), 3.72 (ddd, $J = 5.2$ Hz, $J = 8.2$ Hz, $J = 10.2$ Hz, 2H, CHHO (THP)), 3.43 (m, 2H, CHHO (THP)), 2.96 (t, $J = 2.0$ Hz, 4H, $\text{CH}_2\text{C}\equiv\text{CCH}_2\text{O}$), 1.86-1.50 (m, 12H, CH_2 (THP)); **$^{13}\text{C}\{^1\text{H}\}$ NMR** (100 MHz, CDCl_3): δ 113.8 ($\text{C}\equiv\text{N}$), 97.1 (OCHO), 83.7 ($\text{C}\equiv\text{C}$), 75.9 ($\text{C}\equiv\text{C}$), 62.2 (CHHO (THP)), 54.0 ($\equiv\text{CCH}_2\text{O}$), 36.3 ($\text{C}(\text{CN})_2$), 30.2 (CH_2 (THP)), 27.8 ($\text{CH}_2\text{C}\equiv\text{CCH}_2\text{O}$), 25.3 (CH_2 (THP)), 19.1 (CH_2 (THP)); **HMQC** (400 MHz, CDCl_3): δ 4.68 \leftrightarrow δ 97.1; δ 4.19 \leftrightarrow δ 54.0; δ 3.72 \leftrightarrow δ 62.2; δ 3.33 \leftrightarrow δ 62.2; δ 2.96 \leftrightarrow δ 27.8; **EIMS** m/z calculated for $\text{C}_{21}\text{H}_{25}\text{N}_2\text{O}_4$ (M-H)⁺: 369.18143; found: 369.18186; **Analysis** calculated for $\text{C}_{21}\text{H}_{26}\text{N}_2\text{O}_4$: N, 7.56%; C, 68.09%; H, 7.07%; found: N, 7.49%; C, 66.71%; H, 6.95%.

2,2-Bis(4-bromobut-2-ynyl)malononitrile (**136a**)



In a round bottom flask, to a cold (0 °C) solution of triphenylphosphine (3.39 g, 12.9 mmol) in dichloromethane (30 mL) was added bromine (0.66 mL, 12.9 mmol) dropwise resulting in a white, creamy suspension. To this was added a solution of 2,2-bis(4-(tetrahydro-2*H*-pyran-2-yloxy)but-2-ynyl)malononitrile (1.15 g, 3.10 mmol) in dichloromethane (5 mL) at 0 °C. The mixture was stirred overnight at room temperature. The dark solution was washed with sodium bisulfite, sodium bicarbonate and water and the product was extracted into dichloromethane and the organic layer was dried over magnesium sulfate. The volatiles were removed *in vacuo*. The crude material was purified by flash silica gel chromatography (dichloromethane; R_f 0.70) to yield the dibromide **136a** as a dark-brown, viscous liquid which crystallized upon disturbance after standing for days (0.788 g, 77%). Spectroscopic data for **136a**: IR (neat film, cm^{-1}): 3011 (m), 2960 (m), 2967 (m), 2855 (w), 2275 (w), 2255 (w), 1718 (w), 1426 (s), 1327 (m), 1301 (w), 1269 (w), 1213 (s), 1159 (m), 1087 (m), 1051 (w), 907 (w), 862 (w), 793 (w), 733 (w), 697 (w); $^1\text{H NMR}$ (400 MHz, CDCl_3): δ 3.93 (t, $J = 2.3$ Hz, 4H, CH_2Br), 3.11 (t, $J = 2.3$ Hz, 4H, $\text{CH}_2\text{C}\equiv\text{CCH}_2\text{Br}$); $^{13}\text{C}\{^1\text{H}\}$ NMR (100 MHz, CDCl_3): δ 113.5 ($\text{C}\equiv\text{N}$), 82.6 ($\text{C}\equiv\text{C}$), 76.7 ($\text{C}\equiv\text{C}$), 36.1 ($\text{CH}_2\text{C}\equiv\text{CCH}_2\text{Br}$), 27.9 ($\text{C}(\text{CN})_2$), 13.2 (CH_2Br); **HMQC** (400 MHz, CDCl_3): δ 3.93 \leftrightarrow δ 13.2; δ 3.11 \leftrightarrow δ 27.9; **HMBC** (400 MHz, CDCl_3): δ 3.93 \leftrightarrow δ 82.6, 76.7; δ 3.11 \leftrightarrow δ 113.5, 82.6, 76.7, 36.1, 27.9; **EIMS** m/z calculated for $\text{C}_{11}\text{H}_8\text{N}_2$ ($\text{M}-2\text{Br}$) $^+$: 168.06874; found 168.06873; **Analysis** calculated for $\text{C}_{11}\text{H}_8\text{Br}_2\text{N}_2$: C, 40.28%; N, 8.54%; H, 2.46%; found: C, 40.55%; N, 8.26%; H, 2.61%.

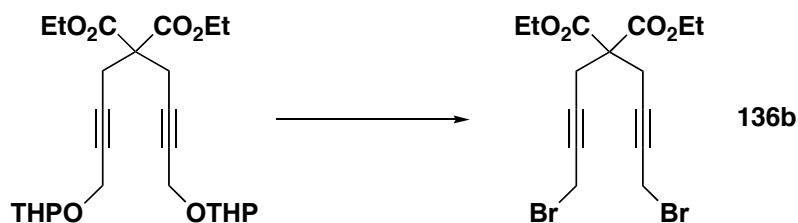
Diethyl 2,2-bis(4-(tetrahydro-2H-pyran-2-yloxy)but-2-ynyl)malonate (135b)



In a round bottom flask, to a cold (0 °C) suspension of sodium hydride (60% in mineral oil, 0.30 g, 7.5 mmol) in dimethylformamide (20 mL) was added diethyl malonate (0.52 g, 3.3 mmol) and 2-(4-bromobut-2-ynyloxy)-tetrahydro-2H-pyran (1.54 g, 6.6 mmol) dropwise. The reaction was stirred overnight at room temperature then diluted with water and extracted into hexanes. The organic layer was dried over magnesium sulfate and the volatiles were evaporated *in vacuo* to give the crude product as a viscous, yellow oil. Purification by flash silica gel chromatography (2 : 1 hexanes : ethyl acetate; R_f 0.39) afforded a diastereotopic mixture of diethyl malonate compound **135b** as a pale yellow oil (0.57 g, 38%). Spectroscopic data for **135b**: **IR** (cast film, cm^{-1}): 2942 (s), 2871 (m), 2743 (w), 2668 (w), 2228 (w), 1738 (s), 1466 (m), 1443 (m), 1429 (m), 1390 (m), 1367 (m), 1346 (m), 1288 (s), 1265 (m), 1242 (m), 1202 (s), 1118 (s), 1096 (s), 1078 (s), 1054 (s), 1025 (s), 972 (m), 945 (m), 903 (m), 871 (m), 816 (m), 785 (w), 754 (w), 678 (w), 668 (w); **$^1\text{H NMR}$** (400 MHz, CDCl_3): δ 4.75 (t, $J = 3.3$ Hz, 2H, OCHO), 4.19 (m, 8H, $\equiv\text{CCH}_2\text{O}$ and OCH_2CH_3), 3.80 (ddd, $J = 11.7$ Hz, $J = 4$ Hz, $J = 9.2$ Hz, $J = 3.4$ Hz, 2H, CHHO (THP)), 3.49 (m, 2H, CHHO (THP)), 2.98 (t, $J = 2.1$ Hz, 2H, $\text{CH}_2\text{C}\equiv\text{CCH}_2\text{O}$), 1.86-1.46 (m, 12H, CH_2 (THP)), 1.24 (t, $J = 7.1$ Hz, 6H, OCH_2CH_3); **$^{13}\text{C}\{^1\text{H}\}$ NMR** (100 MHz, CDCl_3): δ 168.7 (C=O), 96.5 (OCHO), 80.5 ($\equiv\text{CCH}_2\text{O}$), 79.3 ($\text{C}\equiv\text{CCH}_2\text{O}$), 62.0 (CH_2 (THP) or OCH_2CH_3), 61.9 (CH_2 (THP) or OCH_2CH_3), 56.5 ($\text{C}(\text{C}=\text{O})_2$), 54.2 ($\equiv\text{CCH}_2\text{O}$), 30.3 (CH_2 (THP)), 25.3 (CH_2 (THP)), 23.0 ($\text{CH}_2\text{C}\equiv\text{CCH}_2\text{O}$), 19.1 (CH_2 (THP)), 14.0 (OCH_2CH_3); **$^1\text{H}-^1\text{H COSY}$** (400 MHz, CDCl_3): δ 4.19 \leftrightarrow δ 2.98, 1.24; δ 3.80 \leftrightarrow δ 3.49; **HMQC** (400 MHz, CDCl_3): δ 4.75 \leftrightarrow δ 96.5; δ 4.19 \leftrightarrow δ 62.0/61.9¹⁴⁰, 54.2; δ 3.80 \leftrightarrow δ 62.0/61.9¹⁴⁰; δ 3.49 \leftrightarrow δ 62.0/61.9¹⁴⁰; δ 2.98 \leftrightarrow 23.0; δ 1.86-1.46 \leftrightarrow δ 30.3, 25.3, 19.1; δ 1.24 \leftrightarrow δ 14.0; **ESMS** m/z calculated for $\text{C}_{25}\text{H}_{36}\text{O}_8\text{Na}$

(M+Na)⁺: 487.23024; found: 487.23055; **Analysis** calculated for C₂₅H₃₆O₈: C, 64.64%; H, 7.81%; found: C, 64.12%; H, 7.87%.

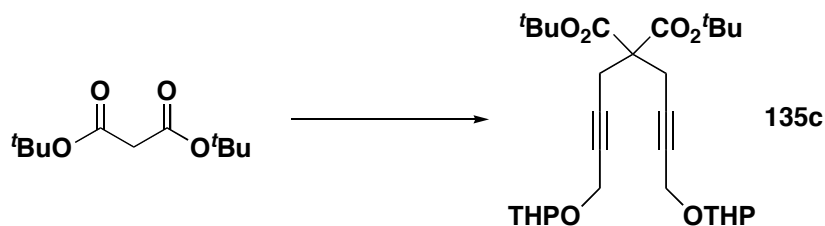
Diethyl 2,2-bis(4-bromobut-2-ynyl)malonate (**136b**)



In a round bottom flask, to a cold (0 °C) solution of triphenylphosphine (0.98 g, 3.7 mmol) in dichloromethane (10 mL) was added bromine (0.58 g, 3.6 mmol) dropwise resulting in a white, creamy suspension. To this was added a solution of diethyl 2,2-bis(4-(tetrahydro-2H-pyran-2-yloxy)but-2-ynyl)malonate (381.4 mg, 0.821 mmol) in dichloromethane (5 mL) at 0 °C. The mixture was stirred overnight at room temperature. The dark solution was filtered through a short plug of silica and the volatiles were evaporated *in vacuo*. The crude material was purified by flash silica gel chromatography (dichloromethane; R_f 0.68) to yield the title dibromide **136b** as an orange liquid (315.2 mg, 91%). Spectroscopic data for **136b**: **IR** (neat, cm⁻¹): 2981 (s), 2937 (m), 2906 (m), 2873 (m), 2372 (w), 2317 (w), 2238 (m), 1737 (s), 1649 (w), 1624 (w), 1465 (m), 1446 (m), 1426 (s), 1390 (m), 1367 (s), 1325 (s), 1296 (s), 1215 (s), 1157 (s), 1095 (s), 1053 (s), 1012 (m), 914 (w), 861 (m), 782 (m), 749 (w), 668 (w); **¹H NMR** (300 MHz, CDCl₃): δ 4.22 (q, *J* = 7.1 Hz, 4H, OCH₂CH₃), 3.85 (t, *J* = 2.3 Hz, 4H, ≡CCH₂Br), 3.00 (t, *J* = 2.3 Hz, 4H, CH₂C≡CCH₂Br), 1.26 (t, *J* = 7.1 Hz, 6H, OCH₂CH₃); **APT ¹³C{¹H} NMR** (100 MHz, CDCl₃): δ 168.4 (p, C=O), 81.8 (p, C≡C), 78.6 (p, C≡C), 62.1 (p, OCH₂CH₃), 56.5 (p, C(C=O)₂), 23.2 (p, CH₂C≡CCH₂Br), 14.5 (p, CH₂C≡CCH₂Br), 14.0 (n, OCH₂CH₃); **HMQC** (300 MHz, CDCl₃): δ 4.22 ↔ δ 62.1; δ 3.85 ↔ δ 14.5; δ 3.00 ↔ δ 23.2; δ 1.26 ↔ δ 14.0; **HMBC** (300 MHz, CDCl₃): δ 4.22 ↔ δ 168.4, 14.0; δ 3.85 ↔ δ 81.8, 78.6; δ 3.00 ↔ δ 168.4, 81.8, 78.6, 56.5, 23.2; δ 1.26 ↔ δ 62.1; **ESMS** *m/z* calculated for

$C_{15}H_{18}O_4Br_2Na$ ($M+Na$)⁺: 442.94640; found: 442.94643; **Analysis** calculated for $C_{15}H_{18}O_4Br_2$: C, 42.68%; H, 4.30%; found: C, 42.64%; H, 4.46%.

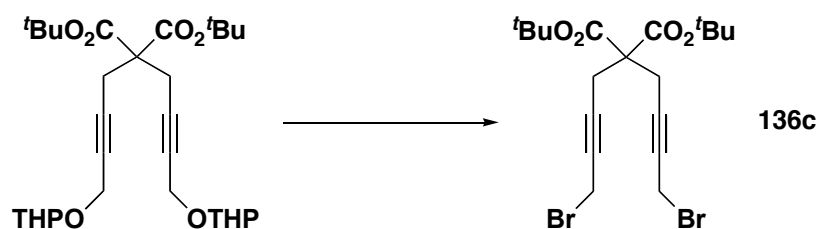
Di-*tert*-butyl 2,2-bis(4-(tetrahydro-2*H*-pyran-2-yloxy)but-2-ynyl)malonate (135c)



In a round bottom flask, to a cold (0 °C) suspension of sodium hydride (60% in mineral oil, 0.12 g, 3.0 mmol) in dimethylformamide (6 mL) was added di-*tert*-butyl malonate (0.25 g, 1.16 mmol) and 2-(4-bromobut-2-ynyloxy)-tetrahydro-2*H*-pyran (0.54 g, 2.32 mmol) dropwise. The reaction was stirred for 1 h then diluted with water and extracted with hexanes. The organic layer was dried over magnesium sulfate and solvents were evaporated *in vacuo* to give the spectroscopically pure malonate compound **135c** as a viscous, orange oil (0.49 g, 82%). No further purification was attempted. Spectroscopic data for **135c**: **IR** (cast film, cm^{-1}): 2942 (m), 2871 (m), 1733 (s), 1455 (w), 1393 (m), 1369 (m), 1323(m), 1301 (m), 1249 (m), 1221 (m), 1202 (m), 1142 (s), 1118 (s), 1078 (m), 1055 (m), 1025 (s), 972 (w), 946 (w), 903 (m), 872 (w), 847 (m), 816 (w), 731 (w); **¹H NMR** (400 MHz, $CDCl_3$): δ 4.77 (t, $J = 3.4$ Hz, 2H, OCHO), 4.23 (dt, $J = 15.5$ Hz, $J = 2.1$ Hz, 2H, $\equiv CCHHO$), 4.18 (dt, $J = 15.5$ Hz, $J = 2.1$ Hz, 2H, $\equiv CCHHO$), 3.82 (ddd, $J = 3.3$ Hz, $J = 9.0$, $J = 11.9$ Hz, 2H, CHHO (THP)), 3.52 (m, 2H, CHHO (THP)), 2.89 (t, $J = 2.1$ Hz, 4H, $CH_2C\equiv CCH_2O$), 1.88-1.50 (m, 12H, CH_2 (THP)), 1.47 (s, 18H, $C(CH_3)_3$); **¹³C{¹H} NMR** (100 MHz, $CDCl_3$): δ 167.9 ($C=O$), 96.5 (OCHO), 81.9 ($OC(CH_3)_3$), 81.0 ($\equiv CCH_2O$), 79.0 ($C\equiv CCH_2O$), 62.1 (CH_2O (THP)), 57.3 ($C(C=O)_2$), 54.2 ($\equiv CCH_2O$), 30.3 (CH_2 (THP)), 27.7 ($C(CH_3)_3$), 25.4 (CH_2 (THP)), 22.8 ($CH_2C\equiv CCH_2O$), 19.2 (CH_2 (THP)); **¹H-¹H COSY** (400 MHz, $CDCl_3$): δ 4.23 \leftrightarrow δ 4.18, 2.89; δ 4.18 \leftrightarrow δ 2.89; δ 3.82 \leftrightarrow δ 3.52; **HMQC** (400 MHz, $CDCl_3$): δ 4.77 \leftrightarrow δ 96.5; δ

4.23 \leftrightarrow δ 54.2; δ 4.18 \leftrightarrow δ 54.2; δ 3.82 \leftrightarrow δ 62.1; δ 3.52 \leftrightarrow δ 62.1; δ 2.89 \leftrightarrow δ 22.8; δ 1.47 \leftrightarrow δ 25.4; **HMBC** (400 MHz, CDCl₃): δ 4.77 \leftrightarrow δ 54.2, 19.2; δ 4.23 \leftrightarrow δ 96.5, 81.0, 79.0, 57.3, 22.8; δ 4.18 \leftrightarrow δ 96.5, 81.0, 79.0, 57.3, 22.8; δ 3.82 \leftrightarrow δ 96.5, 19.2; δ 3.52 \leftrightarrow δ 96.5, 25.4, 22.8; δ 2.89 \leftrightarrow δ 167.9, 81.0, 79.0, 57.3, 22.8; δ 1.47 \leftrightarrow δ 81.9; **ESMS** m/z calculated for C₂₉H₄₄O₈Na (M+Na)⁺: 543.29284; found: 543.29306; **Analysis** calculated for C₂₉H₄₄O₈: C, 66.90%; H, 8.52%; found: C, 65.86%; H, 8.46%.

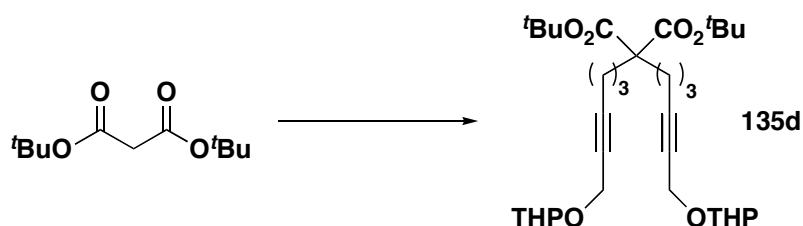
Di-*tert*-butyl 2,2-bis(4-bromobut-2-ynyl)malonate (**136c**)



In a round bottom flask, to a cold (0 °C) solution of triphenylphosphine (1.09 g, 4.16 mmol) in dichloromethane (10 mL) was added bromine (0.62 g, 3.9 mmol) dropwise resulting in a white, creamy suspension. To this was added a solution of di-*tert*-butyl 2,2-bis(4-(tetrahydro-2*H*-pyran-2-yloxy)but-2-ynyl)malonate (0.49 g, 0.94 mmol) in dichloromethane (5 mL) at 0 °C. The mixture was stirred overnight at room temperature. Volatiles were removed *in vacuo* and the product was extracted into hexanes. Evaporation of solvent *in vacuo* left behind the crude solid which was recrystallized from methanol / water to afford the dibromide **136c** as a spectrally homogenous white, fluffy solid (0.45 g, 100%). No further purification was attempted. Spectroscopic data for **136c**: **IR** (cm⁻¹): 3014 (w), 3002 (w), 2974 (m), 2931 (w), 2289 (w), 2235 (w), 1746 (m), 1724 (s), 1475 (w), 1456 (w), 1424 (w), 1393 (w), 1368 (m), 1311 (m), 1248 (m), 1212 (m), 1143 (s), 1073 (m), 1053 (m), 1032 (m), 881 (w), 842 (m), 737 (w), 719 (w), 668 (w); **¹H NMR** (400 MHz, CDCl₃): δ 3.87 (t, J = 2.3 Hz, 4H, \equiv CCH₂Br), 2.91 (t, J = 2.3 Hz, 4H, CH₂C \equiv CCH₂Br), 1.47 (s, 18H, C(CH₃)₃); **¹³C{¹H} NMR** (100 MHz, CDCl₃): δ 167.6 (C=O), 82.34 (OC(CH₃)₃), 82.31 (C \equiv C), 78.2 (C \equiv C), 57.3 (C(C=O)₂), 27.8

(C(CH₃)₃, 23.0 (CH₂C≡CCH₂Br), 14.6 (≡CCH₂Br); **ESMS** *m/z* calculated for C₁₉H₂₆Br₂O₄Na (M+Na)⁺: 499.00900; found: 499.00956; **Analysis** calculated for C₁₉H₂₆Br₂O₄: C, 47.72%; H, 5.48%; found: C, 48.98%; H, 5.55%.

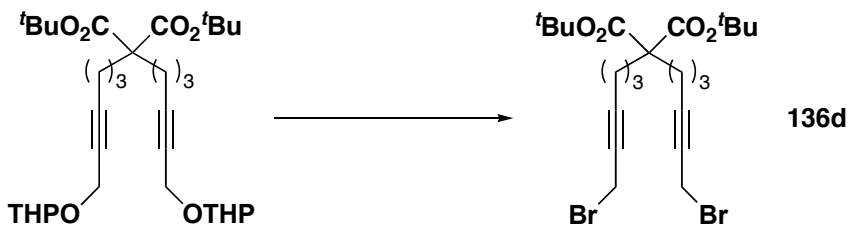
Di-*tert*-butyl 2,2-bis(6-(tetrahydro-2*H*-pyran-2-yloxy)hex-4-ynyl)malonate (135d)



In a round bottom flask, to a cold (0 °C) suspension of sodium hydride (60% in mineral oil, 0.32 g, 8.0 mmol) in dimethylformamide (20 mL) was added di-*tert*-butyl malonate (0.70 g, 3.2 mmol) and 2-(6-bromohex-2-ynyloxy)-tetrahydro-2*H*-pyran (1.64 g, 6.28 mmol) dropwise. The reaction was heated to 60 °C overnight then diluted with water and extracted into hexanes : diethyl ether (1 : 1 *v/v*). The organic layer was dried over magnesium sulfate and the volatiles were evaporated *in vacuo* to give the spectroscopically pure malonate derivative **135d** as a yellow, viscous oil (1.48 g, 82%). Separation of the undetermined mixture of *rac* / *meso* isomers was not attempted and the material was used without further purification. Spectroscopic data for **135d**: **IR** (neat, cm⁻¹): 2941 (s), 2870 (s), 2287 (w), 2223 (w), 1726 (s), 1456 (m), 1392 (m), 1368 (s), 1344 (m), 1323 (m), 1302 (m), 1261 (s), 1202 (s), 1147 (s), 1118 (s), 1079 (s), 1054 (s), 1026 (s), 973 (m), 946 (m), 903 (m), 872 (m), 851 (m), 727 (w); **¹H NMR** (400 MHz, CDCl₃): δ 4.78 (t, *J* = 3.4 Hz, 2H, OCHO), 4.27 (dt, *J* = 15.2 Hz, *J* = 2.1 Hz, 2H, ≡CCHHO), 4.17 (dt, *J* = 15.2 Hz, *J* = 2.1 Hz, 2H, ≡CCHHO), 3.82 (ddd, *J* = 3.2 Hz, *J* = 8.9 Hz, *J* = 11.9 Hz, 2H, CHHO (THP)), 3.52 (m, 2H, CHHO (THP)), 2.22 (tt, *J* = 7.0 Hz, *J* = 2.1 Hz, 4H, CH₂C≡CCH₂O), 1.87 (2nd order m, 2H, CH₂C(C=O)₂), 1.84-1.46 (m, 12H, CH₂ (THP)), 1.44 (s, 18H, C(CH₃)₃), 1.39 (m, 4H, CH₂CH₂CH₂); **¹³C{¹H} NMR** (100 MHz, CDCl₃): δ 170.7 (C=O), 96.7 (OCHO), 85.1 (C≡CCH₂O), 81.0 (OC(CH₃)₃), 76.2 (C≡CCH₂O), 62.0 (CH₂O (THP)), 57.8 (C(C=O)₂), 54.6 (≡CCH₂O), 31.2

(CH₂C(C=O)₂), 30.3 (CH₂ (THP)), 27.9 (C(CH₃)₃), 25.4 (CH₂ (THP)), 23.2 (CH₂CH₂CH₂), 19.2 (CH₂ (THP) *or* CH₂C≡CCH₂O), 19.1 (CH₂ (THP) *or* CH₂C≡CCH₂O); **¹H-¹H COSY** (400 MHz, CDCl₃): δ 4.27 ↔ δ 4.17, 2.22; δ 4.17 ↔ δ 2.22; δ 3.82 ↔ δ 3.52; δ 2.22 ↔ δ 1.39; δ 1.87 ↔ δ 1.39; **HMQC** (400 MHz, CDCl₃): δ 4.78 ↔ δ 96.7; δ 4.27 ↔ δ 54.6; δ 4.17 ↔ δ 54.6; δ 3.82 ↔ δ 62.0; δ 3.52 ↔ δ 62.0; δ 2.22 ↔ δ 19.2/19.1¹⁴⁰; δ 1.87 ↔ δ 31.2; δ 1.44 ↔ δ 27.9; δ 1.39 ↔ δ 23.2; **HMBC** (400 MHz, CDCl₃): δ 4.78 ↔ δ 62.0, 54.6, 19.2/19.1¹⁴⁰; δ 4.27 ↔ δ 96.7, 85.1, 76.2, 23.2; δ 4.17 ↔ δ 96.7, 85.1, 76.2, 23.2; δ 3.82 ↔ δ 85.1, 25.4, 19.2/19.1;¹⁴⁰ δ 3.52 ↔ δ 85.1, 25.4, 19.2/19.1;¹⁴⁰ δ 2.22 ↔ δ 85.1, 76.2, 31.2, 23.2; δ 1.87 ↔ δ 170.7, 57.8, 31.2, 23.2, 19.2/19.1;¹⁴⁰ δ 1.44 ↔ δ 81.0; δ 1.39 ↔ δ 76.2, 57.8, 31.2, 19.2/19.1¹⁴⁰; **ESMS** *m/z* calculated for C₃₃H₅₂O₈Na (M+Na)⁺: 599.35544; found: 599.35640; **Analysis** calculated for C₃₃H₅₂O₈: C, 68.72%; H, 9.09%; found: C, 69.48%; H, 9.80%.

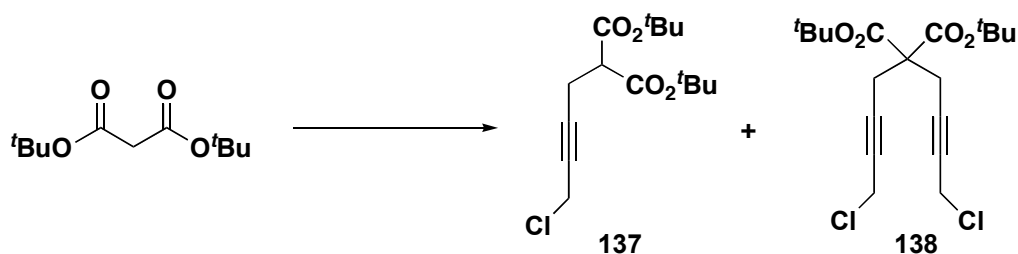
Di-*tert*-butyl 2,2-bis(6-bromohex-4-ynyl)malonate (136d)



In a round bottom flask, to a cold (0 °C) solution of triphenylphosphine (2.48 g, 9.45 mmol) in dichloromethane (20 mL) was added bromine (1.45 g, 9.07 mmol) dropwise resulting in a white, creamy suspension. To this was added a solution of di-*tert*-butyl 2,2-bis(6-(tetrahydro-2H-pyran-2-yloxy)hex-4-ynyl)malonate (1.22 g, 2.16 mmol) in dichloromethane (10 mL) at 0 °C. The mixture was stirred overnight at room temperature. Volatiles were removed *in vacuo* and the product was extracted into hexanes. Evaporation of solvent *in vacuo* left behind a black solid, which was washed with saturated sodium bicarbonate and extracted into hexanes. Evaporation of solvent and purification by flash silica gel chromatography (9 : 1 hexanes : ethyl acetate; R_f

0.24) led to the isolation of dibromide **136d** as a white solid (0.49 g, 43%). Single crystals were obtained by recrystallization from hexanes. Spectroscopic data for **136d**: **IR** (cast film, cm^{-1}): 3003 (w), 2976 (m), 2935 (m), 2873 (w), 2310 (w), 2233 (w), 1807 (w), 1724 (s), 1476 (w), 1457 (m), 1429 (w), 1393 (m), 1368 (m), 1334 (w), 1303 (m), 1257 (m), 1220 (m), 1165 (s), 1147 (s), 1102 (w), 1090 (w), 1039 (w), 998 (w), 850 (m), 746 (w); **^1H NMR** (400 MHz, C_6D_6): δ 3.39 (t, $J = 2.3$ Hz, 4H, $\equiv\text{CCH}_2\text{Br}$), 2.01 (2nd order m, 4H, $\text{CH}_2\text{C}(\text{C}=\text{O})_2$), 1.94 (tt, $J = 7.0$ Hz, $J = 2.3$ Hz, 4H, $\text{CH}_2\text{C}\equiv\text{CCH}_2\text{Br}$), 1.42 (m, 4H, $\text{CH}_2\text{CH}_2\text{CH}_2$), 1.39 (s, 18H, $\text{C}(\text{CH}_3)_3$); **$^{13}\text{C}\{^1\text{H}\}$ NMR** (100 MHz, C_6D_6): δ 170.6 ($\text{C}=\text{O}$), 87.6 ($\text{C}\equiv\text{C}$), 80.6 ($\text{OC}(\text{CH}_3)_3$), 76.4 ($\text{C}\equiv\text{C}$), 58.2 ($\text{C}(\text{CH}_3)_3$), 31.8 ($\text{CH}_2\text{C}(\text{C}=\text{O})_2$), 27.9 ($\text{C}(\text{CH}_3)_3$), 23.5 ($\text{CH}_2\text{CH}_2\text{CH}_2$), 19.4 ($\text{CH}_2\text{C}\equiv\text{CCH}_2\text{Br}$), 15.3 ($\text{CH}_2\text{C}\equiv\text{CCH}_2\text{Br}$); **^1H - ^1H COSY** (400 MHz, C_6D_6): δ 3.39 \leftrightarrow δ 1.94; δ 2.01 \leftrightarrow δ 1.42; δ 1.94 \leftrightarrow δ 1.42; **HMQC** (400 MHz, C_6D_6): δ 3.39 \leftrightarrow δ 15.3; δ 2.01 \leftrightarrow δ 31.8; δ 1.94 \leftrightarrow δ 19.4; δ 1.42 \leftrightarrow δ 23.5; δ 1.39 \leftrightarrow δ 27.9; **ESMS** m/z calculated for $\text{C}_{23}\text{H}_{34}\text{O}_4\text{Br}_2\text{Na}$ ($\text{M}+\text{Na}$)⁺: 555.07160; found: 555.07151; **Analysis** calculated for $\text{C}_{23}\text{H}_{34}\text{O}_4\text{Br}_2$: C, 51.70%; H, 6.04%; found: C, 51.22%; H, 6.28%. For crystal structure report see JMS0838 in Appendix.

Di-tert-butyl 2,2-bis(4-chlorobut-2-ynyl)malonate (138) and Di-tert-butyl 2-(4-chlorobut-2-ynyl)malonate (137)

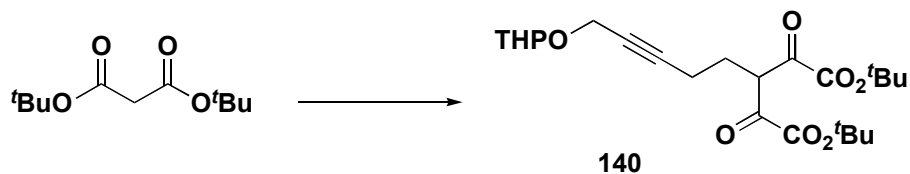


In a round bottom flask, to a cold (0 °C) suspension of sodium hydride (60% in mineral oil, 2.03 g, 50.8 mmol) in dimethylformamide (125 mL) was added di-tert-butyl malonate (4.90 mL, 21.9 mmol) dropwise and stirred until H_2 ceased to evolve. To this solution was then added excess 1,4-dichloro-2-butyne (22 mL, 230 mmol) at 0 °C. After stirring overnight at 50 °C, the reaction was quenched with water then extracted into

dichloromethane. The organic layer was dried over magnesium sulfate and solvents were evaporated *in vacuo* to give the crude product. Vacuum distillation (1 mm Hg) gave the monoalkylated product **137** as a colourless, viscous oil (b.p. 80-86 °C, 1.47 g, 22%) and the dialkylated product **138** as a yellow, viscous oil (b.p. 135-142 °C, 1.16 g, 14%). Spectroscopic data for **138**: **IR** (cast film, cm^{-1}): 2979 (m), 2933 (w), 2241 (w), 1732 (s), 1477 (w), 1457 (w), 1425 (s), 1394 (w), 1370 (m), 1324 (m), 1303 (m), 1263 (m), 1250 (m), 1222 (m), 1164 (s), 1144 (s), 1069 (w), 1054 (w), 1032 (w), 846 (w), 726 (w), 698 (w); **^1H NMR** (300 MHz, CDCl_3): δ 4.08 (t, $J = 2.2$ Hz, 4H, $\equiv\text{CCH}_2\text{Cl}$), 2.89 (t, $J = 2.2$ Hz, 4H, $\text{CH}_2\text{C}\equiv\text{CCH}_2\text{Cl}$), 1.46 (s, 16H, $\text{C}(\text{CH}_3)_3$); **$^{13}\text{C}\{^1\text{H}\}$ NMR** (100 MHz, CDCl_3): δ 167.6 ($\text{C}=\text{O}$), 82.3 ($\text{OC}(\text{CH}_3)_3$), 81.9 ($\text{C}\equiv\text{C}$), 77.9 ($\text{C}\equiv\text{C}$), 57.2 ($\text{C}(\text{C}=\text{O})_2$), 30.6 ($\equiv\text{CCH}_2\text{Cl}$), 27.7 ($\text{C}(\text{CH}_3)_3$), 22.9 ($\text{CH}_2\text{C}\equiv\text{CCH}_2\text{Cl}$); **HMQC** (300 MHz, CDCl_3): δ 4.08 \leftrightarrow δ 30.6; δ 2.89 \leftrightarrow δ 22.9; δ 1.46 \leftrightarrow δ 27.7; **HMBC** (300 MHz, CDCl_3): δ 4.08 \leftrightarrow δ 81.9, 77.9; δ 2.89 \leftrightarrow δ 167.6, 81.9, 77.9, 57.2, 22.9; δ 1.46 \leftrightarrow δ 82.3; **ESMS** m/z calculated for $\text{C}_{19}\text{H}_{26}\text{O}_4\text{Cl}_2\text{Na}$ ($\text{M}+\text{Na}$) $^+$: 411.11004; found: 411.11009; **Analysis** calculated for $\text{C}_{19}\text{H}_{26}\text{O}_4\text{Cl}_2$: C, 58.62%; H, 6.73%; found: C, 58.48%; H, 6.50%.

Spectroscopic data for **137**: **IR** (cast film, cm^{-1}): 2980 (m), 2933 (m), 2243 (w), 1730 (s), 1478 (w), 1458 (w), 1426 (w), 1394 (m), 1370 (s), 1345 (m), 1311 (w), 1283 (w), 1263 (m), 1250 (m), 1165 (s), 1142 (s), 1063 (w), 991 (w), 971 (w), 877 (w), 847 (m), 739 (w), 698 (w); **^1H NMR** (400 MHz, CDCl_3): δ 4.07 (t, $J = 2.3$ Hz, 2H, $\equiv\text{CCH}_2\text{Cl}$), 3.32 (t, $J = 7.7$ Hz, 1H, $\text{CH}(\text{C}=\text{O})_2$), 2.69 (dt, $J = 7.8$ Hz, $J = 2.3$ Hz, 2H, $\text{CH}_2\text{C}\equiv\text{CCH}_2\text{Cl}$), 1.44 (s, 16H, $\text{C}(\text{CH}_3)_3$); **$^{13}\text{C}\{^1\text{H}\}$ NMR** (100 MHz, CDCl_3): δ 167.1 ($\text{C}=\text{O}$), 83.4 ($\text{C}\equiv\text{CCH}_2\text{Cl}$), 82.0 ($\text{OC}(\text{CH}_3)_3$), 76.6 ($\equiv\text{CCH}_2\text{Cl}$), 52.7 ($\text{CH}(\text{C}=\text{O})_2$), 30.7 ($\equiv\text{CCH}_2\text{Cl}$), 27.8 ($\text{C}(\text{CH}_3)_3$), 18.6 ($\text{CH}_2\text{C}\equiv\text{CCH}_2\text{Cl}$); **HMQC** (400 MHz, CDCl_3): δ 4.07 \leftrightarrow δ 30.7; δ 3.32 \leftrightarrow δ 52.7; δ 2.69 \leftrightarrow δ 18.6; δ 1.44 \leftrightarrow δ 27.8; **HMBC** (400 MHz, CDCl_3): δ 4.07 \leftrightarrow δ 83.4, 76.7, 52.7, 18.6; δ 3.32 \leftrightarrow δ 167.1, 83.4, 18.6; δ 2.69 \leftrightarrow δ 167.1, 82.4, 76.6, 52.7, 30.7; δ 1.44 \leftrightarrow δ 167.1, 82.0; **ESMS** m/z calculated for $\text{C}_{15}\text{H}_{23}\text{O}_4\text{ClNa}$ ($\text{M}+\text{Na}$) $^+$: 325.11771; found: 325.11777; **Analysis** calculated for $\text{C}_{15}\text{H}_{23}\text{O}_4\text{Cl}$: C, 59.50%; H, 7.66%; found: C, 59.89%; H, 7.95%.

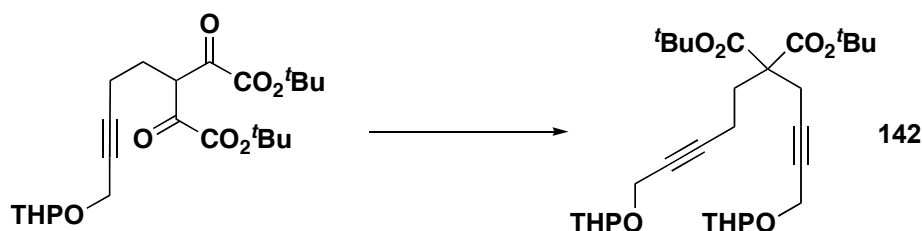
Di-*tert*-butyl 2-(5-(tetrahydro-2H-pyran-2-yloxy)pent-3-ynyl)malonate (**140**)



In a round bottom flask, to a cold (0 °C) suspension of sodium hydride (60% in mineral oil, 0.21 g, 5.3 mmol) in dimethylformamide (20 mL) was added di-*tert*-butyl malonate (1.51 g, 6.98 mmol) and 2-(5-bromopent-2-ynyloxy)-tetrahydro-2H-pyran (1.13 g, 4.57 mmol) dropwise. The mixture was stirred overnight at room temperature then diluted with water and extracted into petroleum ether : diethyl ether (1 : 1 v/v). The organic layer was dried over sodium sulfate and the volatiles were evaporated *in vacuo* ($\sim 4 \times 10^{-3}$ torr) to give the spectroscopically homogenous malonate derivative **140** as an orange liquid (1.16 g, 66%). Spectroscopic data for **140**: **IR** (neat film, cm^{-1}): 2977 (m), 2942 (m), 2872 (w), 1743 (s), 1728 (s), 1479 (w), 1456 (w), 1393 (m), 1369 (m), 1346 (w), 1323 (w), 1288 (w), 1255(m), 1202 (w), 1162 (s), 1140 (s), 1119 (w), 1079 (w), 1054 (w), 1025 (s), 973 (w), 946 (w), 932 (w), 903 (w), 872 (w), 849 (w), 816 (w), 781 (w), 745 (w); **$^1\text{H NMR}$** (400 MHz, CDCl_3): δ 4.79 (t, $J = 3.4$ Hz, 1H, OCHO), 4.27 (dt, $J = 15.3$ Hz, $J = 2.2$ Hz, 1H, $\equiv\text{CHHO}$), 4.18 (dt, $J = 15.3$ Hz, $J = 2.2$ Hz, 1H, $\equiv\text{CHHO}$), 3.83 (ddd, $J = 11.8$ Hz, $J = 8.9$ Hz, 3.2 Hz, 1H, CHHO (THP)), 3.51 (m, 1H, CHHO (THP)), 3.30 (t, $J = 7.4$ Hz, 1H, $\text{CH}(\text{C}=\text{O})_2$), 2.29 (tt, $J = 7.2$ Hz, $J = 2.1$ Hz, 2H, $\text{CH}_2\equiv\text{CH}_2\text{O}$), 2.00 (q, $J = 7.3$ Hz, 2H, $\text{CH}_2\text{CH}_2\equiv\text{CH}_2\text{O}$), 1.88-1.40 (m, 6H, CH_2 (THP)), 1.45 (s, 18H, $\text{C}(\text{CH}_3)_3$); **$^{13}\text{C}\{^1\text{H}\}$ NMR** (100 MHz, CDCl_3): δ 168.4 (C=O), 96.7 (OCHO), 84.8 ($\text{C}\equiv\text{C}$), 81.5 ($\text{OC}(\text{CH}_3)_3$), 76.8 ($\text{C}\equiv\text{C}$), 62.0, 54.5 (CH_2O (THP)), 52.7 ($\text{CH}(\text{C}=\text{O})_2$), 30.3 (CH_2 (THP)), 27.9 ($\text{C}(\text{CH}_3)_3$), 27.5 ($\text{CH}_2\text{CH}_2\equiv\text{CH}_2\text{O}$), 25.4 (CH_2 (THP)), 19.1 (CH_2 (THP)), 16.7 ($\text{CH}_2\equiv\text{CH}_2\text{O}$); **$^1\text{H}-^1\text{H COSY}$** (400 MHz, CDCl_3): δ 4.27 \leftrightarrow δ 4.18, 2.29; δ 4.18 \leftrightarrow δ 2.29; δ 3.83 \leftrightarrow δ 3.51; δ 2.29 \leftrightarrow δ 2.00; **HMQC** (400 MHz, CDCl_3): δ 4.79 \leftrightarrow δ 96.7; δ 4.27, δ 4.18 \leftrightarrow δ 54.5; δ 3.83, δ 3.51 \leftrightarrow δ 62.0; δ 3.30 \leftrightarrow δ 52.7; δ 2.29 \leftrightarrow δ 16.7; δ 2.00 \leftrightarrow δ 27.5; δ 2.29 \leftrightarrow δ 16.7; δ 1.45 \leftrightarrow δ 27.9; **HMBC** (400 MHz, CDCl_3): δ 4.27, δ 4.18 \leftrightarrow δ 96.7, 84.8, 76.8; δ 3.30 \leftrightarrow δ 168.4, 27.5, 16.7; δ 2.29

$\leftrightarrow \delta$ 84.8, 81.5, 76.8, 52.7, 27.5; δ 2.00 $\leftrightarrow \delta$ 168.4, 84.8, 52.7, 16.7; δ 1.45 $\leftrightarrow \delta$ 81.5; **ESMS** m/z calculated for $C_{21}H_{34}O_6Na$ ($M+Na$)⁺: 405.22476; found 405.22487; **Analysis** calculated for $C_{21}H_{34}O_6$: C, 65.94%; H, 8.96%; found: C, 65.68%; H, 8.93%.

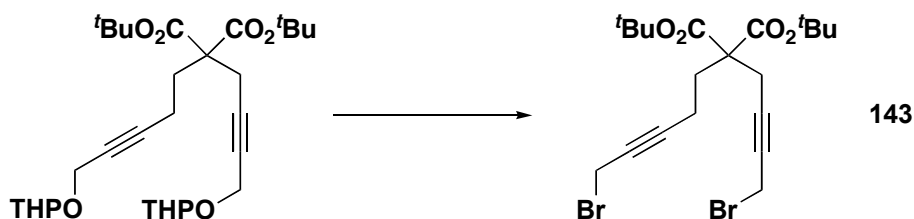
Di-tert-butyl 2-(4-(tetrahydro-2H-pyran-2-yloxy)but-2-ynyl)-2-(5-(tetrahydro-2H-pyran-2-yloxy)pent-3-ynyl)malonate (142)



In a round bottom flask, to a cold (0 °C) suspension of sodium hydride (60% in mineral oil, 0.14 g, 3.5 mmol) in dimethylformamide (20 mL) was added di-tert-butyl 2-(5-(tetrahydro-2H-pyran-2-yloxy)pent-3-ynyl)malonate (0.96 g, 2.51 mmol) and 2-(4-bromobut-2-ynyloxy)-tetrahydro-2H-pyran (0.70 g, 3.0 mmol). After stirring overnight at room temperature, water was added and the product was extracted into petroleum ether: diethyl ether (1 : 1 v/v). The organic layer was dried over sodium sulfate and the solvents were evaporated *in vacuo*. The orange, crude oil was purified by flash silica gel chromatography (4 : 1 petroleum ether : diethyl ether; R_f 0.20) to provide the unsymmetrical malonate **142** as an undetermined mixture of diastereomers and a highly viscous, colourless oil (0.71 g, 53%). Isolation of each diastereomer was not attempted as the removal of the THP protecting groups later in the synthesis results in an achiral molecule. Spectroscopic data for **142**: **IR** (neat film, cm^{-1}): 2942 (m), 2870 (m), 2227 (w), 1729 (s), 1455 (w), 1443 (w), 1393 (w), 1369 (m), 1345 (w), 1323 (w), 1307 (w), 1282 (w), 1249 (m), 1202 (m), 1164 (s), 1143 (s), 1118 (m), 1054 (m), 1038 (m), 1025 (s), 973 (w), 946 (w), 903 (m), 871 (w), 848 (m), 816 (w), 730 (w); **¹H NMR** (400 MHz, $CDCl_3$): δ 4.77 (m, 2H, OCHO), 4.30-4.13 (m, 4H, $\equiv CCH_2O$), 3.81 (m, 2H, CHHO (THP)), 3.51 (m, 2H, CHHO (THP)), 2.73 (t, $J = 2.2$ Hz, 2H, $CH_2C\equiv CCH_2O$), 2.18 (m, 4H, $CH_2CH_2C\equiv CCH_2O$), 1.89-1.48 (m, 12H, CH_2 (THP)), 1.43 (s, 18H, $C(CH_3)_2$);

$^{13}\text{C}\{^1\text{H}\}$ NMR (100 MHz, CDCl_3 , reported as a mixture of diastereomers): δ 168.9, 97.6, 97.4, 97.0, 96.9, 85.3, 81.8, 80.9, 79.0, 76.2, 62.14, 62.05, 61.0, 61.9, 57.3, 54.7, 54.60, 54.56, 31.1, 30.5, 28.0, 27.9, 27.7, 27.6, 25.5, 25.4, 25.2, 19.2, 14.3; **ESMS** m/z calculated for $\text{C}_{30}\text{H}_{46}\text{O}_8\text{Na}$ ($\text{M}+\text{Na}$) $^+$: 557.30849; found 557.30840; **Analysis** calculated for $\text{C}_{30}\text{H}_{46}\text{O}_8$: C, 67.39%; H, 8.67%; found: C, 67.26%; H, 8.81%.

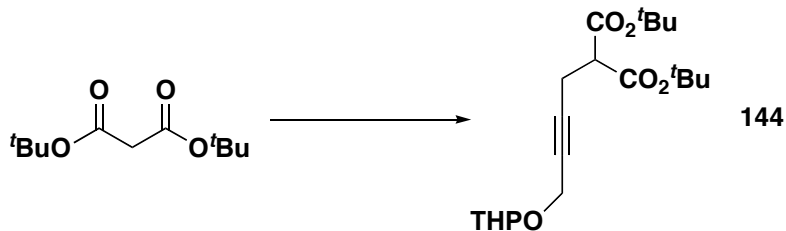
Di-tert-butyl 2-(4-bromobut-2-ynyl)-2-(5-bromopent-3-ynyl)malonate (143)



In a round bottom flask, to a cold (0 °C) solution of triphenylphosphine (0.97 g, 3.7 mmol) in dichloromethane (30 mL) was added carbon tetrabromide (1.23 g, 3.71 mmol) dropwise resulting in a white, creamy suspension. To this was added a solution of di-tert-butyl 2-(4-(tetrahydro-2H-pyran-2-yloxy)but-2-ynyl)-2-(5-(tetrahydro-2H-pyran-2-yloxy)pent-3-ynyl)malonate (381.4 mg, 0.821 mmol) in dichloromethane (5 mL) at 0 °C. The mixture was stirred overnight at room temperature. The solution was frit-filtered to remove the white precipitate and the volatiles were evaporated *in vacuo*. The crude material was triturated with petroleum ether: diethyl ether (1 : 1 v/v), extracting the product from the insoluble byproducts. After solvent removal, the material was purified by flash silica gel chromatography (dichloromethane; $R_f \sim 0.8$) to yield the title dibromide **143** as a white solid (161.8 mg, 39%). Spectroscopic data for **143**: **IR** (neat film, cm^{-1}): 2978 (m), 2933 (w), 2236 (w), 1728 (s), 1477 (w), 1456 (w), 1427 (w), 1394 (w), 1369 (m), 1307 (m), 1284 (m), 1249 (m), 1214 (m), 1165 (s), 1145 (s), 1086 (w), 1071 (w), 1036 (w), 998 (w), 847 (m), 728 (w); ^1H NMR (300 MHz, CDCl_3): δ 3.91 (t, $J = 2.1$ Hz, 2H, $(\text{CH}_2)_2\text{C}\equiv\text{CCH}_2\text{Br}$), 3.88 (t, $J = 2.3$ Hz, 2H, $\text{CH}_2\text{C}\equiv\text{CCH}_2\text{Br}$), 2.79 (t, $J = 2.4$ Hz, 2H, $\text{CH}_2\text{C}\equiv\text{CCH}_2\text{Br}$), 2.28-2.13 (m, 4H, CH_2CH_2), 1.46 (s, 18H, $\text{C}(\text{CH}_3)_3$); $^{13}\text{C}\{^1\text{H}\}$ NMR (100 MHz, CDCl_3): δ 168.7 (C=O), 86.7 ($(\text{CH}_2)_2\text{C}\equiv\text{CCH}_2\text{Br}$), 82.4

(C≡C), 82.1 (OC(CH₃)₃), 78.2 (C≡C), 75.7 ((CH₂)₂C≡CCH₂Br), 57.3 (C(C=O)₂), 30.9 (CH₂CH₂C≡), 27.8 (C(CH₃)₃), 23.4 (CH₂C≡CCH₂Br), 15.4 ((CH₂)₂C≡CCH₂Br), 14.8 (CH₂C≡CCH₂Br), 14.4 (CH₂CH₂C≡); **¹H-¹H COSY** (300 MHz, CDCl₃): δ 3.91 ↔ δ 2.28-2.13; δ 3.88 ↔ δ 2.79; **HMQC** (300 MHz, CDCl₃): δ 3.91 ↔ δ 15.4; δ 3.88 ↔ δ 14.8; δ 2.79 ↔ δ 23.4; δ 2.28-2.13 ↔ δ 30.9, 14.4 (amb.); δ 1.46 ↔ δ 27.8; **HMBC** (400 MHz, CDCl₃): δ 3.91 ↔ δ 86.7, 75.7, 30.9; δ 3.88 ↔ δ 82.4, 78.2, 57.3, 23.4; δ 2.79 ↔ δ 168.7, 82.4, 78.2, 57.3, 30.9; δ 1.46 ↔ δ 82.1; **ESMS** *m/z* calculated for C₂₀H₂₈Br₂O₄Na (M+Na)⁺: 513.02465; found 513.02462; **Analysis** calculated for C₂₀H₂₈Br₂O₄: C, 48.80%; H, 5.73%; found: C, 48.80%; H, 5.75%.

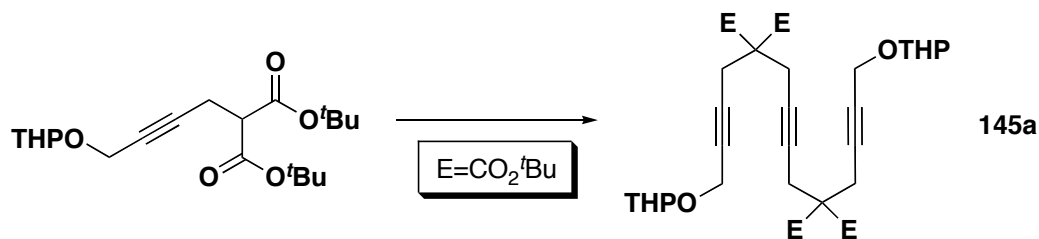
Di-*tert*-butyl 2-(4-(tetrahydro-2*H*-pyran-2-yl)oxy)but-2-ynylmalonate (144)



In a round bottom flask, to a cold (0 °C) suspension of sodium hydride (60% in mineral oil, 0.42 g, 11 mmol) in dimethylformamide (20 mL) was added di-*tert*-butyl malonate (2.11 g, 9.76 mmol) dropwise and stirred until H₂ ceased to evolve. This solution was then transferred by canula to a flask containing 2-(4-bromobut-2-ynyl)oxy-tetrahydro-2*H*-pyran (2.14 g, 9.18 mmol) at 0 °C. After stirring overnight at room temperature, the reaction was quenched with water and extracted into hexanes: diethyl ether (1 : 1 *v/v*). The organic layer was dried over magnesium sulfate and solvents were evaporated *in vacuo* to give the crude product. ¹H NMR spectroscopy of the crude product showed a mixture of unreacted malonate, monoalkylated and dialkylated product. Purification by flash silica gel chromatography (9 : 2 hexanes : ethyl acetate; R_f 0.30) gave the monoalkylated compound **144** as a colourless oil (1.33 g, 39%). Spectroscopic data for **144**: **IR** (cast film, cm⁻¹): 2978 (m), 2941 (m), 2872 (w), 1731 (s), 1456 (w),

1393 (w), 1369 (m), 1345 (m), 1309 (m), 1282 (m), 1249 (m), 1202 (s), 1139 (s), 1079 (m), 1025 (s), 971 (w), 956 (w), 903 (w), 874 (w), 847 (m), 816 (w), 742 (w); $^1\text{H NMR}$ (400 MHz, CDCl_3): δ 4.77 (t, $J = 3.3$ Hz, 1H, OCHO), 4.24 (leaning dt, $J = 2.2$ Hz, $J = 14.6$ Hz, 1H, $\equiv\text{CCHHO}$), 4.17 (leaning dt, $J = 2.2$ Hz, $J = 14.6$ Hz, 1H, $\equiv\text{CCHHO}$), 3.81 (ddd, $J = 3.2$ Hz, $J = 9.2$ Hz, $J = 14.4$ Hz, 1H, CHHO (THP)), 3.50 (m, 1H, CHHO (THP)), 3.34 (t, $J = 7.8$ Hz, 1H, $\text{CH}(\text{C}=\text{O})_2$), 2.70 (dt, $J = 7.8$ Hz, $J = 2.2$ Hz, 2H, $\text{CH}_2\text{C}\equiv\text{CCH}_2\text{O}$), 1.90-1.45 (m, 6H, CH_2 (THP)), 1.47 (s, 18H, $\text{C}(\text{CH}_3)_3$); $^{13}\text{C}\{^1\text{H}\}$ NMR (100 MHz, CDCl_3): δ 167.3 (C=O), 96.5 (OCHO), 82.4 ($\text{C}\equiv\text{CCH}_2\text{O}$), 81.8 ($\text{OC}(\text{CH}_3)_3$), 77.6 ($\text{C}\equiv\text{CCH}_2\text{O}$), 61.9 (CH_2O (THP)), 54.3 ($\equiv\text{CCH}_2\text{O}$), 53.1 ($\text{C}(\text{C}=\text{O})_2$), 30.2 (CH_2 (THP)), 27.9 ($\text{C}(\text{CH}_3)_3$), 25.4 (CH_2 (THP)), 19.1 ($\text{CH}_2\text{C}\equiv\text{CCH}_2\text{O}$), 18.7 (CH_2 (THP)); $^1\text{H}-^1\text{H COSY}$ (400 MHz, CDCl_3): δ 4.24 \leftrightarrow δ 2.70; δ 3.81 \leftrightarrow δ 3.50; δ 3.34 \leftrightarrow δ 2.70; **HMQC** (400 MHz, CDCl_3): δ 4.77 \leftrightarrow δ 96.6; δ 4.24 \leftrightarrow δ 54.3; δ 3.81 \leftrightarrow δ 61.9; δ 3.50 \leftrightarrow δ 61.9; δ 3.34 \leftrightarrow δ 53.1; δ 2.70 \leftrightarrow δ 19.1; **HMBC** (400 MHz, CDCl_3): δ 4.24 \leftrightarrow δ 96.5, 82.4, 77.6; δ 3.34 \leftrightarrow δ 167.3, 82.4, 19.1; δ 2.70 \leftrightarrow δ 167.3, 82.4, 77.6, 53.1; δ 1.47 \leftrightarrow δ 81.8; **ESMS** m/z calculated for $\text{C}_{20}\text{H}_{32}\text{O}_6\text{Na}$ ($\text{M}+\text{Na}$) $^+$: 391.20911; found: 391.20906; **Analysis** calculated for: $\text{C}_{20}\text{H}_{32}\text{O}_6$: C, 65.19%; H, 8.75%; found: C, 64.81%; H, 8.72%.

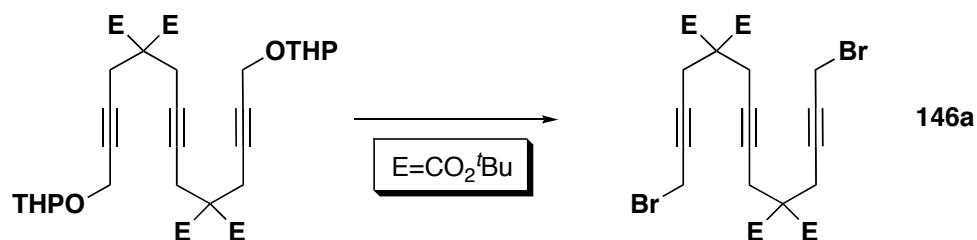
Tetra-*tert*-butyl 1,14-bis(tetrahydro-2*H*-pyran-2-yloxy)tetradeca-2,7,12-triyn-5,5,10,10-tetracarboxylate (145a)



In a round bottom flask, to a cold (0 °C) suspension of sodium hydride (60% in mineral oil, 0.11 g, 2.8 mmol) in dimethylformamide (6 mL) was added di-*tert*-butyl 2-(4-(tetrahydro-2*H*-pyran-2-yloxy)but-2-ynyl)malonate (0.71 g, 1.9 mmol) and 1,4-

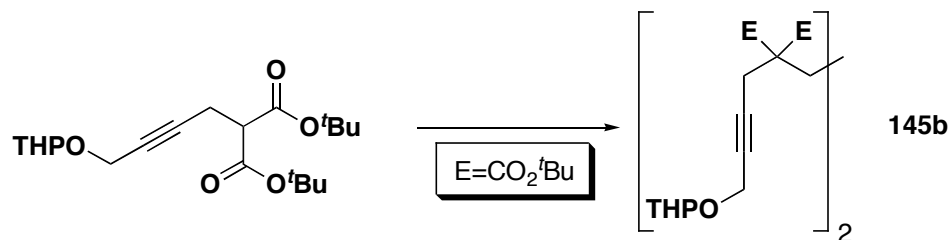
dibromo-2-butyne (0.21 g, 0.99 mmol) dropwise at 0 °C. After stirring overnight at room temperature, the reaction was heated to 50 °C for 1 h before diluting with water and extracting into hexanes. The organic layer was dried over magnesium sulfate and volatiles were evaporated *in vacuo* to give the crude product as a highly viscous, orange oil. Purification by flash silica gel chromatography (5 : 1 hexanes : ethyl acetate; R_f 0.19) gave the triyne **145a** as an undetermined mixture of isomers and a highly viscous, colourless oil (0.43 g, 55%). Spectroscopic data for **145a**: **IR** (cm^{-1}): 2976 (s), 2940 (s), 2871 (m), 2742 (w), 2291 (w), 2225 (w), 1731 (s), 1477 (m), 1456 (m), 1443 (m), 1428 (m), 1393 (m), 1369 (s), 1345 (w), 1324 (m), 1301 (s), 1249 (m), 1221 (m), 1202 (m), 1144 (m), 1119 (w), 1078 (w), 1069 (w), 1054 (w), 1026 (m), 973 (w), 946 (m), 933 (w), 903 (m), 872 (m), 845 (m), 816 (m), 744 (m), 733 (m); **^1H NMR** (400 MHz, CDCl_3): δ 4.77 (t, $J = 3.5$ Hz, 2H, OCHO), 4.19 (m, 4H, $\equiv\text{CCH}_2\text{O}$), 3.81 (ddd, $J = 3.3$ Hz, $J = 8.9$ Hz, $J = 11.7$ Hz, 2H, CHHO (THP)), 3.51 (m, 2H, CHHO (THP)), 2.87 (t, $J = 2.1$ Hz, 4H, $\text{CH}_2\text{C}\equiv\text{CCH}_2\text{O}$), 2.79 (s, 4H, $\text{CCH}_2\text{C}\equiv\text{CCH}_2\text{C}$), 1.86-1.48 (m, 12H, CH_2 (THP)), 1.45 (s, 36H, $\text{C}(\text{CH}_3)_3$); **$^{13}\text{C}\{^1\text{H}\}$ NMR** (100 MHz, CDCl_3): δ 168.0 (C=O), 96.4 (OCHO), 81.8 ($\text{OC}(\text{CH}_3)_3$), 81.1 (C=C), 78.7 (C=C), 77.8 (C=C), 62.1 (CH_2O (THP)), 57.3 ($\text{C}(\text{C}=\text{O})_2$), 54.2 ($\text{CH}_2\text{C}\equiv\text{CCH}_2\text{O}$), 30.3 (CH_2 (THP)), 27.8 ($\text{C}(\text{CH}_3)_3$), 25.4 (CH_2 (THP)), 22.7 ($\text{CCH}_2\text{C}\equiv$), 22.6 ($\text{CCH}_2\text{C}\equiv$), 19.2 (CH_2 (THP)); **^1H - ^1H COSY** (400 MHz, CDCl_3): δ 4.19 \leftrightarrow δ 2.87; δ 3.81 \leftrightarrow δ 3.51; **HMQC** (400 MHz, CDCl_3): δ 4.77 \leftrightarrow δ 96.4; δ 4.19 \leftrightarrow δ 54.2; δ 3.81 \leftrightarrow δ 62.1; δ 3.51 \leftrightarrow δ 62.1; δ 2.87/2.79 \leftrightarrow δ 22.7/22.6¹⁴⁰; δ 1.45 \leftrightarrow δ 27.8; **ESMS** m/z calculated for $\text{C}_{44}\text{H}_{66}\text{O}_{12}\text{Na}$ ($\text{M}+\text{Na}$)⁺: 809.44465; found: 809.44485; **Analysis** calculated for $\text{C}_{44}\text{H}_{66}\text{O}_{12}$: C, 67.15%; H, 8.45%; found: C, 66.78%; H, 8.54%.

Tetra-*tert*-butyl 1,14-dibromotetradeca-2,7,12-triyn-5,5,10,10-tetracarboxylate (146a)



In a round bottom flask, to a cold (0 °C) solution of triphenylphosphine (0.53 g, 2.0 mmol) in dichloromethane (10 mL) was added bromine (0.30 g, 1.9 mmol) dropwise resulting in a white, creamy suspension. To this was added a solution of tetra-*tert*-butyl 1,14-bis(tetrahydro-2*H*-pyran-2-yloxy)tetradeca-2,7,12-triyn-5,5,10,10-tetracarboxylate (0.38 g, 0.48 mmol) in dichloromethane (2 mL) at 0 °C. The mixture was stirred for two days at room temperature. Volatiles were removed *in vacuo* and the product was extracted into hexanes. Evaporation of solvent *in vacuo* and filtration through a plug of silica gel eluting with dichloromethane provided the spectroscopically homogenous dibromide **146a** as a light brown powder (0.12 g, 33%). No further purification was attempted. Spectroscopic data for **146a**: **IR** (cast film, cm^{-1}): 3003 (w), 2978 (m), 2933 (m), 2238 (w), 1732 (s), 1477 (w), 1456 (w), 1427 (w), 1394 (m), 1370 (s), 1325 (m), 1302 (s), 1249 (m), 1221 (s), 1165 (s), 1145 (s), 1069 (m), 1054 (m), 1032 (w), 879 (w), 845 (m), 743 (w), 730 (w); **^1H NMR** (400 MHz, C_6D_6): δ 3.29 (s, 8H, $\equiv\text{CCH}_2\text{Br}$), 3.18 (s, 4H), 1.38 (s, 36H, $\text{C}(\text{CH}_3)_3$); **$^{13}\text{C}\{^1\text{H}\}$ NMR** (100 MHz, C_6D_6): δ 168.7, ($\text{C}=\text{O}$), 83.3 ($\text{C}\equiv\text{C}$), 81.7 ($\text{OC}(\text{CH}_3)_3$), 78.624 ($\text{C}\equiv\text{C}$), 78.615 ($\text{C}\equiv\text{C}$), 57.8 ($\text{C}(\text{C}=\text{O})_2$), 27.8 ($\text{C}(\text{CH}_3)_3$), 23.4 (overlapping $\text{CH}_2\text{C}(\text{C}=\text{O})_2$), 14.7 ($\equiv\text{CCH}_2\text{Br}$); **ESMS** m/z calculated for $\text{C}_{34}\text{H}_{48}\text{O}_8\text{Br}_2\text{Na}$ ($\text{M}+\text{Na}$) $^+$: 765.16081; found: 765.16088; **Analysis** calculated for $\text{C}_{34}\text{H}_{48}\text{O}_8\text{Br}_2\text{Na}$: C, 54.85%; H, 6.50%; found: C, 54.36%; H, 6.69%.

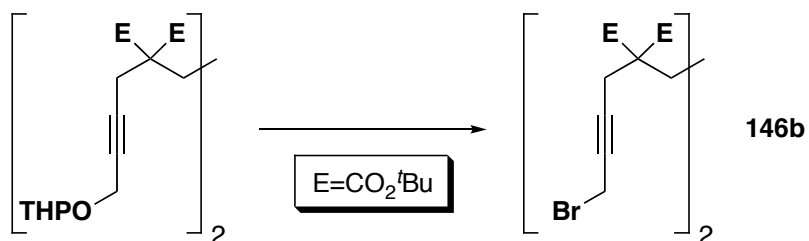
Tetra-*tert*-butyl 1,13-bis(tetrahydro-2*H*-pyran-2-yloxy)trideca-2,11-diyne-5,5,9,9-tetracarboxylate (145b)



In a round bottom flask, to a cold (0 °C) suspension of sodium hydride (60% in mineral oil, 71.8 mg, 1.80 mmol) in dimethylformamide (10 mL) was added di-*tert*-butyl 2-(4-(tetrahydro-2*H*-pyran-2-yloxy)but-2-ynyl)malonate (540.5 mg, 1.47 mmol) and 1,3-dibromopropane (139.8, 0.692 mmol) at 0 °C. After stirring overnight at 50 °C, the reaction was quenched with saturated ammonium chloride and the product was extracted into hexanes. The organic layer was dried over magnesium sulfate and the solvents were evaporated *in vacuo*. Purification by flash silica gel chromatography (6 : 1 hexanes : ethyl acetate; *R_f* 0.15) gave the title compound as a undetermined mixture of diastereomers and a highly viscous colourless oil (168.7 mg, 31%). Spectroscopic data for **145b**: **IR** (cast film, cm⁻¹): 2976 (m), 2939 (m), 2870 (w), 1729 (s), 1457 (w), 1393 (w), 1369 (m), 1258 (m), 1202 (w), 1150 (s), 1116 (m), 1078 (w), 1054 (w), 1025 (s), 945 (w), 903 (w), 871 (w), 847 (w), 816 (w), 668 (w); **¹H NMR** (400 MHz, CDCl₃): δ 4.74 (t, *J* = 3.4 Hz, 2H, OCHO), 4.19 (dt, *J* = 15.4 Hz, *J* = 2.0 Hz, 2H, ≡CCHHO), 4.14 (dt, *J* = 15.4 Hz, *J* = 2.0 Hz, 2H, ≡CCHHO), 3.79 (ddd, *J* = 11.8 Hz, *J* = 9.1 Hz, *J* = 3.4 Hz, 2H, CHHO (THP)), 3.48 (m, 2H, CHHO (THP)), 2.69 (t, *J* = 2.0 Hz, 4H, CH₂C≡CCH₂O), 1.93 (2nd order m, 4H, CH₂CH₂CH₂), 1.82-1.47 (m, 12H, CH₂ (THP)), 1.41 (s, 36H, C(CH₃)₃), 1.13 (m, 2H, CH₂CH₂CH₂); **¹³C{¹H} NMR** (100 MHz, CDCl₃): δ 169.2 (C=O), 96.4 (OCHO), 81.3 (OC(CH₃)₃ or ≡CCH₂O), 81.1 (OC(CH₃)₃ or ≡CCH₂O), 78.5 (C≡CCH₂O), 62.0 (CH₂O (THP)), 57.6 (C(C=O)₂), 54.1 (≡CCH₂O), 31.9 (CH₂CH₂CH₂), 30.2 (CH₂ (THP)), 27.7 (C(CH₃)₃), 25.3 (CH₂ (THP)), 22.9 (CH₂C≡CCH₂O), 19.2 (CH₂ (THP) or CH₂CH₂CH₂), 18.6 (CH₂ (THP) or CH₂CH₂CH₂); **¹H-¹H COSY** (400 MHz, CDCl₃): δ 4.14 ↔ δ 2.69; δ 3.79 ↔ δ 3.48; δ 1.93 ↔ δ 1.13; **HMQC** (400 MHz,

CDCl₃): δ 4.74 \leftrightarrow δ 96.4; δ 4.19 \leftrightarrow δ 54.1; δ 3.79 \leftrightarrow δ 62.0; δ 3.48 \leftrightarrow δ 62.0; δ 2.69 \leftrightarrow δ 22.9; δ 1.93 \leftrightarrow δ 31.9; δ 1.41 \leftrightarrow δ 27.7; **ESMS** *m/z* calculated for C₄₃H₆₈O₁₂Na (M+Na)⁺: 799.46030; found: 799.46007; **Analysis** calculated for C₄₃H₆₈O₁₂: C, 66.47%; H, 8.75%; found: C, 66.13%; H, 8.91%.

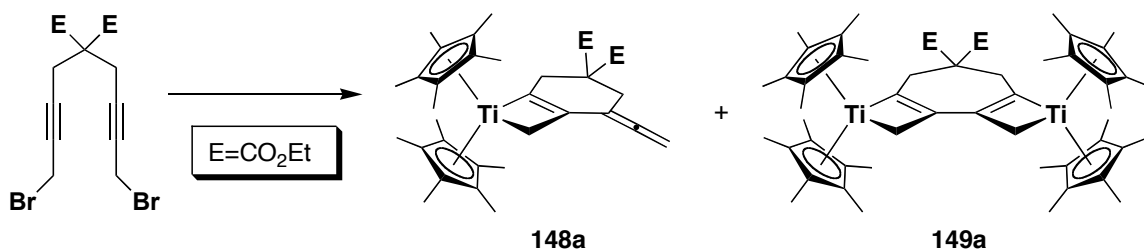
Tetra-*tert*-butyl 1,13-dibromotrideca-2,11-diyne-5,5,9,9-tetracarboxylate (146b)



In a round bottom flask, to a cold (0 °C) solution of triphenylphosphine (2.24 g, 8.54 mmol) in dichloromethane (25 mL) was added bromine (0.44 mL, 8.59 mmol) dropwise resulting in a white, creamy suspension. To this was added a solution of tetra-*tert*-butyl 1,13-bis(tetrahydro-2*H*-pyran-2-yloxy)trideca-2,11-diyne-5,5,9,9-tetracarboxylate (1.60 g, 2.06 mmol) in dichloromethane (12 mL) at 0 °C. The mixture was stirred for overnight at room temperature. The dark solution was successively washed with sodium bisulfite, sodium bicarbonate and water. The organic layer was dried over magnesium sulfate and the volatiles were removed *in vacuo*. Purification by silica gel chromatography (dichloromethane; R_f 0.43) provided the dibromide **146b** as a waxy solid (0.93 g, 61%). Spectroscopic data for **146b**: **IR** (microscope, cm⁻¹): 3004 (m), 2978 (m), 2935 (m), 2232 (w), 1727 (s), 1476 (m), 1456 (m), 1439 (w), 1426 (w), 1393 (m), 1367 (s), 1330 (w), 1305 (m), 1288 (w), 1261 (w), 1234 (m), 1214 (s), 1149 (s), 1116 (s), 1061 (w), 1031 (m), 906 (w), 844 (s), 808 (w), 746 (w), 723 (m), 685 (w); **¹H NMR** (400 MHz, CDCl₃): δ 3.86 (t, *J* = 2.3 Hz, 4H, \equiv CCH₂Br), 2.75 (t, *J* = 2.4 Hz, 4H, CH₂C \equiv CCH₂Br), 1.96 (2nd order m, 4H, CH₂CH₂CH₂), 1.45 (s, 36H, C(CH₃)₃), 1.05 (m, 2H, CH₂CH₂CH₂); **¹³C{¹H} NMR** (100 MHz, CDCl₃): δ 169.2 (C=O), 82.8 (C \equiv C), 81.7 (OC(CH₃)₃), 77.8 (C \equiv C), 57.6 (C(C=O)₂), 32.0 (CH₂CH₂CH₂), 27.8 (C(CH₃)₃), 23.0

(CH₂C≡CCH₂Br), 18.6 (CH₂CH₂CH₂), 14.8 (≡CCH₂Br); ¹H-¹H COSY (400 MHz, CDCl₃): δ 3.86 ↔ δ 2.75; δ 1.96 ↔ δ 1.05; **HMQC** (400 MHz, CDCl₃): δ 3.86 ↔ δ 14.8; δ 2.75 ↔ δ 23.0; δ 1.96 ↔ δ 32.0; δ 1.45 ↔ δ 27.8; δ 1.05 ↔ δ 18.6; **HMBC** (400 MHz, CDCl₃): δ 3.86 ↔ δ 82.8, 77.8; δ 2.75 ↔ δ 169.2, 82.8, 77.8, 57.6, 32.0, 14.8; δ 1.96 ↔ δ 169.2, 57.6, 32.0, 23.0, 18.6; δ 1.45 ↔ δ 81.7; δ 1.05 ↔ δ 32.6; **ESMS** *m/z* calculated for C₃₃H₅₀Br₂O₈Na (M+Na)⁺: 755.17646; found: 755.17638; **Analysis** calculated for C₃₃H₅₀Br₂O₈: C, 53.96%; H, 6.86%; found: C, 53.56%; H, 6.94%.

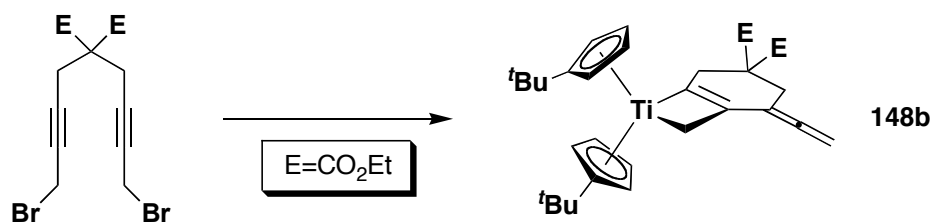
[Cp*₂Ti{3-ethenylidene-5,5-bis(*tert*-ethoxycarbonyl)-2-methanidylcyclohex-1-enyl}] (148a) and [(Cp*₂Ti)₂{2,3-dimethanidyl-6,6-bis(ethoxycarbonyl)cyclohepta-1,3-diene-1,4-diyl}] (149a)



In the glovebox, Cp*₂TiCl (25.9 mg, 73.2 μmol) and SmI₂ (142.5 mg, 235 μmol) were combined with THF (2 mL). In a separate vessel, diethyl 2,2-bis(4-bromobut-2-ynyl)malonate (30.4 mg, 72.0 μmol) was dissolved in THF (1 mL). Both vessels were cooled to -30 °C and combined rapidly. The reaction was allowed to warm to room temperature and stirred overnight, after which the solution had become dark-red and there was a yellow precipitate. The solvent was removed *in vacuo* and the residue was triturated with hexanes and filtered through Celite. Evaporation of volatiles gave a dark-brown oil (31.2 mg). ¹H NMR shows a mixture of **X** and **X** in a 13 : 2 ratio. Crystallization from pentane yields the di(titanacyclobutene) as insoluble X-ray quality purple crystals while the remaining solution containing titanacyclobutene **X** was concentrated and also crystallized from pentane to yield X-ray quality single-crystals. Due to the small quantity of crystals obtained, neither of the purified products were

quantified. Spectroscopic data for mixture: **IR** (microscope, cm^{-1}): 2977 (s), 2906 (s), 2860 (m), 2723 (w), 1956 (w), 1934 (m), 1731 (s), 1653 (w), 1625 (w), 1601 (m), 1559 (w), 1495 (w), 1442 (m), 1378 (m), 1367 (w), 1302 (m), 1244 (s), 1204 (m), 1177 (m), 1095 (m), 1085 (m), 1058 (m), 1024 (m), 955 (w), 889 (w), 861 (m), 843 (m), 805 (w), 712 (w), 674 (w); **NMR** data for titanacycle **X**: **^1H NMR** (400 MHz, C_6D_6): δ 5.02 (br. s, 2H, $\bullet=\text{CH}_2$), 4.16-3.92 (2nd order m, 4H, OCH_2CH_3), 3.48 (br. s, 2H, TiCCH_2), 3.27 (t, $J = 2.7$ Hz, 2H, $\bullet=\text{CCH}_2$), 2.24 (t, $J = 2.5$ Hz, 2H, TiCH_2), 1.72 (s, 30H, $(\text{CH}_3)_5\text{C}_5$), 0.98 (t, $J = 7.5$ Hz, 6H, CH_2CH_3); **$^{13}\text{C}\{^1\text{H}\}$ NMR** (100 MHz, C_6D_6): δ 211.4 ($\text{TiC}=\text{C}$ or $\text{C}=\bullet=\text{CH}_2$), 210.6 ($\text{TiC}=\text{C}$ or $\text{C}=\bullet=\text{CH}_2$), 171.9 ($\text{C}=\text{O}$), 118.8 ($(\text{CH}_3)_5\text{C}_5$), 100.5 ($\bullet=\text{CCH}_2$ or $\text{TiC}=\text{C}$), 97.4 ($\bullet=\text{CCH}_2$ or $\text{TiC}=\text{C}$), 76.9 ($\bullet=\text{CH}_2$), 71.3 (TiCH_2), 61.1 (OCH_2CH_3), 54.6 ($\text{C}(\text{C}=\text{O})_2$), 37.4 (TiCCH_2), 34.9 ($\bullet=\text{CCH}_2$), 14.1 (CH_2CH_3), 12.1 ($(\text{CH}_3)_5\text{C}_5$); **$^1\text{H}-^1\text{H}$ COSY** (400 MHz, C_6D_6): δ 5.02 \leftrightarrow δ 3.48, 3.27, 2.24; δ 4.16-3.92 \leftrightarrow δ 0.98; δ 3.48 \leftrightarrow δ 2.24; **HMQC** (400 MHz, C_6D_6): δ 5.02 \leftrightarrow δ 76.9; δ 4.16-3.92 \leftrightarrow δ 61.1; δ 3.48 \leftrightarrow δ 37.4; δ 3.27 \leftrightarrow δ 34.9; δ 2.24 \leftrightarrow δ 71.3; δ 1.72 \leftrightarrow δ 12.1; δ 0.98 \leftrightarrow δ 14.1; **NMR** data for dititanacycle **X**: **^1H NMR** (400 MHz, C_6D_6): δ 4.01 (q, $J = 7.1$ Hz, 4H, OCH_2CH_3), 3.38 (br. s, 4H, TiCCH_2), 2.61 (br. s, 4H, $\text{TiC}=\text{C}$), 1.87 (s, 60H, $(\text{CH}_3)_5\text{C}_5$), 0.98 (t, $J = 7.5$ Hz, 6H, CH_2CH_3); **$^{13}\text{C}\{^1\text{H}\}$ NMR** (100 MHz, C_6D_6): δ 215.7 ($\text{TiC}=\text{C}$), 173.5 ($\text{C}=\text{O}$), 118.4 ($(\text{CH}_3)_5\text{C}_5$), 107.4 ($\text{TiC}=\text{C}$), 78.2 (TiCH_2), 60.7 (OCH_2CH_3), 54.6 ($\text{C}(\text{C}=\text{O})_2$), 39.1 (TiCCH_2), 13.9 (CH_2CH_3), 12.5 ($(\text{CH}_3)_5\text{C}_5$); **$^1\text{H}-^1\text{H}$ COSY** (400 MHz, C_6D_6): δ 4.01 \leftrightarrow δ 0.98; δ 3.38 \leftrightarrow δ 2.61; **HMQC** (400 MHz, C_6D_6): δ 4.01 \leftrightarrow δ 60.7; δ 3.38 \leftrightarrow δ 39.1; δ 2.61 \leftrightarrow δ 78.2; δ 1.87 \leftrightarrow δ 12.5; δ 0.98 \leftrightarrow δ 13.9; **ESMS** of the mixture failed to detect $[\text{M}+\text{Na}]^+$ of either compound.

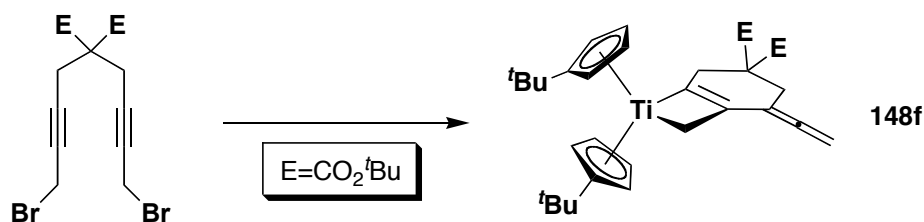
[(^tBuCp)₂Ti{3-ethenylidene-5,5-bis(ethoxycarbonyl)-2-methanidylcyclohex-1-enyl}]
(148b)



In the glovebox, [(^tBuCp)₂TiCl]₂ (33.2 mg, 51 μmol) and SmI₂ (195.8 mg, 323 μmol) were combined with THF (2 mL). In a separate vessel, diethyl 2,2-bis(4-bromobut-2-ynyl)malonate (42.5 mg, 107 μmol) was dissolved in THF (1 mL). Both vessels were cooled to -30 °C and combined rapidly. The colour of the solution changed from dark-blue to red within one minute. The reaction was allowed to warm to room temperature and stirred overnight. The solvent was removed *in vacuo* and the residue was triturated with hexanes and filtered through Celite. Evaporation of volatiles gave the spectroscopically homogenous titanacyclobutene **148b** as dark red oil (40.7 mg, 73%). No further purification was attempted. Spectroscopic data for **148b**: IR (microscope, cm⁻¹): 3101 (w), 2960 (s), 2929 (s), 2903 (m), 2869 (s), 1956 (w), 1936 (w), 1730 (s), 1648 (w), 1624 (w), 1489 (m), 1461 (m), 1446 (w), 1418 (w), 1387 (w), 1364 (m), 1299 (w), 1279 (m), 1243 (s), 1190 (s), 1161 (w), 1096 (m), 1055 (m), 917 (m), 861 (m), 801 (s), 729 (w), 677 (w); ¹H NMR (400 MHz, C₆D₆): δ 6.16 (q, *J* = 2.7 Hz, 2H, ^tBuCpH), 5.65 (q, *J* = 2.7 Hz, 2H, ^tBuCpH), 5.55 (app. sextet, *J* = 2.7 Hz, 4H, ^tBuCpH), 4.96 (br. s, 2H, •=CH₂), 4.06 (dq, *J* = 10.8 Hz, *J* = 7.0 Hz, 2H, OCHHCH₃), 3.97 (dq, *J* = 10.8 Hz, *J* = 7.0 Hz, 2H, OCHHCH₃), 3.46 (br. s, 2H, TiCCH₂), 3.23 (t, *J* = 2.7 Hz, 2H, •=CCH₂), 3.07 (br. t, *J* = 2.2 Hz, TiCH₂), 1.08 (s, 18H, C(CH₃)₃), 0.95 (t, *J* = 7.0 Hz, 6H, CH₂CH₃); ¹³C{¹H} NMR (100 MHz, C₆D₆): δ 212.2 (TiC=C), 210.8 (C=•=CH₂), 171.3 (C=O), 140.1 (*ipso*-^tBuCp), 111.5 (^tBuCp), 111.1 (^tBuCp), 110.8(^tBuCp), 108.8 (^tBuCp), 97.5 (C=•=CH₂), 94.7 (TiC=C), 77.3 (•=CH₂), 64.9 (TiCH₂), 61.2 (OCH₂CH₃), 55.5 (C(C=O)₂), 41.6 (TiCCH₂), 33.8 (•=CCH₂), 32.8 (C(CH₃)₃), 31.6 (C(CH₃)₃), 14.1 (CH₂CH₃); ¹H-¹H COSY (400 MHz, C₆D₆): δ 6.16 ↔ δ 5.65, 5.55; δ 5.65 ↔ δ 5.55; δ 4.96 ↔ δ 3.23; δ 4.06 ↔ δ 3.97, 0.95; δ 3.97 ↔ δ 0.95; δ 3.46 ↔ δ 3.07; HMQC (400

MHz, C₆D₆): δ 6.16 ↔ δ 111.5; δ 5.65 ↔ δ 110.8; δ 5.55 ↔ δ 111.1, 108.8; δ 4.96 ↔ δ 77.3; δ 4.06 ↔ δ 61.2; δ 3.97 ↔ δ 61.2; δ 3.46 ↔ δ 41.6; δ 3.23 ↔ δ 33.8; δ 3.07 ↔ δ 64.9; δ 1.08 ↔ δ 31.6; δ 0.95 ↔ δ 14.1; **HMBC** (400 MHz, C₆D₆): δ 6.16 ↔ δ 140.1; δ 5.65 ↔ δ 140.1; δ 5.55 ↔ δ 140.1; δ 4.96 ↔ δ 210.8, 97.5, 94.7; δ 4.06 ↔ δ 171.3; δ 3.97 ↔ δ 171.3; δ 3.46 ↔ δ 212.2, 171.3, 94.7; δ 3.23 ↔ δ 210.8, 171.3, 97.5, 94.7, 55.5, 41.6; δ 3.07 ↔ δ 212.2, 97.5, 94.7; δ 1.08 ↔ δ 140.1; δ 0.95 ↔ δ 61.2. **EIMS** failed to give M⁺ or any useful fragments.

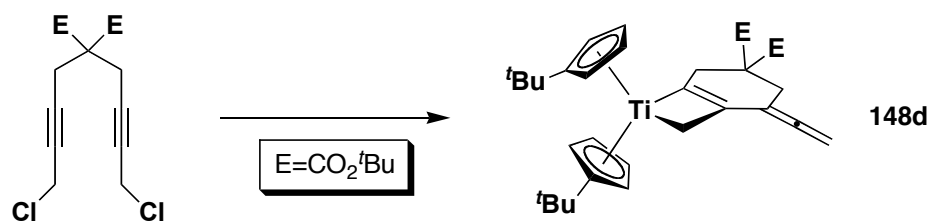
[(^tBuCp)₂Ti{3-ethynylidene-5,5-bis(*tert*-butoxycarbonyl)-2-methanidylcyclohex-1-enyl}] (148f)



In the glovebox, [(^tBuCp)₂TiCl]₂ (83.5 mg, 128 μmol) and SmI₂ (601.9 mg, 885 μmol) were combined with THF (6 mL). In a separate vessel, di-*tert*-butyl 2,2-bis(4-bromobut-2-ynyl)malonate (122.7 mg, 257 μmol) was dissolved in THF (2 mL). Both vessels were cooled to -30 °C and combined rapidly. The reaction was allowed to warm to room temperature and stirred overnight, after which the solution had become dark-red and there was a yellow precipitate. The solvent was removed *in vacuo* and the residue was triturated with hexanes and filtered through Celite. Evaporation of volatiles gave the spectroscopically homogenous titanacyclobutene **X** as a dark-red oil/solid (126.1 mg, 81 %). Further purification was not attempted. Spectroscopic data for **X**: **IR** (cm⁻¹): 3101 (w), 2970 (s), 2869 (s), 1935 (m), 1726 (s), 1616 (w), 1489 (w), 1460 (m), 1418 (w), 1392 (m), 1367 (m), 1270 (m), 1253 (m), 1146 (m), 1085 (w), 1055 (m), 1000 (w), 917 (m), 847 (m), 819 (m), 757 (w), 746 (w), 679 (w); **¹H NMR** (400 MHz, C₆D₆): δ 6.19 (q, *J* = 2.6 Hz, 2H, ^tBuCpH), 5.62 (q, *J* = 2.6 Hz, 2H, ^tBuCpH), 5.57 (q, *J* = 2.6 Hz, 2H,

^tBuCpH), 5.53 (q, *J* = 2.6 Hz, 2H, ^tBuCpH), 4.95 (br. s, 2H, •=CH₂), 3.42 (br. s, 2H, TiCCH₂), 3.09 (m, 4H, TiCH₂ and •=CCH₂), 1.43 (s, 18H, OC(CH₃)₃), 1.09 (s, 18H, CpC(CH₃)₃); ¹³C{¹H} NMR (100 MHz, C₆D₆): δ 213.3 (TiC=C), 210.8 (C=•=CH₂), 170.7 (C=O), 140.0 (*ipso*-^tBuCp), 111.5 (^tBuCp), 111.1 (^tBuCp), 110.6 (^tBuCp), 108.6 (^tBuCp), 98.0 (•=CCH₂), 94.1 (TiC=C), 80.5 (OC(CH₃)₃), 76.8 (•=CH₂), 65.2, 56.8 (C(C=O)₂), 41.6 (TiCCH₂), 34.3 (•=CCH₂), 32.8 (CpC(CH₃)₃), 31.6 (CpC(CH₃)₃), 27.9 (OC(CH₃)₃); ¹H-¹H COSY (300 MHz, C₆D₆): δ 6.19 ↔ δ 5.62, 5.57, 5.53; δ 5.62 ↔ δ 5.57, 5.53; δ 5.57 ↔ δ 5.53; δ 4.95 ↔ δ 3.42, 3.09; δ 3.42 ↔ δ 3.09; **HMQC** (400 MHz, C₆D₆): δ 6.19 ↔ δ 111.5; δ 5.62 ↔ δ 110.6; δ 5.57 ↔ δ 111.1; δ 5.53 ↔ δ 108.6; δ 4.95 ↔ δ 76.8; δ 3.42 ↔ δ 41.6; δ 3.09 ↔ δ 65.2, δ 34.3; δ 1.43 ↔ δ 27.9; δ 1.09 ↔ δ 32.8; **HMBC** (400 MHz, C₆D₆): δ 6.19 ↔ δ 140.0; δ 5.62 ↔ δ 140.0; δ 5.57 ↔ δ 140.0; δ 5.53 ↔ δ 140.0; δ 4.95 ↔ δ 210.8, 98.0, 94.1; δ 3.42 ↔ δ 213.3, 170.7, 94.1; δ 3.09 ↔ δ 213.3, 210.8, 98.0, 94.1, 56.8; δ 1.43 ↔ δ 80.5; δ 1.09 ↔ δ 140.0; **ESMS** *m/z* calculated for C₃₇H₅₂O₄TiNa (M+Na)⁺: 631.32373; found: 631.32406; **Analysis** calculated for C₃₇H₅₂O₄Ti: C, 72.57%; H, 8.56%; found: C, 69.82%; H, 8.61%.

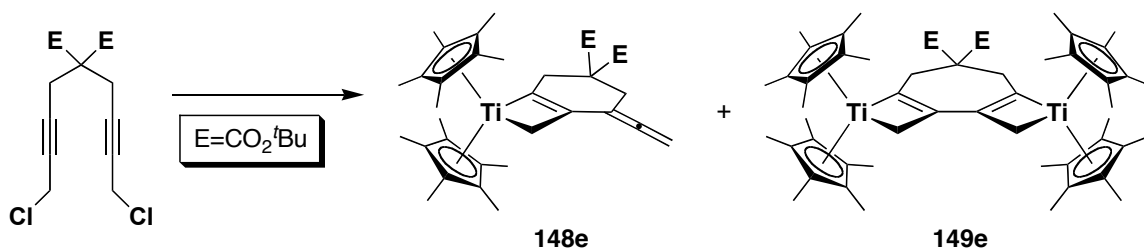
[(^tBuCp)₂Ti{3-ethenylidene-5,5-bis(*tert*-butoxycarbonyl)-2-methanidylcyclohex-1-enyl}] (148d)



In the glovebox, [(^tBuCp)₂TiCl]₂ (48.7 mg, 75 μmol) and SmI₂ (292.4 mg, 482 μmol) were combined with THF (3 mL). In a separate vessel, di-*tert*-butyl 2,2-bis(4-chlorobut-2-ynyl)malonate (57.9 mg, 149 μmol) was dissolved in THF (1 mL). Both vessels were cooled to -30 °C and combined rapidly. The reaction was allowed to warm to room temperature and stirred overnight, after which the solution had become red and

there was a yellow precipitate. The solvent was removed *in vacuo* and the residue was triturated with hexanes and filtered through Celite. Evaporation of volatiles gave the titanacyclobutene **148d** as a dark-red oil (67.3 mg, 74%), which was not further purified. The spectroscopic data were identical to those previously obtained for this complex.

[Cp*₂Ti{3-ethenylidene-5,5-bis(*tert*-butoxycarbonyl)-2-methanidylcyclohex-1-enyl}] (**148e**) and [(Cp*₂Ti)₂{2,3-dimethanidyl-6,6-bis(butoxycarbonyl)cyclohepta-1,3-diene-1,4-diyl}] (**149e**)

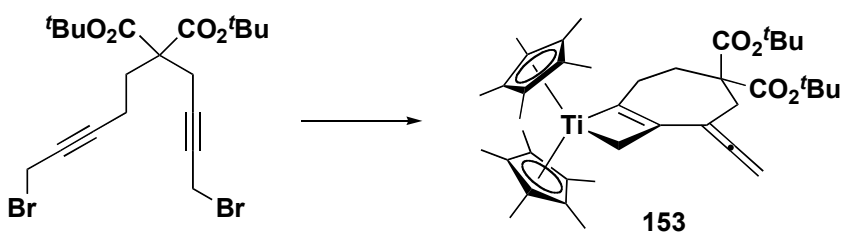


In the glovebox, Cp*₂TiCl (28.3 mg, 80.0 μmol) and SmI₂ (163.5 mg, 269 μmol) were combined in THF (2 mL). In a separate vessel, di-*tert*-butyl 2,2-bis(4-chlorobut-2-ynyl)malonate (30.8 mg, 79.1 μmol) was dissolved in THF (1 mL). Both vessels were cooled to -30 °C and combined rapidly. The reaction was allowed to warm to room temperature while stirring overnight, after which the solution has become dark-red and there was a yellow precipitate. The solvent was removed *in vacuo* and the residue was triturated with hexanes and filtered through Celite. Evaporation of volatiles gave a red oil (42.7 mg, 85%), which by ¹H NMR spectroscopy was a mixture of **148e** and **149e** in a 9 : 1 ratio. No further purification was attempted. Partial spectroscopic data for **148e**: ¹H NMR (400 MHz, C₆D₆): δ 4.99 (br. s, 2H, •=CH₂), 3.40 (br. s, 2H, TiCCH₂), 3.17 (br. s, 2H), 2.24 (br. s, 2H), 1.73 (s, 30H), 1.41 (s, 18H); ¹³C{¹H} NMR (100 MHz, C₆D₆): δ 211.7 (TiC=C or C=•=CH₂), 211.4 (TiC=C or C=•=CH₂), 171.3 (C=O), 118.7 ((CH₃)₅C₅), 100.0 (•=CCH₂ or TiC=C), 97.7 (•=CCH₂ or TiC=C), 80.4 (OC(CH₃)₃), 76.3 (•=CH₂), 71.6 (TiCH₂), 56.2 (C(C=O)₂), 37.1 (TiCCH₂), 34.4 (•=CCH₂), 28.0 (C(CH₃)₃), 12.0 ((CH₃)₅C₅); ¹H-¹H COSY (400 MHz, C₆D₆): δ 4.99 ↔ δ 3.40, 3.17; δ 3.40 ↔ δ

2.24; **HMQC** (400 MHz, C₆D₆): δ 4.99 ↔ δ 76.4; δ 3.40 ↔ δ 37.1; δ 3.17 ↔ δ 34.4; δ 2.24 ↔ δ 71.6; δ 1.73 ↔ δ 12.0; δ 1.41 ↔ δ 28.0.

Limited spectroscopic data for **149e**: **¹H NMR** (400 MHz, C₆D₆): δ 3.21 (br. s, 4H, TiCCH₂), 2.61 (br. s, 4H, TiCH₂), 1.87 (s, 60H, ((CH₃)₅C₅).

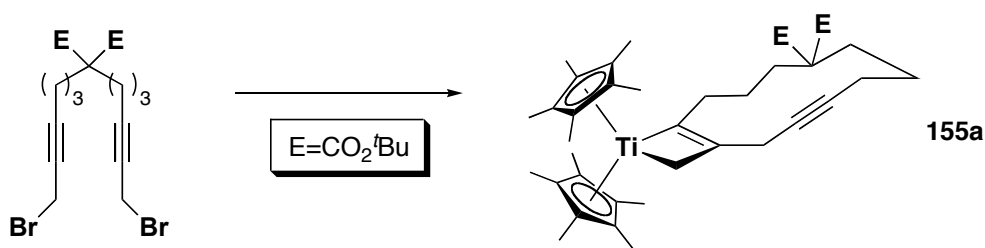
[Cp*₂Ti{3-ethenylidene-5,5-bis(*tert*-butoxycarbonyl)-2-methanidylcyclohept-1-enyl}]
(153)



In the glovebox, Cp*₂TiCl (47.4 mg, 134 μmol) and SmI₂ (193.6 mg, 285 μmol) were combined with THF (5 mL). In a separate vessel, diethyl di-*tert*-butyl 2-(4-bromobut-2-ynyl)-2-(5-bromopent-3-ynyl)malonate (32.6 mg, 66.2 μmol) was dissolved in THF (5 mL). The vessels were removed from the glovebox and were cooled to -78 °C and combined rapidly. The initial dark blue mixture became dark red within five minutes. The reaction was allowed to slowly warm to room temperature overnight, after which there was a yellow precipitate. The solvent was removed *in vacuo* and the residue was triturated with pentane and filtered through Celite. The crude mixture was then triturated with a small amount of pentane at low temperature and crystallized twice from pentane to give the product as a red oil (27.0 mg, 63%). No further purification was performed and impurities were still visible in the spectra. Spectroscopic data for **153**: **¹H NMR** (400 MHz, C₆D₆): δ 4.89 (s, 2H, •=CH₂), 3.30 (s, 2H, •=CCH₂), 2.66 (br. m, 2H, TiCCH₂CH₂), 2.58 (br. m, 2H, TiCCH₂CH₂), 2.25 (s, 2H, TiCH₂), 1.68 (s, 30H, Cp*H), 1.42 (s, 18H, C(CH₃)₂); **¹³C{¹H} NMR** (100 MHz, C₆D₆): δ 216.1 (C=•=C), 213.3 (TiC=C), 171.3 (C=O), 118.9 ((CH₃)₅C₅), 102.4 (TiC=C), 100.3 (C=•=CH₂), 80.2 (OC(CH₃)₃), 75.2 (•=CH₂), 74.5 (TiCH₂), 59.3 (C(C=O)₂), 38.5 (•=CCH₂), 35.2

(TiCCH₂CH₂), 28.0 (C(CH₃)₃), 12.0 ((CH₃)₅C₅)); **¹H-¹H COSY** (400 MHz, C₆D₆): δ 4.89 ↔ δ 3.30, 2.66, 2.25; δ 2.66 ↔ δ 2.58, 2.25; **HMQC** (400 MHz, C₆D₆): δ 4.89 ↔ δ 75.2; δ 3.30 ↔ δ 38.5; δ 2.66 ↔ δ 2.58 ↔ δ 35.2; δ 2.25 ↔ δ 74.5; δ 1.68 ↔ δ 12.0; δ 1.42 ↔ δ 28.0; **HMBC** (400 MHz, C₆D₆): δ 4.89 ↔ δ 213.3, 102.4, 100.3; δ 3.30 ↔ δ 213.3, 171.3, 102.4, 100.3, 59.3, 35.2; δ 2.55 ↔ δ 171.3; δ 2.25 ↔ δ 216.1, 102.4; δ 1.68 ↔ δ 118.9; δ 1.42 ↔ δ 80.2, 28.0.

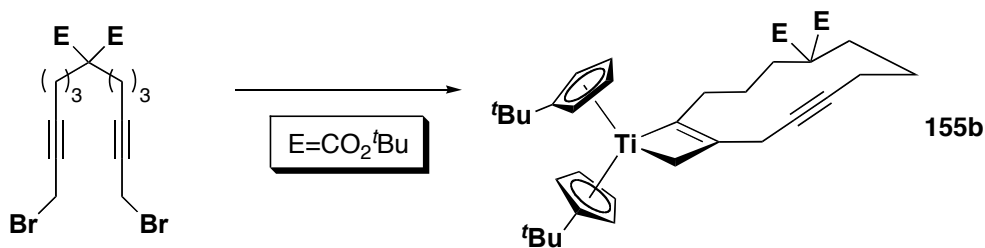
[Cp*₂Ti{9,9-bis(t-butoxycarbonyl)-2-methanidylcyclododec-1-en-4-yn-1-yl}] (155a)



In the drybox, a mixture of Cp*₂TiCl (28.5 mg, 80.6 μmol) and SmI₂ (233.1 mg, 384 μmol) in THF (3 mL) was cooled to -30 °C. In a separate vessel, a solution of *tert*-butyl 2,2-bis(6-bromohex-4-ynyl)malonate (42.0 mg, 78.6 μmol) in THF (0.5 mL) was prepared and also cooled to -30 °C. The solutions were combined at -30 °C and immediately the dark blue solution became dark red with a yellow precipitate forming. The reaction was allowed to stir overnight at 45 °C. The volatiles were removed *in vacuo* and the residue was triturated with pentane and filtered through Celite. Evaporation of the solvent provided the macrocycle **155a** as a crispy, red solid (27.8 mg, 51%). An elemental analysis sample was obtained by recrystallization from pentane at low temperature. This method of purification also afforded single-crystals for X-ray analysis. Spectroscopic data for **155a**: **IR** (microscope, cm⁻¹): 2973 (m), 2921 (m), 2855 (m), 1742 (w), 1721 (s), 1456 (m), 1392 (w), 1366 (m), 1319 (w), 1256 (m), 1231 (w), 1213 (w), 1167 (s), 1147 (s), 1104 (w), 1060 (w), 1017 (w), 846 (w), 797 (w), 714 (w); **¹H NMR** (300 MHz, C₆D₆): δ 3.16 (br. s, 2H, =CCH₂C≡), 2.61 (t, *J* = 7.6 Hz, 2H, TiCCH₂), 2.39 (t, *J* = 6.8 Hz, 2H, ≡C(CH₂)₂CH₂), 2.31 (2nd order m, 2H, TiC(CH₂)₂CH₂),

2.16 (br. s, 2H, TiCH_2), 2.09 (m, 2H, $\equiv\text{CCH}_2\text{CH}_2$), 1.86 (br. m, 2H, $\text{TiCCH}_2\text{CH}_2$), 1.70 (s, 30H, Cp^*H), 1.49 (p, $J = 6.3$ Hz, 2H, $\equiv\text{CCH}_2\text{CH}_2$), 1.41 (s, 18H, $\text{C}(\text{CH}_3)_3$); $^{13}\text{C}\{^1\text{H}\}$ NMR (100 MHz, C_6D_6): δ 211.7 ($\text{TiC}=\text{C}$), 171.1 ($\text{C}=\text{O}$), 118.5 ($(\text{CH}_3)_5\text{C}_5$), 102.5 ($\text{TiC}=\text{C}$), 81.3 ($\text{C}\equiv\text{C}$), 80.2 ($\text{C}\equiv\text{C}$), 79.9 ($\text{OC}(\text{CH}_3)_3$), 79.2 (TiCH_2), 58.7 ($\text{C}(\text{C}=\text{O})_2$), 35.5 (TiCCH_2), 32.6 ($\text{TiC}(\text{CH}_2)_2\text{CH}_2$), 28.9 ($\equiv\text{C}(\text{CH}_2)_2\text{CH}_2$), 28.0 ($\text{C}(\text{CH}_3)_3$), 26.1 ($\text{TiCCH}_2\text{CH}_2$), 24.0 ($=\text{CCH}_2\text{C}\equiv$), 23.1 ($\equiv\text{CCH}_2\text{CH}_2$), 20.2 ($\equiv\text{CCH}_2\text{CH}_2$), 12.1 ($(\text{CH}_3)_5\text{C}_5$); $^1\text{H}-^1\text{H}$ COSY (400 MHz, C_6D_6): δ 3.16 \leftrightarrow δ 2.16; δ 2.66 \leftrightarrow δ 1.86; δ 2.39 \leftrightarrow δ 1.49; δ 2.31 \leftrightarrow δ 1.86; δ 2.09 \leftrightarrow δ 2.16; HMQC (400 MHz, C_6D_6): δ 3.16 \leftrightarrow δ 24.0; δ 2.66 \leftrightarrow δ 35.5; δ 2.39 \leftrightarrow δ 28.9; δ 2.31 \leftrightarrow δ 32.6; δ 2.16 \leftrightarrow δ 79.2; δ 2.09 \leftrightarrow δ 20.2; δ 1.70 \leftrightarrow δ 12.1; δ 1.49 \leftrightarrow δ 23.1; δ 1.41 \leftrightarrow δ 28.0; HMBC (400 MHz, C_6D_6): δ 3.16 \leftrightarrow δ 211.7, 102.5, 81.3, 80.2; δ 2.61 \leftrightarrow δ 211.7, 102.5, 26.1; δ 2.39 \leftrightarrow δ 171.1, 58.7, 32.6, 23.1, 20.2; δ 2.31 \leftrightarrow δ 171.1, 58.7; δ 2.16 \leftrightarrow δ 211.7, 102.5, 26.1, 24.0; δ 1.70 \leftrightarrow δ 118.5; δ 1.41 \leftrightarrow δ 79.9; TOCSY (400 MHz, C_6D_6): Irr. at δ 2.61, obs. δ 2.61 (t, $J = 7.6$ Hz), 2.31 (2nd order m), 2.16 (br. s), 1.86 (br. m); Irr. at δ 2.4, obs. δ 3.16 (s), 2.39 (t, $J = 6.8$ Hz), 2.09 (br. m), 1.49 (p, $J = 6.3$ Hz); ESMS m/z calculated for $\text{C}_{43}\text{H}_{64}\text{O}_4\text{TiNa}$ ($\text{M}+\text{Na}$)⁺: 715.4; found 715.4; Analysis calculated for $\text{C}_{43}\text{H}_{64}\text{O}_4\text{Ti}$: C, 74.44%; H, 9.30%; found: C, 74.68%; H, 9.39%.

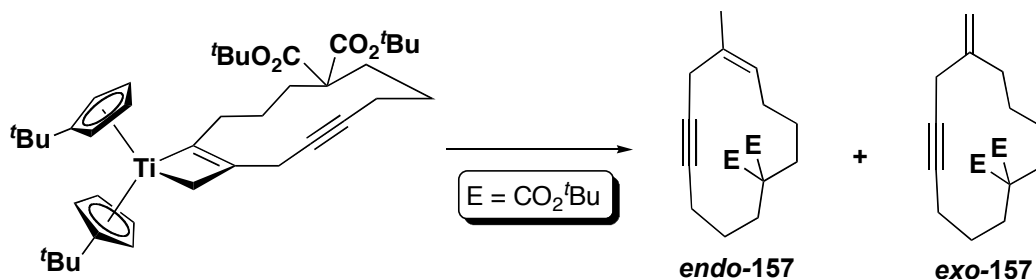
$[(^t\text{BuCp})_2\text{Ti}\{9,9\text{-bis}(\text{t-butoxycarbonyl})\text{-2-methanidylocyclododec-1-en-4-yn-1-yl}\}]$
(155b)



In the drybox, a mixture of $[(^t\text{BuCp})_2\text{TiCl}]_2$ (217.8 mg, 335 μmol) and SmI_2 (1.31 g, 2.16 mmol) in THF (35 mL) was cooled to -30 $^\circ\text{C}$. In a separate vessel, a solution of di-*tert*-butyl 2,2-bis(6-bromohex-4-ynyl)malonate (357.9 mg, 670 μmol) in THF (20 mL)

was prepared and also cooled to -30 °C. The solutions were combined at -30 °C and immediately the dark blue solution became dark red with a yellow precipitate forming. The reaction was and allowed to stir for 20 h. The volatiles were removed *in vacuo* and the residue was triturated with pentane and filtered through Celite. Evaporation of the solvent provided the spectroscopically homogenous macrocycle **155b** as a red solid (247.1 mg, 55%). No further purification was attempted. Spectroscopic data for **155b**: **IR** (microscope, cm⁻¹): 3102 (w), 2962 (s), 2903 (m), 2868 (m), 2286 (w), 1725 (s), 1488 (m), 1460 (m), 1391 (m), 1366 (s), 1259 (s), 1161 (s), 1147 (s), 1093 (m), 1020 (m), 917 (w), 851 (m), 801 (s), 704 (w), 677 (w); **¹H NMR** (300 MHz, C₆D₆): δ 6.01 (apparent q. *J* = 2.7 Hz, 2H, ^tBuCpH), 5.53 (apparent q. *J* = 2.7 Hz, 2H, ^tBuCpH), 5.49 (apparent q. *J* = 2.7 Hz, 2H, ^tBuCpH), 5.44 (apparent q. *J* = 2.7 Hz, 2H, ^tBuCpH), 3.08 (s, 2H, TiCH₂), 2.83 (t, *J* = 7.4 Hz, TiCCH₂), 2.79 (s, 2H, =CCH₂C≡), 2.35 (t, *J* = 7.4 Hz, ≡C(CH₂)₂CH₂), 2.30 (2nd order m, 2H, TiC(CH₂)₂CH₂) 2.03 (br. m, 2H, =CCH₂C≡CCH₂), 1.85 (m, 2H, TiCCH₂CH₂), 1.45 (m, 2H, ≡CCH₂CH₂), 1.41 (s, 18H, OC(CH₃)₃), 1.12 (s, 18H, CpC(CH₃)₃); **¹³C{¹H} NMR** (100 MHz, C₆D₆): δ 213.6 (TiC=C), 171.0 (C=O), 139.4 (*ipso*-^tBuCp), 111.2 (^tBuCp), 110.7 (^tBuCp), 109.7 (^tBuCp), 106.7 (^tBuCp), 93.6 (TiC=C), 81.0 (C≡C), 80.3 (C≡C), 80.1 (OC(CH₃)₃), 74.2 (TiCH₂), 58.6 (C(C=O)₂), 37.7 (TiCCH₂), 32.9 (CpC(CH₃)₃), 31.6 (CpC(CH₃)₃), 31.5 (TiC(CH₂)₂CH₂), 29.0 (≡C(CH₂)₂CH₂), 28.0 (OC(CH₃)₃), 25.0 (TiCCH₂CH₂), 23.1 (≡CCH₂CH₂), 22.6 (=CCH₂C≡), 20.0 (=CCH₂C≡CCH₂); **¹H-¹H COSY** (400 MHz, C₆D₆): δ 6.01 ↔ δ 5.53, 5.49, 5.44; δ 3.08 ↔ δ 2.83; δ 2.83 ↔ δ 1.85; δ 2.79 ↔ δ 2.03; δ 2.35 ↔ δ 1.45; δ 2.30 ↔ δ 1.85; δ 2.03 ↔ δ 1.45; **HMQC** (400 MHz, C₆D₆): δ 6.01 ↔ δ 110.7; δ 5.53 ↔ δ 111.2; δ 5.49 ↔ δ 106.7; δ 5.44 ↔ δ 109.7; δ 3.08 ↔ δ 74.2; δ 2.83 ↔ δ 37.7; δ 2.79 ↔ δ 22.6; δ 2.35 ↔ δ 29.0; δ 2.03 ↔ δ 20.0; δ 1.85 ↔ δ 25.0; δ 1.45 ↔ δ 23.1; δ 1.41 ↔ δ 28.0; δ 1.12 ↔ δ 31.6; **HMBC** (400 MHz, C₆D₆): δ 6.01 ↔ δ 139.4, 111.2/110.7, 106.7; δ 5.53 ↔ δ 139.4, 109.7, 106.7; δ 5.49 ↔ δ 139.4, 109.7; δ 5.44 ↔ δ 139.4, 106.7; δ 3.08 ↔ δ 213.6, 93.6, 22.6; δ 2.83 ↔ δ 213.6, 93.6, 25.0; δ 2.79 ↔ δ 213.6, 93.6, 80.3; δ 1.41 ↔ δ 80.1; δ 1.12 ↔ δ 139.4. Both **ESMS** and **EIMS** failed to give the molecular ion or useful fragments.

(Z)-Di-tert-butyl 8-methyl-cyclododec-8-ene-5-yne-1,1-dicarboxylate (*endo*-157) and Di-tert-butyl 8-methylene-cyclododec-5-yne-1,1-dicarboxylate (*exo*-157)



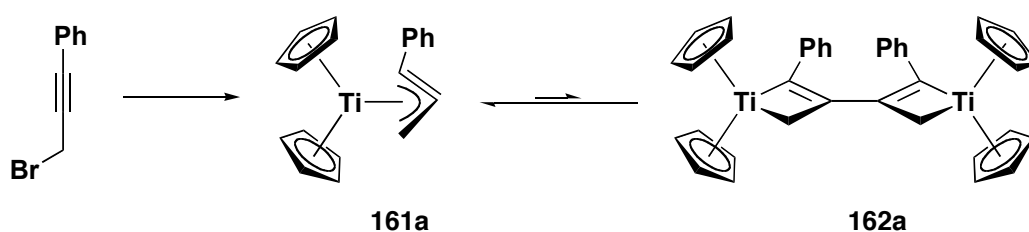
To a -78 °C solution of bicyclic titanacyclobutene **155b** (53.5 mg, 80.5 μmol) in diethyl ether (5 mL) was added anhydrous etheric HCl (1 M, 165 μL). The solution was stirred for 30 minutes at -78 °C then allowed to warm to room temperature. The orange precipitate was filtered, washing with petroleum ether. The filtrate was collected and the solvents were removed *in vacuo*. The crude material was chromatographed on a pipette column using petroleum ether as the eluent and slowly increasing the concentration of diethyl ether. An inseparable 1 : 1 mixture of *endo*-**157** and *exo*-**157** was obtained as a yellow oil. Spectroscopic data for mixture: **IR** (neat film, cm^{-1}): 2976 (s), 2936 (m), 2870 (m), 2212 (w), 1726 (s), 1476 (w), 1459 (m), 1393 (m), 1369 (s), 1322 (w), 1296 (w), 1257 (m), 1211 (w), 1165 (s), 1148 (s), 1030 (w), 932 (w), 881 (w), 850 (m), 793 (w), 747 (w), 702 (w); **endo**-**157**: **^1H NMR** (400 MHz, C_6D_6): δ 5.29 (td, $J = 7.8$ Hz, $J = 1.6$ Hz, 1H, =CH), 2.61 (t, $J = 2.4$ Hz, 2H, =CCH₂C \equiv), 2.26 (2nd order apparent t, $J = 7.4$ Hz, 2H, \equiv CCH₂CH₂), 2.12 (m, 2H, =CCH₂CH₂), 1.88 (m, 2H, \equiv CCH₂CH₂), 1.68 (p, $J = 7.6$ Hz, 2H, =CCH₂CH₂), 1.59 (d, $J = 1.0$ Hz, 3H, CH₃C=), 1.40 (m, 2H, \equiv CCH₂CH₂); **$^{13}\text{C}\{^1\text{H}\}$ NMR** (100 MHz, CDCl_3): δ 132.6 (C=CH), 126.3 (=CH), 81.0 (C \equiv C), 79.6 (C \equiv C), 57.9 (C(C=O)₂), 25.1 (CH₃C=) 22.4 (=CCH₂C \equiv); **^1H - ^1H COSY** (400 MHz, C_6D_6): δ 5.29 \leftrightarrow δ 2.12, 1.59; δ 2.61 \leftrightarrow δ 1.88; **HMQC** (400 MHz, CDCl_3): δ 5.29 \leftrightarrow δ 126.3; δ 2.61 \leftrightarrow δ 22.4; δ 1.88 \leftrightarrow δ 19.1; δ 1.59 \leftrightarrow δ 25.1; **HMBC** (400 MHz, CDCl_3): δ 5.29 \leftrightarrow δ 25.1, 22.7/22.4; ¹⁴⁰ δ 2.61 \leftrightarrow δ 132.6, 126.3, 81.0, 79.6; 57.9; δ 1.59 \leftrightarrow δ 132.6, 126.3.

exo-157: ^1H NMR (400 MHz, C_6D_6): δ 4.78 (dt, $J = 1.3$ Hz, $J = 1.0$ Hz, 1H, =CHH), 4.69 (td, $J = 1.4$ Hz, $J = 1.3$ Hz, 1H, =CHH), 2.68 (t, $J = 2.6$ Hz, 2H, =CCH₂C \equiv), 2.26 (2nd order apparent t, $J = 7.4$ Hz, 2H); 2.05 (m, 2H, =CCH₂CH₂), 1.92 (m, 2H, \equiv CCH₂CH₂), 1.68 (p, $J = 7.6$ Hz, 2H, =CCH₂CH₂), 1.40 (m, 2H, \equiv CCH₂CH₂); $^{13}\text{C}\{^1\text{H}\}$ NMR (100 MHz, CDCl_3): δ 144.8 (C=CH₂), 111.8 (=CH₂), 81.5 (C \equiv C), 79.2 (C \equiv C), 58.4 (C(C=O)₂), 32.1 (=CCH₂CH₂), 28.2 (=CCH₂C \equiv); ^1H - ^1H COSY (400 MHz, C_6D_6): δ 4.78 \leftrightarrow δ 2.68, 2.05; δ 4.69 \leftrightarrow δ 2.05; **HMQC** (400 MHz, CDCl_3): δ 4.78 \leftrightarrow δ 111.8; δ 4.69 \leftrightarrow δ 111.8; δ 2.69 \leftrightarrow δ 28.2; δ 1.82 \leftrightarrow δ 19.8; **HMBC** (400 MHz, CDCl_3): δ 4.78 \leftrightarrow δ 32.1, 28.2; δ 4.69 \leftrightarrow δ 32.1; δ 2.68 \leftrightarrow δ 144.8, 111.8, 81.5, 79.2;

$^{13}\text{C}\{^1\text{H}\}$ NMR (100 MHz, CDCl_3 , remaining signals reported as isomeric mixture): δ 170.9 (C=O), 170.8 (C=O), 80.1 (OC(CH₃)₃), 80.0 (OC(CH₃)₃), 58.4 (C(C=O)₂), 57.9 (C(C=O)₂), 34.4, 30.3, 30.2, 29.0, 28.7, 28.5, 27.9 (C(CH₃)₃), 26.6, 24.1, 23.1, 22.7, 20.8;

ESMS m/z calculated for $\text{C}_{33}\text{H}_{34}\text{O}_4\text{Na}$ (M+Na)⁺: 399.25058; found: 399.24886;

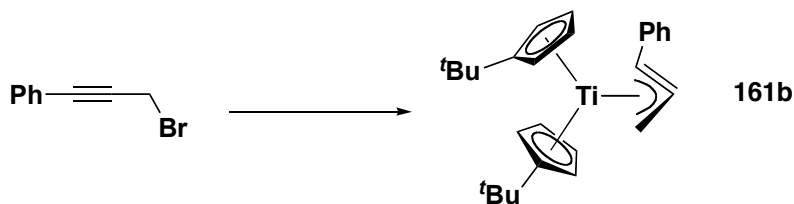
**Bis(cyclopentadienyl)(η^3 -3-phenylpropargyl)titanium (161a) and
tetra(cyclopentadienyl)-2,2'-diphenyl-3,3'-di(titanacyclobutene) (162a)**



In the glovebox, $[\text{Cp}_2\text{TiCl}]_2$ (96.2 mg, 225 μmol) and SmI_2 (551.0 mg, 908 μmol) were combined with THF (6 mL). In a separate vessel, 1-(3-bromoprop-1-ynyl)benzene (86.1 mg, 441 μmol) was dissolved in THF (1 mL). Both vessels were cooled to -30 °C and combined rapidly. The reaction was allowed to warm to room temperature and stirred for six hours after which the solution was dark-green and there was a yellow precipitate. The solvent was removed *in vacuo* and the residue was triturated with hexanes and filtered through Celite. Evaporation of volatiles gave the paramagnetic

propargyl complex **161a** as a dark-green oil (118.9 mg, 92%). Crystallization from toluene at -30 °C gave purple crystals suitable for X-ray crystallography. Analysis of these crystals demonstrated that the product was, in fact, of the diamagnetic titanacyclobutene dimer **162a**. Spectroscopic data for **162a**: **IR** (microscope, cm⁻¹): 2913 (w), 2176 (w), 1924 (m), 1804 (w), 1712 (w), 1593 (m), 1569 (w), 1488 (m), 1441 (m), 1365 (w), 1299 (w), 1275 (w), 1124 (w), 1064 (m), 1016 (s), 904 (w), 797 (s), 759 (s), 694 (s), 666 (w); ¹³C{¹H} **NMR** (100 MHz, toluene-*d*⁸, -80 °C): δ 214.1 (TiC=C), 145.8 (*ipso*-Ph), 110.4 (Cp), 90.4 (TiC=C), 78.8 (TiCH₂); **EIMS** *m/z* calculated for C₁₉H₁₇Ti (M)⁺: 293.0896; found: 293.08090; **Analysis** calculated for C₁₉H₁₇Ti: C, 77.83%; H, 5.84%; found: C, 78.14%; H, 6.10%.

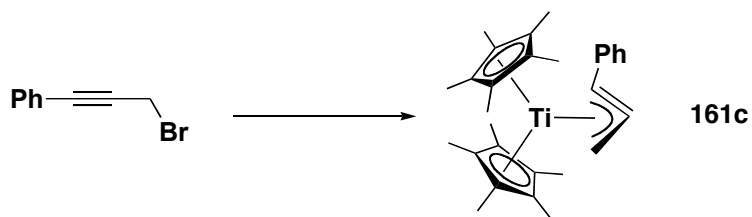
Bis(*tert*-butylcyclopentadienyl)(η³-3-phenylpropargyl)titanium (161b)



In the glovebox, [(^tBuCp)₂TiCl] (96.4 mg, 148 μmol) and SmI₂ (407.8 mg, 600 μmol) were combined with THF (7 mL). In a separate vessel, 1-(3-bromoprop-1-ynyl)benzene (57.3 mg, 294 μmol) was dissolved in THF (3 mL). Both vessels were cooled to -30 °C and combined rapidly. The reaction was allowed to warm to room temperature and stirred overnight, after which the solution had become dark-green and there was a yellow precipitate. The solvent was removed *in vacuo* and the residue was triturated with pentane and filtered through Celite. Evaporation of volatiles gave the propargyl complex **161b** as a paramagnetic dark-green oil (109.3 mg, 92%), which did not crystallize at low temperature. Spectroscopic data for **161b**: **IR** (microscope, cm⁻¹): 3082 (w), 3026 (w), 2958 (m), 2902 (m), 2867 (m), 1598 (w), 1489 (m), 1460 (m), 1418 (w), 1384 (w), 1361 (m), 1279 (m), 1203 (w), 1160 (w), 1045 (w), 1027 (w), 918 (w),

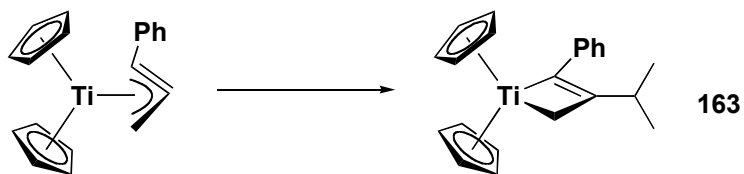
832 (s), 791 (s), 699 (m), 682 (w); EIMS m/z calculated for $C_{27}H_{33}Ti$ (M)⁺: 405.20618; found: 405.20652.

Bis(pentamethylcyclopentadienyl)(η^3 -3-phenylpropargyl)titanium (161c)



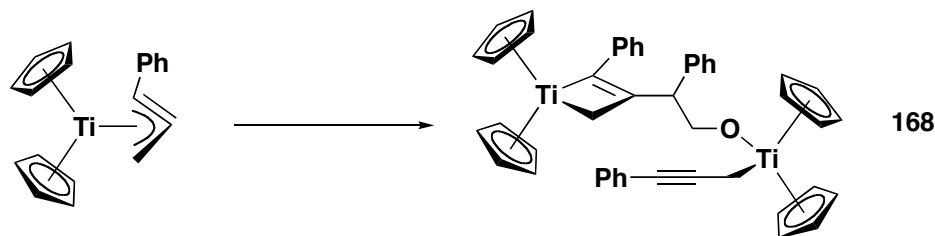
In the glovebox, Cp*₂TiCl (43.5 mg, 123 μ mol) and SmI₂ (227.2 mg, 374 μ mol) were combined with THF (3 mL). In a separate vessel, 1-(3-bromoprop-1-ynyl)benzene (24.0 mg, 123 μ mol) was dissolved in THF (1 mL). Both vessels were cooled to -30 °C and combined rapidly. The reaction was allowed to warm to room temperature and stirred overnight, after which the solution had become very dark and there was a yellow precipitate. The solvent was removed *in vacuo* and the residue was triturated with pentane and filtered through Celite. Evaporation of volatiles gave the propargyl complex **X** as a paramagnetic dark oil (46.7 mg, 69%). Single-crystals were obtained by crystallization from pentane at low temperature. The spectroscopic and mass spectrometric data is consistent with that of the reported compound.⁶¹

$[(\eta^5\text{-C}_5\text{H}_5)_2\text{Ti}\{\eta^2\text{-PhC=C}(\text{iPr})\text{CH}_2\}]$ (**163**)



In the glovebox, a solution of isopropyl iodide (26.5 mg, 156 μmol) in THF (1 mL) was added to a solution of bis(cyclopentadienyl) titanium η^3 -phenyl propargyl (43.7 mg, 149 μmol) and SmI_2 (131.7 mg, 194 μmol) in THF (4 mL) at $-30\text{ }^\circ\text{C}$. The solution was allowed to warm to room temperature and stirred overnight, after which the solution had become dark-red and there was a yellow precipitate. The solvent was removed *in vacuo* and the residue was triturated with pentane and filtered through Celite. Evaporation of volatiles gave the titanacyclobutene **163** as a red crystalline solid (43.1 mg, 86%). Crystallization from a pentane at $-30\text{ }^\circ\text{C}$ gave X-ray quality single crystals. Spectroscopic data for **163**: **IR** (cast film, cm^{-1}): 3118 (w), 3061 (w), 3013 (w), 2951 (m), 2927 (w), 2903 (w), 2862 (w), 1594 (m), 1564 (w), 1480 (w), 1443 (w), 1435 (w), 1403 (w), 1370 (w), 1354 (w), 1296 (w), 1265 (w), 1210 (w), 1166 (w), 1154 (w), 1130 (w), 1099 (w), 1074 (w), 1019 (m), 964 (w), 914 (w), 835 (w), 807 (s), 771 (m), 707 (m); **^1H NMR** (400 MHz, C_6D_6): δ 7.25 (apparent tt, $J = 7.6\text{ Hz}$, $J = 1.7\text{ Hz}$, 2H, *o-* or *m*-PhH), 7.01 (tt, $J = 7.4\text{ Hz}$, $J = 1.3\text{ Hz}$, 1H, *p*-PhH), 6.94 (m, 2H, *o-* or *m*-PhH), 5.58 (s, 10H, CpH), 3.21 (s, 2H, TiCH₂), 2.66 (septet, $J = 6.8\text{ Hz}$, 1H, (CH₃)₂CH), 0.87 (d, $J = 6.8\text{ Hz}$, 6H, (CH₃)₂CH); **$^{13}\text{C}\{^1\text{H}\}$ NMR** (100 MHz, C_6D_6): δ 210.2 (TiC=C), 148.9 (*ipso*-Ph), 128.5 (Ph), 124.9 (Ph), 124.1 (Ph), 111.5 (Cp), 99.7 (TiC=C), 68.9 (TiCH₂), 27.6 ((CH₃)₂CH), 21.3 (CH₃)₂CH); **Analysis** calculated for $\text{C}_{22}\text{H}_{24}\text{Ti}$: C, 78.57%; H, 7.19%; found: C, 78.87%; H, 7.31%.

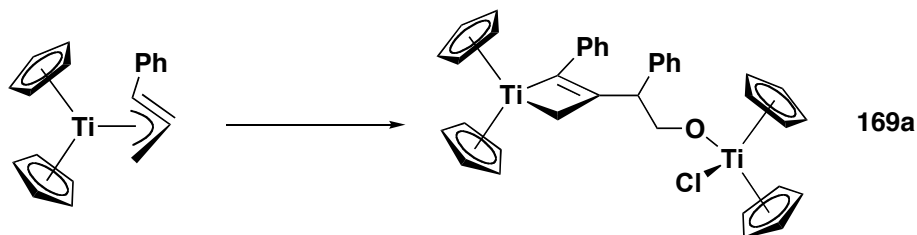
[Cp₂Ti{PhC=C(CHPhCH₂OTi(η¹-CH₂C≡CPh)Cp₂)CH₂}] (**168**)



In the drybox, a dark green solution of [bis(cyclopentadienyl)titanium(η³-phenyl propargyl)] (40.7 mg, 0.139 mmol) in THF (3 mL) was cooled to -30 °C. In a separate vessel, a solution of styrene oxide (8.5 mg, 0.071 mmol) in THF (0.5 mL) was prepared and also cooled to -30 °C. The solutions were combined at -30 °C and allowed to stir at room temperature. Within 1 h, the solution became dark red. After stirring overnight, the volatiles were removed *in vacuo* and the residue was triturated with hexanes and filtered through Celite. Evaporation of the solvent provided the bimetallic complex **168** as an analytically pure red solid (46.9 mg, 96%). Spectroscopic data for **168**: **IR** (microscope, cm⁻¹): 3060 (w), 3025 (w), 2973 (m), 2921 (m), 2853 (m), 2176 (s), 1593 (m), 1565 (w), 1489 (m), 1478 (w), 1443 (m), 1365 (w), 1350 (w), 1261 (m), 1099 (s), 1018 (s), 977 (w), 908 (w), 815 (w), 799 (s), 751 (w), 729 (w), 689 (w); **¹H NMR** (300 MHz, C₆D₆): δ 7.77 (d, *J* = 7.8 Hz, 2H, PhH), 7.35-6.93 (m, 13H, PhH), 5.68 (s, 5H, CpH), 5.61 (s, 5H, CpH), 5.56 (s, 5H, CpH), 5.42 (s, 5H, CpH), 4.65 (dd, *J* = 11.2 Hz, *J* = 9.7 Hz, 1H, OCHHCH), 4.44 (dd, *J* = 11.2 Hz, *J* = 6.0 Hz, 1H, OCHHCH), 3.78 (dd, *J* = 9.7 Hz, *J* = 6.0 Hz, 1H, PhCH), 3.11 (d, *J* = 11.7 Hz, 1H, TiCHHC=C), 2.84 (d, *J* = 11.7 Hz, 1H, TiCHHC=C), 2.06 (d, *J* = 12.5 Hz, 1H, ≡CCHH), 1.91 (d, *J* = 12.5 Hz, 1H, ≡CCHH); **¹³C{¹H} NMR** (100 MHz, C₆D₆): δ 211.2 (TiC=C), 148.7 (Ph), 142.0 (Ph), 131.1 (Ph), 129.1 (Ph), 128.8 (Ph), 128.6 (Ph), 128.1 (Ph), 127.6 (Ph), 126.2 (Ph), 126.0 (Ph), 125.0 (Ph), 124.5 (Ph), 113.2 (C₅H₅), 113.0 (C₅H₅), 112.2 (C₅H₅), 111.5 (C₅H₅), 102.0 (PhC≡C), 97.0 (TiC=C), 86.4 (PhC≡C), 80.6 (OCH₂), 69.5 (TiCH₂C=C), 48.8 (PhCH), 26.5 (≡CCH₂); **¹H-¹H COSY** (300 MHz, C₆D₆): δ 4.65 ↔ δ 4.44, 3.78; δ 4.44 ↔ δ 3.78; δ 3.11 ↔ δ 2.84; δ 2.06 ↔ δ 1.91; **HMQC** (300 MHz, C₆D₆): δ 5.68 ↔ δ 113.0; δ 5.61 ↔ δ 112.2; δ 5.56 ↔ δ 113.2; δ 5.42 ↔ δ 111.5; δ 4.65 ↔ δ 80.6; δ 4.44

$\leftrightarrow \delta$ 80.6; δ 3.78 $\leftrightarrow \delta$ 48.8; δ 3.11 $\leftrightarrow \delta$ 69.5; δ 2.84 $\leftrightarrow \delta$ 69.5; δ 2.06 $\leftrightarrow \delta$ 26.5; δ 1.91 $\leftrightarrow \delta$ 26.5; **HMBC** (400 MHz, C₆D₆): δ 7.77 $\leftrightarrow \delta$ 86.4; δ 4.65 $\leftrightarrow \delta$ 142.0, 97.0, 48.8; ; δ 4.44 $\leftrightarrow \delta$ 142.0, 97.0, 48.8; δ 3.78 $\leftrightarrow \delta$ 211.2, 142.0, 97.0, 80.6, 69.5; δ 3.11 $\leftrightarrow \delta$ 211.2, 148.7, 97.0, 48.8; 2.84 $\leftrightarrow \delta$ 211.2, 148.7, 97.0, 48.8; δ 2.06 $\leftrightarrow \delta$ 131.1, 102.0, 86.4; δ 1.91 $\leftrightarrow \delta$ 131.1, 102.0, 86.4; **EIMS** *m/z* calculated for C₂₇H₂₆TiO (M+H-Cp₂Ti(PhCCCH₂))⁺: 414.14630; found: 414.14434; **Analysis** calculated for C₄₆H₄₂Ti₂O : C, 78.20%; H, 5.99%; found: C, 78.18%; H, 6.44%.

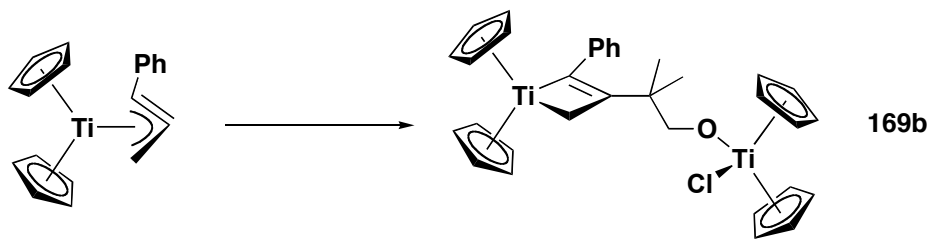
[Cp₂Ti{PhC=C(CHPhCH₂OTiClCp₂)CH₂}] (169a)



In the glovebox, a solution of styrene oxide (51.3 mg, 427 μ mol) in THF (1.5 mL) was added to [bis(cyclopentadienyl)titanium(η^3 -phenyl propargyl)] (118.9 mg, 405 μ mol) in THF (3 mL) at -30 °C. To this dark green solution, was added [Cp₂TiCl]₂ (87.1 mg, 408 μ mol) in THF (1.5 mL). Immediately the reaction mixture became dark-red. The vessel was stored at -30 °C for two days. The volatiles were removed *in vacuo* to give a red foam. Trituration with benzene and filtration through Celite removed a small amount of grey powder. Evaporation of solvent provided the bimetallic complex **169a** as a red foam (279.5 mg, quantitative). Crystallization from a benzene / pentane solution at -30 °C yielded dark-red crystals suitable for X-ray crystallography. Spectroscopic data for **169a**: **IR** (film, cm⁻¹): 3108 (w), 3059 (w), 3023 (w), 2917 (m), 2838 (w), 1593 (m), 1564 (w), 1493 (w), 1479 (m), 1444 (m), 1368 (w), 1330 (w), 1262 (w), 1091 (s), 1019 (s), 976 (w), 811 (s), 760 (m), 722 (w), 701 (m), 664 (w); **¹H NMR** (400 MHz, C₆D₆): δ 7.38-7.03 (m, 10H, PhH), 5.87 (s, 5H, CpH), 5.77 (s, 5H, CpH), 5.70 (s, 5H, CpH), 5.43 (s, 5H, CpH), 4.76 (d, *J* = 7.8 Hz, 2H, OCH₂), 3.92 (t, *J* = 7.8 Hz, 1H, PhCH), 3.25 (d, *J* =

11.6 Hz, 1H, TiCHH), 2.89 (d, $J = 11.6$ Hz, 1H, TiCHH); $^{13}\text{C}\{^1\text{H}\}$ NMR (100 MHz, C_6D_6): δ 210.8 (TiC=C), 148.7 (Ph), 141.8 (Ph), 129.0 (Ph), 128.7 (Ph), 128.6 (Ph), 128.1 (Ph), 126.3 (Ph), 125.2 (Ph), 124.4 (Ph), 116.5 (C_5H_5), 116.1 (C_5H_5), 112.4 (C_5H_5), 111.5 (C_5H_5), 97.5 (TiC=C), 84.0 (OCH_2), 69.4 (TiCH₂), 48.4 (PhCH); $^1\text{H}-^1\text{H}$ COSY (400 MHz, C_6D_6): δ 4.76 \leftrightarrow δ 3.92; δ 3.25 \leftrightarrow δ 2.89; **HMQC** (400 MHz, C_6D_6): δ 5.87 \leftrightarrow δ 116.1; δ 5.77 \leftrightarrow δ 116.5; δ 5.70 \leftrightarrow δ 112.4; δ 5.43 \leftrightarrow δ 111.5; δ 4.76 \leftrightarrow δ 84.0; δ 3.92 \leftrightarrow δ 48.4; δ 3.25 \leftrightarrow δ 69.4; δ 2.89 \leftrightarrow δ 69.4; **HMBC** (400 MHz, C_6D_6): δ 4.76 \leftrightarrow δ 141.8, 97.5, 48.4; δ 3.92 \leftrightarrow δ 210.8, 141.8, 97.5, 84.0, 69.4; δ 3.25 \leftrightarrow δ 210.8, 112.4, 111.5, 97.5, 48.4; δ 2.89 \leftrightarrow δ 210.8, 112.4, 111.5, 97.5, 48.4; **EIMS** m/z calculated for $\text{C}_{27}\text{H}_{26}\text{TiO}$ ($\text{M}+\text{H}-\text{Cp}_2\text{TiCl}$)⁺: 414.14630; found: 414.14566; **Analysis** calculated for $\text{C}_{37}\text{H}_{35}\text{Ti}_2\text{OCl}$: C, 70.89%; H, 5.63%; found: C, 70.84%; H, 5.70%.

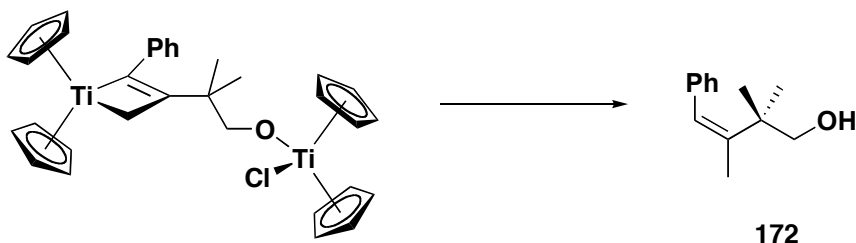
[Cp₂Ti{PhC=C(CH(CH₃)₂)CH₂OTiClCp₂}CH₂}] (169b)



In the glovebox, a cold solution of isobutylene oxide (18 μL , 203 μmol) in THF (1.5 mL) was added to [bis(cyclopentadienyl)titanium(η^3 -phenyl propargyl)] (55.9 mg, 191 μmol) in THF (3 mL) at -30 °C. To this dark green solution, was added $[\text{Cp}_2\text{TiCl}]_2$ (40.5 mg, 95 μmol) in THF (1.5 mL). The mixture slowly turned dark red over the period of several hours. The solution was stirred overnight at room temperature and the volatiles were removed *in vacuo* to give a red foam. Washing with several portions of pentane gave the bimetallic complex **169b** as a red solid (87.6 mg, 80%) pure by spectral analysis. No further purification was done. Spectroscopic data for **169b**: **IR** (cast film, cm^{-1}): 3109 (w), 3066 (w), 3015 (w), 2961 (m), 2922 (m), 2867 (m), 1737 (w), 1595 (m), 1563 (w), 1490 (w), 1477 (m), 1443 (m), 1377 (w), 1354 (w), 1275 (w), 1172 (w), 1152 (w), 1072

(s), 1019 (s), 912 (w), 808 (s), 761 (m), 720 (m), 703 (m), 661 (w); ^1H NMR (400 MHz, C_6D_6): δ 7.19 (m, 2H, *m*-Ph), 6.98 (d, $J = 8.0$ Hz, 2H, *o*-Ph), 6.91 (t, $J = 7.5$ Hz, 1H, *p*-Ph), 5.91 (s, 10H, CpH), 5.66 (s, 10H, CpH), 4.20 (s, 2H, OCH_2), 3.24 (s, 2H, TiCH_2), 0.98 (s, 6H, $(\text{CH}_3)_2\text{C}$); $^{13}\text{C}\{^1\text{H}\}$ NMR (100 MHz, C_6D_6): δ 204.8 (TiC=C), 151.2 (*ipso*-Ph), 128.6 (*m*-Ph), 124.0 (*o*- or *p*-Ph), 123.1 (*o*- or *p*-Ph), 116.2 (C_5H_5), 112.7 (C_5H_5), 100.5 (TiC=C), 93.2 (OCH_2), 71.4 (TiCH_2), 44.1 ($(\text{CH}_3)_2\text{C}$), 25.8 ($(\text{CH}_3)_2\text{C}$); **HMQC** (400 MHz, C_6D_6): δ 5.91 \leftrightarrow δ 116.2; δ 5.66 \leftrightarrow δ 112.7; δ 4.20 \leftrightarrow δ 93.2; δ 3.24 \leftrightarrow δ 71.4; δ 0.98 \leftrightarrow δ 25.8; **HMBC** (400 MHz, C_6D_6): δ 7.19 \leftrightarrow δ 128.6; δ 6.98 \leftrightarrow δ 124.0; δ 4.20 \leftrightarrow δ 100.5, 44.1, 25.8; δ 3.24 \leftrightarrow δ 204.8, 124.0, 100.5, 44.1; δ 0.98 \leftrightarrow δ 100.5, 93.2, 44.1.

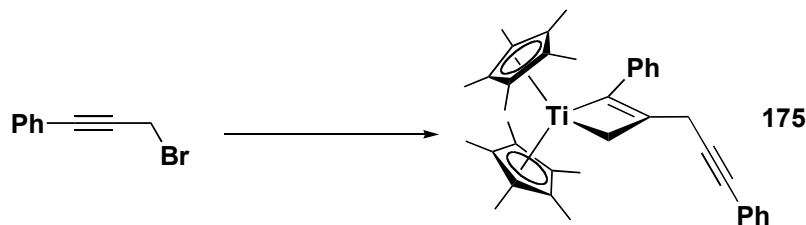
(Z)-2,2,3-Trimethyl-4-phenylbut-3-en-1-ol (172)



To a solution of $[\text{Cp}_2\text{Ti}\{\text{PhC}=\text{C}(\text{CH}(\text{CH}_3)_2\text{CH}_2\text{OTiClCp}_2)\text{CH}_2\}]$ (26.7 mg, 46.1 μmol) in diethyl ether (5 mL) was added anhydrous HCl (1M in diethyl ether, 150 μL , 150 μmol) at -78 $^\circ\text{C}$. Immediately, the colour of the solution changed from a dark-red to orange. The mixture was stirred overnight at -78 $^\circ\text{C}$ and then saturated sodium bicarbonate was added. The product was extracted into several portions of diethyl ether and the organic layer was dried over sodium sulfate. Removal of volatiles *in vacuo* followed by flash silica gel chromatography (dichloromethane; R_f 0.28) gave the homoallylic alcohol **172** as a pale yellow oil (5.3 mg, 60%). Spectroscopic data for **172**: **IR** (neat film, cm^{-1}): 3387 (m), 3056 (w), 3018 (w), 2966 (s), 2929 (s), 2872 (m), 1942 (w), 1734 (w), 1636 (w), 1598 (w), 1575 (w), 1491 (m), 1442 (m), 1377 (m), 1263 (w), 1155 (w), 1111 (w), 1047 (m), 916 (w), 846 (w), 821 (w), 751 (s), 701 (s), 668 (w); ^1H

NMR (400 MHz, CDCl₃): δ 7.31-7.14 (m, 5H, PhH), 6.57 (s, 1H, =CH), 3.31 (d, *J* = 6.5 Hz, 2H, CH₂OH), 1.91 (t, *J* = 1.3 Hz, 3H, =CCH₃), 1.55 (s, 1H, OH), 1.00 (s, 6H, C(CH₃)₂); **APT** ¹³C{¹H} **NMR** (100 MHz, CDCl₃): δ 141.9 (p, *ipso*-Ph or =CH), 140.5 (p, *ipso*-Ph or =CCH₃), 128.6 (n, *o*- or *m*-Ph), 127.93 (n, *o*- or *m*-Ph or =CCH₃), 127.89 (n, *o*- or *m*-Ph or =CCH₃), 126.3 (n, *p*-Ar), 70.9 (p, =CH), 42.2 (p), 25.9 (n, C(CH₃)₂), 23.7 (n, =CCH₃); **NOE** (400 MHz, CDCl₃): Irr. δ 6.57, Obs. δ 7.31-7.14 (0.01%), 3.31 (-0.31%), 1.91 (4.60%), 1.00 (-0.75%); Irr. δ 6.57, Obs. δ 7.31-7.14 (0.74%), 6.57 (2.76%), 3.31 (0.55%), 1.55 (-1.02%), 1.00 (2.07%); **HSQC** (400 MHz, CDCl₃): δ 6.57 ↔ δ 127.9; δ 3.31 ↔ δ 70.9; δ 1.91 ↔ δ 23.7; δ 1.00 ↔ δ 25.9; **EIMS** *m/z* calculated for C₁₃H₁₈O₁ (M)⁺: 190.13577; found: 190.13628.

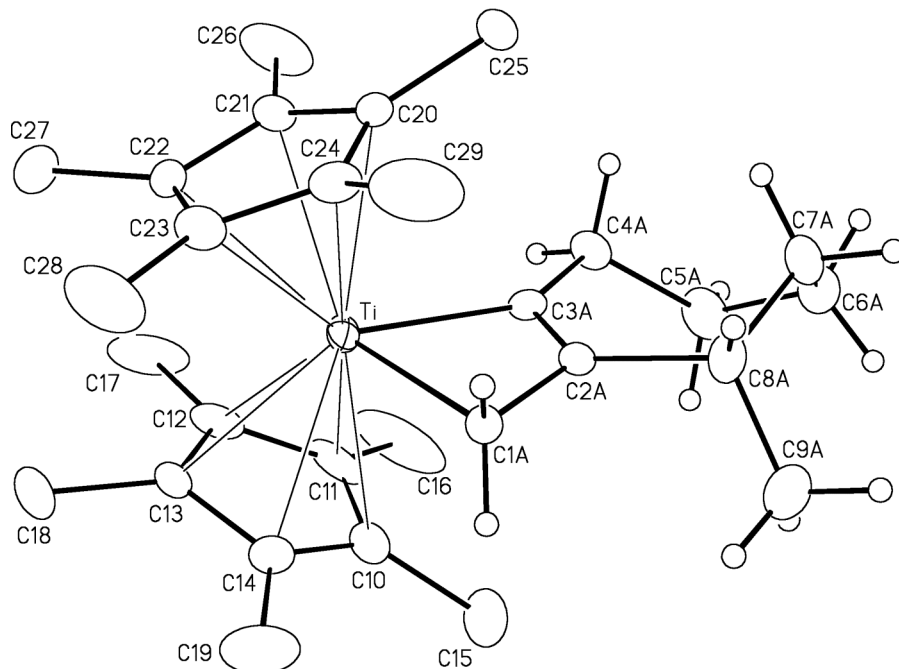
[(η⁵-C₅Me₅)₂Ti{η²-PhC=C(CH₂C≡CPh)CH₂}] (175)⁶¹



In the glovebox, Cp*₂TiCl (23.8 mg, 67.3 μmol) and SmI₂ (135.6 mg, 357 μmol) were combined with THF (2 mL). In a separate vessel, 1-(3-bromoprop-1-ynyl)benzene (12.3 mg, 63.1 μmol) was dissolved in THF (0.5 mL). Both vessels were cooled to -30 °C and combined rapidly. To the resulting green mixture was added bromodiethyl malonate (16.3 mg, 68.2 μmol) and the solution immediately became red. The reaction was allowed to warm to room temperature and stirred overnight. The solvent was removed *in vacuo* and the residue was triturated with hexanes and filtered through Celite. Evaporation of volatiles gave the titanacyclbutene **175** as an impure dark red-brown oil (21.5 mg, '124%'). Crystallization from pentane at -30 °C gave dark crystals suitable for X-ray analysis. The spectroscopic data match that of the reported compound.

Appendix: Crystallographic Data

A. Selected crystallographic data for **129**. Additional information (including structure factors, etc.) can be obtained directly from Dr. Robert McDonald or Dr. Michael Ferguson at the X-Ray Crystallography Laboratory, University of Alberta, Department of Chemistry, Edmonton AB T6G 2G2 Canada. Request .cif file or report # JMS0859.



Crystallographic Experimental Details for Titanacyclobutene **129**

A. Crystal Data

formula	C ₂₉ H ₄₄ Ti
formula weight	440.54
crystal dimensions (mm)	0.52 × 0.24 × 0.16
crystal system	monoclinic
space group	<i>P</i> 2 ₁ / <i>n</i> (an alternate setting of <i>P</i> 2 ₁ / <i>c</i> [No. 14])
unit cell parameters ^a	
<i>a</i> (Å)	10.1565 (4)
<i>b</i> (Å)	19.4029 (8)
<i>c</i> (Å)	12.6834 (5)
β (deg)	99.2770 (10)
<i>V</i> (Å ³)	2466.77 (17)
<i>Z</i>	4
ρ _{calcd} (g cm ⁻³)	1.186

μ (mm ⁻¹)	0.360
<i>B. Data Collection and Refinement Conditions</i>	
diffractometer	Bruker D8/APEX II CCD ^b
radiation (λ [Å])	graphite-monochromated Mo K α (0.71073)
temperature (°C)	-100
scan type	ω scans (0.3°) (20 s exposures)
data collection 2θ limit (deg)	50.50
total data collected	17360 ($-12 \leq h \leq 12$, $-23 \leq k \leq 23$, $-15 \leq l \leq 15$)
independent reflections	4463 ($R_{\text{int}} = 0.0249$)
number of observed reflections (<i>NO</i>)	3691 [$F_o^2 \geq 2\sigma(F_o^2)$]
structure solution method	direct methods (<i>SHELXS-97</i> ^c)
refinement method	full-matrix least-squares on F^2 (<i>SHELXL-97</i> ^c)
absorption correction method	Gaussian integration (face-indexed)
range of transmission factors	0.9440–0.8348
data/restraints/parameters	4463 [$F_o^2 \geq -3\sigma(F_o^2)$] / 0 / 356
goodness-of-fit (<i>S</i>) ^d	1.055 [$F_o^2 \geq -3\sigma(F_o^2)$]
final <i>R</i> indices ^e	
R_1 [$F_o^2 \geq 2\sigma(F_o^2)$]	0.0573
wR_2 [$F_o^2 \geq -3\sigma(F_o^2)$]	0.1592
largest difference peak and hole	0.550 and -0.665 e Å ⁻³

^aObtained from least-squares refinement of 8865 reflections with $4.58^\circ < 2\theta < 49.02^\circ$.

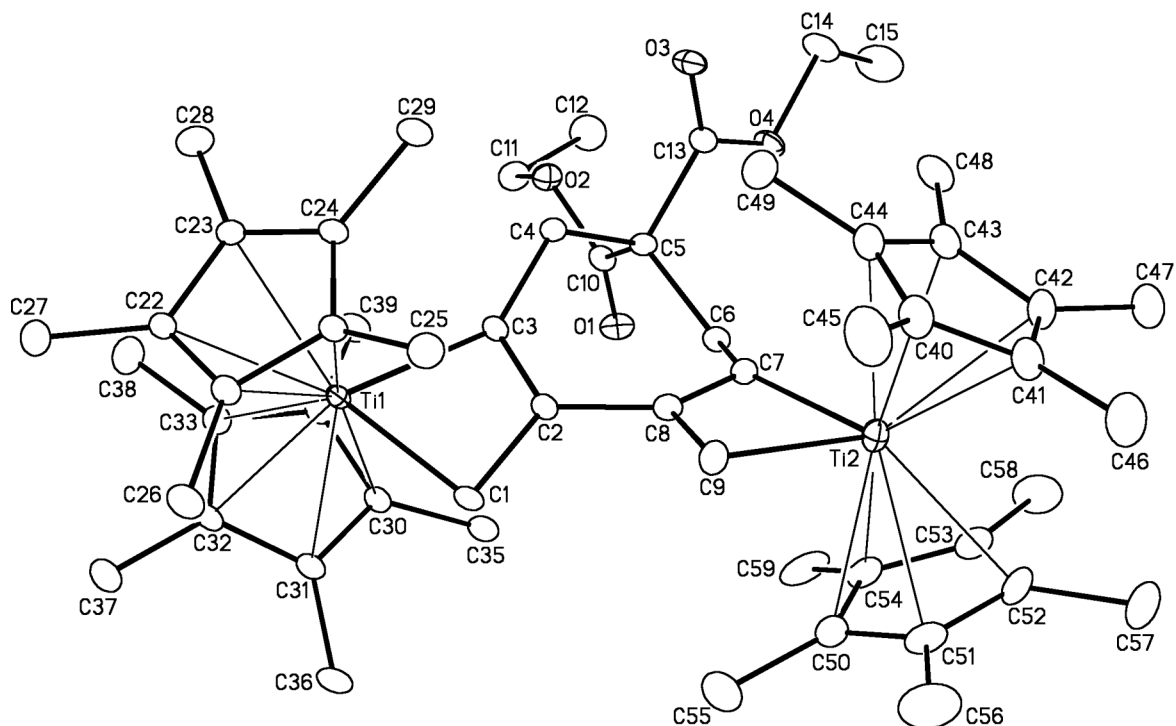
^bPrograms for diffractometer operation, data collection, data reduction and absorption correction were those supplied by Bruker.

^cSheldrick, G. M. *Acta Crystallogr.* **2008**, *A64*, 112–122.

^d $S = [\sum w(F_o^2 - F_c^2)^2 / (n - p)]^{1/2}$ (n = number of data; p = number of parameters varied; $w = [\sigma^2(F_o^2) + (0.0776P)^2 + 2.2339P]^{-1}$ where $P = [\text{Max}(F_o^2, 0) + 2F_c^2]/3$).

^e $R_1 = \sum ||F_o| - |F_c|| / \sum |F_o|$; $wR_2 = [\sum w(F_o^2 - F_c^2)^2 / \sum w(F_o^4)]^{1/2}$.

B. Report # JMS0905.



Crystallographic Experimental Details for Titanacyclobutene **149a**

A. Crystal Data

formula	C ₅₅ H ₇₈ O ₄ Ti ₂
formula weight	898.97
crystal dimensions (mm)	0.35 × 0.19 × 0.08
crystal system	triclinic
space group	<i>P</i> $\bar{1}$ (No. 2)
unit cell parameters ^a	
<i>a</i> (Å)	10.1008 (16)
<i>b</i> (Å)	15.732 (3)
<i>c</i> (Å)	16.667 (3)
α (deg)	73.319 (2)
β (deg)	85.482 (2)
γ (deg)	74.164 (2)
<i>V</i> (Å ³)	2440.8 (7)
<i>Z</i>	2
ρ _{calcd} (g cm ⁻³)	1.223
μ (mm ⁻¹)	0.371

B. Data Collection and Refinement Conditions

diffractometer Bruker D8/APEX II CCD^b

radiation (λ [Å])	graphite-monochromated Mo K α (0.71073)
temperature (°C)	-100
scan type	ω scans (0.3°) (20 s exposures)
data collection 2θ limit (deg)	50.50
total data collected	17393 ($-12 \leq h \leq 12, -18 \leq k \leq 18, -20 \leq l \leq 20$)
independent reflections	8809 ($R_{\text{int}} = 0.0643$)
number of observed reflections (NO)	5704 [$F_o^2 \geq 2\sigma(F_o^2)$]
structure solution method	direct methods (<i>SHELXS-97</i> ^c)
refinement method	full-matrix least-squares on F^2 (<i>SHELXL-97</i> ^c)
absorption correction method	Gaussian integration (face-indexed)
range of transmission factors	0.9695–0.8807
data/restraints/parameters	8809 [$F_o^2 \geq -3\sigma(F_o^2)$] / 0 / 570
goodness-of-fit (S) ^d	1.007 [$F_o^2 \geq -3\sigma(F_o^2)$]
final R indices ^e	
R_1 [$F_o^2 \geq 2\sigma(F_o^2)$]	0.0601
wR_2 [$F_o^2 \geq -3\sigma(F_o^2)$]	0.1757
largest difference peak and hole	0.745 and -0.557 e Å ⁻³

^aObtained from least-squares refinement of 4863 reflections with $4.28^\circ < 2\theta < 44.68^\circ$.

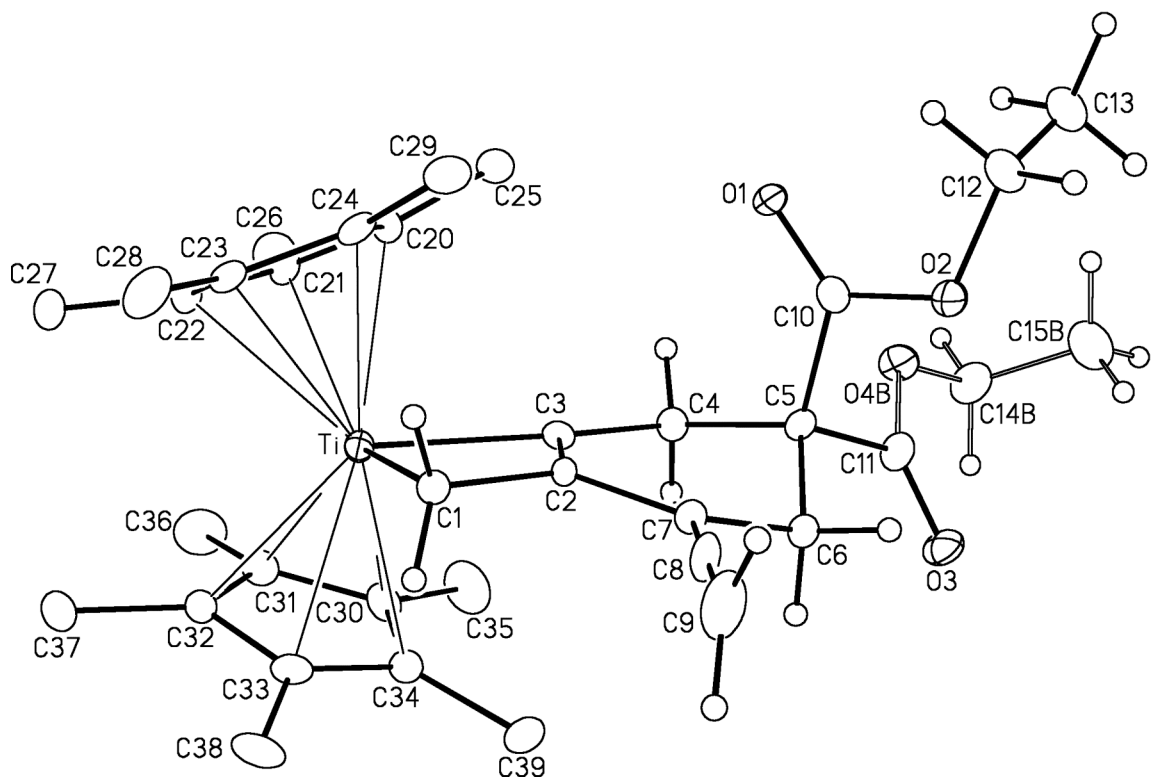
^bPrograms for diffractometer operation, data collection, data reduction and absorption correction were those supplied by Bruker.

^cSheldrick, G. M. *Acta Crystallogr.* **2008**, *A64*, 112–122.

^d $S = [\sum w(F_o^2 - F_c^2)^2 / (n - p)]^{1/2}$ (n = number of data; p = number of parameters varied; $w = [\sigma^2(F_o^2) + (0.0942P)^2]^{-1}$ where $P = [\text{Max}(F_o^2, 0) + 2F_c^2]/3$).

^e $R_1 = \sum ||F_o| - |F_c|| / \sum |F_o|$; $wR_2 = [\sum w(F_o^2 - F_c^2)^2 / \sum w(F_o^4)]^{1/2}$.

C. Report # JMS0909.



Crystallographic Experimental Details for Titanacyclobutene **148a**

A. *Crystal Data*

formula	C ₃₅ H ₄₈ O ₄ Ti
formula weight	580.63
crystal dimensions (mm)	0.63 × 0.21 × 0.02
crystal system	orthorhombic
space group	<i>Pna</i> 2 ₁ (No. 33)
unit cell parameters ^a	
<i>a</i> (Å)	21.163 (7)
<i>b</i> (Å)	16.803 (6)
<i>c</i> (Å)	8.799 (3)
<i>V</i> (Å ³)	3129.0 (19)
<i>Z</i>	4
ρ_{calcd} (g cm ⁻³)	1.233
μ (mm ⁻¹)	0.310

B. *Data Collection and Refinement Conditions*

diffractometer	Bruker D8/APEX II CCD ^b
radiation (λ [Å])	graphite-monochromated Mo K α (0.71073)
temperature (°C)	-100
scan type	ω scans (0.3°) (20 s exposures)

data collection 2θ limit (deg)	50.50
total data collected	21657 ($-25 \leq h \leq 25$, $-20 \leq k \leq 20$, $-10 \leq l \leq 10$)
independent reflections	5680 ($R_{\text{int}} = 0.1438$)
number of observed reflections (NO)	3476 [$F_o^2 \geq 2\sigma(F_o^2)$]
structure solution method	direct methods (<i>SHELXS-97</i> ^c)
refinement method	full-matrix least-squares on F^2 (<i>SHELXL-97</i> ^c)
absorption correction method	Gaussian integration (face-indexed)
range of transmission factors	0.9938–0.8298
data/restraints/parameters	5680 [$F_o^2 \geq -3\sigma(F_o^2)$] / 0 / 398
Flack absolute structure parameter ^d	–0.03(4)
goodness-of-fit (S) ^e	1.006 [$F_o^2 \geq -3\sigma(F_o^2)$]
final R indices ^f	
R_1 [$F_o^2 \geq 2\sigma(F_o^2)$]	0.0541
wR_2 [$F_o^2 \geq -3\sigma(F_o^2)$]	0.1060
largest difference peak and hole	0.288 and –0.255 e Å ⁻³

^aObtained from least-squares refinement of 4147 reflections with $4.84^\circ < 2\theta < 39.56^\circ$.

^bPrograms for diffractometer operation, data collection, data reduction and absorption correction were those supplied by Bruker.

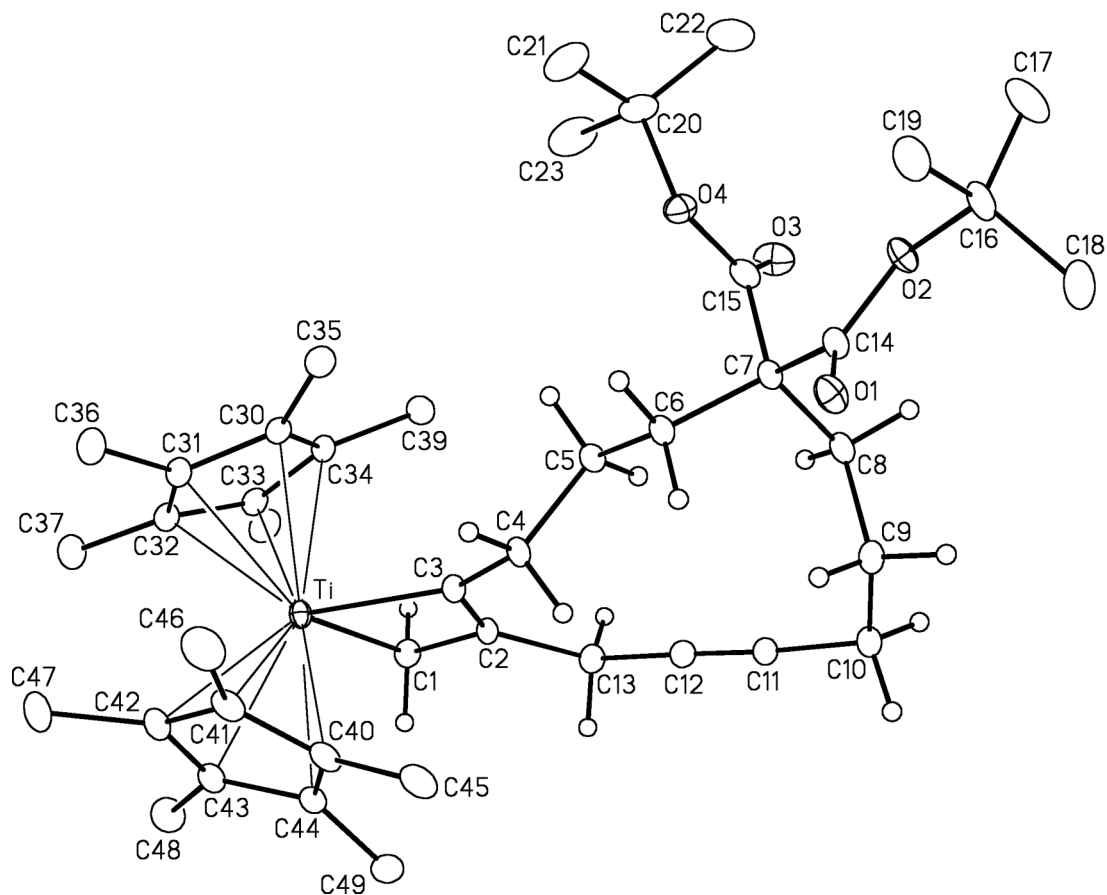
^cSheldrick, G. M. *Acta Crystallogr.* **2008**, *A64*, 112–122.

^dFlack, H. D. *Acta Crystallogr.* **1983**, *A39*, 876–881; Flack, H. D.; Bernardinelli, G. *Acta Crystallogr.* **1999**, *A55*, 908–915; Flack, H. D.; Bernardinelli, G. *J. Appl. Cryst.* **2000**, *33*, 1143–1148. The Flack parameter will refine to a value near zero if the structure is in the correct configuration and will refine to a value near one for the inverted configuration.

^e $S = [\sum w(F_o^2 - F_c^2)^2 / (n - p)]^{1/2}$ (n = number of data; p = number of parameters varied; $w = [\sigma^2(F_o^2) + (0.0325P)^2 + 0.3359P]^{-1}$ where $P = [\text{Max}(F_o^2, 0) + 2F_c^2] / 3$).

^f $R_1 = \sum ||F_o| - |F_c|| / \sum |F_o|$; $wR_2 = [\sum w(F_o^2 - F_c^2)^2 / \sum w(F_o^4)]^{1/2}$.

D. Report # JMS0854.



Crystallographic Experimental Details for Titanacyclobutene **155a**

A. Crystal Data

formula	C _{45.50} H ₇₀ O ₄ Ti
formula weight	728.92
crystal dimensions (mm)	0.33 × 0.27 × 0.02
crystal system	monoclinic
space group	<i>P</i> 2 ₁ / <i>c</i> (No. 14)
unit cell parameters ^a	
<i>a</i> (Å)	18.8700 (15)
<i>b</i> (Å)	13.8626 (11)
<i>c</i> (Å)	16.3507 (13)
β (deg)	96.8940 (10)
<i>V</i> (Å ³)	4246.2 (6)
<i>Z</i>	4
ρ _{calcd} (g cm ⁻³)	1.140
μ (mm ⁻¹)	0.241

B. Data Collection and Refinement Conditions

diffractometer	Bruker D8/APEX II CCD ^b
radiation (λ [Å])	graphite-monochromated Mo K α (0.71073)
temperature (°C)	-100
scan type	ω scans (0.3°) (30 s exposures)
data collection 2θ limit (deg)	50.50
total data collected	29676 ($-22 \leq h \leq 22$, $-16 \leq k \leq 16$, $-19 \leq l \leq 19$)
independent reflections	7699 ($R_{\text{int}} = 0.0996$)
number of observed reflections (NO)	4685 [$F_o^2 \geq 2\sigma(F_o^2)$]
structure solution method	direct methods (<i>SIR97</i> ^c)
refinement method	full-matrix least-squares on F^2 (<i>SHELXL-97</i> ^d)
absorption correction method	multi-scan (<i>SADABS</i>)
range of transmission factors	0.9952–0.9258
data/restraints/parameters	7699 [$F_o^2 \geq -3\sigma(F_o^2)$] / 15 ^e / 475
goodness-of-fit (S) ^f	1.032 [$F_o^2 \geq -3\sigma(F_o^2)$]
final R indices ^g	
R_1 [$F_o^2 \geq 2\sigma(F_o^2)$]	0.0614
wR_2 [$F_o^2 \geq -3\sigma(F_o^2)$]	0.1938
largest difference peak and hole	1.150 and -0.816 e Å ⁻³

^aObtained from least-squares refinement of 3953 reflections with $4.58^\circ < 2\theta < 41.50^\circ$.

^bPrograms for diffractometer operation, data collection, data reduction and absorption correction were those supplied by Bruker.

^cAltomare, A.; Burla, M. C.; Camalli, M.; Cascarano, G. L.; Giacovazzo, C.; Guagliardi, A.; Moliterni, A. G. G.; Polidori, G.; Spagna, R. *J. Appl. Cryst.* **1999**, *32*, 115–119.

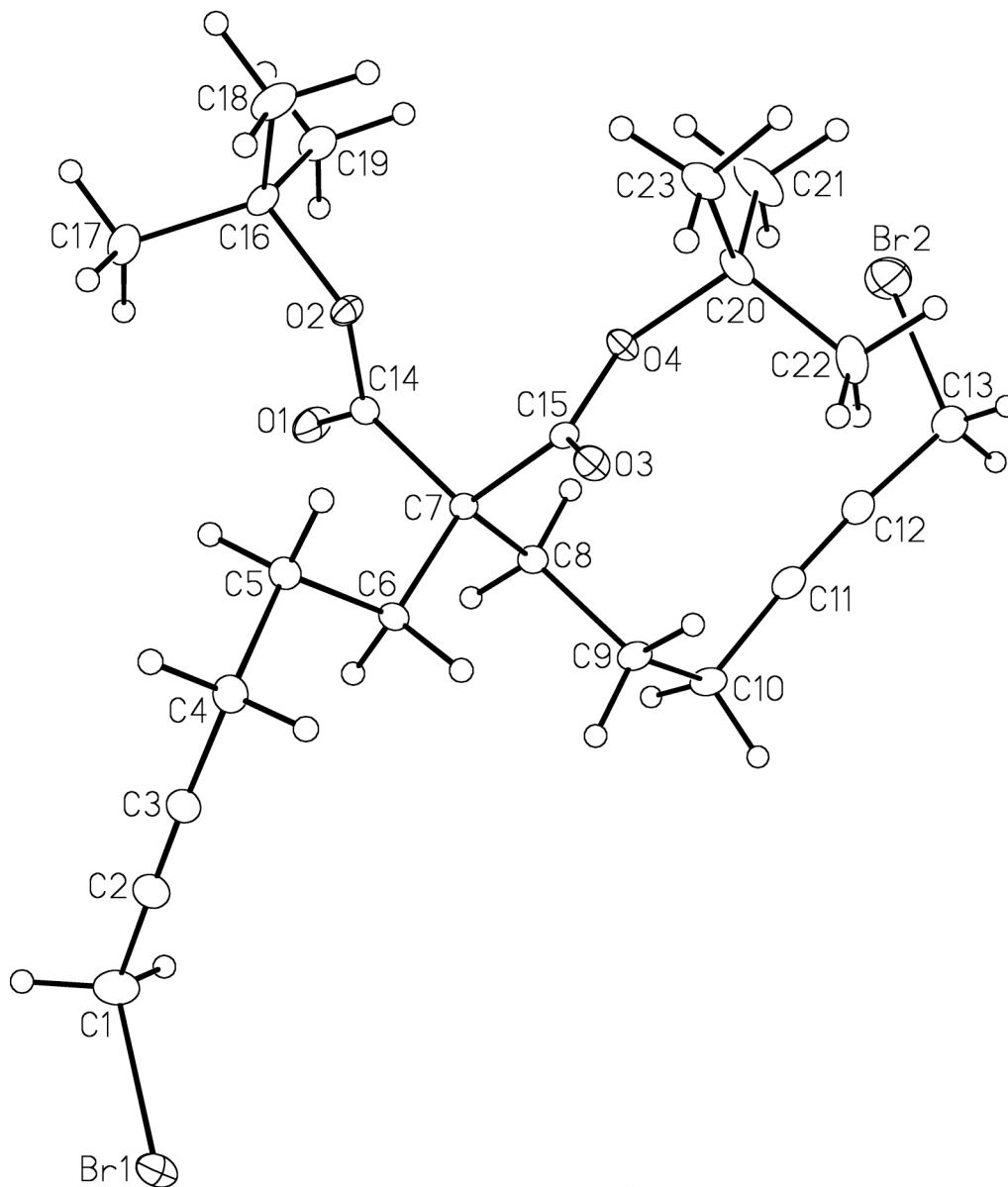
^dSheldrick, G. M. *Acta Crystallogr.* **2008**, *A64*, 112–122.

^eThe C–C and C...C distances within the disordered solvent pentane molecules were restrained to be 1.530(2) and 2.500(2) Å, respectively. Additionally, the C2S...C5S distance was restrained to be not less than 2.80(3) Å.

^f $S = [\sum w(F_o^2 - F_c^2)^2 / (n - p)]^{1/2}$ (n = number of data; p = number of parameters varied; $w = [\sigma^2(F_o^2) + (0.0965P)^2 + 2.8230P]^{-1}$ where $P = [\text{Max}(F_o^2, 0) + 2F_c^2]/3$).

^g $R_1 = \sum ||F_o| - |F_c|| / \sum |F_o|$; $wR_2 = [\sum w(F_o^2 - F_c^2)^2 / \sum w(F_o^4)]^{1/2}$.

E. Report # JMS0838.



Crystallographic Experimental Details for Malonate **136d**

A. Crystal Data

formula	$C_{23}H_{34}Br_2O_4$
formula weight	534.32
crystal dimensions (mm)	0.53 x 0.48 x 0.14
crystal system	triclinic
space group	$P\bar{1}$ (No. 2)
unit cell parameters ^a	
<i>a</i> (Å)	9.1808 (9)

b (Å)	10.1193 (10)
c (Å)	14.5188 (14)
α (deg)	71.7407 (11)
β (deg)	76.1738 (12)
γ (deg)	85.2861 (13)
V (Å ³)	1243.8 (2)
Z	2
ρ_{calcd} (g cm ⁻³)	1.427
μ (mm ⁻¹)	3.283

B. Data Collection and Refinement Conditions

diffractometer	Bruker D8/APEX II CCD ^b
radiation (λ [Å])	graphite-monochromated Mo K α (0.71073)
temperature (°C)	-100
scan type	ω scans (0.4°) (10 s exposures)
data collection 2θ limit (deg)	52.80
total data collected	9939 ($-11 \leq h \leq 11$, $-12 \leq k \leq 12$, $-18 \leq l \leq 18$)
independent reflections	5074 ($R_{\text{int}} = 0.0206$)
number of observed reflections (NO)	4149 [$F_o^2 \geq 2\sigma(F_o^2)$]
structure solution method	direct methods (<i>SIR97</i> ^c)
refinement method	full-matrix least-squares on F^2 (<i>SHELXL-97</i> ^{c,d})
absorption correction method	Gaussian integration (face-indexed)
range of transmission factors	0.6543–0.1891
data/restraints/parameters	5074 [$F_o^2 \geq -3\sigma(F_o^2)$] / 0 / 262
goodness-of-fit (S) ^e	1.025 [$F_o^2 \geq -3\sigma(F_o^2)$]
final R indices ^f	
R_1 [$F_o^2 \geq 2\sigma(F_o^2)$]	0.0342
wR_2 [$F_o^2 \geq -3\sigma(F_o^2)$]	0.0836
largest difference peak and hole	1.016 and -0.769 e Å ⁻³

^aObtained from least-squares refinement of 5827 reflections with $4.56^\circ < 2\theta < 54.84^\circ$.

^bPrograms for diffractometer operation, data collection, data reduction and absorption correction were those supplied by Bruker.

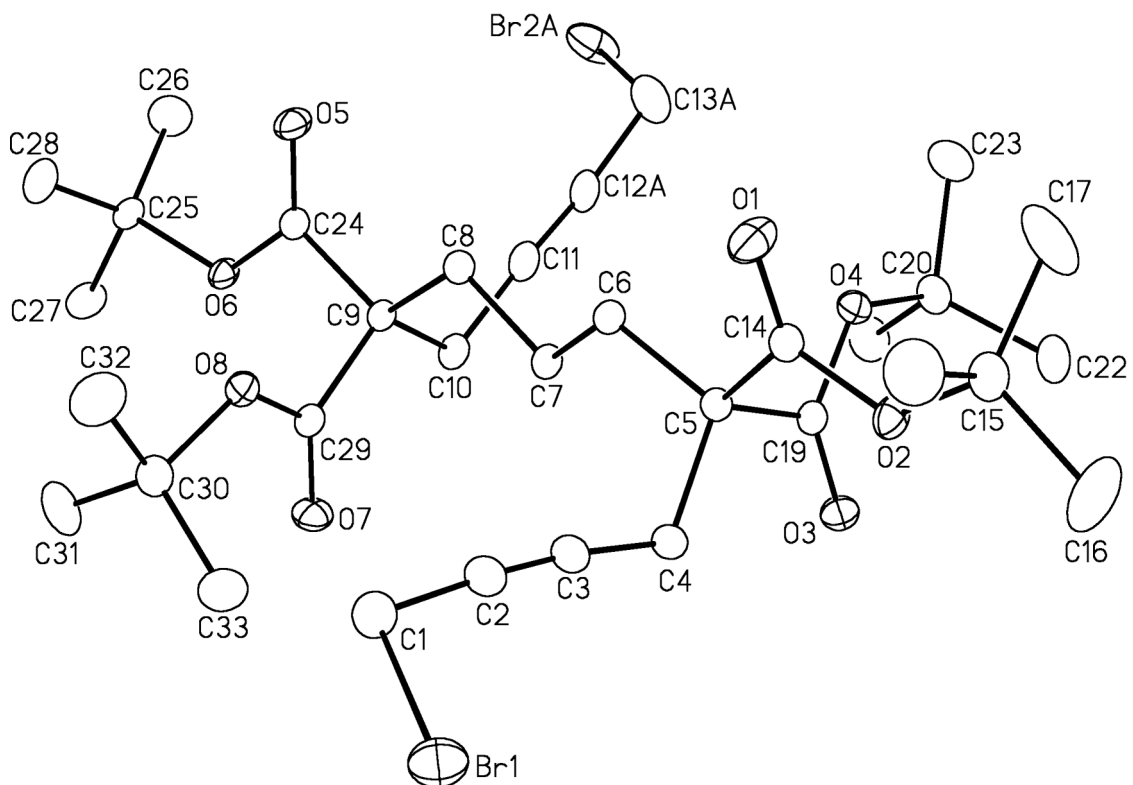
^cAltomare, A.; Burla, M. C.; Camalli, M.; Cascarano, G. L.; Giacovazzo, C.; Guagliardi, A.; Moliterni, A. G. G.; Polidori, G.; Spagna, R. *J. Appl. Cryst.* **1999**, *32*, 115–119.

^dSheldrick, G. M. *Acta Crystallogr.* **2008**, *A64*, 112–122.

^e $S = [\sum w(F_o^2 - F_c^2)^2 / (n - p)]^{1/2}$ (n = number of data; p = number of parameters varied; $w = [\sigma^2(F_o^2) + (0.0268P)^2 + 1.2856P]^{-1}$ where $P = [\text{Max}(F_o^2, 0) + 2F_c^2] / 3$).

^f $R_1 = \sum ||F_o| - |F_c|| / \sum |F_o|$; $wR_2 = [\sum w(F_o^2 - F_c^2)^2 / \sum w(F_o^4)]^{1/2}$.

F. Report # JMS0840.



Crystallographic Experimental Details for Malonate **146b**

A. Crystal Data

formula	C ₃₃ H ₅₀ Br ₂ O ₈
formula weight	734.55
crystal dimensions (mm)	0.60 × 0.59 × 0.37
crystal system	monoclinic
space group	<i>P</i> 2 ₁ / <i>n</i> (an alternate setting of <i>P</i> 2 ₁ / <i>c</i> [No. 14])
unit cell parameters ^a	
<i>a</i> (Å)	14.3841 (9)
<i>b</i> (Å)	10.9981 (7)
<i>c</i> (Å)	24.0670 (15)
β (deg)	95.3990 (10)
<i>V</i> (Å ³)	3790.5 (4)
<i>Z</i>	4
ρ _{calcd} (g cm ⁻³)	1.287
μ (mm ⁻¹)	2.181

B. Data Collection and Refinement Conditions

diffractometer Bruker D8/APEX II CCD^b

radiation (λ [Å])	graphite-monochromated Mo K α (0.71073)
temperature (°C)	-100
scan type	ω scans (0.3°) (20 s exposures)
data collection 2θ limit (deg)	54.98
total data collected	32304 ($-18 \leq h \leq 18, -14 \leq k \leq 14, -31 \leq l \leq 31$)
independent reflections	8670 ($R_{\text{int}} = 0.0257$)
number of observed reflections (NO)	6647 [$F_o^2 \geq 2\sigma(F_o^2)$]
structure solution method	direct methods (<i>SIR97</i> ^c)
refinement method	full-matrix least-squares on F^2 (<i>SHELXL-97</i> ^d)
absorption correction method	Gaussian integration (face-indexed)
range of transmission factors	0.5835–0.3479
data/restraints/parameters	8670 [$F_o^2 \geq -3\sigma(F_o^2)$] / 0 / 403
goodness-of-fit (S) ^e	1.017 [$F_o^2 \geq -3\sigma(F_o^2)$]
final R indices ^f	
R_1 [$F_o^2 \geq 2\sigma(F_o^2)$]	0.0397
wR_2 [$F_o^2 \geq -3\sigma(F_o^2)$]	0.1074
largest difference peak and hole	0.563 and -0.987 e Å ⁻³

^aObtained from least-squares refinement of 9975 reflections with $4.66^\circ < 2\theta < 52.46^\circ$.

^bPrograms for diffractometer operation, data collection, data reduction and absorption correction were those supplied by Bruker.

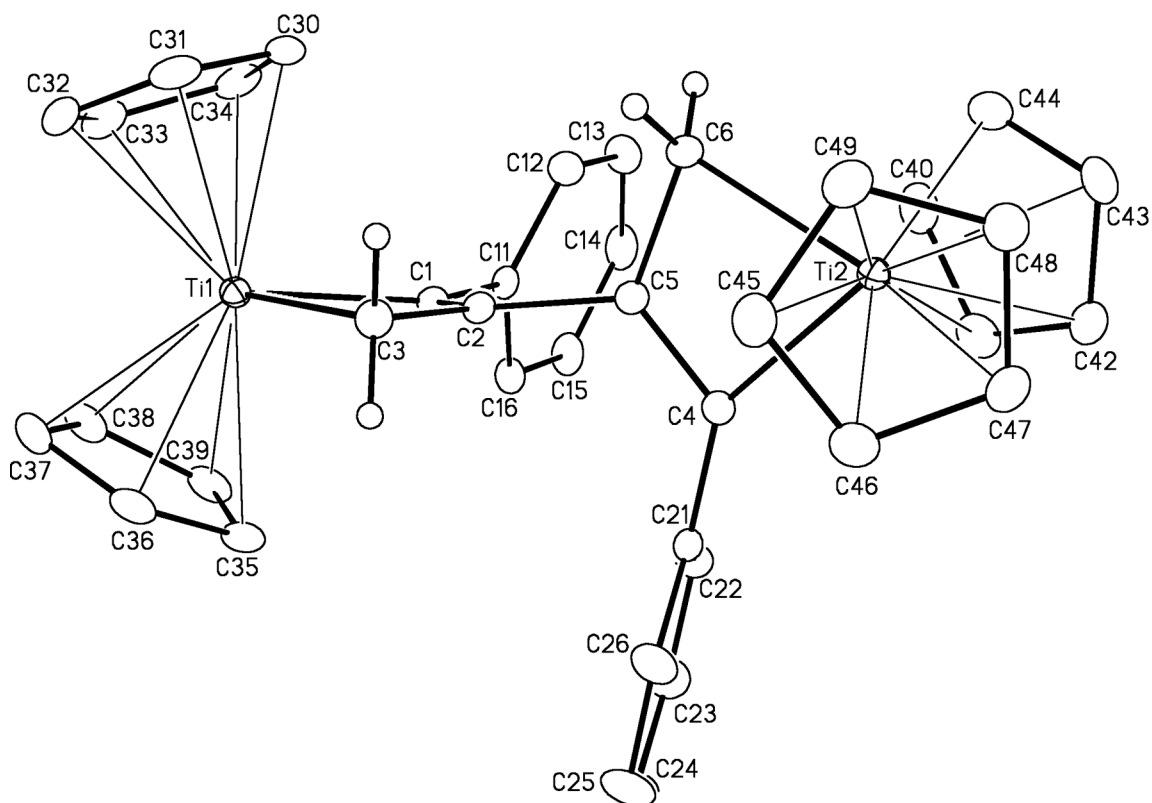
^cAltomare, A.; Burla, M. C.; Camalli, M.; Cascarano, G. L.; Giacovazzo, C.; Guagliardi, A.; Moliterni, A. G. G.; Polidori, G.; Spagna, R. *J. Appl. Cryst.* **1999**, *32*, 115–119.

^dSheldrick, G. M. *Acta Crystallogr.* **2008**, *A64*, 112–122.

^e $S = [\sum w(F_o^2 - F_c^2)^2 / (n - p)]^{1/2}$ (n = number of data; p = number of parameters varied; $w = [\sigma^2(F_o^2) + (0.0466P)^2 + 2.4154P]^{-1}$ where $P = [\text{Max}(F_o^2, 0) + 2F_c^2] / 3$).

^f $R_1 = \sum ||F_o| - |F_c|| / \sum |F_o|$; $wR_2 = [\sum w(F_o^2 - F_c^2)^2 / \sum w(F_o^4)]^{1/2}$.

G. Report # JMS0857.



Crystallographic Experimental Details for Ditanacyclobutene **162a**

A. Crystal Data

formula	C ₄₅ H ₄₂ Ti ₂
formula weight	678.59
crystal dimensions (mm)	0.40 × 0.25 × 0.19
crystal system	monoclinic
space group	<i>P</i> 2 ₁ / <i>c</i> (No. 14)
unit cell parameters ^a	
<i>a</i> (Å)	11.1838 (9)
<i>b</i> (Å)	35.677 (3)
<i>c</i> (Å)	9.4379 (7)
β (deg)	114.9315 (8)
<i>V</i> (Å ³)	3414.8 (5)
<i>Z</i>	4
ρ _{calcd} (g cm ⁻³)	1.320
μ (mm ⁻¹)	0.499

B. Data Collection and Refinement Conditions

diffractometer	Bruker D8/APEX II CCD ^b
radiation (λ [Å])	graphite-monochromated Mo Kα (0.71073)

temperature (°C)	−100
scan type	ω scans (0.3°) (25 s exposures)
data collection 2θ limit (deg)	52.88
total data collected	27175 ($-14 \leq h \leq 14$, $-44 \leq k \leq 44$, $-11 \leq l \leq 11$)
independent reflections	7006 ($R_{\text{int}} = 0.0266$)
number of observed reflections (NO)	6000 [$F_o^2 \geq 2\sigma(F_o^2)$]
structure solution method	direct methods (<i>SIR97</i> ^c)
refinement method	full-matrix least-squares on F^2 (<i>SHELXL-97</i> ^d)
absorption correction method	numerical (<i>SADABS</i>)
range of transmission factors	0.9115–0.8264
data/restraints/parameters	7006 [$F_o^2 \geq -3\sigma(F_o^2)$] / 0 / 425
goodness-of-fit (S) ^e	1.089 [$F_o^2 \geq -3\sigma(F_o^2)$]
final R indices ^f	
R_1 [$F_o^2 \geq 2\sigma(F_o^2)$]	0.0349
wR_2 [$F_o^2 \geq -3\sigma(F_o^2)$]	0.1014
largest difference peak and hole	0.300 and -0.273 e Å ⁻³

^aObtained from least-squares refinement of 9914 reflections with $4.62^\circ < 2\theta < 52.70^\circ$.

^bPrograms for diffractometer operation, data collection, data reduction and absorption correction were those supplied by Bruker.

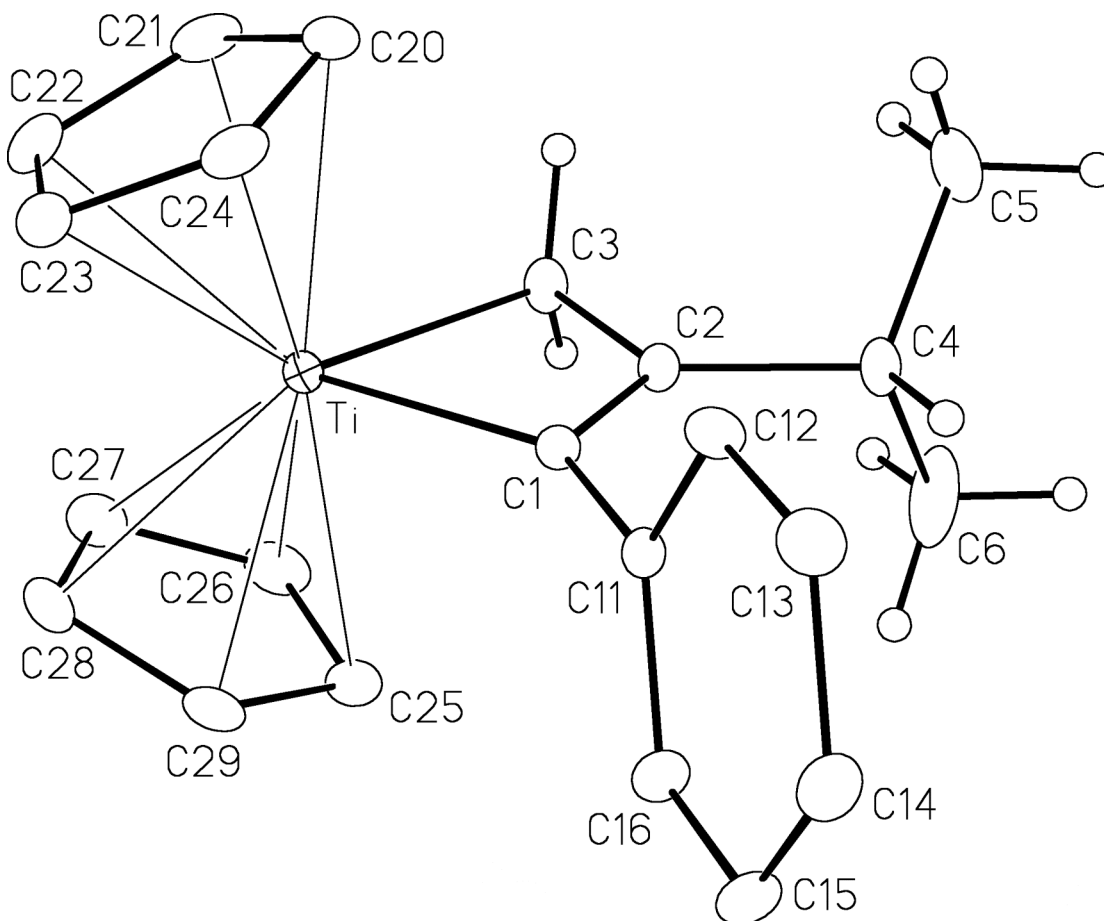
^cAltomare, A.; Burla, M. C.; Camalli, M.; Cascarano, G. L.; Giacovazzo, C.; Guagliardi, A.; Moliterni, A. G. G.; Polidori, G.; Spagna, R. *J. Appl. Cryst.* **1999**, *32*, 115–119.

^dSheldrick, G. M. *Acta Crystallogr.* **2008**, *A64*, 112–122.

^e $S = [\sum w(F_o^2 - F_c^2)^2 / (n - p)]^{1/2}$ (n = number of data; p = number of parameters varied; $w = [\sigma^2(F_o^2) + (0.0490P)^2 + 1.6759P]^{-1}$ where $P = [\text{Max}(F_o^2, 0) + 2F_c^2] / 3$).

^f $R_1 = \sum ||F_o| - |F_c|| / \sum |F_o|$; $wR_2 = [\sum w(F_o^2 - F_c^2)^2 / \sum w(F_o^4)]^{1/2}$.

H. Report # JMS0908.



Crystallographic Experimental Details for Titanacyclobutene **163**

A. Crystal Data

formula	C ₂₂ H ₂₄ Ti
formula weight	336.31
crystal dimensions (mm)	0.45 × 0.34 × 0.24
crystal system	triclinic
space group	<i>P</i> $\bar{1}$ (No. 2)
unit cell parameters ^a	
<i>a</i> (Å)	8.196 (3)
<i>b</i> (Å)	9.338 (3)
<i>c</i> (Å)	12.585 (4)
<i>α</i> (deg)	98.963 (3)
<i>β</i> (deg)	106.739 (3)
<i>γ</i> (deg)	99.146 (4)
<i>V</i> (Å ³)	889.7 (5)
<i>Z</i>	2
<i>ρ</i> _{calcd} (g cm ⁻³)	1.255

μ (mm ⁻¹)	0.478
<i>B. Data Collection and Refinement Conditions</i>	
diffractometer	Bruker D8/APEX II CCD ^b
radiation (λ [Å])	graphite-monochromated Mo K α (0.71073)
temperature (°C)	-100
scan type	ω scans (0.4°) (10 s exposures)
data collection 2θ limit (deg)	55.32
total data collected	7815 ($-10 \leq h \leq 10$, $-12 \leq k \leq 12$, $-16 \leq l \leq 16$)
independent reflections	4055 ($R_{\text{int}} = 0.0186$)
number of observed reflections (NO)	3589 [$F_o^2 \geq 2\sigma(F_o^2)$]
structure solution method	Patterson/structure expansion (<i>DIRDIF-2008</i> ^c)
refinement method	full-matrix least-squares on F^2 (<i>SHELXL-97</i> ^d)
absorption correction method	Gaussian integration (face-indexed)
range of transmission factors	0.8930–0.8125
data/restraints/parameters	4055 [$F_o^2 \geq -3\sigma(F_o^2)$] / 0 / 208
goodness-of-fit (S) ^e	1.070 [$F_o^2 \geq -3\sigma(F_o^2)$]
final R indices ^f	
R_1 [$F_o^2 \geq 2\sigma(F_o^2)$]	0.0333
wR_2 [$F_o^2 \geq -3\sigma(F_o^2)$]	0.0917
largest difference peak and hole	0.278 and -0.244 e Å ⁻³

^aObtained from least-squares refinement of 4719 reflections with $5.08^\circ < 2\theta < 55.32^\circ$.

^bPrograms for diffractometer operation, data collection, data reduction and absorption correction were those supplied by Bruker.

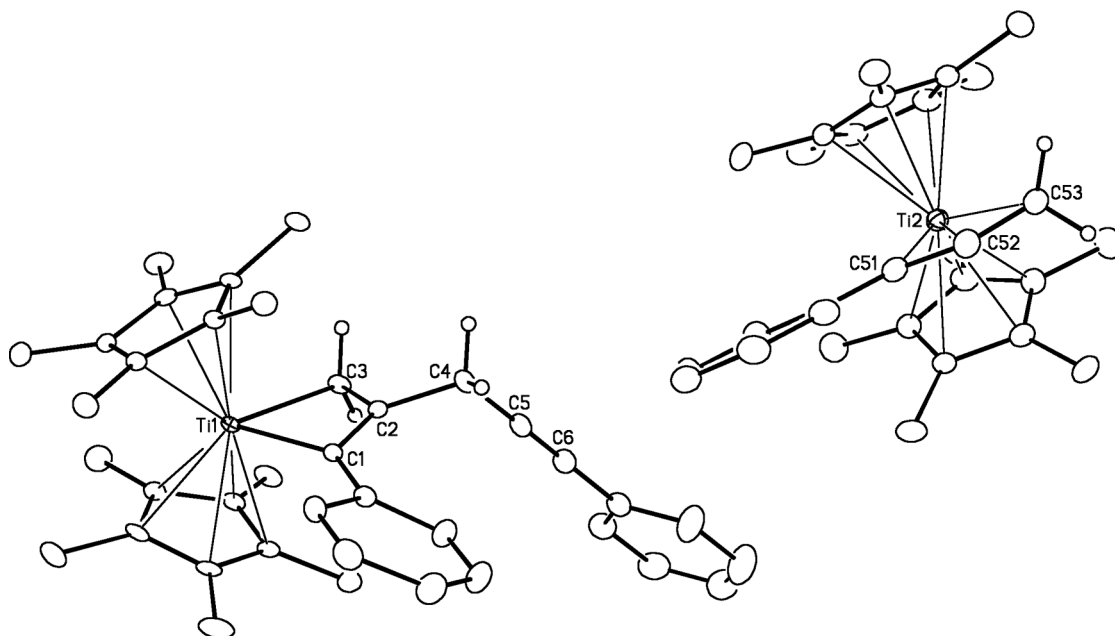
^cBeurskens, P. T.; Beurskens, G.; de Gelder, R.; Smits, J. M. M.; Garcia-Granda, S.; Gould, R. O. (2008). The *DIRDIF-2008* program system. Crystallography Laboratory, Radboud University Nijmegen, The Netherlands.

^dSheldrick, G. M. *Acta Crystallogr.* **2008**, *A64*, 112–122.

^e $S = [\sum w(F_o^2 - F_c^2)^2 / (n - p)]^{1/2}$ (n = number of data; p = number of parameters varied; $w = [\sigma^2(F_o^2) + (0.0467P)^2 + 0.2314P]^{-1}$ where $P = [\text{Max}(F_o^2, 0) + 2F_c^2]/3$).

^f $R_1 = \sum |F_o| - |F_c| / \sum |F_o|$; $wR_2 = [\sum w(F_o^2 - F_c^2)^2 / \sum w(F_o^4)]^{1/2}$.

I. Report # JMS0938.



Crystallographic Experimental Details for Co-Crystallite **161c** and **175**

A. Crystal Data

formula	$C_{67}H_{81}Ti_2$
formula weight	982.12
crystal dimensions (mm)	$0.58 \times 0.20 \times 0.03$
crystal system	monoclinic
space group	$P2_1/n$ (an alternate setting of $P2_1/c$ [No. 14])
unit cell parameters ^a	
a (Å)	10.1251 (10)
b (Å)	38.713 (4)
c (Å)	14.0094 (14)
β (deg)	93.548 (2)
V (Å ³)	5480.8 (10)
Z	4
ρ_{calcd} (g cm ⁻³)	1.190
μ (mm ⁻¹)	0.331

B. Data Collection and Refinement Conditions

diffractometer	Bruker D8/APEX II CCD ^b
radiation (λ [Å])	graphite-monochromated Mo $K\alpha$ (0.71073)
temperature (°C)	-100
scan type	ω scans (0.3°) (60 s exposures)
data collection 2θ limit (deg)	50.50
total data collected	38640 ($-12 \leq h \leq 12$, $-46 \leq k \leq 46$, $-16 \leq l \leq 16$)

independent reflections	9910 ($R_{\text{int}} = 0.0955$)
number of observed reflections (NO)	6193 [$F_o^2 \geq 2\sigma(F_o^2)$]
structure solution method	direct methods (<i>SHELXS-97</i> ^c)
refinement method	full-matrix least-squares on F^2 (<i>SHELXL-97</i> ^c)
absorption correction method	Gaussian integration (face-indexed)
range of transmission factors	0.9895–0.8297
data/restraints/parameters	9910 [$F_o^2 \geq -3\sigma(F_o^2)$] / 0 / 642
goodness-of-fit (S) ^d	1.079 [$F_o^2 \geq -3\sigma(F_o^2)$]
final R indices ^e	
R_1 [$F_o^2 \geq 2\sigma(F_o^2)$]	0.0622
wR_2 [$F_o^2 \geq -3\sigma(F_o^2)$]	0.1843
largest difference peak and hole	0.496 and -0.502 e \AA^{-3}

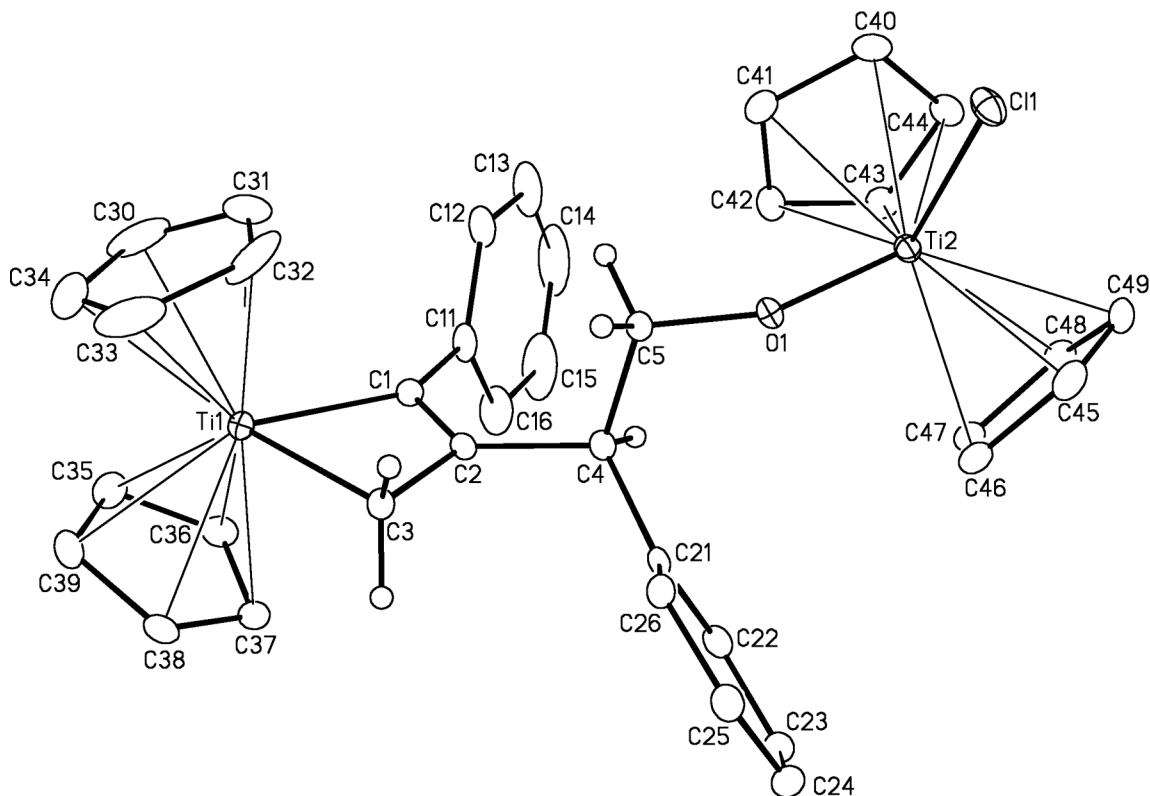
^aObtained from least-squares refinement of 6301 reflections with $4.54^\circ < 2\theta < 43.98^\circ$.

^bPrograms for diffractometer operation, data collection, data reduction and absorption correction were those supplied by Bruker.

^cSheldrick, G. M. *Acta Crystallogr.* **2008**, *A64*, 112–122.

^d $S = [\sum w(F_o^2 - F_c^2)^2 / (n - p)]^{1/2}$ (n = number of data; p = number of parameters varied; $w = [\sigma^2(F_o^2) + (0.0664P)^2 + 9.9395P]^{-1}$ where $P = [\text{Max}(F_o^2, 0) + 2F_c^2]/3$).

^e $R_1 = \sum ||F_o| - |F_c|| / \sum |F_o|$; $wR_2 = [\sum w(F_o^2 - F_c^2)^2 / \sum w(F_o^4)]^{1/2}$.



Crystallographic Experimental Details for Titanacyclobutene **169a**

A. Crystal Data

formula	$C_{37}H_{35}ClOTi_2$
formula weight	626.9
crystal dimensions (mm)	$0.48 \times 0.14 \times 0.10$
crystal system	monoclinic
space group	$P2_1/c$ (No. 14)
unit cell parameters ^a	
<i>a</i> (Å)	11.514 (2)
<i>b</i> (Å)	28.360 (5)
<i>c</i> (Å)	18.560 (3)
β (deg)	90.562 (3)
<i>V</i> (Å ³)	6060.2 (19)
<i>Z</i>	8
ρ_{calcd} (g cm ⁻³)	1.374
μ (mm ⁻¹)	0.644

B. Data Collection and Refinement Conditions

diffractometer	Bruker D8/APEX II CCD ^b
----------------	------------------------------------

radiation (λ [Å])	graphite-monochromated Mo K α (0.71073)
temperature (°C)	-100
scan type	ω scans (0.3°) (30 s exposures)
data collection 2θ limit (deg)	50.50
total data collected	42800 ($-13 \leq h \leq 13, -34 \leq k \leq 34, -22 \leq l \leq 22$)
independent reflections	10972 ($R_{\text{int}} = 0.0622$)
number of observed reflections (NO)	7992 [$F_o^2 \geq 2\sigma(F_o^2)$]
structure solution method	direct methods (<i>SHELXS-97</i> ^c)
refinement method	full-matrix least-squares on F^2 (<i>SHELXL-97</i> ^c)
absorption correction method	numerical (<i>SADABS</i>)
range of transmission factors	0.9408–0.7466
data/restraints/parameters	10972 [$F_o^2 \geq -3\sigma(F_o^2)$] / 0 / 739
goodness-of-fit (S) ^d	1.014 [$F_o^2 \geq -3\sigma(F_o^2)$]
final R indices ^e	
R_1 [$F_o^2 \geq 2\sigma(F_o^2)$]	0.0422
wR_2 [$F_o^2 \geq -3\sigma(F_o^2)$]	0.1091
largest difference peak and hole	0.457 and -0.422 e Å ⁻³

^aObtained from least-squares refinement of 8656 reflections with $4.38^\circ < 2\theta < 45.82^\circ$.

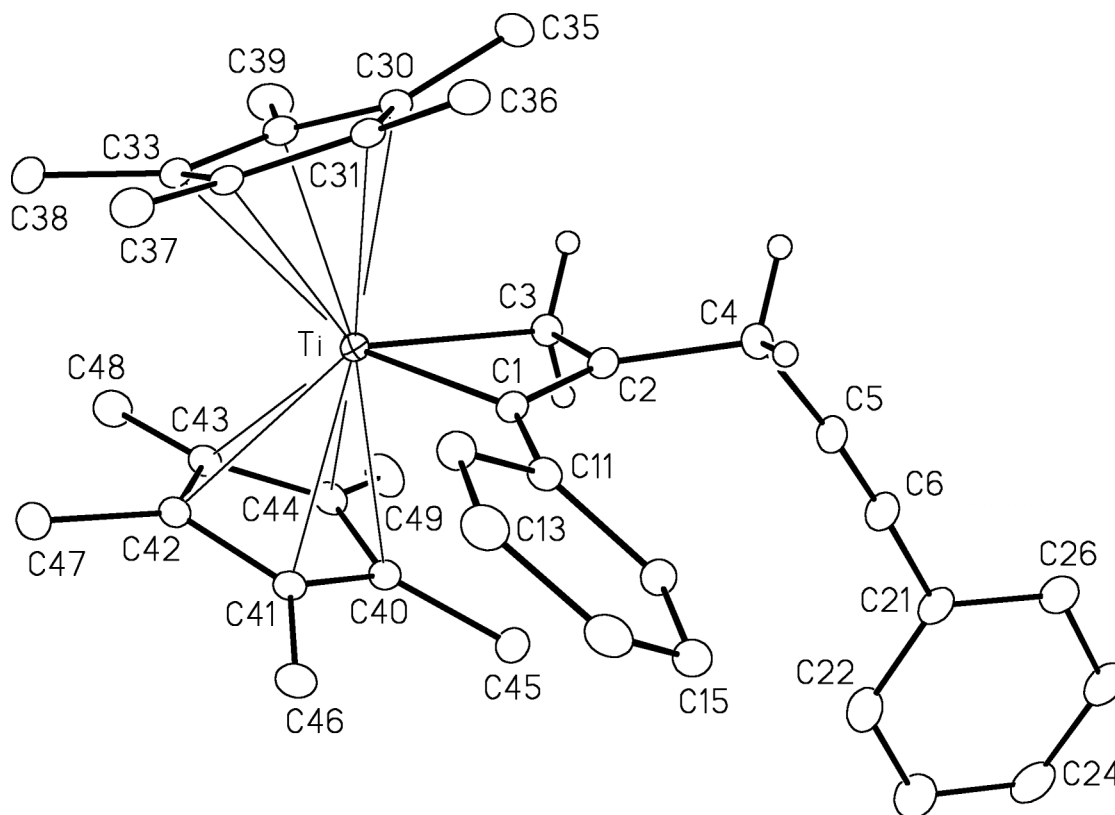
^bPrograms for diffractometer operation, data collection, data reduction and absorption correction were those supplied by Bruker.

^cSheldrick, G. M. *Acta Crystallogr.* **2008**, *A64*, 112–122.

^d $S = [\sum w(F_o^2 - F_c^2)^2 / (n - p)]^{1/2}$ (n = number of data; p = number of parameters varied; $w = [\sigma^2(F_o^2) + (0.0433P)^2 + 6.0491P]^{-1}$ where $P = [\text{Max}(F_o^2, 0) + 2F_c^2] / 3$).

^e $R_1 = \sum ||F_o| - |F_c|| / \sum |F_o|$; $wR_2 = [\sum w(F_o^2 - F_c^2)^2 / \sum w(F_o^4)]^{1/2}$.

K. Report # JMS0911.



Crystallographic Experimental Details for Titanacyclobutene **175**.

A. Crystal Data

formula	C ₃₈ H ₄₄ Ti
formula weight	548.63
crystal dimensions (mm)	0.61 × 0.44 × 0.30
crystal system	monoclinic
space group	<i>P</i> 2 ₁ / <i>c</i> (No. 14)
unit cell parameters ^a	
<i>a</i> (Å)	16.6487 (8)
<i>b</i> (Å)	17.3689 (9)
<i>c</i> (Å)	10.9951 (5)
β (deg)	108.3236 (6)
<i>V</i> (Å ³)	3018.2 (3)
<i>Z</i>	4
ρ _{calcd} (g cm ⁻³)	1.207
μ (mm ⁻¹)	0.308

B. Data Collection and Refinement Conditions

diffractometer	Bruker D8/APEX II CCD ^b
radiation (λ [Å])	graphite-monochromated Mo K α (0.71073)
temperature (°C)	−100
scan type	ω scans (0.3°) (15 s exposures)
data collection 2θ limit (deg)	55.02
total data collected	26165 ($-21 \leq h \leq 21$, $-22 \leq k \leq 22$, $-14 \leq l \leq 14$)
independent reflections	6920 ($R_{\text{int}} = 0.0215$)
number of observed reflections (NO)	6091 [$F_o^2 \geq 2\sigma(F_o^2)$]
structure solution method	Patterson/structure expansion (<i>DIRDIF-2008</i> ^c)
refinement method	full-matrix least-squares on F^2 (<i>SHELXL-97</i> ^d)
absorption correction method	Gaussian integration (face-indexed)
range of transmission factors	0.9143–0.8334
data/restraints/parameters	6920 [$F_o^2 \geq -3\sigma(F_o^2)$] / 0 / 362
goodness-of-fit (S) ^e	1.026 [$F_o^2 \geq -3\sigma(F_o^2)$]
final R indices ^f	
R_1 [$F_o^2 \geq 2\sigma(F_o^2)$]	0.0364
wR_2 [$F_o^2 \geq -3\sigma(F_o^2)$]	0.1037
largest difference peak and hole	0.319 and −0.340 e Å ^{−3}

^aObtained from least-squares refinement of 9852 reflections with $4.56^\circ < 2\theta < 54.94^\circ$.

^bPrograms for diffractometer operation, data collection, data reduction and absorption correction were those supplied by Bruker.

^cBeurskens, P. T.; Beurskens, G.; de Gelder, R.; Smits, J. M. M; Garcia-Granda, S.; Gould, R. O. (2008). The *DIRDIF-2008* program system. Crystallography Laboratory, Radboud University Nijmegen, The Netherlands.

^dSheldrick, G. M. *Acta Crystallogr.* **2008**, *A64*, 112–122.

^e $S = [\sum w(F_o^2 - F_c^2)^2 / (n - p)]^{1/2}$ (n = number of data; p = number of parameters varied; $w = [\sigma^2(F_o^2) + (0.0536P)^2 + 1.3680P]^{-1}$ where $P = [\text{Max}(F_o^2, 0) + 2F_c^2] / 3$).

^f $R_1 = \sum ||F_o| - |F_c|| / \sum |F_o|$; $wR_2 = [\sum w(F_o^2 - F_c^2)^2 / \sum w(F_o^4)]^{1/2}$.

References and notes

- (1) (a) Beck, A. L. *Tetrahedron* **1981**, *37*, 3073-3100; (b) Beck, A. L.; Schiesser, C. H. *Tetrahedron* **1985**, *41*, 3925-3941; (c) Spellmeyer, D. C.; Houk, K. N. *J. Org. Chem.* **1987**, *52*, 959-974.
- (2) Roxburgh, C. J. *Tetrahedron* **1995**, *51*, 9767-9822.
- (3) Sandeep, H. and Pattenden, G. *Contemp. Org. Synth.* **1997**, *4*, 196-215.
- (4) Faraco, R. F. P.; Pires, M. C.; Rocha, A. P. C.; Prado, M. A. F. *Quim. Nova.* **2008**, *31*, 1499-1513.
- (5) For examples of macrocycles by photochemical methods see: (a) Abad, S.; Bosca, Griesbeck, A. G.; Henz, A.; Kramer, W.; Lex, J.; Nerowski, F.; Oelgemöller, M. *Helv. Chim. Acta* **1997**, *80*, 912-933; (b) Griesbeck, A. G. *Chimia*, **1998**, *52*, 272-283; (c) Xue, J.; Zhu, L.; Fun, H.-K.; Xu, J.-H. *Tetrahedron Lett.* **2000**, *41*, 8553-8557; (d) Griesbeck, A. G.; Oelgemöller, M.; Lex, J. *J. Org. Chem.* **2000**, *65*, 9028-9032; (e) Yoo, D. J.; Kim, E. Y.; Oelgemöller, M. *Photochem. Photobiol. Sci.* **2004**, *3*, 311-316; (f) Abad, S.; Bosca, F.; Domingo, L. R.; Gil, S.; Pischel, U.; Miranda, M. A. *J. Am. Chem. Soc.* **2007**, *129*, 7407-7420.
- (6) For examples of transannular cyclization from macrocyclic radical intermediates see: (a) Hitchcock, S. A. and Pattenden, G. *Tetrahedron Lett.* **1992**, *33*, 4843-4846 (corrigendum; *Tetrahedron Lett.* **1992**, *33*, 7448.); (b) Pattenden, G.; Smithies, A. J.; Walkter, D. S. *Tetrahedron Lett.* **1994**, *35*, 2413-2416; (c) Jahn, U. and Curran, D. P. *Tetrahedron Lett.* **1995**, *36*, 8921-8924; (d) Pattenden, G.; Smithies, A. J.; Tapolczay, D.; Walkter, D. S. *J. Chem. Soc., Perkin Trans. 1* **1995**, 7-19; (e) Houldsworth, S. J.; Pattenden, G.; Pryde, D. C.; Thomson, N. M. *J. Chem. Soc., Perkin Trans. 1* **1997**, 1091-1093; (f) Hitchcock, S. A.; Houldsworth, S. J.; Pattenden, G.; Pryde, D. C.; Thomson, N. M.; Blake, A. J. *J. Chem. Soc., Perkin Trans. 1* **1998**, 3181-3206.
- (7) Walton, J. C. "Unusual Radical Cyclizations" in *Topics in Current Chemistry* **2006**, Springer, Berlin.
- (8) Porter, N. A.; Magnin, D. R.; Wright, B. T. *J. Am. Chem. Soc.* **1986**, *108*, 2787-2788.
- (9) Porter, N. A. and Chang, V. H.-T. *J. Am. Chem. Soc.* **1987**, *109*, 4976-4981.

- (10) Porter, N. A.; Chang, V. H.-T.; Magnin, D. R.; Wright, B. T. *J. Am. Chem. Soc.* **1988**, *110*, 3554-3560.
- (11) Porter, N. A.; Lacher, B.; Chang, V. H.-T.; Magnin, J. *Am. Chem. Soc.* **1989**, *111*, 8309-8310.
- (12) (a) Feldman, K. S. and Lee, Y. B. *J. Am. Chem. Soc.* **1987**, *109*, 5850-5851; (b) Feldman, K. S.; Bobo, J. S.; Tewalt, G. L. *J. Org. Chem.* **1992**, *57*, 4573-4574.
- (13) Scott, D. M.; McPhail, A. T.; Porter, N. A. *J. Org. Chem.* **1993**, *58*, 1178-1186.
- (14) (a) Miracle, G. S.; Cannizzaro, S. M.; Porter, N. A. *J. Am. Chem. Soc.* **1992**, *114*, 9683-9685; (b) Porter, N. A.; Miracle, G. S.; Cannizzaro, S. M.; Carter, R. L.; McPhail, A. T.; Liu, L. *J. Am. Chem. Soc.* **1994**, *116*, 10255-10266.
- (15) Ingold, K. U.; Luszyk, J.; Scaiano, J. C. *J. Am. Chem. Soc.* **1984**, *106*, 343-348.
- (16) (a) Baldwin, J. E.; Adlington, R. M.; Mitchell, M. B.; Robertson, J. *J. Chem. Soc., Chem. Commun.* **1990**, 1574-1575; (b) Baldwin, J. E.; Adlington, R. M.; Mitchell, M. B.; Robertson, J. *Tetrahedron* **1991**, *47*, 5901-5918.
- (17) Barth, F. and O-Yang, C. *Tetrahedron Lett.* **1990**, *31*, 1121-1124.
- (18) Chambers, R. D. *Fluorine in Organic Chemistry* **2004**, Wiley-Interscience, New York.
- (19) (a) Oki, M. and Nakanishi, H. *Bull. Chem. Soc. Jpn.* **1970**, *43*, 2558-2566; (b) Fisher, H.; Wu, L. M. *Helv. Chim. Acta* **1983**, *66*, 138-147; (c) Beckwith, A. L. J. and Glover, S. A. *Aust. J. Chem.* **1987**, *40*, 157-173; (d) Wiberg, K. B. and Wong, M. W. *J. Am. Chem. Soc.* **1993**, *115*, 1078-1084.
- (20) (a) Troyansky, E. I.; Ismagilov, R. F.; Strelenko, Y. A.; Samoshin, V.V.; Demchuk, D. V.; Nikishin, G. I.; Lindeman, S. V.; Khrustalyov, V. N.; Struchkov, Y. T. *Tetrahedron Lett.* **1995**, *36*, 2293-2294; (b) Troyansky, E. I.; Ismagilov, R. F.; Samoshin, V.V.; Strelenko, Y. A.; Demchuk, D. V.; Nikishin, G. I.; Lindeman, S. V.; Khrustalyov, V. N.; Struchkov, Y. T. *Tetrahedron* **1995**, *51*, 11431-11444.
- (21) Ryu, I.; Nagahar, K.; Yamazaki, H.; Tsunoi, S.; Sonoda, N. *Synlett.* **1994**, 643-645.
- (22) Macrocyclization *via* acyl radicals have also been generated from phenyl selenoesters: Boger, D. L.; and Mathvink, R. J. *J. Am. Chem. Soc.* **1990**, *112*, 4008-4011.

- (23) (Ni) Boivin, J.; Yousfi, M.; Zard, S. Z. *Tetrahedron Lett.* **1994**, *35*, 5629-5632; (Ru, Fe) Iqbal, J.; Bhatia, B.; Nayyar, N. K. *Chem. Rev.* **1994**, *94*, 519-564.
- (24) Clark, A. J. *Chem. Soc. Rev.* **2002**, *31*, 1-11.
- (25) De Campo, F.; Lastécouères, D.; Verlhac, J.-B. *J. Chem. Soc., Perkin Trans. 1* **2000**, 575-580.
- (26) Curran, D. P. and Seong, C. M. *J. Am. Chem. Soc.* **1990**, *112*, 9401-9403.
- (27) Curran reported a systematic study using this methodology: Curran, D. P. and Seong, C. M. *Synlett.* **1991**, 107-108.
- (28) Gerlach, U. *Tetrahedron Lett.* **1995**, *36*, 5159-5162.
- (29) (a) Li, C.-J. and Chan, T.-H. *Organic Reactions in Aqueous Media*; John Wiley & Sons: New York, **1997**; (b) Grieco, P. A. *Organic Synthesis in Water*; Blackie Academic & Professional, London, **1998**; (c) Lubineau, A. and Auge, J. In *Modern Solvents in Organic Synthesis*; Knochel, P., Ed.; Springer-Verlag: Berlin Heidelberg, **1999**; (d) Li, C.-J. *Chem Rev.* **1993**, *93*, 2023-2035.
- (30) Yorimitsu, H.; Nakamura, T.; Shinokubo, H.; Oshima, K.; Omoto, K.; Fujimoto, H. *J. Am. Chem. Soc.* **2000**, *122*, 11041-11047.
- (31) For anionic and cationic methods see: (a) Yokota, K.; Matsumura, M.; Yamaguchi, K.; Takada, Y. *Makromol. Chem. Rapid Commun.* **1983**, *4*, 721-724; (b) Longone, D. T. and Glatzhofer, D. T. *J. Polym. Sci., Part A: Polym. Chem.* **1986**, *24*, 1725-1733; (c) Hashimoto, T. and Kodaira, T. *J. Polym. Sci., Part A: Polym. Chem.* **2003**, *41*, 281-292; (d) Hashimoto, T.; Watanabe, K.; Kodaira, T. *J. Polym. Sci., Part A: Polym. Chem.* **2004**, *42*, 3373-3379; (e) Sakai, R.; Satoh, T.; Kakuchi, R.; Kaga, H.; Kakuchi, T. *Macromolecules*, **2004**, *37*, 3996-4003; For metal-catalyzed see: (f) Sanda, F.; Kawano, T.; Masuda, T. *Polym. Bull.* **2005**, *55*, 341-347.
- (32) Ochiai, B.; Ootani, Y.; Endo, T. *J. Am. Chem. Soc.* **2008**, *130*, 10832-10833.
- (33) Costa, A. I.; Barata, P. D.; Prata, J. V. *React. Funct. Polym.* **2005**, *38*, 465-470.
- (34) Intramolecular macrocyclization of benzyl radicals on styrene have been reported: Shea, K. J.; O'Dell R.; Sasaki, D. Y. *Tetrahedron Lett.* **1992**, *33*, 4699-4702.
- (35) Jasperse, C. P.; Curran, D. P.; Fevig, T. L. *Chem. Rev.* **1991**, *91*, 1237-1286.

- (36) (a) Stork, G. and Baine, N. H. *J. Am. Chem. Soc.* **1982**, *104*, 2321-2323; (b) Stork, G. and Mook, R. *J. Am. Chem. Soc.* **1983**, *105*, 3720-3722; (c) Stork, G.; Mook, R.; Biller, S. A. (Jr.); Rychovsky, S. D. *J. Am. Chem. Soc.* **1983**, *105*, 3741-3742; (d) Stork, G. and Baine, N. H. *Tetrahedron Lett.* **1985**, *26*, 5927-5930; (e) Stork, G. and Mook, R. *Tetrahedron Lett.* **1986**, *27*, 4529-4532; (f) Stork, G.; Sher, P. M.; Chen, H.-L. *J. Am. Chem. Soc.* **1986**, *108*, 6384-6385.
- (37) Weinstock, J.; Hieble, J. P.; Wilson, J. W. *Drugs Future*, **1985**, *10*, 646-697.
- (38) (a) Lamas, C.; Saá, C.; Castedo, L.; Domínguez, D. *Tetrahedron Lett.* **1992**, *33*, 5653-5654; (b) Rodríguez, G.; Magdalena Cid, M.; Saá, C.; Castedo, L.; Domínguez, D. *J. Org. Chem.* **1996**, *61*, 2780-2782; (c) Rodríguez, G.; Castedo, L.; Domínguez, D. Saá, C. *Tetrahedron Lett.* **1998**, *39*, 6551-6554; (d) Rodríguez, G.; Castedo, L.; Domínguez, D. Saá, C. *J. Org. Chem.* **1999**, *64*, 877-883; (e) Rodríguez, G.; Castedo, L.; Domínguez, D. Saá, C. *J. Org. Chem.* **1999**, *64*, 4830-4833.
- (39) (a) Prado, M. A. F.; Alves, R. J.; Souza Filho, J. D.; Alves, R. B.; Pedrosa, M. T. C.; Prado, R. F.; Faraco, A. A. G. *J. Chem. Soc., Perkin Trans. 1* **2000**, 1853-1857; (b) Binatti, I.; Prado, M. A. F.; Alves, R. J.; Souza Filho, J. D. *J. Braz. Chem. Soc.* **2002**, *13*, 570-575; (c) Faraco, A. A. G.; Prado, M. A. F.; Alves, R. J.; Souza Filho, J. D.; Alves, R. B.; Faraco, R. F. P. *Synth. Commun.* **2003**, *33*, 463-474; (d) Oliveira, R. B.; Souza Filho, J. D.; Prado, M. A. F.; Eberlin, M. N.; Meurer, E. C.; Santos, L. S.; Alves, R. J. *Tetrahedron* **2004**, *60*, 9901-9908; (e) Binatti, I.; Alves, R. B.; Souza Filho, J. D.; Dias, D. F.; Prado, M. A. F.; Alves, R. J. *Quim. Nova.* **2005**, *28*, 1023-1029; (f) Dias, D. F.; Prado, M. A. F.; Alves, R. J.; Binatti, I.; Alves, R. B.; Souza Filho, J. D. *Quim. Nova.* **2006**, *29*, 444-451; (g) Oliveira, M. T.; Prado, M. A. F.; Alves, R. B.; Cesar, A.; Alves, R. J.; Queiroga, C. G.; Santos, L. S.; Eberlin, M. N. *J. Braz. Chem. Soc.* **2007**, *18*, 364-369.
- (40) Klausner, R. D.; Donaldson, J. G.; Lippincott-Schwartz, J. *J. Cell. Biol.* **1992**, *116*, 1071-1080.
- (41) Feldman, K. S.; Berven, H. M.; Romanelli, A. L. *J. Org. Chem.* **1993**, *58*, 6851-6856.

- (42) Betina, V. *Zearalenone and its Derivatives in Mycotoxins: Chemical, Biological and Environmental Aspects*; Elsevier: Amsterdam, **1989**.
- (43) Syntheses of (\pm)-zearalenone: (a) Taub, D.; Girotra, N. N.; Hoffsommer, R. D.; Kuo, C. H.; Slates, H. K.; Weber, S.; Wendler, N. L. *Chem. Commun.* **1967**, 225-226; (b) Girotra, N. N.; Wendler, N. L. *Chem. & Ind.* **1967**, 35, 1493; (c) Taub, D.; Girotra, N. N.; Hoffsommer, R. D.; Kuo, C. H.; Slates, H. K.; Weber, S.; Wendler, N. L. *Tetrahedron*, **1968**, 24, 2443-2452; (d) Vlattas, I.; Harrison, I. T.; Tokes, L.; Fried, J. H.; Cross, A. D. *J. Org. Chem.* **1968**, 33, 4176-4179; (e) Hurd, R. N. and Shah, D. H. *J. Med. Chem.* **1973**, 16, 543-545; (f) Takahashi, T.; Kasuga, K.; Takahashi, M.; Tsuji, J. *J. Am. Chem. Soc.* **1979**, 101, 5072-5073.
- (44) Syntheses of (-)-zearalenone: (a) Kalivretenos, A.; Stille, J. K.; Hegedus, L. S. *J. Org. Chem.* **1991**, 56, 2883-2894; (b) Keinan, E. I. Sinha, S. C.; Sinhabagchi, A. *J. Chem. Soc., Perkin Trans. 1* **1991**, 3333-3339.
- (45) (a) Hitchcock, S. A. and Pattenden, G. *Tetrahedron Lett.* **1990**, 31, 3641-3644; (b) Hitchcock, S. A. and Pattenden, G. *J. Chem. Soc., Perkin Trans. 1* **1992**, 1323-1328.
- (46) Ruzicka, L. *Helv. Chim. Acta* **1926**, 9, 715-729.
- (47) Examples of (\pm)-muscone syntheses: (a) Mookherjee, B. D.; Trenkle, R. W.; Patel, R. R. *J. Org. Chem.* **1971**, 36, 3266-3270; (b) Ito, Y. and Saegusa, T. *J. Org. Chem.* **1977**, 42, 2326-2327; (c) Tsuji, J.; Yamada, T.; Shimizu, I. *J. Org. Chem.* **1980**, 45, 5209-5211.
- (48) Examples of (-)-(*R*)-muscone syntheses: (a) Mamdapur, V. R.; Chakravarti, K. K.; Nayak, U. G.; Bhattacharyya, S. C. *Tetrahedron* **1964**, 20, 2601-2604; (b) Baumann, M.; Hoffman, W.; Müller, N. *Tetrahedron Lett.* **1976**, 17, 3585-3588; (c) Nelson, K. A. and Mash, E. A. *J. Org. Chem.* **1986**, 51, 2721-2724; (d) Bulic, B.; Lücking, U.; Pfaltz, A. *Synlett.* **2006**, 1031-1034.
- (49) Goodwin, T. W. *Aspects of Terpenoid Chemistry and Biochemistry*, Acad. Press, London, New York, **1971**.
- (50) Jonas, D.; Özlü, Y.; Parsons, P. J. *Synlett.* **1995**, 255-256.

- (51) (a) Cox, N. J. G.; Pattenden, G.; Mills, S. D. *Tetrahedron Lett.* **1989**, *30*, 621-624; (b) Cox, N. J. G.; Mills, S. D.; Pattenden, G. *J. Chem. Soc., Perkin Trans. 1* **1992**, 1313-1321.
- (52) (a) Patil, V. D.; Nayak, U. R.; Dev, S. *Tetrahedron* **1973**, *29*, 341-348; (b) Prasad, R. S. and Dev, S. *Tetrahedron* **1976**, *32*, 1437-1441.
- (53) Fenical, W.; Okuda, R. K.; Bandurraga, M. M.; Culver, P.; Jacobs, R. S. *Science* **1981**, *212*, 1512-1514.
- (54) Hayakawa, Y.; Kawakami, K.; Seto, H. *Tetrahedron Lett.* **1992**, *33*, 2701-2704.
- (55) Roseophilin: (a) Fürstner, A. and Weintritt, H. *J. Am. Chem. Soc.* **1998**, *120*, 2817-2825; (b) Fürstner, A.; Gastner, T.; Weintritt, H. *J. Org. Chem.* **1999**, *64*, 2361-2366; (c) Bamford, S. J.; Luker, T. Speckamp, W. N.; Hiemstra, H. *Org. Lett.* **2000**, *2*, 1157-1160; (d) Trost, B. M. and Doherty, G. A. *J. Am. Chem. Soc.* **2000**, *122*, 3801-3810; (e) Harrington, P. E. and Tius, M. A. *J. Am. Chem. Soc.* **2001**, *123*, 8509-8514.
- (56) (±)-Roseophilin: Bitar, A. Y. and Frontier, A. *J. Org. Lett.* **2009**, *11*, 49-52.
- (57) (ent)-Roseophilin: Boger, D. L. and Hong, J. *J. Am. Chem. Soc.* **2001**, *123*, 8515-8519.
- (58) (a) Robertson, J.; Burrows, J. N.; Stuppel, P. A. *Tetrahedron* **1997**, *53*, 14807-14820; (b) Robertson, J. and Hatley, R. J. D. *Chem. Commun.* **1999**, 1455-1456; (c) Robertson, J.; Hatley, R. J. D.; Watkin, D. J. *J. Chem. Soc., Perkin Trans. 1* **2000**, 3389-3396.
- (59) Balraju, V.; Reddy, D. S.; Periasamy, M.; Iqbal, J. *Tetrahedron Lett.* **2005**, *46*, 5207-5210.
- (60) (a) Casty, G. L. and Stryker, J. M. *J. Am. Chem. Soc.* **1995**, *117*, 7814-7815; (b) Carter, C. A. G.; McDonald, R.; Stryker, J. M. *Organometallics* **1999**, *18*, 820-822; (c) Carter, C. A. G.; Greidanus, G.; Chen, J.-X.; Stryker, J. M. *J. Am. Chem. Soc.* **2001**, *123*, 8872-8873; (d) Carter, C. A. G.; Casty, G. L.; Stryker, J. M. *Synlett* **2001**, 1046-1049.
- (61) Ogoshi, S. and Stryker, J. M. *J. Am. Chem. Soc.* **1998**, *120*, 3514-3515.
- (62) For simplicity it is understood that “ η^3 -propargyl” is referring to “ η^3 -propargyl/allenyl” indicating the indeterminate hybridization of the organic ligand.
- (63) Girard, P.; Namy, J. L.; Kagan, H. B. *J. Am. Chem. Soc.* **1980**, *102*, 2693-2698.
- (64) Bauer, R. C. Ph. D. Dissertation Thesis, University of Alberta, **2009**.

- (65) Stephan, D. W. *Organometallics* **2005**, *24*, 2548-2560.
- (66) Morita, M. and Stryker, J. M. *Unpublished results* **2008**.
- (67) (a) Lauher, J. W. and Hoffmann, R. *J. Am. Chem. Soc.* **1976**, *98*, 1729-1742; (b) Curtis, M. D. and Eisenstein, O. *Organometallics* **1984**, *3*, 887-895; (c) Green, J. C. *Chem. Soc. Rev.* **1998**, *27*, 263-271.
- (68) (a) Chen, J.-X. Ph. D. Dissertation Thesis, University of Alberta, **1999**; (b) Tiege, P. B. Ph. D. Dissertation Thesis, University of Alberta, **2001**.
- (69) (a) Beesley, R. M.; Ingold, C. K.; Thorpe, J. F. *J. Chem. Soc.* **1915**, *107*, 1080-1106; (b) Ingold, C. K. *J. Chem. Soc.* **1921**, *119*, 305-329; (c) Ingold, C. K.; Sako, S.; Thorpe, J. F. *J. Chem. Soc.* **1922**, *120*, 1117-1198; (d) Jung, M. E. and Piizzi, G. *Chem. Rev.* **2005**, *105*, 1735-1766.
- (70) Nomuran N. and Stryker, J. M. *Unpublished results* **1995**.
- (71) von Ragué Schleyer, P. *J. Am. Chem. Soc.* **1961**, *83*, 1368-1373.
- (72) Binisti, C.; Assogba, L.; Touboul, E.; Mounier, C.; Huet, J.; Ombetta, J.-E.; Dong, C.Z.; Redeuilh, C.; Heymans, F.; Godfroid, J.-J. *Eur. J. Med. Chem.* **2001**, *36*, 809-828.
- (73) Kerwin, S. M. *Tetrahedron Lett.* **1994**, *35*, 1023-1026.
- (74) Earl, R. A. and Townsend, L. B. *Org. Synth. Coll. Vol. 7*, **1990**, 334.
- (75) Dumez, E.; Faure, R.; Dulcère, J-P. *Eur. J. Org. Chem.* **2001**, 2577-2588.
- (76) Brillion, D.; Deslongchamps, P. *Can. J. Chem.* **1987**, *65*, 43-55.
- (77) This material was prepared by a previous member of the Stryker group. Distillation was performed prior to use.
- (78) Roy, C. D. *Aust. J. Chem.* **2006**, *59*, 657-659.
- (79) Yadav, V. K. and Fallis, A. G. *J. Org. Chem.* **1986**, *51*, 3372-3374.
- (80) Node, M.; Kajimoto, T.; Nishide, K.; Fujita, E.; Fugii, K. *Tetrahedron Lett.* **1984**, *25*, 219-222.
- (81) Amouroux, R.; Jatczak, M.; Chastrette, M. *Bull. Soc. Chim. Fr.* **1987**, 505-510.
- (82) Oehlschlager, A. C.; Czyzewska, E.; Aksela, R.; Pierce, Jr. H. D. *Can. J. Chem.* **1986**, *64*, 1407-1413.
- (83) Jagasia, R. and Stryker, J. M. *Unpublished Results* **2000**.

- (84) Cundari, S.; Dalpozzo, R.; De Nino, A.; Procopio, A.; Sindona, G. *Tetrahedron* **1999**, *55*, 10155-10162.
- (85) Guss, C. O. and Rosenthal, R. *J. Am. Chem. Soc.* **1955**, *77*, 2549.
- (86) Khan, Ab. T.; Choudhury, L. H.; Ghosh, S. *Tetrahedron Lett.* **2004**, *45*, 7891-7894.
- (87) Verhe, R.; De Kimpe, N.; De Buyck, L.; Schamp, N. *Synth. Commun.* **1981**, *11*, 35-42.
- (88) Grigsby, W.E., Hind, J., Chanley, J., Westheimer, F.H., *J. Am. Chem. Soc.*, **1942**, *64*, 2606-2610.
- (89) Wheeler, O. H. and Granell de Rodriguez, E. E. *J. Org. Chem.* **1964**, *29*, 1227-1229.
- (90) Fauq, A.H., Kache, R., Khan, M.A., Vega, I.E., *Bioconjugate Chem.*, **2006**, *17*, 248-254.
- (91) Yebga, A.; Ménager, S.; Vérité, P.; Comber Farnoux, C.; Lafont, O. *Eur. J. Med. Chem.* **1995**, *30*, 769-777.
- (92) Wagner, A.; Heitz, M-P.; Mioskowski, C. *J. Chem. Soc. Chem. Comm.* **1989**, 1619-1620.
- (93) Gansäuer, A.; Winkler, I.; Worgull, D.; Franke, D.; Lauterbach, T.; Okkel, A.; Nieger, M. *Organometallics*, **2008**, *27*, 5699-5707.
- (94) Kagan, H. B. *Tetrahedron*, **2003**, *59*, 10351, 10372.
- (95) Fernández-Mateos, A.; Herrero Teijó, P.; Radanedo Clemente, R.; Rubio González, R. *Tetrahedron Lett.* **2006**, *47*, 7755-7758.
- (96) (a) Petasis, N. A. and Fu, D.-K. *Organometallics* **1993**, *12*, 3776-3780; (b) Doxsee, K. M.; Juliette, J. J. J.; Mouser, J. K. M.; Zientara, K. *Organometallics* **1993**, *12*, 4682-4686; (c) Tomita, I. and Ueda, M. *J. Inorg. Organomet. Polym. Mater.* **2005**, *15*, 511-518.
- (97) The sample was prepared by P. Tiege during his Ph.D work at the Univeristy of Alberta.
- (98) Zhang, X.-M. and Bordwell, F. G. *J. Phys. Org. Chem.* **1994**, *7*, 751-756.
- (99) (a) Bräse, S.; Wertal, H.; Frank, D.; Vidović, D.; Meijere, A. *Eur. J. Org. Chem.* **2005**, 4167-4178; (b) Toullec, P. Y.; Genin, E.; Antoniotti, S.; Genêt, J-P.; Michelet, V. *Synlett*, **2008**, 707-711.

- (100) (a) Chen, J.-T.; Chen, Y.-K.; Chu, J.-B.; Lee, G.-H.; Wang, Y. *Organometallics*, **1997**, *16*, 1476-1483; Cheng, Y.-C.; Chen, Y.-K.; Huang, T.-M.; Yu, C.-I.; Lee, G.-H.; Wang, Y.; (b) Chen, J.-T. *Organometallics* **1998**, *17*, 2953-2957.
- (101) Avakyan, V. G.; Litmanovich, A. D.; Cherkezyan, V. O. *Bulletin of the Academy of Sciences of the USSR, Division of Chemical Science* **1984**, *33*, 292-296.
- (102) (a) Deslongchamps, P.; Lamothe, S.; Lin, H.-S. *Can. J. Chem.* **1984**, *62*, 2395-2398; (b) Brillon, D.; Deslongchamps, P. *Tetrahedron Lett.* **1986**, *27*, 1131-1134; (c) Brillon, D.; Deslongchamps, P. *Can. J. Chem.* **1987**, *65*, 56-68.
- (103) Crich, D. and Fortt, S. M. *Tetrahedron Lett.* **1987**, *28*, 2895-2898.
- (104) Collin, J. and Lossing, F. P. *Can. J. Chem.* **1957**, *35*, 778-787.
- (105) Lambert, J. B.; Shurvell, H. F.; Lightner, D. A.; Graham Cooks, R. *Organic Structural Spectroscopy*, Prentice-Hall, New Jersey, **2001**.
- (106) (a) Fernandez-Matéos, A.; Martin de la Nava, E.; Pascuala Coca, G.; Ramos Silva, A.; Rubio González, R. *Org. Lett.* **1999**, *1*, 607-610; (b) Fernandez-Matéos, A.; Mateos Burón, L.; Rabanedo Clemente, R.; Ramos Silva, A. I.; Rubio González, R. *Synlett.* **2004**, 1011-1014.
- (107) Gansäuer, A.; Piestert, F.; Huth, I.; Lauterbach, T. *Synthesis* **2008**, 3509-3515.
- (108) Nugent, W. A. and RajanBabu, T. V., *J. Am. Chem. Soc.* **1988**, *110*, 8561-8562.
- (109) (a) Fürstner, A. *Chem. Eur. J.* **1998**, *4*, 567-570; Gansäuer, A. and Bluhm, H. *Chem. Rev.* **2000**, *100*, 2771-2788; (b) Barrero, A. F.; Quílez del Moral, J. F.; Sánchez, E. M.; (c) Arteaga, J. F. *Eur. J. Org. Chem.* **2006**, 1627-1641.
- (110) Nugent, W. A. and RajanBabu, T. V. *J. Am. Chem. Soc.* **1989**, *112*, 6408-6409.
- (111) (a) Nugent, W. A. and RajanBabu, T. V. *J. Am. Chem. Soc.* **1989**, *112*, 6408-6409; (b) RajanBabu, T. V. and Nugent, W. A. *J. Am. Chem. Soc.* **1994**, *116*, 986-997; (c) Gansäuer, A.; Bluhm, H.; Pierobon, M. *J. Am. Chem. Soc.* **1998**, *120*, 12849-12859.
- (112) Barrero, A. F.; Rosales, A.; Cuerva, J. M.; Oltra, J. E. *Org. Lett.* **2003**, *5*, 1935-1938.
- (113) Justicia, J.; Campaña, A. G.; Bazdi, B.; Robles, R.; Cuerva, J. M.; Oltra, J. E. *Adv. Synth. Catal.* **2008**, *350*, 571-576.

- (114) Barrero, A. F.; Quílez del Moral, J. F.; Sánchez, E. M.; Arteaga, J. F. *Eur. J. Org. Chem.* **2006**, 1627-1641.
- (115) Qiu, X. M.Sc. Dissertation Thesis, University of Alberta, **2000**.
- (116) (a) Gansäuer, A.; Lauterbach, T.; Bluhm, H.; Noltemeyer, M. *Angew. Chem. Int. Ed.* **1999**, *38*, 2909-2910; (b) Gansäuer, A.; Fan, C.-A.; Keller, F.; Keil, J. *J. Am. Chem. Soc.* **2007**, *129*, 3484-3485.
- (117) Casty, G. L. Ph. D. Dissertation Thesis, University of Alberta, **1994**.
- (118) (a) Casey, C. P. and Yi, C. S. *J. Am. Chem. Soc.* **1992**, *114*, 6597-6598; (b) Casey, C. P.; Nash, J. R.; Yi, C. S.; Selmezy, A. D.; Chung, S.; Powell, D. R.; Hayashi, R. K. *J. Am. Chem. Soc.* **1998**, *120*, 722-733; (c) Casey, C. P.; Boller, T. M.; Same, J. S. M.; Reinert-Nash, J. R. *Organometallics*, **2009**, *28*, 123-131.
- (119) Ogoshi, S. and Stryker, J. M. *Unpublished results* **1998**.
- (120) (a) Rodriguez, G. and Bazan, G. C. *J. Am. Chem. Soc.* **1997**, *119*, 343-352; (b) Chen, J.-T. *Coordination Chemistry Reviews.* **1999**, *192*, 1143-1168.
- (121) Crabtree, R. H. *The Organometallic Chemistry of the Transition Metals*, Wiley-Interscience, Hoboken, NJ, **2005**.
- (122) Daasbjerg, K.; Svith, H.; Grimme, S.; Gerenkamp, M.; Mück-Lichtenfeld, C.; Gansäuer, A.; Barchuk, A.; Keller, F. *Angew. Chem. Int. Ed.* **2006**, *45*, 2041-2044.
- (123) Gansäuer, A.; Barchuk, A.; Keller, F.; Schmitt, M.; Grimme, S.; Gerenkamp, M.; Mück-Lichtenfeld, C.; Daasbjerg, K.; Svith, H. *J. Am. Chem. Soc.* **2007**, *129*, 1359-1371.
- (124) Matsukawa, M.; Tabuchi, T.; Inanaga, J.; Yamaguchi, M. *Chem. Lett.* **1987**, 2101-2102.
- (125) (a) Molander, G. A. and Harris, C. R. *Tetrahedron* **1998**, *54*, 3321-3354; (b) Jung, D. Y. and Kim, Y. H. *Synlett.* **2005**, 3019-3032.
- (126) Meinhart, J. D. and Grubbs, R. H. *Bull. Chem. Soc. Jpn.* **1980**, *61*, 171-180.
- (127) Doxsee, K. M. and Mouser, J. K. M. *Tetrahedron Lett.* **1991**, *32*, 1687-1690.
- (128) Curran, D. P.; Chen, M.-H.; Spletzer E.; Seong, C. M.; Chang, C.-T. *J. Am. Chem. Soc.* **1989**, *111*, 8872-8878.
- (129) Zhou, H.; Huang, X.; Chen, W. *J. Org. Chem.* **2004**, *69*, 5471-5472.

- (130) Fairlamb, I. and Lynam J. *Organometallic Chemistry Volume 34*, **2008**, The Royal Society of Chemistry, Cambridge, UK.
- (131) (a) Tebbe, F. N. and Harlow, R. L. *J Am. Chem. Soc.* **1980**, *102*, 6149-6151; (b) McKinney, R. J.; Tulip, T. H.; Thorn, D. L.; Coolbaugh, T. S.; Tebbe, F. N. *J. Am. Chem. Soc.* **1981**, *103*, 5584-5586; (c) Shono, T.; Nagasawa, T.; Tsubouchi, A.; Noguchi, K.; Takeda, T. *Chem. Commun.* **2008**, *30*, 3537-3539; (d) Beckhaus, R.; Sang, J.; Wagner, T.; Ganter, B. *Organomet.* **1996**, *15*, 1176-1187.
- (132) All averages are calculated at the 95% confidence level.
- (133) Allen, F. H.; Kennard, O.; Watson, D. G.; Brammer, L.; Orpen, A. G.; Taylor, R. *J. Chem. Soc. Perkin. Trans.* **1987**, *12*, S1-S19.
- (134) (a) Harvey, B. G.; Mayne, C. L.; Arif, A. M.; Ernst, R. D. *J. Am. Chem. Soc.* **2005**, *127*, 16426-16435; (b) Scheins, S.; Messerschmidt, M.; Gembicky, M.; Pitak, M.; Volkov, A.; Coppens, P.; Harvey, B. G.; Turpin, G. C.; Arif, A. M.; Ernst R. D. *J. Am. Chem. Soc.* **2009**, *131*, 6154-6160.
- (135) Harvey, B. G.; Arif, A. M.; Ernst, R. D. *J. Organomet.* **2006**, 5211-5217.
- (136) Coutts, R. S. P.; Wailes, P. C.; Martin, R. L. *J. Organomet. Chem.* **1973**, *47*, 375-382.
- (137) (a) Sekine, M.; Tsuruoka, H.; Limura, S.; Kusuoku, H.; Wada, T. *J. Org. Chem.* **1996**, *61*, 4087-4100; (b) Edwards, P. G.; Paisey, S. J.; Tooze, R. P. *J. Chem. Soc., Perkin Trans. 1* **2000**, 3122-3128.
- (138) Srinivasan, R.; Chandrasekharam, M.; Vani, P. V. S. N.; Chida, A. S.; Singh, A. K. *Synth. Commun.* **2002**, *32*, 1853-1858.
- (139) Lee, J. C.; Bae, Y. H.; Chang, S.-K. *Bull. Korean. Chem. Soc.* **2003**, *24*, 407-408.
- (140) Unable to ambiguously assign.